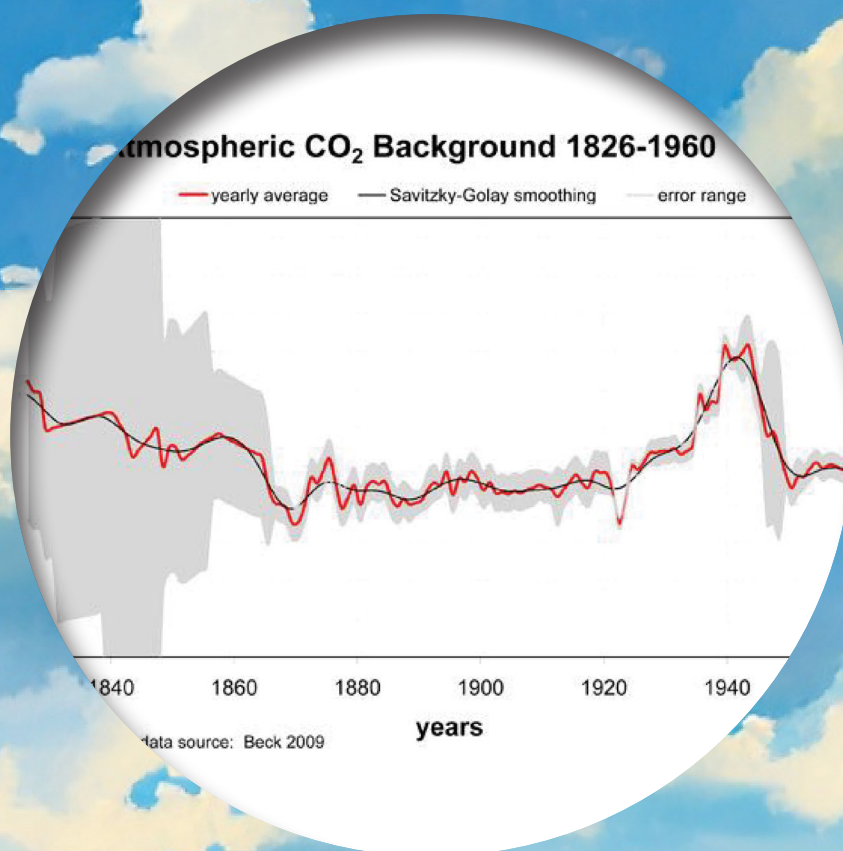


SCIENCE OF CLIMATE CHANGE

Volume 2.2

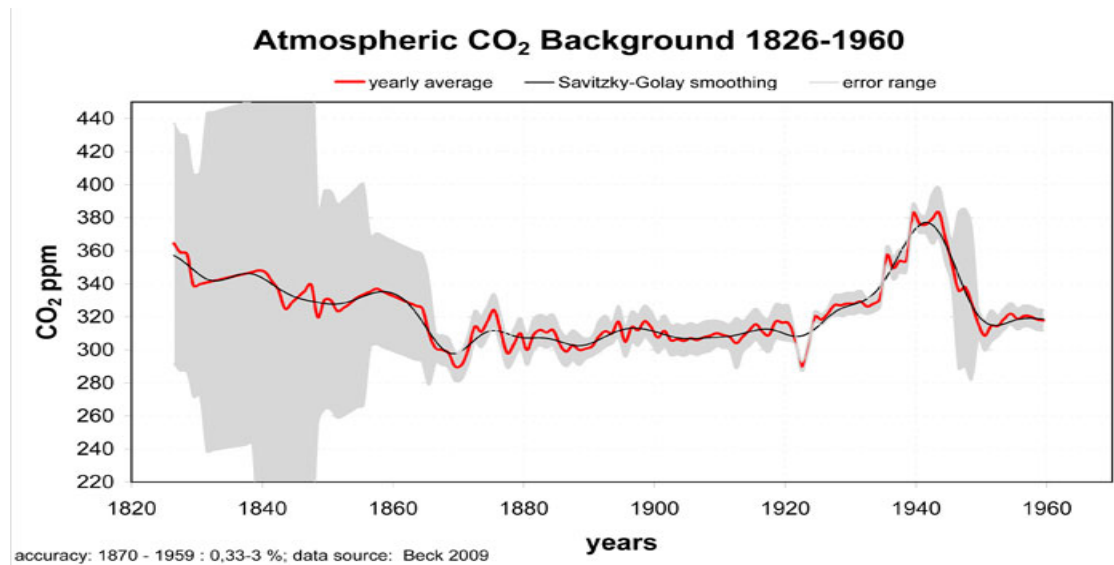
2022

<https://scienceofclimatechange.org>



Published by: Klimarealistene (Org. no. 995 314 592)

ISSN 2703-9080 (print) ISSN 2703-9072 (online)



Atmospheric CO₂ background level 1826-1960 estimated from directly measured data (red). The black line is a smoothed value, and the shaded gray is the estimated error range.

From an article by Ernst-Georg Beck: *Reconstruction of Atmospheric CO₂ Background Levels since 1826 from Direct Measurements near Ground*

Figure 24, page 173

SCIENCE OF CLIMATE CHANGE

Volume 2.2

June 2022

ISSN 2703-9072

Klimarealistene, P.O. Box 33, 3901 Porsgrunn, Norway

Table of Content

	Page
Editorial.....	
Hermann Harde, How Much CO ₂ and the Sun Contribute to Global Warming:.....	105
Harald Yndestad, Publication of Ernst-Georg Beck's Atmospheric CO ₂ Time series from 1826-1960.....	134
Francis Massen, Ernst-Georg Beck, Hans Jelbring, Antoine Kies, Observed Temporal and Spatial CO ₂ Variations Useful for the Evaluation of Regionally Observed CO ₂ Data.....	137
Ernst-Georg Beck, Reconstruction of Atmospheric CO ₂ Background Levels since 1826 from Direct Measurements near Ground (inclusive Supplements 3 & 5).....	148

Editorial

We have the pleasure to publish the monumental work of Ernst-Georg Beck with the title: *Reconstruction of Atmospheric Background Levels since 1826 from Direct Measurements near Ground*, which was submitted to a journal in 2010, but were not accepted for publication before Beck died in September 2010. In this work he analyzed CO₂ measurements from 979 technical papers and made use of methods to find the yearly average model, based on simultaneous wind measurements, precipitation measurements and other information about the observations. He showed he this way could estimate the atmospheric CO₂ level within a few per cent of the Mauna Loa reference observations. Analysis of the time series show that it has the same pattern as the Sea Surface Temperature and the Lunar Nodal tide variations which are controlled by the Moon.

In this issue we also publish the result of advanced energy-radiation balance model calculations with added solar radiative forcing amplified by induced cloud cover changes. The result is that CO₂ should not have contributed more than one third of the last century warming and the Sun the other two thirds.

Good reading

Jan-Erik Solheim
Editor

The Editorial Board consists of Stein Storlie Bergsmark, Ole Henrik Ellestad, Martin Hovland, Ole Humlum and Olav Martin Kvalheim.

A digital version of this volume can be found here: <https://doi.org/10.53234/scc202308/15>



Correspondence to
harde@hsu-hh.de

Vol. 2.2 (2022)

pp. 105-133

How Much CO₂ and the Sun Contribute to Global Warming: Comparison of Simulated Temperature Trends with Last Century Observations

Hermann Harde

Helmut-Schmidt-University, Hamburg, Germany

Abstract

The Intergovernmental Panel on Climate Change classifies the human influence on our climate as extremely likely to be the main reason of global warming over the last decades. Particularly anthropogenic emissions of carbon dioxide are made responsible for the observed temperature changes, while any natural forcings are almost completely excluded. However, detailed own calculations with an advanced energy-radiation-balance model indicate that the temperature increase and its variations over the last 140 years can much better be explained by additionally including solar radiative forcing and its amplification by induced cloud cover changes. We present simulations based on different time series of the total solar irradiance and compare them with composed land-ocean-surface temperature measurements of the Northern Hemisphere. From these simulations we follow that CO₂ should not have contributed more than about one third to global warming over the last century, while solar variations over this period can well explain two thirds of the increase.

Keywords: Solar variability; global warming; temperature time series; CO₂ radiative forcing; solar radiative forcing; climate sensitivity; solar sensitivity; thermal feedbacks; solar feedback.

Submitted Dec. 02, 2021. Accepted Feb. 11, 2022. <https://doi.org/10.53234/scc202206/10>

1. Introduction

The Fifth and Sixth Assessment Report (AR5 and AR6) [1, 2] of the Intergovernmental Panel on Climate Change (IPCC) announced new evidence of an anthropogenic climate change based on many independent scientific analyses from observations of the climate system, paleoclimate archives, theoretical studies of climate processes, and simulations using climate models. In these reports the IPCC classifies the human influence as extremely likely to be the dominant cause of the observed warming since the mid-20th century (e.g., AR5-WG1-SPM-D3), while contributions from natural forcings and internal variability would only likely be in the range of -0.1°C to 0.1°C . Particularly increasing emissions of carbon dioxide (CO₂) over the last century are made responsible for this change, and the Equilibrium Climate Sensitivity (ECS) as a measure for the Earth's temperature increase at doubled CO₂ concentration in the atmosphere is specified with an assessed best estimate of 3°C and a *likely* range of 2.5°C to 4°C (high confidence, AR6-WG1-SPM, A.4.4) - acronyms see Annex.

However, explanations of the observed global warming over the last 170 years, in particular anthropogenic contributions to this warming, are still quite contradictorily discussed, and it is surprising:

- (i) that the well documented delayed and pure native emissions of CO₂ and methane (CH₄) to sea and air temperature changes (see, e.g., Petit et al. [3]; Monnin et al. [4]; Caillon et al. [5]; Torn & Harte [6]; Humlum et al. [7]; Salby [8]) are not further considered in AR5 or AR6 with their consequences for interpreting actual climate changes (for a detailed con-

sideration of the "hen-or-egg causality" see also Koutsoyiannis & Kundzewicz [9]);

- (ii) that any observed increase of CO₂ since the Little Ice Age is allocated only to anthropogenic emissions and assumed to cumulate in the atmosphere over thousands of years, while any temporal and temperature dependent variations of the 25 times larger natural emissions and their uptake are excluded (see, Harde [10, 11]);
- (iii) that Radiative Forcings (RF) of greenhouse (GH) gases with their feedbacks are referred, which are mostly valid for clear sky conditions, while the impact of clouds is usually omitted (AR5-WG1- Chap.8.3.1);
- (iv) that important effects like convection and evaporation feedback, which can contribute to significant negative feedback (Harde [12, 13]), are not considered;
- (v) and that the IPCC denies any noticeable solar influence on the actual climate, although there exists strong evidence of an increasing solar activity over the last century (see, e.g., Hoyt & Schatten [14]; Willson & Mordvinov [15]; Shapiro et al. [16]; Ziskin & Shaviv [17]; Scafetta & Willson [18]; Usoskin et al. [19]; Zhao & Feng [20]; Soon et al. [21]; Connolly et al. [22]).

Despite these deficits and simplifications, the GH-gases are assigned with very high confidence (95%) to be responsible for the actual climate change. Because of the far-reaching consequences for future climate predictions, it is particularly important to scrutinize, how far this assertion can really be confirmed by the observed changes of GH-gas concentrations, the global temperature and the solar activity. Also, the impact of some native effects like thermally and solar induced cloud cover changes, which affect our climate, but which are not always well understood, has carefully to be investigated with its implications on the observed temperature changes.

Therefore, in this contribution we compare composed land and sea surface temperature measurements of the Northern Hemisphere (Soon et al. [21]) with simulations performed by an advanced 2-Layer Climate Model (2LCM) (Harde [12, 13]), which allows to calculate the influence of CO₂ and solar variations on the climate. This model with its main features is briefly presented in Section 2. The different external forcings like the CO₂ radiative forcing and the solar radiative forcing with their specific feedbacks are discussed in Section 3 and can directly be compared with calculations within the Coupled Model Intercomparison Project Phase 5 (CMIP5) and Phase 6 (CMIP6). In Section 4 we present simulations for the temperature trend over the last 140 years, based on the CMIP5 and CMIP6 data, and on the other hand on our own calculations, this for six different Total Solar Irradiance (*TSI*)-time-series, which we oppose to respective measurements. Section 5 gives a summary with future perspectives.

2. Two-Layer-Climate Model

Climate models are the primary tools available for investigating the response of the climate system to various forcings, for making climate predictions on seasonal to decadal time scales and for making projections of future climate over the coming century and beyond (see AR5-Chap.9 [1]).

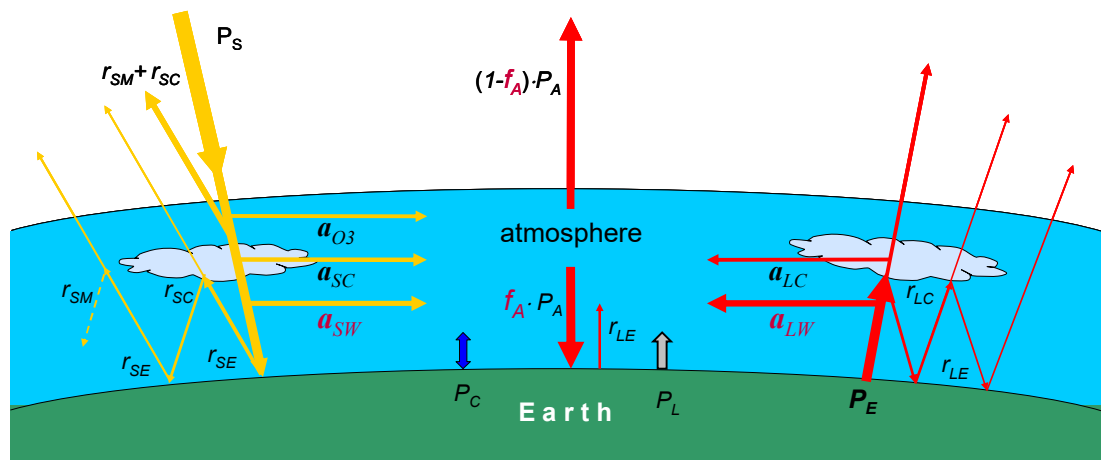
Over recent years models of different complexity were developed. Atmosphere–Ocean General Circulation Models (AOGCMs) are primarily aiming to understand the dynamics of the physical components of the climate system (atmosphere, ocean, land and sea ice), and to make projections based on future GH-gas and aerosol forcing. These models are extensively used for seasonal to decadal climate predictions, often with a focus on particular regions.

Earth System Models (ESMs) expand on AOGCMs and try to include various biogeochemical cycles such as the carbon-, the sulphur- or ozone-cycle. They are the most comprehensive tools available for simulating the response of the climate to external forcing with biogeochemical feedbacks.

Earth System Models of Intermediate Complexity (EMICs) attempt to include relevant components often in an idealized manner or at lower resolution than the models described above. EMICs are more focussed on certain scientific questions such as understanding climate feedbacks on millennial time scales or exploring sensitivities in which long model integrations are required. This class of models often includes Earth system components not yet included in all ESMs (e.g., ice sheets).

Different to the AOGCMs and ESMs, which with their higher local and temporal resolution have to solve complex coupled nonlinear differential equations - making these calculations extremely time consuming and even unstable - we use a much simpler but not less expressive model, which is based on a global energy and radiation balance and averages over larger local variations. Its primary objective is comparable with EMICs to better understand climate feedbacks and the sensitivity of some impacts, which have not been considered previously in other models. Our direct approach to the model evaluation is to compare model output with observations and to analyse the resulting difference. Figure 1 shows the main features of our model with its relevant parameters.

This model is especially appropriate to calculate the influence of increasing CO₂ concentrations on global warming as well as the impact of solar variations on the climate. It considers the atmosphere and the Earth's surface as two main layers acting as absorbers for short wave (sw) and long wave (lw) radiation and simultaneously working as Planck radiators for lw radiation. In addition, it includes heat transfer between these layers due to convection and evaporation (P_C and P_L), and it considers sw and lw scattering processes at the atmosphere and at clouds. Further it includes all common feedback processes like water vapor, lapse rate, and albedo feedback but additionally takes into account temperature dependent sensible and latent heat fluxes as well as temperature induced and solar induced cloud cover feedback.



P – power; r – reflectivity (scattering); a – absorptivity; f_A – back-radiated fraction

Figure 1: Two-layer climate model for the Earth-atmosphere system with the main parameters.

At equilibrium the Earth's surface and atmosphere release as much power as they suck up from the Sun and the neighbouring layer. This gives a coupled balance equation system, which can be solved for the radiated power P_E of the surface and the emitted power P_A of the atmosphere. With Stefan-Boltzmann's law the global mean temperatures at the surface and for the atmosphere are derived.

Primarily this 2LCM was developed to assess the Equilibrium Climate Sensitivity ECS and also the Equilibrium Solar Sensitivity ESS (temperature change at 1‰ variation of the Total Solar Irradiance TSI), i.e., it uses steady-state conditions for the energy and radiation balance to derive from this the respective Earth and atmospheric temperatures T_E and T_A at a given CO₂ concentration and TSI . But such calculation can also be applied to track the smaller temperature variations caused by the year-to-year CO₂ and TSI changes. The faster adjustments to the RF like

tropospheric and stratospheric temperature adjustments already achieve equilibrium within a few months, only the surface temperature is adapting over much longer periods. But with CO₂ concentration changes of about 130 ppm over 170 years, corresponding to an average increase of 0.8 ppm/yr, also the slower thermal feedbacks are all the time close to equilibrium conditions, which compared to a transient response only slightly shift the absolute temperature level by not more than one or two tenth of a degree. At the same time this defines an upper limit of these impacts without affecting their relative contributions to global warming. In addition, for comparison with the observed temperature series, which are expected to suffer from a larger delay to an internal or external forcing, the calculated temperatures in any way have to be considered as moving average over 15 to 20 years, thus, further reducing any differences between the transient response and the equilibrium climate calculations.

Different to other climate models, where the influence of GH-gases is expressed by the radiative forcing F_{RG} in the tropopause, in this model the key parameters controlling the fluxes are the sw- and lw-absorptivities a_{SW} and a_{LW} of the GH-gases as well as the back-radiated fraction f_A of the atmosphere (see Fig. 1.) These parameters are changing with the atmospheric composition of the gases, their partial and total pressure as well as with their temperature. This requires detailed Line-By-Line sw absorption and lw Radiation Transfer (LBL-RT) calculations for the up- and down-welling fluxes in the atmosphere (for details see Harde [12, 13, 23, 24]), this for different CO₂ concentrations (in this case 14 concentrations from 0 - 770 ppm), for three climate zones with different ground temperatures and humidity, and for different cloud covers. Such calculations include up to 900,000 lines for the most important GH-gases water vapor (WV), carbon dioxide, methane, and ozone and are based on the HITRAN database [25].

Since the partial pressure of the GH-gases and the atmospheric pressure are changing with temperature and altitude, the atmosphere is segmented into up to 228 sub-layers from ground to 86 km height. The layer thickness up to the tropopause is 100 m and is increasing over the stratosphere. For each slice the individual spectral absorptivities and re-emission are calculated, summed up over the propagation path and are integrated over the spectral distribution to obtain the respective key parameters for the different CO₂ concentrations, for different ground temperatures (with changing WV concentrations), and for different cloud covers. With these parameters integrated in the climate model, the Earth's surface temperature T_E and the lower tropospheric temperature T_A (in about 800m altitude) are simulated as a function of the CO₂ concentration and the solar anomaly. For comparison with other models from these data we also derive the CO₂ radiative forcing F_{CO_2} .

Pressure and temperature changes with altitude are based on the US Standard Atmosphere Model (for details see Harde [12], Subsec. 2.1.2). Some other parameters (cloud and sw ozone absorptivities, scattering coefficients at clouds and the atmosphere, as well as the sw and lw Earth's reflectivities) are adapted in such a way that all radiation and heat fluxes almost exactly reproduce the widely accepted radiation and energy budget scheme of Trenberth, Fassulo and Kiehl (TFK-scheme) [26], which essentially relies on data from satellite measurements within the ERBE and CERES program [27–31]. This adaptation yields a calibration of the model to the observed up- and downwelling fluxes under standard conditions in the atmosphere and for constant heat fluxes between the surface and atmosphere.

To reproduce also the measured temperature variations with the observed cloud cover changes over the 80s and 90s, we relate to the temperature anomaly data of the Hadley Centre and Climate Research Unit (HadCRUT3) as a function of the monthly global cloud cover data of the International Satellite Cloud Climatology Project (ISCCP) [32] yielding a response of $-0.065^{\circ}\text{C}/\%$ of cloud cover changes (see also O. Humlum [33]).

All relevant parameters are listed in Harde [13], Table 6. Together with an assumed $TSI = 1365.2 \text{ W/m}^2$, a mean cloud cover $C_C = 66\%$ and a CO₂ concentration of 380 ppm they determine a reference temperature $T_R = 16^{\circ}\text{C}$ of the Earth's surface (see TFK-scheme [26]). Since over the period from 1850 to present the CO₂ concentration increased from 280 to actually 410

ppm, and most of the TSI time series investigated in this contribution are varying around a mean TSI of 1360 W/m^2 , it is preferential to avoid larger deviations from the reference, particularly for feedbacks with a larger non-linear response. Therefore, we use here as references for our simulations the lower TSI of $S_R = 1360 \text{ W/m}^2$ and a lower CO₂ concentration of $C_R = 350 \text{ ppm}$, which together with the other parameters now define a reference temperature of $T_R = 15.5^\circ\text{C}$. These references together tie up a working point, around which smaller deviations in the CO₂ concentration and the solar anomaly are considered.

3. External Forcings and their Feedbacks

For our actual studies, which aim towards distinction of anthropogenic and natural contributions to global warming, it is important to clearly assign the different drivers and forcings with their respective feedbacks. This is the subject of this section. The strength of drivers is quantified as radiative forcing RF in units of W/m^2 and represents the change in energy flux caused by a driver. It is calculated at the tropopause or at the top of the atmosphere.

Independent of the model's complexity, almost all known models are based on the simple relation that the ground temperature changes ΔT_E^i are scaling proportional to the changes of an external forcing ΔF_i :

$$\Delta T_E^i = \lambda_i \cdot \Delta F_i, \quad (1)$$

where λ_i is a sensitivity parameter representing the response of the Earth-Atmosphere-System (EASy) to the forcing. This equation holds for transient as well as for equilibrium conditions. The IPCC assigns almost all global warming to the emitted GH-gases and in particular to the impact of CO₂. Therefore, here we only consider the increase of the CO₂ concentration over the Industrial Era from 280 ppm to 410 ppm, while any contributions due to CH₄ or N₂O variations can well be neglected.

3.1 CO₂ Radiative Forcing

With (1) then we can write for the temperature increase due to CO₂ radiative forcing ΔF_{CO_2} (units: W/m^2):

$$\Delta T_E^{CO_2} = \lambda_p \cdot \Delta F_{CO_2} = -\frac{1}{\alpha_p} \Delta F_{CO_2}, \quad (2)$$

with λ_p as the Planck sensitivity or climate sensitivity parameter and α_p as the Planck response or Planck feedback, which represents the additional thermal or lw emission to space arising from vertically uniform warming of the surface and the atmosphere (AR6-WG1-Chap.7.4.2.1). It plays a fundamental stabilizing role in Earth's climate and has a strongly negative value: a warmer planet radiates more energy to space.

A calculation of the Earth's temperature T_E with the 2LCM as a function of the CO₂ concentration is displayed in Fig. 2 (Red Diamonds, for further details see also Harde [13], Subsec. 4.2).

In good agreement with the literature (e.g., Myhre et al. 1998 [34]) for higher concentrations our LBL-RT calculations reveal an almost logarithmic increase (Green Triangles) of the CO₂ forcing with rising CO₂ concentration C_{CO_2} relative to the reference concentration C_R of 350 ppm:

$$\Delta T_E^{CO_2} = \lambda_p \cdot \Delta F_{2xCO_2} \frac{\ln(C_{CO_2}/C_R)}{\ln 2} = ECS_B \frac{\ln(C_{CO_2}/C_R)}{\ln 2}. \quad (3)$$

For doubling the concentration from 350 to 700 ppm, at a mean cloud cover of 66% we find a forcing of $\Delta F_{2xCO_2} = 3.69 \text{ W/m}^2$ ([13], Table 3). However, due to some deviations from a pure logarithmic progression, for smaller concentrations from 280 to 560 ppm this reduces to $\Delta F_{2xCO_2} = 3.32 \text{ W/m}^2$. Since forcing and ECS are mostly considered for a doubling of CO₂ from pre-

industrial times with 280 ppm to 560 ppm, here we also relate to these changes - different to [13].

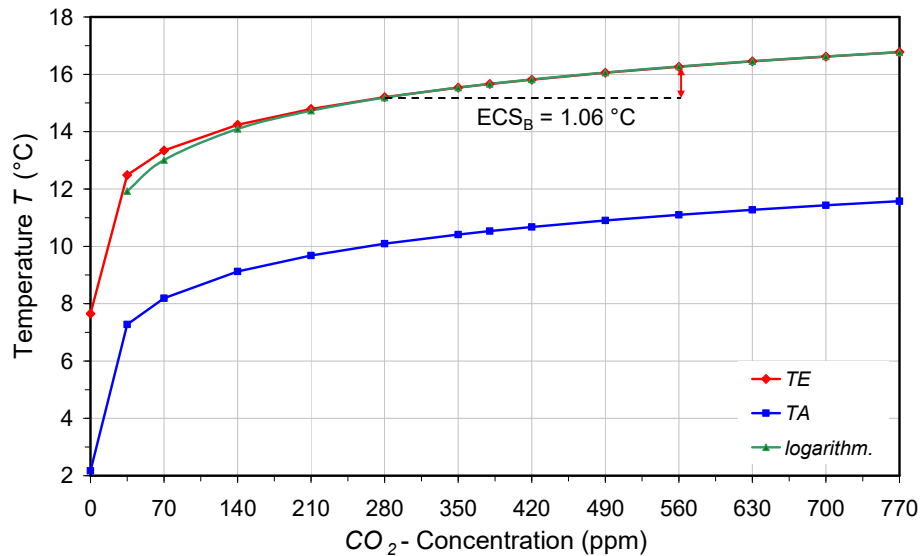


Figure 2: Calculated Earth temperature T_E (Red Diamonds) and atmospheric temperature T_A (Blue Squares) as a function of increasing CO₂ concentration at mean cloud cover without feedbacks. The Earth temperature can well be represented by a logarithmic graph (Green Triangles) with a basic equilibrium climate sensitivity $ECS_B = 1.06^\circ\text{C}$.

For the 2LCM with its key parameters a_{SW} , a_{LW} and f_A we then calculate a basic ECS (without feedbacks) of $ECS_B = 1.06^\circ\text{C}$ (see Fig. 2, Red Diamonds), and with $\lambda_P = ECS_B/\Delta F_{2\times CO_2}$ together with the above forcing a Planck sensitivity $\lambda_P = 0.319^\circ\text{C}/(\text{W}/\text{m}^2)$.

The atmospheric temperature T_A (Blue Squares) reflects the temperature of the lower troposphere in an altitude of about 800 m as a function of the CO₂ concentration (for details see [12], Subsec. 4.4).

We note that the climate sensitivity, which we derive from a radiation and energy balance at the surface and TOA, also includes atmospheric sw absorptivity changes, while the forcing $\Delta F_{2\times CO_2} = 3.32 \text{ W}/\text{m}^2$ only represents the instantaneous lw RF at TOA (without stratospheric adjustment). With AR5 the IPCC introduced the concept of an effective RF, which includes short-time adjustments. However, for a simulation with the 2LCM another RF only changes the Planck sensitivity, not the basic equilibrium climate sensitivity as the relevant quantity for our further investigations.

This basic climate sensitivity with $ECS_B = \lambda_P \cdot \Delta F_{2\times CO_2} = 1.06^\circ\text{C}$ exactly reproduces the value used in the CMIP5 AOGCMs (see AR5-WG1-Tab.9.5), only the forcing of CMIP5 with $\Delta F_{2\times CO_2} = 3.39 \text{ W}/\text{m}^2$ is 2% larger, and thus the Planck sensitivity with $\lambda_P = -1/\alpha_P = 0.313^\circ\text{C}/\text{W}\cdot\text{m}^2$ accordingly smaller. A second approach listed in AR5-WG1-Tab.9.5 uses an RF of $3.71 \text{ W}/\text{m}^2$ with the same Planck sensitivity and therefore calculates with an $ECS_B = 1.16^\circ\text{C}$. The CMIP6 ESMs actually emanate from values for $\lambda_P = 0.311^\circ\text{C}/\text{W}\cdot\text{m}^2$ and for $\Delta F_{2\times CO_2} = 3.93 \text{ W}/\text{m}^2$ with an $ECS_B = 1.22^\circ\text{C}$ (AR6-WG1-Chap.7.4).

3.1.1 Thermal Feedbacks

However, by far the largest inconsistencies between different climate models result from feedback processes. Their combined effect is to amplify the base climate response (Planck response), and they are mainly responsible that the ECS as one of the most important but also most controversially discussed measures in climate science diverges by more than a factor of 20 from about 0.4°C up to more than 8°C .

Certainly one reason of these large discrepancies is the complexity of some effects, from which their interrelated actions and their mutual interference are often not really known. Other reasons are the wrong or undifferentiated assignment of a feedback to a specific climate driver, and also the simple neglect of effects.

Feedback effects are generally included in (1) or (2) as additional terms, which to first order are assumed to respond linearly and independently to the temperature changes ΔT_E . Eq. (2) then extends to:

$$\Delta T_E^{CO_2} = \lambda_P \cdot (\Delta F_{CO_2} + \sum_k f_k \cdot \Delta T_E^{CO_2}), \quad (4a)$$

or after transposition

$$\Delta T_E^{CO_2} = \frac{1}{1 - \lambda_P \cdot \sum f_k} \cdot \lambda_P \cdot \Delta F_{CO_2} = \lambda_P \cdot A_{FT} \cdot \Delta F_{CO_2}, \quad (4b)$$

where the f_k designate different feedbacks (units: W/m²/°C) and $A_{FT} = (1 - \lambda_P \cdot \sum f_k)^{-1} = \alpha_P / (\alpha_P + \sum f_k)$ is the thermal feedback amplification or attenuation factor of the radiative forcing. While in AR6 feedbacks are now abbreviated as α_k , here we further use f_k .

CMIP5 explicitly considers 4 feedbacks (AR5-WG1-Tab.9.5), which are listed in Table 1, column 2 as the mean of 30 AOGCMs. For the sake of clarity, only the values for the lower RF are listed in Table 1. CMIP6 additionally discusses biogeochemical and biogeophysical feedbacks (AR6-WG1-Chap.7.4), but does not closer specify their size. The average of 35 models with an even larger spread than CMIP5, is listed in column 3.

Table 1: Thermal feedbacks for CO₂ radiative forcing

	CMIP5			CMIP6			2LCM		
λ_P (°C/W·m ²)	0.313			0.311			0.319		
ΔF_{2xCO_2} (W/m ²)	3.39			3.93			3.32		
ECS_B (°C)	1.06			1.22			1.06		
feedbacks	f_k W/m ² /°C	A_k	ΔT_k °C	f_k W/m ² /°C	A_k	ΔT_k °C	f_k W/m ² /°C	A_k	ΔT_k °C
water vapor f_{WV}	1.6	2.0	1.06	1.77	2.22	1.5	0.38	1.14	0.14
lapse rate f_{LR}	-0.6	0.84	-0.17	-0.50	0.87	-0.16	-0.6	0.84	-0.17
surf. albedo f_{SA}	0.3	1.10	0.11	0.35	1.12	0.15	0.3	1.11	0.11
clouds therm f_{TC}	0.3	1.10	0.11	0.49	1.18	0.22	0.3	1.11	0.11
convection f_{CO}							-0.02	0.99	-0.01
evaporation f_{EV}							-2.51	0.55	-0.47
total feedbacks by CO ₂	f_{TG} W/m ² /°C	A_{FT}	ECS °C	f_{TG} W/m ² /°C	A_{FT}	ECS °C	f_{TG} W/m ² /°C	A_{FT}	ECS °C
	2.14	3.01	3.2	2.18	3.10	3.78	-1.77	0.64	0.68

Water-Vapor-Feedback: While the lapse-rate, the surface albedo and the thermally induced cloud changes only moderately affect the ground temperature changes, the IPCC assumes as the dominant impact on global warming the water vapor feedback (AR6-WG1-Chap.7.4.2.2). CMIP5 uses a feedback of $f_{WV} = 1.6$ W/m²/°C, yielding an amplification of the basic ECS_B of

$A_{WV} = 2$, CMIP6 even emanates from $f_{WV} = 1.77 \text{ W/m}^2/\text{°C}$ with an amplification of $A_{WV} = 2.22$ (for an assessment of feedbacks, see also AR6-WG1-Tab.7.10 and Fig.7.10).

Our own investigations, however, show a significantly smaller influence of WV. From LBL-RT calculations for three different climate zones and thus different temperatures and humidity we derive a water vapor feedback of $f_{WV} = 0.38 \text{ W/m}^2/\text{°C}$ with an amplification at mean cloud cover of only $A_{WV} = 1.14$ or +14% (for details see, Harde [13], subsection 4.3.1). The reasons for this discrepancy are fourfold:

- (i) So, our calculations also consider the sw absorptivity, which causes negative feedback. Apparently, this contribution is not considered and specified in AR5. Whereas the lw outgoing radiation is more efficiently blocked and thus contributes to positive feedback, the sw radiation is also more strongly absorbed with increasing WV in the atmosphere and less of it reaches the surface, which contributes to slightly negative feedback.
- (ii) Further, the IPCC neglects a declining absorption cross-section of GH-gases with increasing temperature over the troposphere (see Harde [24]).
- (iii) The main differences, however, relate to cloud and saturation effects. In AR5-WG1-Chap.8.3.1 we can read that *"most intercomparison studies of the RF of GH-gases are for clear sky and aerosol-free conditions, while the introduction of clouds would greatly complicate the targets of research and are usually omitted in the intercomparison exercises of GCM radiation codes and LBL codes"*.

Therefore, obviously also for an assessment of the WV feedback cloud effects were neglected. Our studies show that calculations for clear sky give a feedback of $f_{WV} = 1.04 \text{ W/m}^2/\text{°C}$ with an amplification $A_{WV} = 1.54$, which for its own already contributes to a 4x larger temperature increase of 54% compared to mean cloudiness conditions with only 14%. Since at clear sky also the ECS_B with 1.68°C is much larger than at 66% cloud cover with 1.06°C , this would result in an increase due to WV-feedback of $\Delta T_E = 1.54 \times 1.68^\circ\text{C} = 2.59^\circ\text{C}$, while at mean cloudiness this does not contribute more than $\Delta T_E = 1.14 \times 1.06^\circ\text{C} = 1.2^\circ\text{C}$.

- (iv) Finally, most of the AOGCMs emanate from a mean WV concentration of 7,750 ppm, in agreement with the US Standard Atmosphere 1976, representing mid-latitude but not global mean conditions. In our calculations we use a global mean WV concentration (at standard conditions) of 14,615 ppm, which was derived from GPS measurements (Vey [35]) of the water content in different climate zones (see Harde [12], Fig. 1).

Similar to CO₂, also the water lines are already strongly saturating over wider spectral regions. Therefore, with increasing vapor concentration only the far wings of these lines and weak absorption bands can further contribute to an additional absorption, which roughly logarithmically increases with the vapor concentration. Despite an exponential increase of the vapor concentration with rising temperature, due to the Clausius-Clapeyron relation together this only results in a linear increase of the absorptivities. For the lw absorptivity, e.g., this increase with temperature is only one third under global mean conditions compared to US Standard Atmosphere conditions.

Altogether, consideration of the sw and lw effects with temperature, the strong impact of clouds and the larger saturation at higher water vapor level leads to a significantly lower response to temperature changes than assumed in most AOGCMs and ESMs. So, our analysis of the WV feedback only contributes to an increase of the basic climate sensitivity of 14%, while the IPCC follows from a gain of 120%, which is more than 8 times larger.

Lapse-Rate and Surface Albedo Feedback: When the vertical temperature profile changes, also the back-radiation varies with temperature and concentration changes of the GH gases. As a direct consequence also the radiation balance is modified and known as lapse rate feedback.

Both theory and climate models indicate that global warming will reduce the rate of temperature decrease with altitude, producing a negative lapse rate feedback, considered in CMIP5 with $f_{LR} = -0.6 \text{ W/m}^2/\text{°C}$ (AR5-WG1-Tab.9.5), in CMIP6 with $-0.5 \text{ W/m}^2/\text{°C}$ (AR6-WG1-Chap.7.4.2). In our accounting scheme this is expressed as a temperature dependent back-radiated fraction $df_A/dT_E = -0.0875\%/^\circ\text{C}$ with an attenuation of $A_{LR} = 0.84$.

The surface albedo influence is estimated as a positive feedback, in CMIP5 with $f_{SA} = 0.3 \pm 0.1 \text{ W/m}^2/\text{°C}$, in CMIP6 with $f_{SA} = 0.35 \pm 0.1 \text{ W/m}^2/\text{°C}$. In our simulations we introduce this albedo feedback as a temperature dependent change of the Earth's reflectivity with $dr_{SE}/dT_E = -0.158 \text{ } \%/^\circ\text{C}$, which at mean overcast contributes to an increase of the climate sensitivity of 11%.

For the lapse-rate and the surface albedo these are the same feedbacks as specified in AR5-WG1-Tab.9.5.

Cloud-Feedback: *"Clouds respond to climate forcing mechanisms in multiple ways, and differences in cloud feedbacks constitute by far the primary source of spread of both equilibrium and transient climate responses simulated by climate models"* (Dufresne & Bony [36]).

So, quite contradictory observations are reported, where on the one side regional meteorological conditions over the Pacific are described, providing modelling evidence for a positive low level cloud feedback in this region on decadal time scales (Clement et al. [37]), and on the other side, particularly in the tropics, the opposite trend is observed that with increasing temperature and thus rising humidity also the cloud formation is increasing, which then contributes to negative feedback (Lindzen et al. [38]; Laken & Pallé [39]; Cho et al. [40]; Caldwell et al. [41]).

The IPCC exclusively considers a Thermally Induced Cloud (TIC)-feedback f_{TC} and lists in AR6-WG1-Chap.7.4.2.4.3 a best estimate of the net cloud feedback of $f_{TC} = 0.42 \text{ W/m}^2/\text{°C}$ with a *very likely* range of -0.1 to $0.94 \text{ W/m}^2/\text{°C}$, which is less than the value published in AR5 with $f_{TC} = 0.6$ (-0.2 to $+2.0$) $\text{W/m}^2/\text{°C}$ (see AR5-WG1-Chap.7). On the other hand, CMIP5 models were assuming a model mean half of $f_{TC} = 0.3 \pm 0.7 \text{ W/m}^2/\text{°C}$ (AR5-WG1-Tab.9.5), while CMIP6 now uses a value of $f_{TC} = 0.49 \pm 0.6 \text{ W/m}^2/\text{°C}$. This new and higher cloud feedback together with the water vapor feedback and also the higher assumed RF of $\Delta F_{2xCO_2} = 3.93 \text{ W/m}^2$ determine the main difference between CMIP5 and CMIP6. At the same time it flattens the discrepancies between the different specified values.

But even the largest value by far cannot explain the observed cloud cover changes over the 80s and 90s within the ISCCP program. This would require an $f_{TC} \geq 2 \text{ W/m}^2/\text{°C}$ and together with the other feedbacks used in CMIP5/6 then lead to an unrealistically high ECS of more than 15°C . Also, with the smaller WV-feedback as derived from our calculations and assuming a cloud feedback of $2 \text{ W/m}^2/\text{°C}$ would give an ECS of 2.8°C and contribute to 1.7°C to global warming over the last century, much more than observed.

All this is a strong indication that apparently still another mechanism is responsible for cloud changes which are in agreement with the ISCCP observations. This has to be discussed in the next subsection. But to account also for a thermal impact on cloud changes, in our further simulations we include a CO₂ and thus thermally induced feedback as used in CMIP5 with $f_{TC} = 0.3 \text{ W/m}^2/\text{°C}$.

Convection Feedback: Additionally, to these standard feedbacks we see from our calculations that the air temperature is less sensitively responding to CO₂ concentration changes than the Earth temperature (see Fig. 2). Therefore, the temperature difference in the convection zone is further increasing with ascending CO₂ concentration. As a consequence, also the sensible heat flux of about 17 W/m^2 is growing with the concentration, which altogether results in negative feedback. A more detailed consideration shows that this feedback is larger for clear sky and reduces at mean cloud cover to $f_{CO} = -0.02 \text{ W/m}^2/\text{°C}$ with a damping of 1% (differences to [12], subsection 4.4 and 5.4.4, and [13], subsection 4.3.4 result from considering here a doubling of CO₂ from 280 to 560 ppm).

Evaporation Feedback: Similar to convection also evaporation of water and sublimation of ice contribute to cooling of the surface. Since an increasing Earth temperature further forces these processes, they also result in negative feedback, which we call evaporation feedback.

Although in more general terms this is also one part of convection, we further distinguish convection and evaporation feedbacks to assign them to sensible and latent heat contributions. According to Kirchhoff's equation changes in latent heat are directly proportional to temperature changes with a proportionality factor, given by the difference of the specific heats in the two phases.

From this we derive for a latent heat flux of 80 W/m² an evaporation feedback at clear sky of $f_{EV} = -2.0$ W/m²/°C with an attenuation factor $A_{EV} = 0.59$, and at mean cloud cover this results in an even larger negative feedback of $f_{EV} = -2.51$ W/m²/°C, yielding an attenuation factor of $A_{EV} = 0.55$. So, latent heat can contribute to significant negative feedback and work as a strong stabilizer for the climate system. All the more, it is surprising that apparently this feedback is not considered in CMIP5/6 and also not mentioned in AR5 or AR6.

3.1.2 Total Feedback and ECS

CMIP5 specifies a model mean ECS of 3.2°C, however, obviously this is in clear contradiction to the mainstream feedback theory. With a Planck sensitivity of $\lambda_P = 0.313$ °C/W·m² as negative reciprocal of the model mean Planck feedback $\alpha_P = -3.2$ W/m²/°C (see AR5-Tab.9.5) and for a total feedback of 1.6 W/m²/°C (sum of the four feedbacks in column 2, Table 1) the respective amplification should be $A_{FT} = 2$. Thus, from (4b) with an $ECS_B = 1.06$ °C we only expect an $ECS = 2.12$ °C or with the other CMIP5-approach ($ECS_B = 1.16$ °C) an $ECS = 2.32$ °C.

For the CMIP6 ESMs the discrepancy to the mainstream theory is less obvious but still noticeable. With a minimally smaller Planck sensitivity of $\lambda_P = 0.311$ °C/W·m² and a total feedback of 2.11 W/m²/°C now the respective amplification should be $A_{FT} = 2.91$; and with an $ECS_B = 1.22$ °C we deduce an $ECS = 3.55$ °C, while CMIP6 lists a model mean of 3.78°C (AR6-WG1-Table7.SM.5).

Indeed, it is well known that generally different feedback processes do not act linearly and independently of each other, so that for stronger impacts a larger nonlinear response is expected. For reliable calculations, therefore, it is strongly recommended to consider the different effects simultaneously, but in quite small steps for the energy budget and to repeat this procedure till self-consistency of the balance equation system for the radiated power of the surface P_E and of the atmosphere P_A is achieved.

So, when applying this method and inserting the feedbacks as displayed in Table 1, for CMIP5 only a slightly increasing total feedback and amplification with $f_{TG} = 1.63$ W/m²/°C and $A_{FT} = 2.03$ can be found, while for CMIP6 with $f_{TG} = 2.18$ W/m²/°C and $A_{FT} = 3.10$ we derive values, which now exactly reproduce the specified ECS of CMIP6 with 3.78°C.

For the 2LCM with a total negative feedback we observe the opposite behavior. While the direct sum of feedbacks in Table 1, column 4, is -2.16 W/m²/°C with an amplification $A_{FT} = 0.59$, the self-consistency calculation gives $f_{TG} = -1.77$ W/m²/°C and an $A_{FT} = 0.64$ with an $ECS = 0.68$ °C.

So, to attain for CMIP5 an $ECS = 3.2$ °C, a significantly higher total feedback of $f_{TG} = 2.14$ W/m²/°C is required yielding an amplification of $A_{FT} = 3.01$. For our later simulations this is achieved by increasing the respective cloud feedback from $f_{TC} = 0.3$ to 0.74 W/m²/°C.

However, the main discrepancies of CMIP5/6 to our approach result from the much larger WV feedback and neglect of negative evaporation feedback (see Table 1, right). At mean cloud cover we get a very moderate ECS of only 0.68°C. Thus, the CO₂ contribution to global warming is found to be 5.6x smaller than derived from CMIP6.

3. 2 Solar Radiative Forcing

As pure native contribution to global warming we consider here only variations caused by the solar anomaly. In analogy to (2) we can write for the temperature increase due to solar radiative forcing changes ΔF_{Sun} :

$$\Delta T_E^{Sun} = \lambda_{Sun} \cdot \Delta F_{Sun}, \quad (5)$$

with $\lambda_{Sun} = 0.065 \text{ W}^{-1}\text{m}^2 \text{ }^\circ\text{C}$ as the solar sensitivity parameter, which now reflects the temperature response of the 2LCM to the incident solar intensity at mean cloud cover. For $\Delta F_{Sun} = \Delta TSI = 0.1\%$ of the reference intensity $S_R = 1360 \text{ W/m}^2$ this defines the basic equilibrium solar sensitivity with $ESS_B = 0.088^\circ\text{C}$.

3.2.1 Solar Induced Thermal Feedback

The solar induced temperature changes underlie the same thermal feedbacks as the CO₂ radiative forcing and can be included as an additional term in (5) similar to (4a) with:

$$\Delta T_E^{Sun} = \lambda_{Sun} \cdot \Delta F_{Sun} + \lambda_p \cdot \sum_k f_k \cdot \Delta T_E^{Sun}, \quad (6a)$$

which now is proportional to ΔT_E^{Sun} , and after transposing (6a) this gives

$$\Delta T_E^{Sun} = \frac{1}{1 - \lambda_p \cdot \sum_k f_k} \lambda_{Sun} \cdot \Delta F_{Sun} = \lambda_{Sun} \cdot A_{FT} \cdot \Delta F_{Sun}. \quad (6b)$$

But different to (4b) now we have to differentiate on the one hand between the temperature response due to the solar influence described by λ_{Sun} , and on the other hand the response of the feedbacks, which due to their definition relate to the Planck sensitivity λ_p . We call this a Solar Induced Thermal (SIT)-feedback f_{ST} . With a total feedback amplification factor $A_{FT} = ECS/ECS_B = 3.10$ under CMIP6 conditions the solar sensitivity becomes $ESS = A_{FT} \cdot ESS_B = 0.27^\circ\text{C}$, while in our case it reduces to 0.06°C and is almost negligible. But nature is somewhat more complicated and presents us always new challenging puzzles.

3.2.2 Solar Induced Cloud Feedback

Various investigations of the solar anomaly over the last century indicate a much larger response of the global temperature on solar radiation than this can be explained only by thermal feedbacks (see, e.g., Ziskin & Shaviv [17]; Vahrenholt & Lüning [42]; Harde [12,13]; Soon et al. [21]; Connolly et al. [22]). Since observations also show that the cloud cover varies over the solar cycles, there exists strong evidence that the solar activity directly acts back on the cloud formation. Actual publications indicate that with an increasing solar activity and, therefore, an increasing solar magnetic field the cosmic flux, which hits the atmosphere, is reduced and causes direct feedback on the cloud cover C_C (for a comprehensive summary see Svensmark [43]). So, it is expected that the generation rate of aerosols as condensation seeds for the formation of water droplets in the lower atmosphere is directly influenced by the cosmic radiation flux (Svensmark-effect), which therewith also controls the cloud cover.

A reduced cloud formation at an increased solar activity then reinforces the initial TSI induced temperature increase, and it can be included in the 2LCM as a feedback term, which now is controlled by variations of the TSI and initiates reciprocal changes in the cloud cover C_C (see Harde [13], Eq.(21)):

$$C_C(TSI) = \begin{cases} C_{C,\min} + (C_{CR} - C_{C,\min}) \cdot e^{-s_f(TSI - S_R)/S_R} & \text{for } TSI \geq S_R \\ C_{CR} + (C_{CR} - C_{C,\min}) \cdot (1 - e^{s_f(TSI - S_R)/S_R}) & \text{for } TSI < S_R \end{cases}, \quad (7)$$

with S_R as the reference solar constant and s_f as a solar induced cloud cover parameter.

Since even at very high TSI values clouds would not completely disappear, we suppose a rest cloudiness of $C_{C,min} = 20\%$ and an exponential approach to this lower limit. For TSI values smaller than the reference solar constant S_R we use for reasons of uniqueness the same functional relation.

In our simulations we do not differentiate between low- and high-level cloud contributions but use a more general description, how such feedback can be derived and quantified from observations within the ISCCP program. So, the cloud cover variation from 1983 to 2000 of -4% at an observed TSI increase of $\Delta TSI = 0.1\%$ (Willson & Mordvinov [15]) can be reproduced by a cloud cover parameter $s_f = 90$. A smaller supposed increase of only $\Delta TSI = 0.05\%$, as assumed in some other publications (Fröhlich & Lean [44]), raises s_f to ≈ 180 and thus increases the respective Solar Induced Cloud (SIC)-feedback f_{SC} .

With this additional feedback integrated in the 2LCM, analogous to (4a) and (6a), but now with a feedback term which relates to λ_{Sun} , we can write (for the moment still without thermal feedback):

$$\begin{aligned}\Delta T_E^{Sun} &= \lambda_{Sun} \cdot (\Delta TSI + f_{SC} \cdot \Delta T_E^{Sun}) \Rightarrow \\ \Delta T_E^{Sun} &= \frac{1}{1 - \lambda_{Sun} \cdot f_{SC}} \lambda_{Sun} \cdot \Delta TSI = \lambda_{Sun} \cdot A_{SC} \cdot \Delta TSI\end{aligned}\quad (8a)$$

For a cloud cover parameter of $s_f = 90$ the respective SIC -feedback becomes $f_{SC} = 11.0 \text{ W/m}^2/\text{°C}$ and the SIC -amplification factor $A_{SC} = 3.5$. This feedback includes all sw and lw effects, which are responding to cloud cover changes in our model. Under these conditions the basic solar sensitivity of 0.088°C rises to $ESS = 0.31\text{°C}$. For $s_f = 180$ the feedback inclines nonlinear to $f_{SC} = 12.7 \text{ W/m}^2/\text{°C}$, the amplification becomes $A_{SC} = 5.7$ and the solar sensitivity $ESS = 0.51\text{°C}$.

An equivalent formulation for SIC -feedback is to express this as amplification of the TSI changes with a feedback factor $f'_{SC} = \lambda_{Sun} \cdot f_{SC}$ (for $s_f = 90$, e.g.: $f'_{SC} = 0.72$) and the same amplification A_{SC} :

$$\begin{aligned}\Delta F_{Sun} &= \Delta TSI + f'_{SC} \cdot \Delta F_{Sun} \Rightarrow \\ \Delta F_{Sun} &= \frac{1}{1 - f'_{SC}} \Delta TSI = A_{SC} \cdot \Delta TSI\end{aligned}\quad (8b)$$

3.2.3 Combined Solar Induced Thermal and Cloud Feedback

Inserting (8b) into (6b) gives the total temperature change caused by solar radiative forcing, now including SIT -and SIC -feedbacks:

$$\begin{aligned}\Delta T_E^{Sun} &= \frac{1}{1 - \lambda_p \cdot \sum f_k} \lambda_{Sun} \cdot \left(\frac{1}{1 - \lambda_{Sun} \cdot f_{SC}} \Delta TSI \right) \\ &= \lambda_{Sun} \cdot A_{FT} \cdot A_{SC} \cdot \Delta TSI\end{aligned}\quad (9)$$

For a solar variability of $\Delta TSI = 0.1\%$, a SIC -amplification $A_{SC} = 3.5$ and a thermal feedback amplification of $A_{FT} = 0.64$ for the 2LCM (Table 1, right column) we calculate an equilibrium solar sensitivity of $ESS = 0.20\text{°C}$, while with the CMIP6 data this would rise up to 0.96°C , more than the observed temperature increase over the last century.

3. 3 Total Temperature Change

The total temperature change as the sum of (4b) and (9) then gives:

$$\begin{aligned}\Delta T_E &= \frac{\lambda_p}{1 - \lambda_p \cdot \sum f_k} \cdot \left(\Delta F_{CO_2} + \frac{\lambda_{Sun} / \lambda_p}{1 - \lambda_{Sun} \cdot f_{SC}} \Delta TSI \right) \\ &= \lambda_p \cdot A_{FT} \cdot (\Delta F_{CO_2} + \kappa \cdot A_{SC} \cdot \Delta TSI)\end{aligned}\quad (10)$$

with $\kappa = \lambda_{Sun}/\lambda_P$ as ratio of the solar to Planck sensitivity.

Fig. 3 displays the respective block diagram for the CO₂ and solar radiative forcings with their feedbacks and represents the principal scheme, how the Earth's temperature is affected by these external forcings. We note that this is only a first order (linear) approach for the two forcings with their feedbacks to better address the different processes. In any way, the further simulations of the temperature trend as a function of the CO₂ concentration and solar variability over time have to be performed by solving the radiation and energy balance system in smaller steps for all forcings and feedbacks simultaneously, till self-consistency of the radiated power of the surface P_E and of the atmosphere P_A is obtained. This accounts for all kinds of nonlinearities and inter-relations of the different contributions.

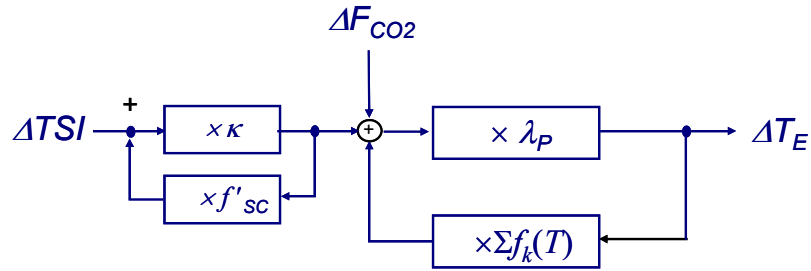


Figure 3: Schematic block diagram of the forcings with their feedbacks.

Table 2 contains a compilation of the climate and solar sensitivities with the respective feedbacks.

Table 2: Equilibrium climate and solar sensitivity for the CMIP5/6 models and the 2LCM.

ECS_B (°C)	CMIP5 1.06			CMIP6 1.22			2LCM 1.06		
CO ₂ feedback	f_{TG} W/m ² /°C	A_{FT}	ECS °C	f_{TG} W/m ² /°C	A_{FT}	ECS °C	f_{TG} W/m ² /°C	A_{FT}	ECS °C
	2.14	3.01	3.2	2.18	3.10	3.78	-1.77	0.64	0.68
ESS_B (°C)	0.088			0.088			0.088		
solar thermal feedback	f_{ST} W/m ² /°C	A_{FT}	ESS °C	f_{ST} W/m ² /°C	A_{FT}	ESS °C	f_{ST} W/m ² /°C	A_{FT}	ESS °C
	2.05	2.80	0.25	2.12	2.93	0.26	-9.5	0.62	0.06
solar cloud feedback	f_{SC} W/m ² /°C	A_{SC}	ESS °C	f_{SC} W/m ² /°C	A_{SC}	ESS °C	f_{SC} W/m ² /°C	A_{SC}	ESS °C
$c_f = 90$	11.2	3.67	0.33	11.0	3.49	0.31	11.0	3.49	0.31
$c_f = 180$	12.9	6.24	0.55	12.7	5.80	0.51	12.7	5.72	0.51
solar-thermal-cloud feedback		A_{FT}^* A_{SC}	ESS °C		A_{FT}^* A_{SC}	ESS °C		A_{FT}^* A_{SC}	ESS °C
$c_f = 90$		10.2	0.90		10.2	0.90		2.16	0.19
$c_f = 180$		17.4	1.53		17.0	1.48		3.54	0.32

They form the basis for the further calculations of the temperature series and show some smaller deviations from the direct accounting scheme. So, the self-consistency calculation for the solar sensitivity with a thermal amplification for the 2LCM of $A_{FT} = 0.62$ (slightly smaller than for pure CO₂ feedback) and a solar cloud amplification of $A_{SC} = 3.5$ gives a small correction with $ESS = 0.19^\circ\text{C}$ compared to Eq. (9) with 0.2°C . The respective calculation for the CMIP6 data gives 0.90°C compared to the directly deduced value of 0.96°C . Larger deviations have to be expected for the total temperature at increasing feedbacks and solar variability.

4. Simulation of Temperature Records

In this section we present simulations for the temperature trend over the last 140 years, based on the one hand on the CMIP5 and CMIP6 data, and on the other hand on our own calculations. For these simulations we use our advanced 2LCM, which allows to consider the simultaneous influence of CO₂ and solar variations on the climate. The calculations rely on six different *TSI*-time-series and can directly be compared with composed land-sea surface temperature measurements of the Northern Hemisphere (Soon et al. [21]).

4.1 Simulation with CMIP5/6 Data

Our simulations and their comparison with observed temperature time series cover the period from 1880 up to now (as far as data are available). For the CO₂ increase before 1958 we use palaeo-climate data assuming a level of 280 ppm in 1850, which is continuously increasing up to 315 ppm in 1957, and since 1958 we consult the Mauna Loa measurements (Tans & Keeling [45]).

4.1.1 CMIP5-Simulation

The CO₂ record used for our calculations is displayed in Fig.4a (Green Squares) and can directly be compared with the calculated temperature series T_C based on the 2LCM (Magenta Diamonds) at a constant $TSI = 1360 \text{ W/m}^2$, but with the CMIP5 data (Table 1). Only a larger *TIC*-feedback of $f_{TC} = 0.74 \text{ W/m}^2/^\circ\text{C}$ was applied to overcome the inconsistency in the specified *ECS* value for the CMIP5 AOGCMs with 3.2°C .

Within the observed interval of CO₂ concentration changes from 280 to 400 ppm (right scale) and with a relatively high feedback amplification of $A_{FT} = 3.01$ the temperature increases almost linearly with the CO₂-concentration. As this simulation only relies on CO₂ radiative forcing, both graphs proceed parallel to each other with a temperature increase over 135 years of 1.47°C . Also displayed is a logarithmic plot according to (3) with the specifications as listed in Table 1 for CMIP5 (Plum Dots). Over this considered period it develops even faster with 1.7°C , while at 560 ppm both graphs are crossing.

Fig. 4b shows the same simulation only as temperature anomaly ΔT_C (15.2°C subtracted) and as moving average over 20 years (Magenta Diamonds). This graph can be compared with a composed data set (Blue Triangles) consisting on the one hand of rural land data of the Northern Hemisphere (Soon & Connolly [21]) with a weighting of 30% and on the other hand the sea surface data of Kennedy et al. [46] with a weighting of 70%. The temperature increase of 1.2°C , which due to the averaging procedure is now 0.27°C smaller, is still too large, and particularly stronger deviations show up from 1920 till 1970.

So, CO₂ forcing can only explain a monotonic increase of the temperature, and it completely fails to trace any variations over the observed period. Also, it cannot reproduce the observed cloud variations over the 80s and 90s, which would require a much larger thermal cloud feedback, then causing a temperature increase of even 8°C over the Industrial Era.

On the other hand, also considering solar forcing with *SIC*-feedback included and reproducing the observed cloud cover changes, this contributes to additional warming. So, for an increasing

TSI of typically 0.1 - 0.3% over the considered period, together with the CO₂ warming this gives a total warming of 1.6 - 3.2°C. Even using only *TSI* time series with a very flat variation of less than 0.03% ($< 0.4 \text{ W/m}^2$ after averaging over the Schwabe cycles, see e.g., Wang et al. [47] and Matthes et al. [48]), this results in a temperature anomaly over the Industrial Era of 1.2 - 1.5°C, which is in clear contradiction to the measured records.

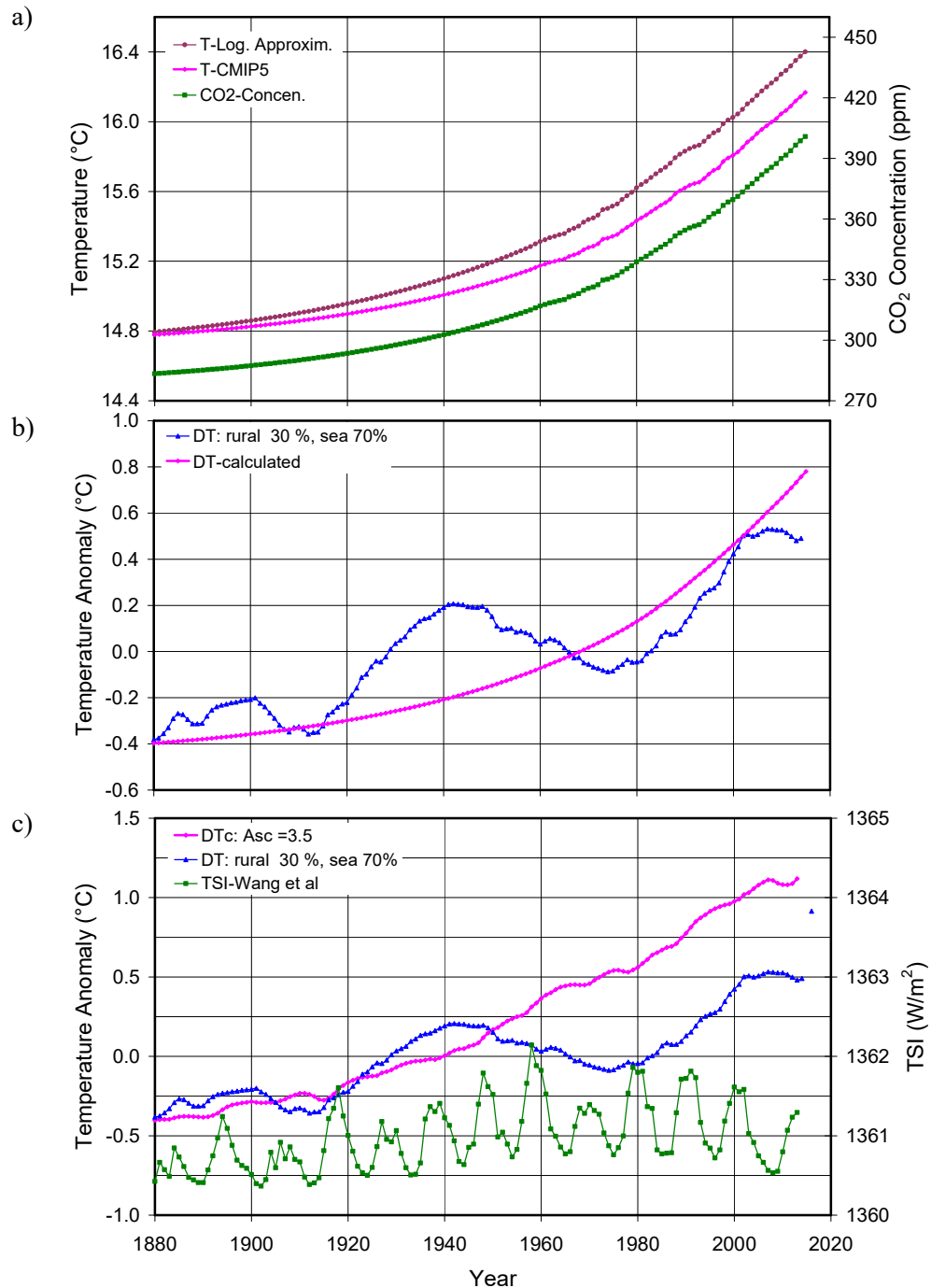


Figure 4: a) Atmospheric CO₂ concentration over time (Green Squares), calculated Earth's temperature with CMIP5 data (Magenta Diamonds) and logarithmic plot (Plum Dots). b) CMIP5 simulation of temperature anomaly (Magenta Diamonds) compared with composed temperature anomaly (30% rural land, 70% Sea Surface Temperature (SST)) (Blue Triangles). c) TSI time series of Wang et al. (Green Squares) with calculated temperature anomaly ΔT_c using CMIP5- and TSI-data (Magenta Diamonds) and comparison with composite rural land-sea temperature times series.

Fig. 4c shows the *TSI* series of Wang et al. [47] (Green Squares), which was recommended for the CMIP5 AOGCMs as solar variation over recent years and which is even characterized by a downward trend since the 1970s. The simulated temperature time series based on this *TSI* series with an $ESS = 0.9^{\circ}\text{C}$ and otherwise the CMIP5 feedbacks with $ECS = 3.2^{\circ}\text{C}$, is displayed as Magenta Diamonds. To compare it with the composed rural land-sea temperature measurements (Blue Triangles), it is plotted as temperature anomaly (in this case 15.5°C subtracted). It reveals an even larger discrepancy with an increase of more than 1.5°C over the Industrial Era than only considering CO₂ forcing (see Fig. 4b).

4.1.2 CMIP6-Simulation

Fig. 5a shows the respective calculation for the CMIP6 data (Table 1), this for a slightly modified 2LCM with an adapted $ECS_B = 1.22^{\circ}\text{C}$, a constant $TSI = 1360 \text{ W/m}^2$ and an $ECS = 3.78^{\circ}\text{C}$ (Magenta Diamonds). Over the displayed concentration range, it proceeds again proportional to the CO₂ record (Green Squares) and also to the logarithmic plot (Plum Dots), only with a slightly different slope. Over the considered period of 135 years the temperature increases by 1.81°C (no averaging).

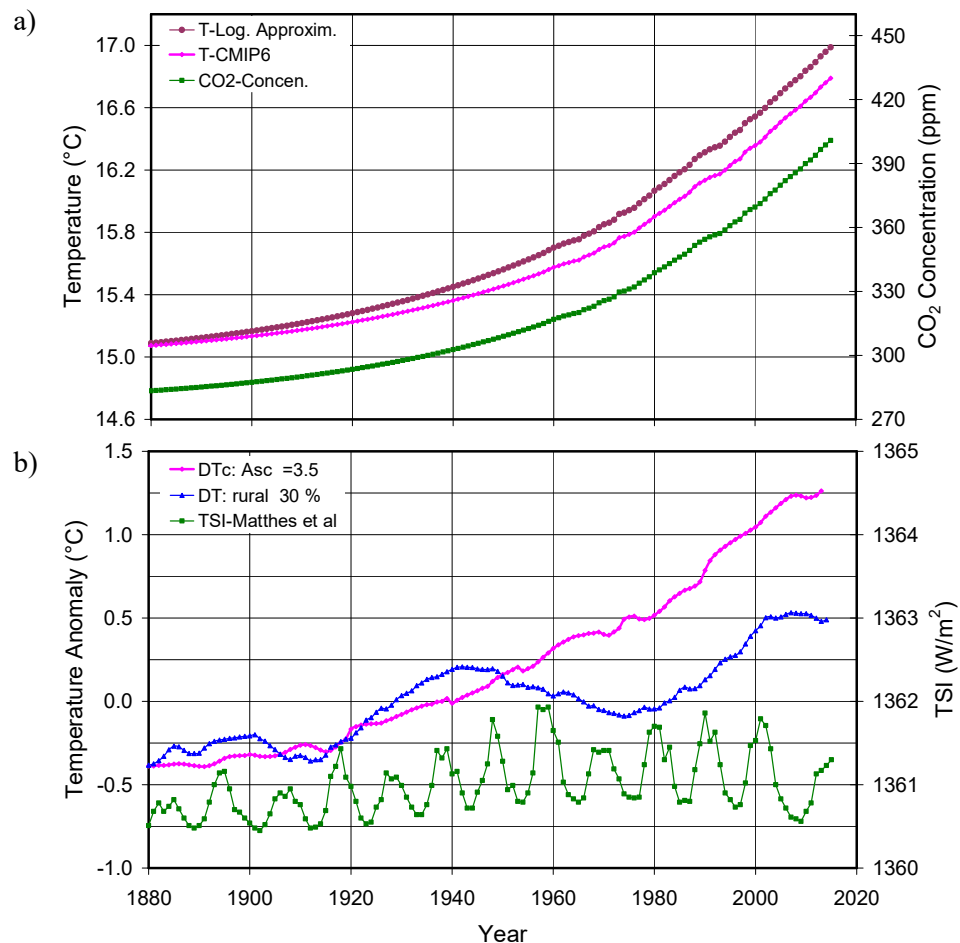


Figure 5: a) Atmospheric CO₂ concentration over time (Green Squares), calculated Earth's temperature T_c with CMIP6 data (Magenta Diamonds) and logarithmic plot (Plum Dots).

b) TSI time series of Matthes et al. (Green Squares) with calculated temperature anomaly ΔT_c using CMIP6- and TSI-data (Magenta Diamonds) compared with composed temperature anomaly (30% rural land, 70% SST) (Blue Triangles).

As solar variation for the CMIP6 ESMs is the *TSI* series of Matthes et al. [48] recommended. Fig. 5b shows this series (Green Squares), which significantly differs from the CMIP5 forcing dataset, mainly due to an official reduction of the average *TSI* during solar minimum from

1365.4 W/m² to 1361.0 W/m² with inevitable implications for understanding the Earth's radiation budget. Besides this significant correction this series is characterized by a very flat progression over time with a variation over the solar cycles (minimum-to-maximum) of 1.5 W/m², but for the solar minima of not more than 0.25 W/m². For the period from 1983 - 2010, which is important for comparison with the ISCCP observations, it even displays a negative trend like the Wang et al. data. The simulated temperature anomaly based on the Matthes et al. data for an $ESS = 0.9^{\circ}\text{C}$ and otherwise the CMIP6 feedbacks is displayed as running average (Magenta Diamonds) and can be compared with the composed rural land-sea temperature measurements (Blue Triangles). With a temperature increase of almost 1.7°C over the Industrial Era it reveals an even larger discrepancy than the CMIP5 simulation. A recent study of Scafetta (2021) [49] comes to a similar conclusion that CMIP6 ESMs are significantly overestimating global warming over the last 40 years.

All this is a strong indication that the observed temperature and cloud changes over the Industrial Era cannot satisfactorily be explained under conditions assumed for the CMIP5 AOGCMs or the CMIP6 ESMs, neither by CO₂ forcing alone nor with additional solar forcing. Although the preceding calculations were performed with our 2LCM, they allow to clearly identify the origin of these deficits. Primarily, we trace them back to the too large total thermal feedbacks used in CMIP5/6 models; and to avoid a still larger dissent to observations, the smallest possible solar influence - and neglecting *SIC*-feedback - is assumed in these models. Instead, IPCC and CMIP5/6 have to consult other effects like negative aerosol feedback to get not too large discrepancies to the observed global warming over the last century.

4. 2 Simulations with Different TSI Time Series Using own Feedback Data

In this subsection we consider simulations, which are only based on our own calculations for the thermal feedbacks and which include solar radiative forcing with *SIC*-feedback. As *TSI* time series we use the records of Matthes et al. [48], Usoskin et al. [50], Muscheler et al. [51], Bard et al. [52, 53] and Hoyt & Schatten [14, 18] to compare the simulations with composed rural land-sea surface temperature time series of different relative weighting.

4.2.1 TSI Time Series of Matthes et al.

The *TSI*-time series of Matthes et al. [48] has already been used for the CMIP6 simulation (Fig. 5b, Green Squares) and is characterized by a very flat progression over time with a variation over the solar cycles (minimum-to-maximum) of 1.5 W/m², but for the solar minima of not more than 0.25 W/m². This series is again plotted as Green Squares in Fig. 6.

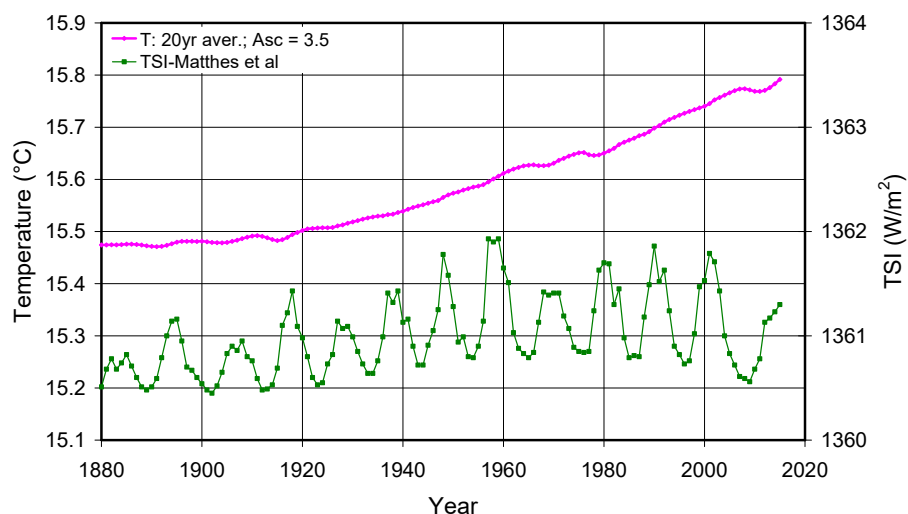


Figure 6: *TSI*-time-series of Matthes et al. [48] (Green Squares) and simulated Earth's temperature with $A_{SC} = 3.5$ (Magenta Diamonds).

Apparently for the solar cycles 21 - 23 Matthes et al. and Wang et al. rely on the so called PMOD approach suggested by Fröhlich and Lean [44], who tried to compose two *TSI* satellite datasets within the Active Cavity Radiometer Irradiance Monitor (ACRIM) program, for which data over a gap of 2 yrs were missing. They modified published contributory *TSI* results with the effect of conforming the ACRIM1/ACRIM2 ratio to Earth Radiation Budget Satellite (ERBS) data during the ACRIM gap and matching composite *TSI* to the lower values predicted by solar-proxy models during the activity maximum of solar cycle 21.

This stands in strong contradiction to the ACRIM composite of Willson & Mordvinov [15], who used results originally published by the science teams of contributory experiments and the NIMBUS7/ERB comparisons to relate ACRIM1 and ACRIM2. From their analysis Willson & Mordvinov derived a positive minimum-to-minimum *TSI* trend of 0.05% per decade. They explain the differences to the PMOD approach as an artifact of uncorrected ERBS degradation.

For our further simulations we essentially rely on a positive trend between 0.025% and 0.05% per decade and explain the observed lower cloud cover of 4% within the ISCCP program by this increase (see Eq. (7)). With a $\Delta TSI = 0.025\%$ per decade this requires a solar cloud parameter of $s_f = 180$ and then causes a further amplification of $A_{SC} = 5.7$ and an $ESS = 0.32^\circ\text{C}$, for $\Delta TSI = 0.05\%$ per decade s_f is 90, $A_{SC} = 3.5$ and $ESS = 0.19^\circ\text{C}$.

The calculated temperature time series based on the Matthes et al. composite is also displayed in Fig. 6 (Magenta Diamonds) and represents a moving average over 20 yr to account for a delayed response of land and oceans to the CO₂ and solar radiative forcings. CO₂ with an increase of almost 120 ppm from 1880 to 2015 and with the thermal feedbacks used for the 2LCM (see Table 1) contributes to a temperature increase of $\Delta T_E^{CO_2} = 0.34^\circ\text{C}$.

The small solar anomaly of just 0.3 W/m² till the mid-century does not donate more than 0.07°C (for $A_{SC} = 3.5$). In such case of a very flat progression, it is close-by to apply also a weaker *TSI* increase over the 80s and 90s for the same cloud change of 4%. Within the observational uncertainties this is a quite realistic scenario. So, with $\Delta TSI = 0.05\%$ over the considered period (2 decades) the cloud parameter rises to $s_f = 180$ and the cloud feedback amplification increases to $A_{SC} = 5.7$ (slightly nonlinear), which then contributes to a solar heating of $\Delta T_E^{Sun} = 0.12^\circ\text{C}$.

Altogether this results in a total calculated warming over the Industrial Era of 0.46°C and only represents about half of the observed warming (see Fig. 4b). Opposite to Subsec. 4.1 now this might be explained by too small thermal feedback, but particularly the very monotonic trend over time, dominated by the CO₂ radiative forcing, is a strong indication that some larger native impact is missing, which may be caused by larger solar variations and/or superimposed internal oscillations like the Atlantic-Multi-Decadal-Oscillation (AMO) or Pacific-Decadal-Oscillation (PDO).

4.2.2 *TSI Time Series of Usoskin et al.*

The time series of Usoskin et al. [50] shows a stronger dip around 1910 before it continuously rises till 1960 by about 2 W/m² and then remains at an almost constant level (Fig. 7a, Green Squares). With a cloud amplification of $A_{SC} = 3.5$ the temperature change over the displayed period amounts 0.53°C (Magenta Diamonds).

Better agreement between measured temperatures and our simulations can be found, when assuming a higher *SIC*-feedback amplification of $A_{SC} = 5.7$. This is again justified due to the flat *TSI* trend over the 80s and 90s. Fig. 7b shows the direct comparison of the calculated anomaly (Magenta Diamonds) with the land-ocean temperature time series (Blue Triangles).

While the stronger decline in the early 20th century and the subsequent increase can acceptably be reproduced, the simulation fails to explain the deeper dip around 1970.

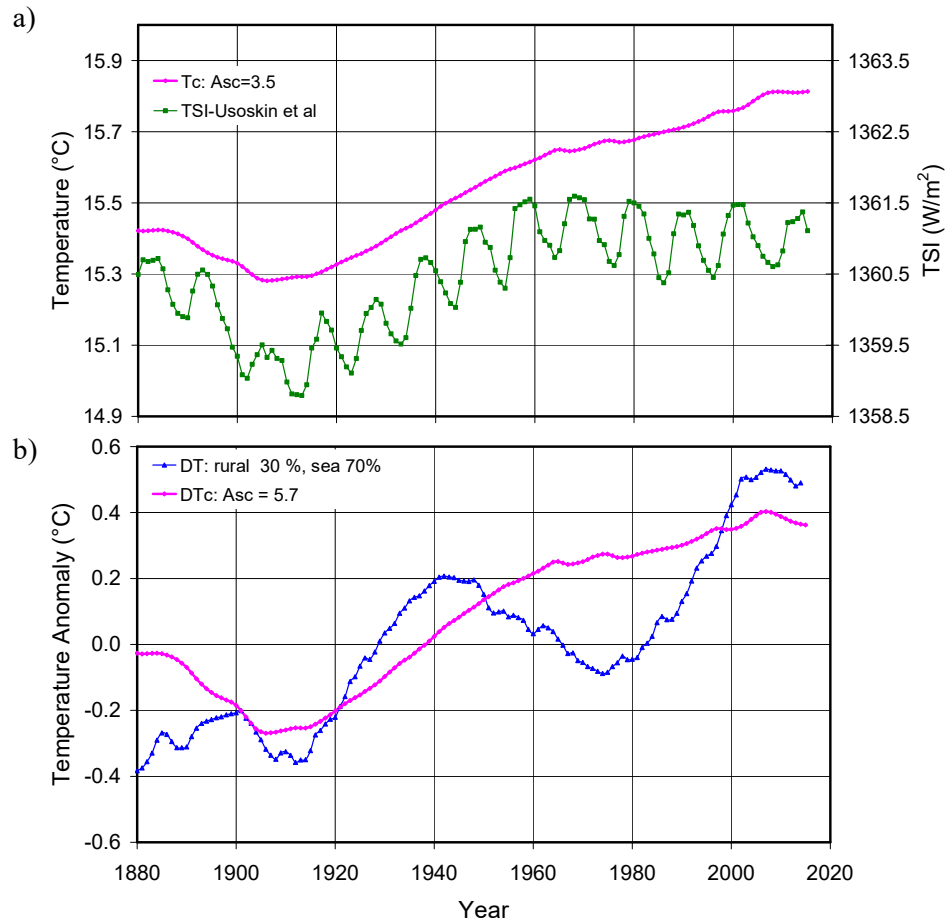


Figure 7: a) TSI-time-series of Usoskin et al. [50] (Green Squares) and simulated temperature T_c with $A_{SC} = 3.5$ (Magenta Diamonds). b) Simulated temperature series anomaly ΔT_c applying TSI data of Usoskin et al. for $A_{SC} = 5.7$ (Magenta Diamonds) compared with composed land-sea temperature anomaly (30% rural, 70% SST) (Blue Triangles).

4.2.3 TSI Time Series of Muscheler et al.

A TSI time series similar to Usoskin et al. has been published by Muscheler et al. [51], which also shows a stronger drop around 1910 and then an almost continuous growth till 2015 altogether of 3 W/m² (Fig. 8).

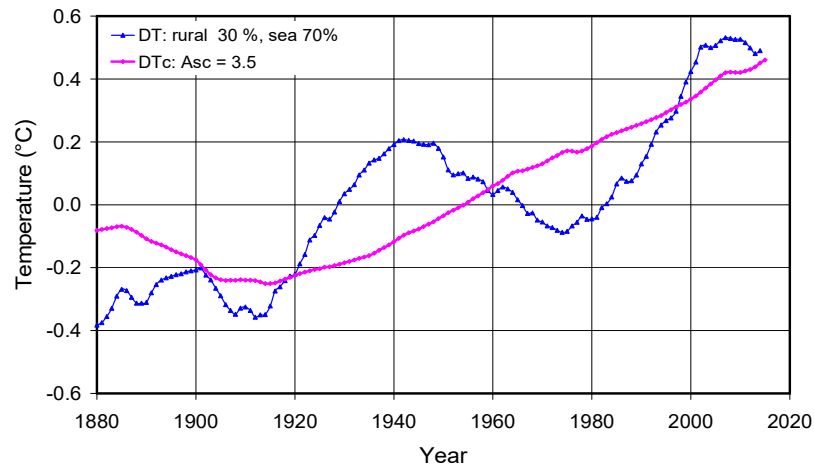


Figure 8: Simulated temperature time series anomaly ΔT_c applying TSI data of Muscheler et al. [51] with $A_{SC} = 3.5$ (Magenta Diamonds) compared with composed land-sea temperature series (30% rural land, 70% SST) (Blue Triangles).

Additionally, Fig. 8 displays the respective simulation with this *TSI* time series assuming a solar cloud feedback of $A_{SC} = 3.5$ (Magenta Diamonds).

This simulation reproduces the general temperature increase over the Industrial Era as combination of the CO₂ radiative forcing with an $ECS = 0.68^\circ\text{C}$ and a solar radiative forcing with $ESS = 0.19^\circ\text{C}$ (*SIC*-amplification: $A_{SC} = 3.5$).

But also with this *TSI* time series the stronger temperature variations between the 50s and 80s cannot be explained.

4.2.4 *TSI* Time Series of Bard et al.

Different to the preceding records the *TSI* time series of Bard et al. [52], updated by Amman et al. [53], shows absolute values, which are about 7 W/m² larger than the others (Fig. 9a, Green Squares). This series was derived from cosmogenic isotope records (¹⁰Be and ¹⁴C) and then adapted to the older recommended *TSI* of 1365.4 W/m². As a consequence, also the calculated global temperatures are rising by about 0.5°C. The variations of 1 W/m² around the mean *TSI* of 1367 W/m² are comparatively small but they confirm quite well the larger decline at the early 20th century, before the intensity is again rising till 1940. For the second half of the century this time series reveals a further wider, pronounced minimum, before the *TSI* rapidly inclines over the 80s and 90s.

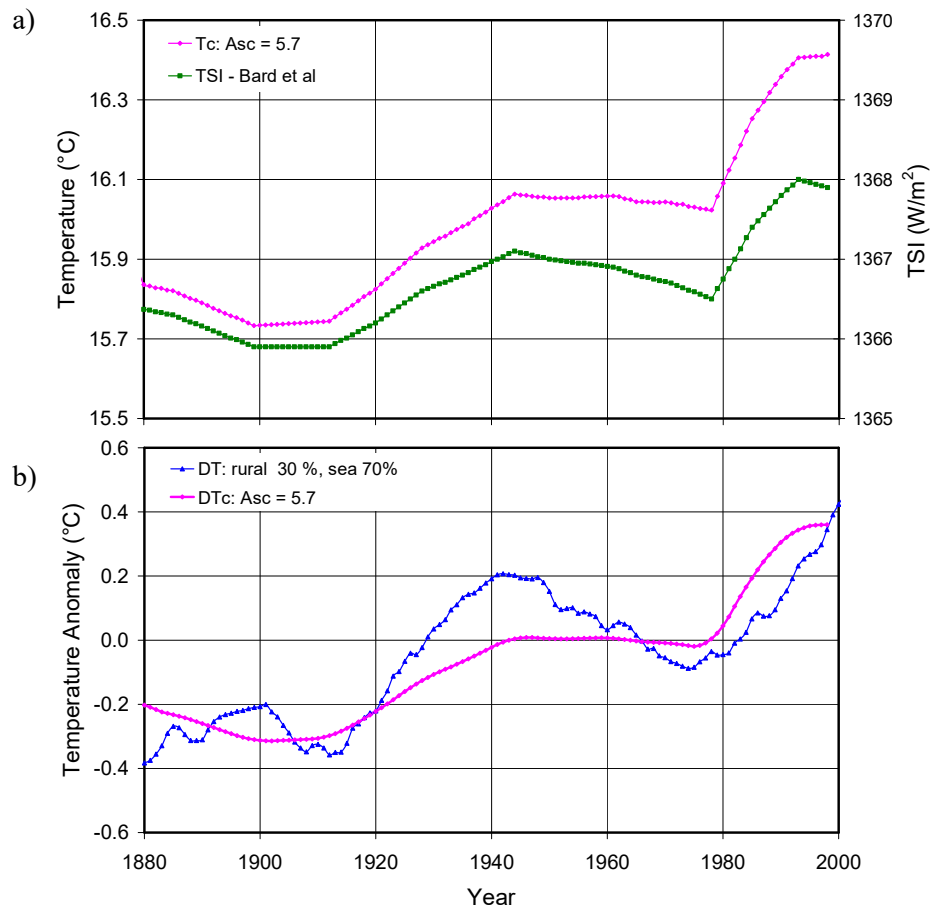


Figure 9: a) *TSI* time series after Bard et al. [52] (Green Squares) and calculated Earth's temperature T_C assuming a *SIC*-amplification of $A_{SC} = 5.7$ (Magenta Diamonds). b) Calculated temperature anomaly ΔT_C (Magenta Diamonds) compared with the composed land ocean temperature time series (30% rural land, 70% SST) (Blue Triangles).

The simulation based on this time series is represented as Magenta Diamonds in Fig. 9a and as temperature anomaly plotted in Fig. 9b, the latter allowing direct comparison with the composed

land-sea temperature series (Blue Triangles). This calculation was performed for a *SIC*-amplification of $A_{SC} = 5.7$ to compensate for the relatively flat trend of the *TSI* series over the full-time scale.

Although this simulation cannot completely reproduce the distinct modulation of the observed data, this is a clear indication that at least part of these variations could have solar origin.

4.2.5 *TSI Time Series of Hoyt & Schatten*

Finally, we consider the *TSI* time series of Hoyt & Schatten [14], updated by Scafetta & Willson [18], which similar to the Bard et al. series also shows a reduced solar activity over the 50s till 80s but much more pronounced with a decline of almost 2 W/m² (Fig. 10a, Green Squares). This strong solar variability has already extensively been discussed by Soon et al. [21] and shown to be the dominant influence on Northern Hemisphere temperature trends since at least 1881.

Our actual simulations with this *TSI* time series integrated in the 2LCM confirm the strong correlation between the solar variations and observed temperature records over the last century. Fig. 10a displays the non-averaged calculated temperature trend (Plum Dots) to compare this directly with the *TSI* series and to demonstrate how the calculation closely tracks the solar variations. Additionally, Fig. 10a reveals the smoothed data as running average over 20 yr (Magenta Diamonds), clearly exposing the phase shift mainly expected due to the delayed response by the oceans.

Fig. 10b shows the simulated temperature anomaly (Magenta Diamonds) and the composed rural land-ocean temperature series with a weighting of 30% rural land and 70% oceans (Blue Triangles). Similar to the calculation with the other *TSI* series also here we find better agreement with observations, when assuming a larger cloud feedback with an amplification of $A_{SC} = 5.7$, respectively an equilibrium solar sensitivity of $ESS = 0.32^{\circ}\text{C}$. Apparently this is an indication of a more sensitive cloud response to *TSI* changes than assuming a solar cloud cover parameter of $s_f = 90$ ($A_{SC} = 3.5$) and $ESS = 0.19^{\circ}\text{C}$.

A larger deviation is only found for the late 19th and early 20th century. The correlation factor for this calculation with the composed temperature data is $r = 0.95$. Assuming a composed temperature series of only 10% land and 90% ocean weighting (Fig. 10c, Blue Triangles) and starting the comparison with the calculation (Magenta Diamonds) at 1908, this correlation is almost perfect ($r = 0.99$), indicating a slightly larger sensitivity of our simulation to the SST-data.

The deviations between 1880 and 1910 can reasonably well be explained by the AMO with its positive phase during this interval and with a dominant oscillation period of 50 to 70 years. This oscillation also shapes the further temperature development over the 20th and beginning 21st century and apparently develops synchronously with the solar variations. So, part of the distinctive temperature modulation may also be assigned to this or additional superimposed native forcings. But also without these impacts solar radiative forcing and its amplification by induced cloud changes can already well explain the observed temperature changes. In any way can the AMO like other observed beats in a more general way be traced back to solar wind and planetary gravitation interactions, reflecting harmonic and sub-harmonic beats of the solar cycles (for a detailed discussion, see Mörner et al., 2020 [54], Subsec. 8.1; for the 60-yrs beats and their origin see also: Scafetta, 2010 [55], 2013 [56]; Solheim 2013 [57]). Therefore, in a wider sense may also these additional forcings be understood as solar and gravitation-controlled drivers, whose strength and periodicity to some part is also mirrored in the *TSI*-variations.

While the CO₂ increase over the Industrial Era alone can only explain a temperature growth of 0.34°C of the total observed incline of about 0.9°C, solar radiative forcing in this case contributes about 60% to global warming. For a CO₂ increase of 82 ppm over the last century the respective contribution is not more than 0.24°C or 30% of the calculated increase of 0.84°C over this period.

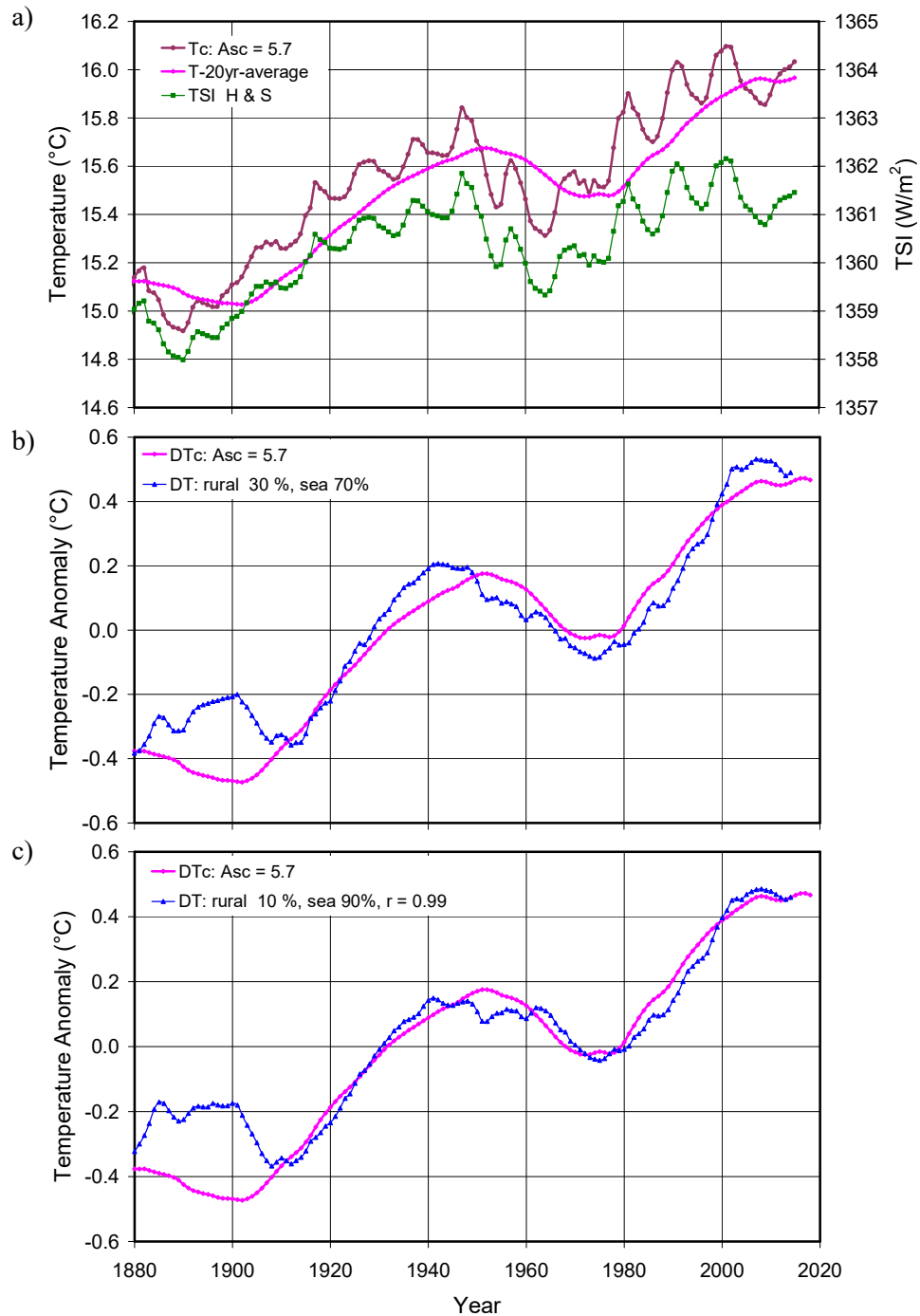


Figure 10: a) TSI time series after Hoyt & Schatten [14] (Green Squares) and calculated temperature trend T_C assuming a SIC-amplification of $A_{SC} = 5.7$ without averaging (Plum Dots) and with 20 yrs running average (Magenta Diamonds. b) and c) Calculated temperature anomaly ΔT_C (Magenta Diamonds) compared with composed land-sea temperature series b) for 30% rural, 70% SST and c) for 10% rural and 90% SST (Blue Triangles).

5. Conclusion

We have performed detailed studies of CO₂ and solar radiative forcing with their mutual influence on global warming. While the IPCC assumes that most of the temperature trends since the 1950s are due to changes in atmospheric greenhouse gas concentrations (AR5-WG1-SPM-D3

[1] and AR6-WG1-SPM [2]), our own calculations indicate that the temperature increase and its variations over the last 140 years can best be explained by combined CO₂ and solar radiative forcing.

For these investigations we have used an advanced energy-radiation-balance model (Harde [12, 13]), which allows to simulate the global temperature trend under the simultaneous impact of increasing CO₂ concentrations and solar variability. These simulations can directly be compared with observed temperature time series, for which - due to the different response of continents and oceans - we refer to the combined land-ocean-temperature composite of the Northern Hemisphere as derived by Soon & Connolly [21].

Our studies cover simulations under quite contrasting conditions, on the one hand based on the model means of the CMIP5 AOGCMs and CMIP6 ESMs characterized by Equilibrium Climate Sensitivities of $ECS = 3.2^{\circ}\text{C}$ (AR5-WG1-Tab.9.5 [1]) and $ECS = 3.78^{\circ}\text{C}$ (AR6-WG1-Table 7.SM.5 [2]), on the other hand based on our own calculations of CO₂ radiative forcing with an $ECS = 0.68^{\circ}\text{C}$ (Harde [13]). For the solar radiative forcing we considered six different *TSI* time series with significantly different trends (Wang et al. [47]; Matthes et al. [48], Usoskin et al. [50], Muscheler et al. [51], Bard et al. [52, 53] and Hoyt & Schatten [14, 18]), which with respect to their impact on global warming are subject of a further amplification by thermally induced feedbacks as well as solar induced cloud feedback (Harde [12, 13]). Together these amplifications are denoted by the Equilibrium Solar Sensitivity *ESS* (temperature change at $\Delta TSI = 0.1\%$) with values varying between 0.19°C and 0.9°C depending on the prevailing feedbacks. The amplification due to cloud changes was derived from observations within the International Satellite Cloud Climatology Project [32] over the 80s and 90s.

From these simulations we see that under CMIP5/6 conditions with large thermal feedback but very flat solar variability (Wang et al. [47] and Matthes et al. [48]) the calculated temperature increase over the Industrial Era is distinctly larger than found from observations. Even CO₂ forcing alone would contribute to a too large warming. Apparently, some inconsistencies between observations and calculations result from the temperature and *TSI* records themselves, which on their part reveal significant differences between each other. Also, the *ECS* and *ESS* values applied in our simulations contain larger uncertainties. But it is also clear that the observed dominant temperature variations over the last century with a broader dip over the 50s to 80s cannot be traced back only to CO₂, which was only monotonically increasing over the considered period and mistakenly is assumed to be only of anthropogenic origin, while a much larger fraction of native origin (about 85%) is obviously embezzled (see Harde [10,11]; Harde & Salby [58]; Salby & Harde [59,60]).

On the other hand, calculations relying on our own CO₂ radiative forcing data with significantly smaller thermal feedback but larger solar variability show excellent agreement with the land-ocean-temperature composite. So a simulation with an $ECS = 0.68^{\circ}\text{C}$, an $ESS = 0.32^{\circ}\text{C}$ and based on the *TSI* time series of Hoyt & Schatten [14] reproduces the stronger temperature drop over the 50s till 80s and also the total warming of $\sim 0.9^{\circ}\text{C}$ over the considered time interval with a correlation factor of $r = 0.95$.

Our findings confirm the actual studies of Connolly et al. [22] and Stefani [61], who are using a multiple regression analysis to quantify the relative contribution of CO₂ and solar generated global warming. Connolly et al. demonstrate that even up to 98% of global warming over the last 170 years may be explained by solar radiative forcing, depending on the underlying *TSI*-series and temperature time series. Based on a double regression analysis of the temperature data with the geomagnetic aa-index and the logarithm of the CO₂ concentration Stefani derives a correlation around 87% and a transient climate response *TCR* between 0.6°C and 1.6°C for doubling CO₂, which also points to a significant influence of solar variability on the climate.

In this context we emphasize that different to a regression analysis in our studies we independently deduce the absolute CO₂ radiative forcing and solar radiative forcing - the latter only dependent on the assumed *TSI* satellite datasets within the ACRIM-program over the 80s and

90s - which we compare with the composed land-sea surface temperature measurements.

Consideration of additional forcings like AMO or other native oscillations may even improve this agreement (see Fig. 10b and 10c), but as long as their size and origin cannot better be identified, is solar radiative forcing and its amplification by induced cloud changes the most plausible explanation for the observed temperature changes, all the more as also the other forcings are more or less controlled by the solar wind and superposed planetary gravitational impacts (Mörner et al. [54]).

From the preceding calculations we derive a CO₂ affected portion to global warming over the Industrial Era of not more than 0.34°C and over the last century of only 0.24°C, which is 30% of the total warming, while apparently two thirds are caused by the solar impact. As human CO₂ emissions should not have contributed more than 15% to the increase over the Industrial Era, the anthropogenic fraction to global warming is expected to be only 0.05°C.

Funding

This research did not receive any specific grant from funding agencies in the public, commercial, or not-for-profit sectors.

Guest-Editor: Prof. Jan-Erik Solheim; Reviewers were anonymous.

Acknowledgements

The author thanks Dr. Willie Soon and Dr. Ronan Connolly, both Center for Environmental Research and Earth Science, Salem, MA, USA, and Dr. Michael Connolly, independent scientist, Dublin, for encouraging this study and for many stimulating discussions.

Special thanks go also to the guest editor Prof. Jan-Erik Solheim and editor Geir Hasnes for additional suggestions and support of this publication.

References

1. Fifth Assessment Report (AR5), IPCC, 2013: T. F. Stocker, D. Qin, G.-K. Plattner et al., Eds., *Climate Change 2013: The Physical Science Basis*, Cambridge University Press, New York, NY, USA, 2014.
2. Sixth Assessment Report (AR6), IPCC, 2021: V. Masson-Delmotte, P. Zhai, A. Pirani et al.: *Climate Change 2021: The Physical Science Basis. Contribution of Working Group I to the Sixth Assessment Report of the Intergovernmental Panel on Climate Change*, Cambridge University Press. In Press.
3. J. R. Petit, J. Jouzel, D. Raynaud et al., 1999: *Climate and atmospheric history of the past 420,000 years from the Vostok ice core*, Antarctica, *Nature*, vol. 399, no. 6735, pp. 429–436.
4. E. Monnin, A. Indermöhle, A. Dällenbach et al., 2001: *Atmospheric CO₂ concentrations over the last glacial termination*, *Science*, vol. 291, no. 5501, pp. 112–114.
5. N. Caillon, J. P. Severinghaus, J. Jouzel, J.-M. Barnola, J. Kang, and V. Y. Lipenkov, 2003: *Timing of atmospheric CO₂ and antarctic temperature changes across termination III*, *Science*, vol. 299, no. 5613, pp. 1728–1731.
6. M. S. Torn and J. Harte, 2006: *Missing feedbacks, asymmetric uncertainties, and the underestimation of future warming*, *Geophysical Research Letters*, vol. 33, no. 10, Article ID L10703.

7. O. Humlum, K. Stordahl, and J.-E. Solheim, 2013: *The phase relation between atmospheric carbon dioxide and global temperature*, Global and Planetary Change, vol. 100, pp. 51–69.
8. M. L. Salby, 2013: *Relationship between Greenhouse Gases and Global Temperature*, video presentation, April 2013, Hamburg, Germany, <https://www.youtube.com/watch?v=2ROwcDKwc0>.
9. D. Koutsoyiannis, Z. W. Kundzewicz, 2020: *Atmospheric Temperature and CO₂: Hen-Or-Egg Causality?*, Sci 2020, 2, 72; <https://doi.org/10.3390/sci2040083>
10. H. Harde, 2017: *Scrutinizing the carbon cycle and CO₂ residence time in the atmosphere*, Global and Planetary Change 152, pp. 19–26, <http://dx.doi.org/10.1016/j.gloplacha.2017.02.009>.
11. H. Harde, 2019: *What Humans Contribute to Atmospheric CO₂: Comparison of Carbon Cycle Models with Observations*. Earth Sciences, Vol. 8, No. 3, pp. 139–158, <https://doi.org/10.11648/j.earth.20190803.13>.
12. H. Harde, 2014: *Advanced two-layer climate model for the assessment of global warming by CO₂*, Open Journal of Atmospheric and Climate Change, vol. 1, no. 3, pp. 1–50, <http://citeseerx.ist.psu.edu/viewdoc/download?doi=10.1.1.909.4771&rep=rep1&type=pdf>.
13. H. Harde, 2017: *Radiation Transfer Calculations and Assessment of Global Warming by CO₂*, International Journal of Atmospheric Sciences, Volume 2017, Article ID 9251034, pp. 1–30, <https://www.hindawi.com/journals/ijas/2017/9251034/>, <https://doi.org/10.1155/2017/9251034>.
14. D. V. Hoyt, K. H. Schatten, 1993: *A discussion of plausible solar irradiance variations, 1700–1992*, Journal of Geophysical Research: Space Physics 98 18895–906.
15. R. C. Willson and A. V. Mordvinov, 2003: *Secular total solar irradiance trend during solar cycles 21–23*, Geophysical Research Letters, vol. 30, no. 5, pp. 1–4.
16. A. Shapiro, W. Schmutz, E. Rozanov, M. Schoell, M. Haberreiter, and S. Nyeki, 2011: *A new approach to long-term reconstruction of the solar irradiance leads to large historical solar forcing*, Astronomy & Astrophysics, vol. 529, article 67.
17. S. Ziskin and N. J. Shaviv, 2012: *Quantifying the role of solar radiative forcing over the 20th century*, Advances in Space Research, vol. 50, no. 6, pp. 762–776.
18. N. Scafetta and R. C. Willson, 2014: *ACRIM total solar irradiance satellite composite validation versus TSI proxy models*, Astrophysics and Space Science, vol. 350, no. 2, pp. 421–442, <http://dx.doi.org/10.1007/s10509-013-1775-9>.
19. I. G. Usoskin, G. Hulot, Y. Gallet et al., 2014: *Evidence for distinct modes of solar activity*, Astronomy & Astrophysics, vol. 562, article L10.
20. X. Zhao and X. Feng, 2014: *Periodicities of solar activity and the surface temperature variation of the Earth and their correlations*, Chinese Science Bulletin, vol. 59, no. 14, pp. 1284–1292.
21. W. Soon, R. Connolly, and M. Connolly, 2015: *Re-evaluating the role of solar variability on Northern Hemisphere temperature trends since the 19th century*, Earth-Science Reviews, vol. 150, pp. 409–452.
22. R. Connolly, W. Soon, M. Connolly, S. Baliunas, J. Berglund, C. J. Butler, R. G. Cionco, A. G. Elias, V. M. Fedorov, H. Harde, G. W. Henry, D. V. Hoyt, O. Humlum, D. R. Legates, S. Lüning, N. Scafetta, J.-E. Solheim, L. Szarka, H. van Loon, V. M. V. Herrera, R. C. Willson, H. Yan and W. Zhang, 2021: *How much has the Sun influenced Northern Hemisphere temperature trends? An ongoing debate*, Research in Astronomy and Astrophysics 2021 Vol. 21 No. 6, 131(68pp), <http://www.raa-journal.org/raa/index.php/raa/article/view/4906>.

23. H. Harde, 2011: *Was trägt CO₂ wirklich zur Globalen Erwärmung bei?: Spektroskopische Untersuchungen und Modellrechnungen zum Einfluss von H₂O, CO₂, CH₄ und O₃ auf unser Klima*, Books on Demand, Norderstedt, Germany.
24. H. Harde, 2013: *Radiation and heat transfer in the atmosphere: a comprehensive approach on a molecular basis*, International Journal of Atmospheric Sciences, vol. 2013, Article ID 503727, 26 pages, <http://dx.doi.org/10.1155/2013/503727>.
25. L. S. Rothman, I. E. Gordon, A. Barbe et al., 2008: *The HITRAN 2008 molecular spectroscopic database*, Journal Of Quantitative Spectroscopy and Radiative Transfer, vol. 110, no. 9-10, pp. 533–572, 2008,
New Version (2016): High-Resolution Transmission Molecular Absorption data base, Harvard-Smithsonian Center for Astrophysics: <https://www.cfa.harvard.edu/hitran/>.
26. K. E. Trenberth, J. T. Fasullo, and J. Kiehl, 2009: *Earth's global energy budget*, Bulletin of the American Meteorological Society, vol. 90, no. 3, pp. 311–323.
27. B. Barkstrom, E. Harrison, G. Smith et al., 1985: *Earth Radiation Budget Experiment (ERBE) archival and April 1985 results*, Bulletin of the American Meteorological Society, vol. 70, pp. 1254–1262.
28. T. D. Bess and G. L. Smith, 1993: *Earth radiation budget: results of outgoing longwave radiation from Nimbus-7, NOAA-9 and ERBS satellites*, Journal of Applied Meteorology, vol. 32, no. 5, pp. 813–824.
29. B. A. Wielicki, B. R. Barkstrom, E. F. Harrison, R. B. Lee III, G. L. Smith, and J. E. Cooper, 1996: *Clouds and the Earth's radiant energy system (CERES): an earth observing system experiment*, Bulletin of the American Meteorological Society, vol. 77, no. 5, pp. 853–868.
30. B. A. Wielicki, B. R. Barkstrom, E. F. Harrison et al., 2006: *CERES radiation budget accuracy overview*, in Proceedings of the 12th Conference on Atmospheric Radiation, vol. 9.1, American Meteorological Society, Madison, Wis, USA.
31. T. Wong, B. A. Wielicki, R. B. Lee III, G. L. Smith, K. A. Bush, and J. K. Willis, 2006: *Reexamination of the observed decadal variability of the earth radiation budget using altitude-corrected ERBE/ERBS nonscanner WFOV data*, Journal of Climate, vol. 19, no. 16, pp. 4028–4048.
32. International Satellite Cloud Climatology Project (ISCCP),
<http://isccp.giss.nasa.gov/products/onlineData.html>.
33. O. Humlum, <http://www.climate4you.com/index.htm>.
34. G. Myhre, E. J. Highwood, K. P. Shine, and F. Stordal, 1998: *New estimates of radiative forcing due to well mixed greenhouse gases*, Geophysical Research Letters, vol. 25, no. 14, pp. 2715–2718.
35. S. Vey, 2007: *Bestimmung und Analyse des atmosphärischen Wasserdampfgehaltes aus globalen GPS-Beobachtungen einer Dekade mit besonderem Blick auf die Antarktis* [Ph.D. thesis], Technical University Dresden.
36. J.-L. Dufresne and S. Bony, 2008: *An assessment of the primary sources of spread of global warming estimates from coupled atmosphere-ocean models*, Journal of Climate, vol. 21, no. 19, pp. 5135–5144.
37. A. C. Clement, R. Burgman, and J. R. Norris, 2009: *Observational and model evidence for positive low-level cloud feedback*, Science, vol. 325, no. 5939, pp. 460–464.
38. R. S. Lindzen, M.-D. Chou, and A. Y. Hou, 2001: *Does the earth have an adaptive infrared iris?*, Bulletin of the American Meteorological Society, vol. 82, no. 3, pp. 417–432.

39. B. A. Laken and E. Pallé, 2012: *Understanding sudden changes in cloud amount: the Southern Annular Mode and South American weather fluctuations*, Journal of Geophysical Research Atmospheres, vol. 117, no. 13, pp. 1984–2012.
40. H. Cho, C.-H. Ho, and Y.-S. Choi, 2012: *The observed variation in cloud-induced longwave radiation in response to sea surface temperature over the Pacific warm pool from MTSAT-IR imagery*, Geophysical Research Letters, vol. 39, no. 18, Article ID L18802.
41. P. M. Caldwell, Y. Zhang, and S. A. Klein, 2013: *CMIP3 subtropical stratocumulus cloud feedback interpreted through a mixed layer model*, Journal of Climate, vol. 26, no. 5, pp. 1607–1625.
42. F. Vahrenholt, S. Lüning, 2012: *Die Kalte Sonne*, Hoffmann und Campe, Hamburg, Germany.
43. H. Svensmark, 2019: *FORCE MAJEURE - The Sun's Role in Climate Change*, The Global Warming Policy Foundation, ISBN 978-0-9931190-9-5.
44. C. Fröhlich and J. Lean, 1998: *The Sun's total irradiance: cycles and trends in the past two decades and associated climate change uncertainties*, Geophys. Res. Lett., 25, 4377–4380.
45. P. Tans, NOAA/ESRL and R. Keeling, Scripps Institution of Oceanography (scrippsco2.ucsd.edu), 2017, <https://www.esrl.noaa.gov/gmd/ccgg/trends/data.html>.
46. J. J. Kennedy, N. A. Rayner, C. P. Atkinson and R. E. Killick, 2019: *An Ensemble Data Set of Sea Surface Temperature Change From 1850: The Met Office Hadley Centre HadSST.4.0.0.0 Data Set*, Journal of Geophysical Research: Atmospheres 124, pp. 7719–63.
47. Y.-M. Wang, J. L. Lean, N. R. Sheeley Jr., 2005: *Modelling the Sun's magnetic field and irradiance since 1713*, Astrophys. J. 625, 522–538, <http://dx.doi.org/10.1085/429689>.
48. K. Matthes, B. Funke, M. E. Andersson et al., 2017: *Solar forcing for CMIP6*, Geosci. Model Dev., 10, 2247, <https://www.geosci-model-dev.net/10/2247/2017/gmd-10-2247-2017.pdf>.
49. N. Scafetta, 2021: *Testing the CMIP6 GCM Simulations versus Surface Temperature Records from 1980–1990 to 2011–2021: High ECS Is Not Supported*, Climate 9, p. 161, <https://doi.org/10.3390/cli9110161>
50. I. G. Usoskin, Y. Gallet, F. Lopes, G. A. Kovaltsov & G. Hulot, 2016: *Solar activity during the Holocene: the Hallstatt cycle and its consequence for grand minima and maxima*, Astronomy & Astrophysics, V 587, A150, 10 pp, <https://ui.adsabs.harvard.edu/abs/2016A%26A...587A.150U/abstract>
51. R. Muscheler, F. Adolphi, K. Herbst & A. Nilsson, 2016: *The Revised Sunspot Record in Comparison to Cosmogenic Radionuclide-Based Solar Activity Reconstructions*, Sol. Phys., 291, 3025, <https://ui.adsabs.harvard.edu/abs/2016SoPh..291.3025M/abstract>
52. E. Bard, G. Raisbeck, F. Yiou, J. Jouzel, 2000: *Solar irradiance during the last 1200 years based on cosmogenic nuclides*, Tellus 52B, 985–992, <http://dx.doi.org/10.3402/tellusb.v52i3.17080>.
53. C. M. Ammann, F. Joos, D. S. Schimel, B. L. Otto-Bliesner, R. A. Tomas, 2007: *Solar influence on climate during the past millennium: results from transient simulations with the NCAR Climate System Model*, Proc. Natl. Acad. Sci. 104, 3713–3718, <http://dx.doi.org/10.1073/pnas.0605064103>.
54. N.-A. Mörner, J.-E. Solheim, O. Humlum, S. Falk-Petersen, 2020: *Changes in Barents Sea Ice Edge Positions in the Last 440 Years: A Review of Possible Driving Forces*, Intern. Journal of Astronomy and Astrophysics, 2020, 10, 97-164, <https://www.scirp.org/journal/ijaa>.

55. N. Scafetta, 2010: *Empirical Evidence for a Celestial Origin of the Climate Oscillations and its Implications*, Journal of Atmospheric and Solar-Terrestrial Physics , 72, pp. 951-970, <https://doi.org/10.1016/j.jastp.2010.04.015>.
56. N. Scafetta, 2013: *Solar and Planetary Oscillation Control on Climate Change: Hind-Cast, Forecast and a Comparison with CMIP5 GCMS*, Energy & Environment, 24, pp. 455-496, <https://doi.org/10.1260/0958-305X.24.3-4.455>.
57. J.-E. Solheim, 2013: *Signals from the Planets, via the Sun to the Earth*, Pattern Recognition in Physics , 1, pp. 177-184, <https://doi.org/10.5194/prp-1-177-2013>.
58. H. Harde, M. L. Salby, 2021: *What Controls the Atmospheric CO₂ Level?*, Science of Climate Change and Philosophy Vol. 1, No.1, pp. 54 - 69, <https://doi.org/10.53234/scc202106/22>.
59. M. L. Salby, H. Harde, 2021: *Control of Atmospheric CO₂ - Part I: Relation of Carbon 14 to Removal of CO₂*, Science of Climate Change and Philosophy Vol. 1, No.2, pp. 177-195, <https://doi.org/10.53234/scc202112/30>.
60. M. L. Salby, H. Harde, 2021: *Control of Atmospheric CO₂ - Part II: Influence of Tropical Warming*, Science of Climate Change and Philosophy Vol. 1, No.2, pp. 196-212, <https://doi.org/10.53234/scc202112/12>.
61. F. Stefani, 2021: *Multiple regression analysis of anthropogenic and heliogenic climate drivers, and some cautious forecasts*, Climate 9(11), p. 163, <https://doi.org/10.3390/cli9110163>.

Annex: Acronyms

Abbreviation	meaning
2LCM	Two-Layer Climate Model
ACRIM	Active Cavity Radiometer Irradiance Monitor
A_{FT}, A_{SC}	thermal feedback amplification, solar induced cloud amplification
AGW	Anthropogenic Global Warming
AMO, PDO	Atlantic-Multi-Decadal-Oscillation, Pacific-Decadal-Oscillation
a_{LW}	long wave absorptivity (of CO ₂ , WV, CH ₄ and O ₃)
a_{SW}	short wave absorptivity (of CO ₂ , WV, CH ₄ and O ₃)
AR5	Fifth Assessment Report of the IPCC (2013)
AR6	Sixth Assessment Report of the IPCC (2021)
AOGCMs	atmosphere-ocean general circulation models
C, C_R	CO ₂ concentration, reference concentration 350 ppm
C_C, C_{CR}	cloud cover, reference cloud cover 66%
CERES	Clouds and the Earth's Radiant Energy System
CMIP5, CMIP6	Coupled Model Intercomparison Project Phase 5, Phase 6
$\Delta F_{CO_2}, \Delta F_{Sun}$	CO ₂ and solar radiative forcing
ΔT_C	calculated temperature anomaly
ΔT_{SI}	total solar irradiance variability
EASy	Earth-Atmosphere-System
ECS	equilibrium climate sensitivity

EMICs	Earth System Models of Intermediate Complexity
ERBE	Earth Radiation Budget Experiment
ERBS	Earth Radiation Budget Satellite
ESMs	Earth-system models
ESS	equilibrium solar sensitivity
α_P	Planck feedback
f_A	downward directed fraction of atmospheric radiation
$f_{WV}, f_{LR}, f_{SA}, f_{CO}, f_{EV}, f_{TC}$	feedbacks: WV, lapse rate, surface albedo, convection, evaporation, cloud
f_{TG}, f_{SC}, f_{ST}	total thermal feedbacks, solar induced cloud, solar induced thermal feedb.
GH-gases	green house gases
GPS	global positioning satellite
HadCRUT	Hadley Centre and Climate Research Unit
IPCC	Intergovernmental Panel of Climate Change
ISCCP	International Satellite Cloud Climatology Project
λ_P	Planck sensitivity - climate sensitivity parameter
λ_{Sun}	solar sensitivity parameter
LBL-RT calculations	line-by line radiation transfer calculations
lw radiation	long wave radiation
P_A, P_E	radiated power of atmosphere and of Earth's surface
ppm, ppmv	parts per million by volume
r	correlation factor
RF	radiative forcing
s_f	solar induced cloud cover parameter
SIC-feedback	solar induced cloud feedback
S_R	reference solar constant
SST	sea surface temperature
sw radiation	short wave radiation
T_A, T_E	atmospheric temperature (lower troposphere), Earth (surface) temperature
T_C, T_{Cl}	calculated temperature series, cloud temperature,
T_R	reference temperature (15.5 °C)
TCR	Transient Climate Response
TFK-scheme	energy and radiation budget scheme after Trenberth et al. [26]
TIC-feedback	thermally induced cloud feedback
TSI	total solar irradiance
WV	water vapor



Publication of Ernst-Georg Beck's Atmospheric CO₂ Time series from 1826-1960

Correspondence to

harald.yndestad@ntnu.no

Vol. 2.2 (2022)

pp. 134-136

Harald Yndestad

Norwegian University of Science and Technology,
N-6025, Aalesund, Norway.

Submitted 08-10-2022, Accepted 04-11-2022. <https://doi.org/10.53234/scc202112/15>

A surprise e-mail

On Christmas Day 2008, I received an e-mail from the German researcher Ernst-Georg Beck. He asked me to analyze an atmospheric CO₂ time-series from 1820 to 1960. A CO₂ time-series from 1820 was something special. Next day I went to work, analyzed the time-series, wrote a short note and e-mailed back a comment. It was all done in an hour. I wrote that there was nothing special about this time-series. The CO₂ variations coincided with North Atlantic water surface temperature from 1900 to 1960 (Yndestad et al. 2008) [1].

In August 2009 he came from Germany and visited me in Ålesund, Norway. He wanted to know more about the CO₂ time-series signature. In a golden moment, the wavelet spectrum analysis revealed a coincidence between the CO₂ signature, the Atlantic Water temperature, and the lunar nodal tide spectrum (Yndestad et al. 2008) [1]. Beck found what he was looking for. After the CO₂ signature was estimated, I started to ask him about possible errors in the time-series. Slowly I began to understand, the magnitude of the job he had done. This was a life's work, which should have been presented as a PhD thesis.

Summary of the work

The estimated Marine Boundary Layer (MBL) CO₂ time-series was derived from around 90,000 measurements associated with meteorological data selected from a basis of around 200,000 recorded measurements. The data had been presented in 979 technical papers. Among the authors were two Nobel Laureates. The standard analytical procedures of the time had been employed, including intercalibration between some laboratories. The uncertainty was quite large the first decades but narrowed over time to a level within 3 % (Beck 2007) [2]. For measurements over time in the same laboratory, the relative uncertainty would be reduced. That should give adequate comparisons with modern data including a fairly good overlap with the Mauna Loa data from 1958 the last 5 years. Thus, the data set should be considered at least partly adequate which would justify further detailed studies by the international scientific community. After all, the resolution of these in situ data is far beyond the ice core data being widely accepted.

Becks last manuscript

Beck started to work a revised paper and the first update came in October 2009. In the new paper he explained how Francis Massen had found an empirical relation between the CO₂ level and wind speed (where meteorological data were available), demonstrating that high winds

mixed the atmosphere gases so the ground measurements near the sea showed almost the same (level) concentration as the Mauna Loa reference station at elevation near 4000 m. (Massen and Beck, 2011) [3] He also showed that a similar empirical relation existed between CO₂ level and precipitation, and that estimates based on measurement on certain times of the day or at certain times of the year gave values close to Mauna Loa observations (Beck 2022) [4].

The challenge was to summarize his extensive material. Late in the autumn 2009, I received a message that he had been reduced due to disease. In January 2010, I was informed that he had got cancer. It was urgent to get the manuscript published. In spring 2010, he worked in good periods. During the spring, he received help from his own university. In August, the manuscript was submitted to Journal of Climate for publication. He died September 21, 2010. A rejection came November 15, 2010. The last comment from the second reviewer was: "*I must categorically recommend the rejection of this article without the possibility of a new submission or revision*". The atmospheric CO₂ from 1820 did not coincide with published CO₂ variations from Antarctic ice core samples, over the past 1,000 years. After Beck, the manuscript was no longer publishable or transferable.

Becks vs Keeling

The discussion about the time-series coincidences was not new. Beck had published a first version of his data series in 2007 (Beck 2007) [2]. In this publication, Beck allowed himself to comment that the Mauna Loa data series lacked data for the period before 1959. This comment led to a reaction from Ralph F. Keeling [(Keeling 2007) [5]. Beck's data series had an unexpected CO₂ growth from 1930 to 1945 and a subsequent relaxation over the next 10 years. The credibility of the data series now was dependent on Beck being able to clarify the source of CO₂ growth in this period. Beck believed the source was variations in the sea temperature. In a new article, he showed that the CO₂ variation was correlated with measured temperature variations in Antarctica (Beck, 2008a) [6], (Beck 2008b) [7]. In the autumn 2008, a new publication appeared (Yndestad et al. 2008) [1] which confirmed that the Atlantic Ocean had a temperature increase from 1930 to 1945. This increased sea surface temperature coincided with the CO₂ increase from 1930 to 1945 in Beck's data. Beck's article was handed over to the journal *Science of Climate Change* in 2021. They took the responsibility to publish the Beck February 2010 paper, as (Beck 2022) [3].

Atmospheric CO₂ signatures

There are no other known atmospheric CO₂ data series, that goes back to 1820. The question remained. What is the reference that may verify an atmospheric CO₂ time-series from 1820 to 1960. The solution was to estimate spectrum signature coincidences. Global sea surface temperature signature from 1850 to 2022 was known (Yndestad 2022a) [8]. The next step was to estimate atmospheric CO₂ at Mauna Loa signature 1959-2020 and the Atlantic CO₂ spectrum signature 1826-1960. It turned out that atmospheric CO₂ signatures coincides with the lunar nodal tide. Atmospheric CO₂ is controlled by sea temperature variations. Global sea surface temperature variations are controlled by the lunar nodal tide (Yndestad 2022b) [9]. The lunar nodal tides are controlled by the moon. Beck's extensive work was not in vain. The CO₂ time-series, estimated by Beck, is confirmed by the lunar nodal signature. The atmospheric CO₂ time-series 1820-1960 then should be published and made available for the scientific community and further studies.

References

1. Yndestad H, Turrell W R, and Ozhigin V 2008. Lunar Nodal Tide Effects on Variability of Sea Level, Temperature, and Salinity in the Faroe-Shetland Channel and the Barents

- Sea. Deep Sea Res. I. Oceanographic Res. Pap. 55__ (10), 1201–1217.
<https://doi.org/10.1016/j.dsr.2008.06.003>
2. Beck E-G 2007. 180 Years of Atmospheric CO₂ Gas Analysis by Chemical Methods. *Energy & Environment*. 18. 259-282. <https://doi.org/10.1260/095830507780682147>
 3. Massen F and Beck E-G 2011. Accurate Estimation of CO₂ Background Level from Near Ground Measurements at Non-Mixed Environments. In: *Leal Filho, W. (eds) The Economic, Social and Political Elements of Climate Change, Climate Change Management*. Springer: Berlin, Heidelberg.
 4. Beck E-G 2022. Reconstruction of Atmospheric CO₂ Background Levels since 1826 from direct measurements near ground, *Science of Climate Change*, 2, pp.
<https://doi.org/10.53234/scc202111/xxx>
 5. Keeling R F 2007. Comment on “180 Years of Atmospheric Co₂ Gas Analysis by Chemical Methods” by Ernst-Georg Beck, *Energy & Environment*. 18. 637-639.
https://citeseerx.ist.psu.edu/viewdoc/download?doi=10.1.1.861.5583&rep=rep1&type=pdfhttps://doi.org/10.1007/978-3-642-14776-0_31
 6. Beck E-G 2008a. Evidence of variability of atmospheric CO₂ concentration during the 20th century (discussion paper, May 2008).
 7. Beck E-G 2008b. 50 Years of Continuous Measurement of CO₂ on Mauna Loa, *Energy & Environment*. 19. 1017-1028. <https://doi.org/10.1260/095830508786238288>
 8. Yndestad H 2022. Jovian Planets and Lunar Nodal Cycles in the Earth's Climate Variability. *Frontiers in Astronomy and Space Sciences*, 10 May.
<https://www.frontiersin.org/article/10.3389/fspas.2022.839794>.
 9. Yndestad H 2022. Lunar forced Mauna Loa and Atlantic CO₂ variability. *Science of Climate Change*. In review.



Correspondence to
francis.mas-
sen@education.lu

Vol. 2.3 (2022)

pp. 137-147

Observed Temporal and Spatial CO₂ Variations Useful for the Evaluation of Regionally Observed CO₂ Data

Francis Massen^a, Ernst-Georg Beck^{†b}, Hans Jelbring^c, Antoine Kies^d

^ameteoLCD, Lycée classique Diekirch, Diekirch, Luxembourg

^bBiology Lab, Merian-Schlule, Freiburg, Germany

^cDept. of Physical Geography and Quaternary, Stockholm University, Sweden (ret.)

^dUniversity of Luxembourg, Radiation Laboratory, Luxembourg, Luxembourg

Abstract

Observed ocean and land CO₂ data show both seasonal and spatial variations, where latitude is the most important in addition to the increase in time. A simple, approximative corrective procedure is proposed which will be of use when comparing contemporary CO₂ data from land and ocean influenced stations, and for the validation of historical CO₂ measurements. This could help to validate regional CO₂ measurements against the Mauna Loa reference, or to analyse historical measurements done at different locations by applying common corrections.

The original paper has been finalized the 17 May 2007; except some editing for typing errors, layout and links, no changes have been made in this version which should be seen as a tribute to the late Ernst-Georg Beck, (Francis Massen 2022)

Keywords: CO₂ variations; latitudinal CO₂ variations; hemispheric CO₂ variations; land/sea differences.

Submitted 23-06-2022, Accepted 05-07-2022. <https://doi.org/10.53234/scc202206/12>

1. The variations of global CO₂ with latitude and time

Figure 1 shows the global distribution of CO₂ 1996-2005 as given by NOAA (NOAA, Globalview-CO₂, gv files). Clearly CO₂ varies with time (continuous increase), season (high and low) and latitude. The aim of this paper is to find an easy approximative procedure to validate CO₂ measurements from different stations taken at the same time. The procedure should allow handling differences in latitude, in location-type as sea- or land-based, and in hemisphere. Thus, it should be considered as a first step, before the application of full-grown models like MATCH (CGD, Match model).

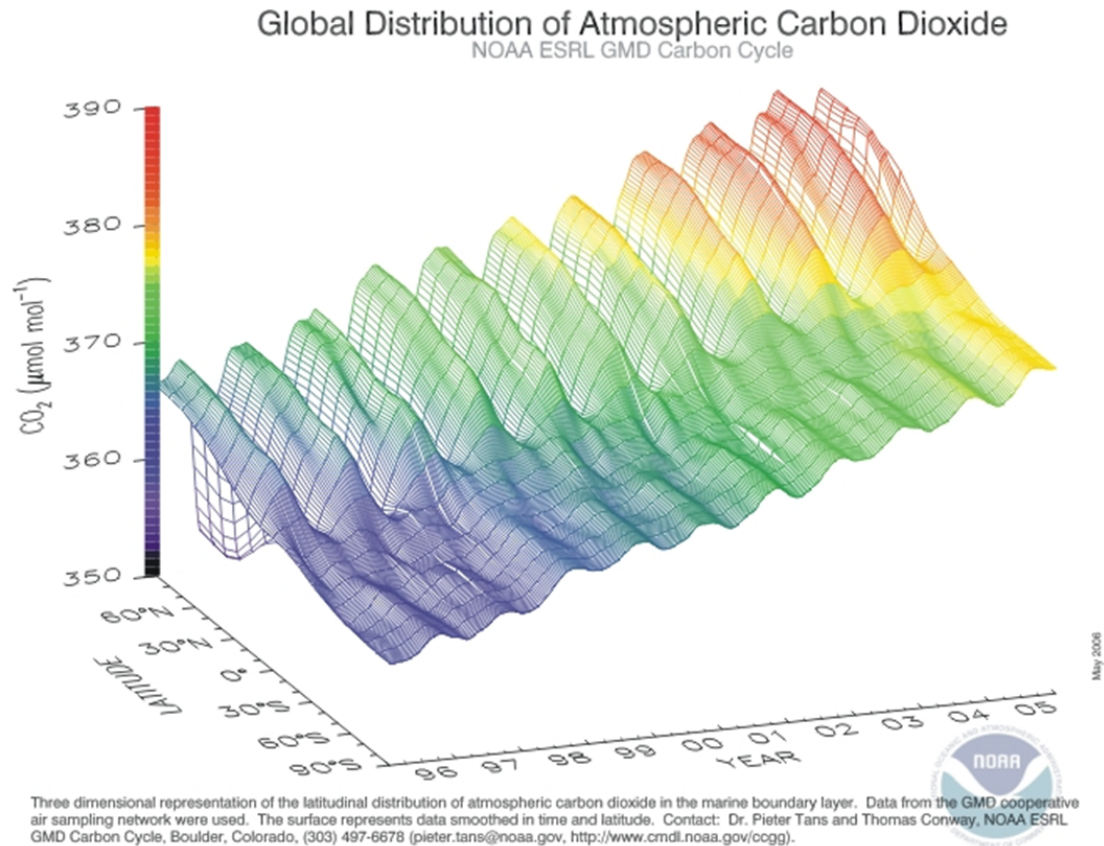


Figure 1. Seasonal and latitudinal variation of CO₂ Mixing ratios

2. Stations and time-span used

All data in the present study come from the NOAA Globalview ftp site [1]

The data files hold 4 columns like:

Creation Date: Thu Aug 31 09:28:42 2006

of rows after column header: 1297

UTC	S(t)	REF(t)	diff
1979.000000	335.4340	336.7548	-1.3208
1979.020833	335.7970	337.1502	-1.3532

The CO₂ mixing ratio is S(t), or if not available the sum of REF(t) + diff.

23 stations from South-Pole to Spitsbergen are used in this study; start of the year (SOY) and mid of the year (MOY) data are from 1985, 1990, 1995, 2000 and 2005; with SOY corresponding to the yyyy.0000 and MOY to the yyyy.5000 records. Ocean based stations are stations located at the coast or on an island; land-based stations are at a distance from sea of at least 50 km.

3. Stations of the southern hemisphere

A quick check shows that stations south of -40° latitude measure practically identical CO₂ mixing ratios and do not show any latitudinal gradient. The linear increase in time from 1985 to 2005 is 1.575 ppm*y⁻¹ (1.642 for the SOY, 1.504 for the MOY data). Adjusting the MOY data for the 6 months delay from SOY shows only small (less than 1 ppm, except for 1985) positive and negative differences. This reflects the well-known fact that the circumpolar vortex blocks or damps

Table 1. Stations used in this paper: SEA=1 means sea or coast-based station

	1 LAT	2 Location	3 file	4 Alt	5 SEA
spo	-90	south pole	spo_01D0	2810	0
maa	-68	mawson station, antarctica	maa_02D0	32	1
bhd	-41	baring head (NZ)	mhd_15C0	80	1
cgo	-40	cape grim, tasmania	cgo_01D0	94	1
ams	-37	amsterdam island (F)	ams_11C0	150	1
smo	-14	samoa island (USA)	smo_04D0	42	1
asc	-8	ascension island (UK)	asc_01D0	54	1
chr	2	christmas island	chr_01D0	3	1
mlo	20	mauna loa	mlo_01D0	3397	1
haa	21	molokai uisland, hawaii	haa005_01D2	500	1
ask	23	assekrem, algeria	ask_01D0	2728	0
wis	31	Sede Boker, Neguev	wis_01D0	400	0
ljo	33	la jolla pier, california	ljo_04D0	10	1
goz	36	gozo, malta	goz_01D0	30	1
wlg	36	mount waliguan (PRC)	wlg_01D0	3810	0
uta	40	wendover, utah	uta_1D0	1320	0
cmn	44	monte cimone (I)	cmn_17C0	2165	0
sch	48	schauinsland (D)	sch_23C0	1205	0
mhd	53	mace head (Eire)	mhdcbc_11C0	25	1
wes	55	westerland island (D)	wes_23C0	8	1
pal	68	pallas, Finland	palcbc_30C0	560	0
brw	71	barrow head, alaska	brw_01D0	11	1
zep	79	spitzbergen	zep_01D0	475	1

rapid and massive air mass intrusions from North to South; no major vegetation cover also means there are no photosynthesis-driven seasonal forcings.

Table 2 linear regression slopes for SH stations and latitudes between -40° and 0°

Year	SH SOY latitudinal gradient	SH MOY lati- tudinal gradi- ent
	Sea	Sea
1985	0.0303	0.0659
1990	0.0347	0.0455
1995	0.0363	0.0504
2000	0.0398	0.0604
2005	0.0547	0.0886
Mean stdev	0.0392 0.0062	0.0622 0.0168

The situation is different for the region between -40° and 0° .; the subset used in this study only has ocean-based stations. The SOY and MOY data series both have positive latitudinal gradients, with of a mean $0.0392 \pm 0.0093 \text{ ppm} \cdot \text{y}^{-1}$ for the SOY and $0.0622 \pm 0.0168 \text{ ppm} \cdot \text{y}^{-1}$ for the MOY season.

The SOY latitudinal gradients increase with time, whereas the MOY gradients are more or less constant. An exception is the year 2005, where both gradients show an unusual large increase in respect to the preceding year. Figure 2 shows the linear regression lines. The mean annual CO₂ concentration increases for all SH stations are between 1.580 and $1.642 \text{ ppm} \cdot \text{y}^{-1}$; at all stations except South-Pole MOY mixing ratios increase slightly faster than SOY ones.

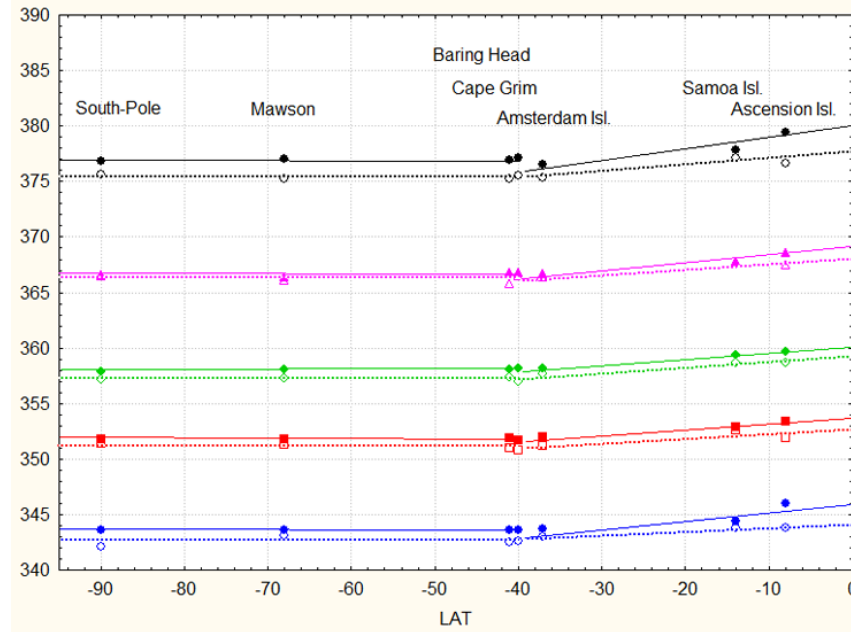


Figure 2. Variations of SH CO₂ mixing ratios with latitude (SOY = hollow symbols and dotted lines , MOY = full symbols and lines), 1985 to 2005

Table 3. Compared SOY and MOY annual linear increases for SH, 1985-2005

location	latitude	Mean annual in-crease at SOY	Mean annual increase at MOY
South-Pole	-90	1.642	1.624
Mawson	-68	1.580	1.628
Baring Head	-41	1.604	1.630
Cape Grim	-40	1.632	1.645
Amsterdam Island	-37	1.596	1.606
Samoa Island	-14	1.632	1.634
Ascension Island	-8	1.622	1.641
Mean/stdev for SH		1.615 0.023	1.630 0.013
Mean/stdev for SH latitude >-40°		1.617 0.019	1.627 0.019

The difference between same year SOY and MOY observations is small if the MOY data are corrected for the 6 months delay by subtracting 0.815. (see table 4 for the year 2005 situation).

Table 4. SOY and delay corrected MOY data are very close (Year 2005)

location	latitude	SOY	Time-delay adjusted MOY	delta ppm
South-Pole	-90	375.6	376.0	0.4
Mawson	-68	375.2	376.2	1.0
Baring Head	-41	375.2	376.0	0.8
Cape Grim	-40	377.1	376.3	0.8
Amsterdam Island	-37	375.3	375.9	0.6
Samoa Island	-14	377.1	377.0	0.1
Ascension Island	-8	379.4	378.6	0.8

Conclusion: To validate SH CO₂ data for latitudes higher than -40° an approximate latitudinal gradient of 0.04 ppm*degree⁻¹ for the SOY and 0.06 ppm*degree⁻¹ for the MOY period is suggested. Stations located below -40° latitude do not need to be corrected. The increase with time is approx. 1.6 ppm*y⁻¹ for all SH stations. The small difference between SOY and MOY readings shows that SH stations do not have a large seasonal effect. The maximum difference caused by the latitudinal gradient is 2.4 ppm for the most distant stations.

4. Stations of the Northern Hemisphere

The simple SH situation becomes more complicated in the NH due to much greater landmasses and vegetation. 16 stations, 9 sea and 7 land based are used in this study. The paucity of land-based stations represents a real problem, as no ensemble of evenly spaced land stations exists. We use land stations between latitude 23° (Assekrem, Algeria) and 68° (Pallas, Finland).

As shown in table 5, the SOY latitudinal gradients all are positive and higher than the corresponding SH gradients; the gradient for land stations are up to 2 times higher than those of the sea-based stations.

The MOY trends are negative for all sea and land-based stations; land stations have negative gradients 6 to 18 times higher than sea stations! This big change clearly shows the importance of making a difference between land and ocean-based stations during the summer periods: if in a first approximation SH sea and land stations of the same latitude could be treated in a similar manner, the huge difference of the latitudinal influence during the summer season makes that distinction mandatory for NH stations. During the NH winter season, the difference becomes smaller with the land gradients practically the double of the sea gradients. The similar magnitude of the negative MOY land gradients and the positive SOY sea gradients shows that summer-time land regions are as much a CO₂ sink as winter sea regions are a source (fig. 3 and 4).

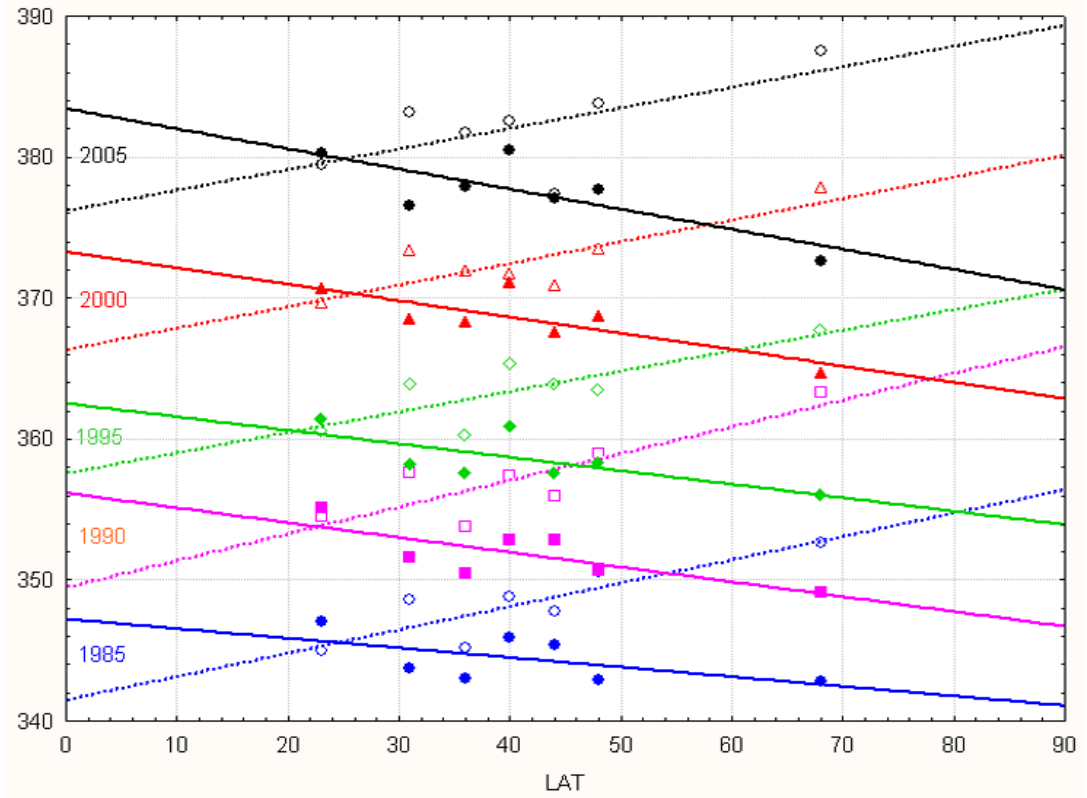


Figure 3. Variations of NH land station CO₂ mixing ratios with latitude (SOY = hollow symbols and dotted lines, MOY = full symbols and lines). 1985 to 2005

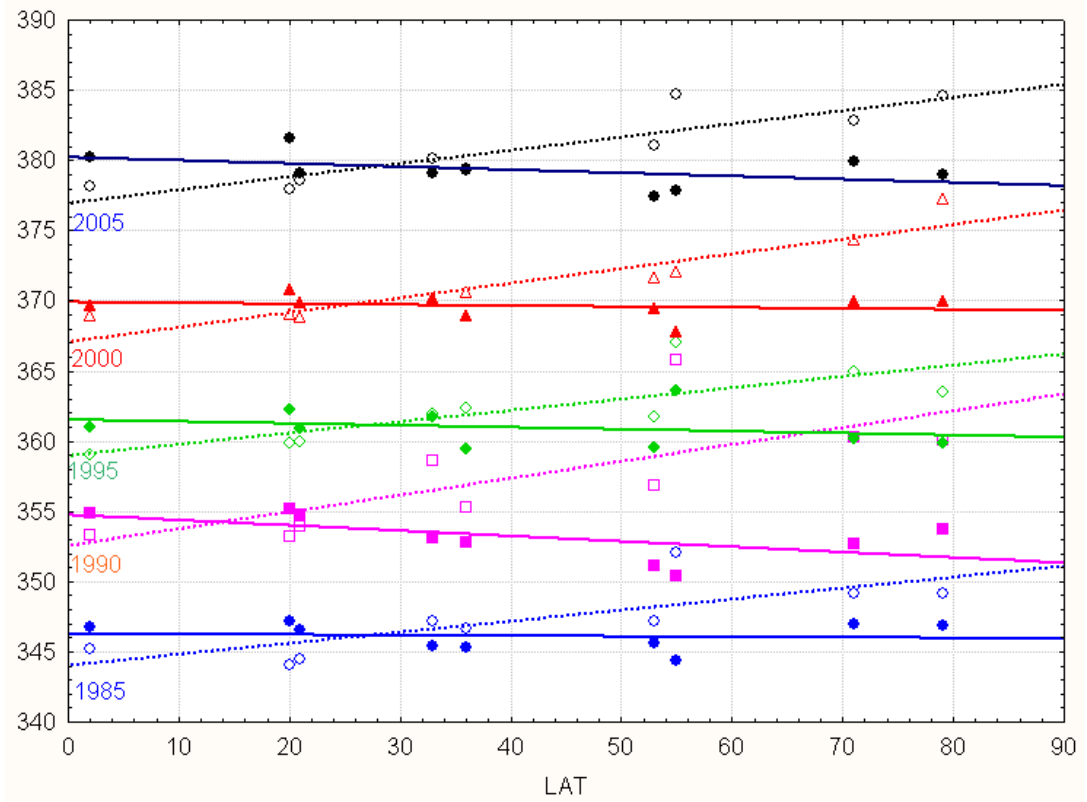


Figure 4. Variations of NH sea stations CO₂ mixing ratios with latitude (SOY = hollow symbols and dotted lines, MOY = full symbols and lines). 1985 to 2005

The magnitude of negative MOY gradients of the sea stations remains more or less constant with time (table 5), whereas the latitudinal gradients of land stations change remarkably (trend is - 0.0032 per year) and suggest a rising summertime CO₂ uptake in the more northern regions, possibly due to an ongoing greening of the northern NH land-masses (fig. 5).

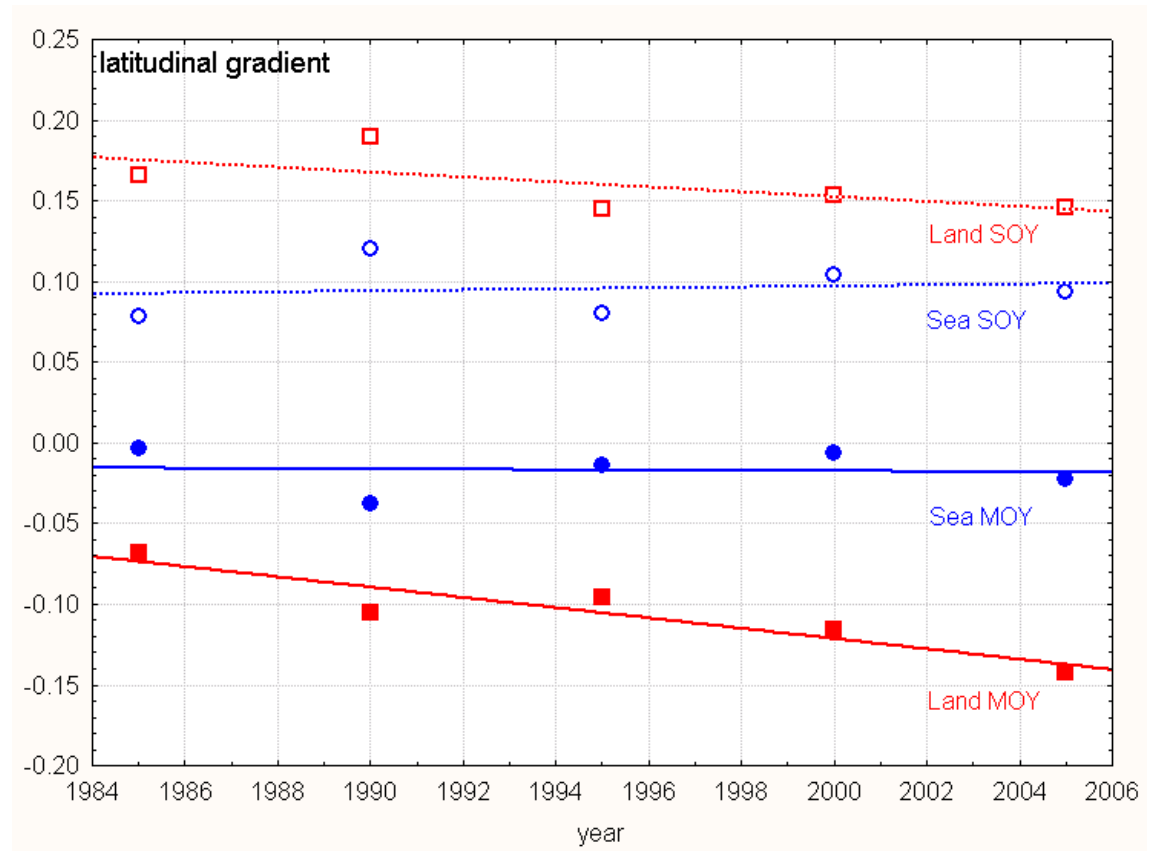


Figure 5. . Time dependency of NH latitudinal gradients (MOY = solid, SOY = dotted lines)

Table 5. SOY and MOY latitudinal gradients for the NH

Year	NH SOY latitudinal gradient			NH MOY latitudinal gradient		
	Sea	Land	L/S	Sea	Land	L/S
1985	0.0786	0.1656	2.1	-0.0038	-0.0683	18.0
1990	0.1200	0.1899	1.6	-0.0146	-0.1051	7.2
1995	0.0804	0.1450	1.8	-0.0139	-0.0957	6.9
2000	0.1044	0.1534	1.5	-0.0067	-0.1159	17.3
2005	0.0940	0.1459	1.6	-0.0225	-0.1426	6.3
Mean	0.0955	0.1600	1.7	-0.0123	-0.1055	11.1
stdev	0.0173	0.0187	0.2	0.0073	0.0272	6.0

As the latitudinal temperature drop becomes greater during the winter season, one should expect a high negative trend for the sea stations during wintertime, and a positive one during summertime. The data show the opposite: the positive trend may be caused by a predominance of the massive wintertime land sources which flips a "natural" trend from negative to positive and vice-versa. The magnitude of the winter sea and land stations latitudinal gradients differs by a factor 2, the sea gradient being always smaller than the corresponding land gradient

The gradients from table 5 may be compared to those reported in Warneke (2005) for the total CO₂ column measured during a ship cruise in Jan/Feb 2003, where the authors report a variation of about 1.3 ppm between 0° and 10° latitude; their measurements at higher latitudes give a negative gradient, opposite to this study and the MATCH model used by the authors. This paper clearly shows that a single trip from one hemisphere to the other cannot yield a correct estimation of the latitudinal gradient.

Table 6. Difference between SO and MOY mixing ratios.

Location	Lat. °	Alt. masl	Sea or Land	SOY	Time-delay adjusted MOY	delta
Christmas Island	2	3	Sea	378.1	379	0.9
Mauna Loa, Hawaii	20	3397	Sea	378.0	381	3.0
Molokai Island, Hawaii	21	500	Sea	378.6	378	0.6
Assekrem, Algeria	23	2728	Land	379.5	379	0.5
Sede Boker, Israel	31	400	Land	383.1	382.3	0.8
La Jolla, USA	33	10	Sea	380.1	378	2.1
Gozo, Malta	36	30	Sea	379.4	378	0.6
Mount Waliguan, PRC	36	3810	Land	381.8	377	4.8
Wendover, UT, USA	40	1320	Land	382.5	380	2.5
Monte Cimone, Italy	44	2165	Land	377.4	376	1.4
Schauinsland, Germany	48	1205	Land	383.8	377	6.8
Mace Head, Ireland	53	25	Sea	381.0	377	4.0
Westerland, Germany	55	8	Sea	384.7	377	7.7
Pallas, Finland	68	560	Land	387.5	371.8	15.7
Barrow, AL, USA	71	11	Sea	382.8	379	3.8
Spitsbergen, Norway	79	475	Sea	384.6	378	6.6

To estimate the seasonal amplitude for 2005, we will adjust the MOY data by subtracting 0.82, as the yearly increase for all stations of the NH is about 1.64 ppm*y⁻¹:

As can be seen, the seasonal difference is small for isolated islands (Christmas, Gozo) and desert locations (Assekrem, Sede Boker). It is higher in vegetation rich locations as Schauinsland and especially Pallas (large surrounding forests). Westerland island is very close to the mainland, and shows similar seasonal behavior. Spitsbergen with its much shorter summer season comes a bit as a surprise; the important seasonal swing might be a spill-over from the inflow of large easterly land-based winter sources.

5. How to apply a seasonal and latitudinal corrector

The stations in this report were different according to land or sea locations, SH or NH hemisphere, latitude, and period of the year. Our report shows that the sole qualifier of sea- or land-based does not point to a clear applicable different seasonal correction, as the seasonal gradients rises from negligible to important in a comparable manner when going from South to North. NH Southern stations located in arid regions do not differ much from sea stations at the same latitude; and this holds even for more northern locations. An exception are large forest area stations as Pallas.

The situation is easy for SH stations located lower then -40°: no correction is needed! For the SH stations located between -40° and the equator, correctors as +0.04 ppm per degree and +0.06 ppm per degree are suggested for the SOY and MOY seasons. As a first check, one could even neglect the seasonal difference and retain a single latitudinal gradient of 0.05 ppm per degree for all seasons.

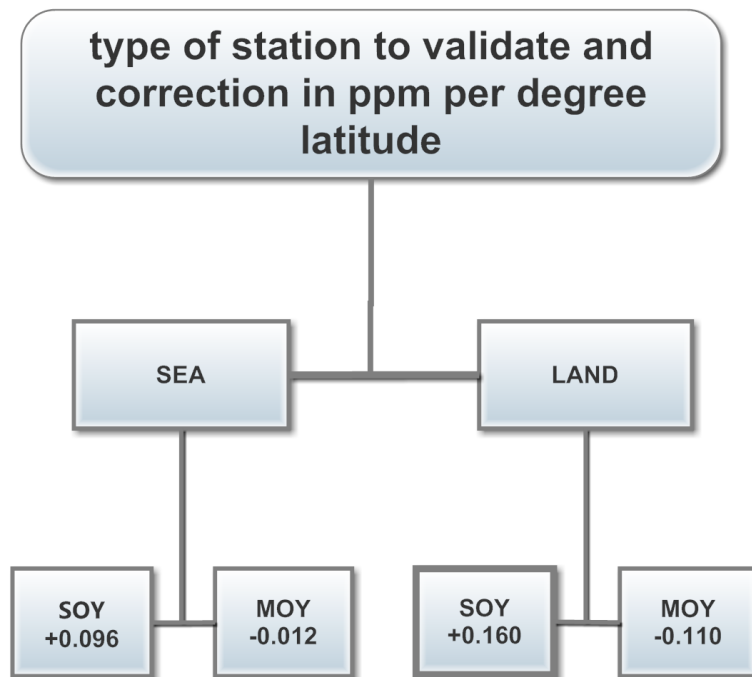


Figure 6. Method of correction for latitude

For the NH the seasonal latitudinal gradient remains the most important corrector. Four different situations should be respected (fig. 6):

sea and SOY:	+0.096 ppm per degree
sea and MOY:	-0.012 ppm per degree
land and SOY:	+0.160 ppm per degree
land and MOY:	-0.110 ppm per degree

Ideally only stations of the same type should be compared; when this is not possible, use the correct sea/land latitudinal gradient and apply a best guest corrector for extremely different locations (coast/sea and forest covered mainland).

6. Applying the correction to a historical data series

As an example, we will use the measurements done by Steinhauser in Wien during the Mai-August 1957 (Steinhauser 1958). This is one of the few well documented chemical measurement series overlapping with the first NDIR measurements by Keeling.

To compare with the first Keeling measurements, we will use the results from fig.7.

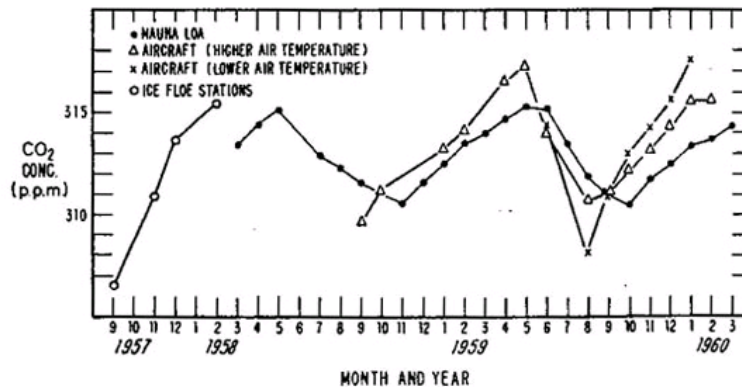


Figure 7.The early Keeling curve (from Scripps Institution of Oceanography)

Keeling made early measurements at Mauna Loa, lat. 20°, in 1958; the July mixing ratio is 313 ppm.

The latitude of Wien is 48°; applying the gradient to the Keeling data gives the following results:

Steinhauser, Wien, July 1957 (mean): 319 ppm (from Steinhauser 1958)

Keeling, Mauna Loa, July 1958: 313 ppm (fig. 7)

MLO MOY sea latitude correction: $28^{\circ}(-0.01) = -0.3$

adjusted MLO 313 -0.3 = 312.7 ppm = result if Keeling had measured at the latitude of Wien

subtract estimated increase of 1.6 for 1 year difference between time of measurements

definitive adjusted MLO: ~311 ppm (no other sea/land correction)

difference between chemical and NDIR measurements: 8 ppm = 2.6%

A further problem comes from the fact that the whole MLO annual cycle is time-shifted by about 3 months versus Wien (Wien minima happen in June, MLO minima in Sept-Oct. If we compare a full yearly cycle from Wien (mean of Jan57 to Dec57 is 320 ppm) to the May58 to April58 MLO mean (313 ppm), the difference becomes ~10 ppm (+3.2% relative to MLO) after applying the latitudinal (-0.3) and time (-2.4) corrections to the MLO readings.

7. Conclusion

This report shows the importance in applying latitudinal and seasonal correctors when comparing or validating CO₂ data from different stations. For SH stations, the latitudinal gradient is the sole corrector needed. For NH stations of the same sea/land type one can use one of the 4 mean gradients from table 5, according to SOY, MOY, SH and NH. If the stations belong to different sea-land categories, the comparison is hampered by the uncertain magnitude of the sea/land corrector.

Funding

No funding.

Guest-Editor: Jan-Erik Solheim; **Reviewer:** anonymous.

References

Beck E-G 2007, *180 Years of Atmospheric CO₂ Gas Analysis by Chemical Methods*, Energy & Environment 18, 259–282. <https://doi.org/10.1177/0958305X0701800206>

CGD-UCAR, MATCH model.

Link accessible via the Internet Archive/Wayback Machine (web.archive.org)

Search for "Atmospheric tracer-transport model – MATCH (Rasch)"

NOAA, *Globalview-CO₂ GLOBALVIEW-CO₂: Cooperative Atmospheric Data Integration. Project - Carbon Dioxide*. CD-ROM, NOAA/CMDL, Boulder, Colorado.

https://daac.ornl.gov/ISLSCP_II/guides/globalview_co2_point.html

Zip file with gv

data: https://meteo.lcd.lu/papers/co2_pattern/co2_and_latitude/GLOBALVIEW.zip

Scripps Institute, The early Keeling Curve. https://scrippsco2.ucsd.edu/history_legacy/early_keeling_curve.html

Steinhauser F 1958, *Der Kohlendioxyd-Gehalt der Luft in Wien und seine Abhängigkeit von verschiedenen Faktoren*. <http://nbn-resolving.de/urn:nbn:de:101:1-201601251147>

Warneke T 2005, *Seasonal and latitudinal variations of column averaged volume-mixing ratios of atmospheric CO₂*. GRL, vol.32,

L03808 <https://epic.awi.de/id/eprint/11860/1/War2005a.pdf>

Reconstruction of Atmospheric CO₂ Background Levels since 1826 from Direct Measurements near Ground

*Ernst-Georg Beck†,
Institute of Biology III, University of Freiburg*

Abstract

A new data set of annually averaged CO₂ background levels directly measured from 1826 to 1960 is presented. It is based on a selection process of about 100,000 single samples from more than 200,000 available near ground on land and sea, mainly in the northern hemisphere. Analysing the data, methods, sampling stations, meteorological conditions and air masses it is possible to reconstruct the past yearly CO₂ background levels. New methods to estimate annual marine boundary levels from near ground data from the historical data are presented. This allows the reconstruction within an estimated error range of $\pm 2.5\%$ and a methodical error range since 1870 of $\pm 3\%$. A definite fluctuation of levels can be seen around 1860 and especially around 1940 showing levels of more than 380 ppm, almost like today. A slow rise of atmospheric CO₂ since 1880 is confirmed. The difference in averages of CO₂-levels in the 19th and 20th century of 2.6 % is within error range of 3 % of methods.

Keywords: CO₂ background level, marine boundary level, direct chemical methods, vertical profiles, wind and precipitation corrections.

Submitted 19-02-2010; Accepted 30-05-2022. <https://doi.org/10.53234/scc202112/16>

A summary of acronyms see at the end of the paper.

1. Introduction:

Atmospheric CO₂ concentrations have been measured since the beginning of the 19th century with remarkable precision. Carl Wilhelm Scheele was the first person, who from a number of ingeniously contrived experiments, concluded that the atmospheric air is a mixed fluid composed of about two parts of nitrogen, and one part of oxygen, along with a very small admixture of carbon dioxide. This statement by Joseph Black (1806), the discoverer of CO₂, dates back to 1806 and marked the beginning of accurate gas analysis and the end of the phlogiston theory—a former heresy in science. (Rörsch 2007).

As outlined in Beck (2007, 2008) about 200 000 single samples of air have been collected and analysed by the scientists who established knowledge of modern natural science. Theodore de Saussure (1830) was the first who continuously analysed air samples in the Swiss alpine area since about 1809 up to 1830 and established accurate gas analysis by dissolving defined volumes of air in alkaline solution and subsequently dried and weighted them to calculate the corresponding concentration of CO₂ in air. He found the today well known characteristics of the atmospheric fluctuations of CO₂ during daytime and night time, the seasons, influence by vegetation and weather (fog, rain, snow) and burning fuels by man. Max Pettenkofer introduced the titrimetric CO₂ method around 1855 which became the standard in CO₂ gas analysis for the subsequent 100 years. Since about 1870 it was possible to validate the sampling and analyzing within an error range of $\pm 3\%$ or about ± 10 ppm.

In the 20th century hundreds of thousands of samples have been analysed on continents and over the oceans as well as investigating the vertical profile of air using a refined Pettenkofer method down to 0.33 % error in 1935. Modern NDIR spectroscopic analysis of air streams was introduced in 1938, exhibiting a much better accuracy of 0.1 % since the early 1950s and is still used for today's atmospheric monitoring by NOAA. Meanwhile globally acting networks monitor CO₂ contents in the atmosphere or the hydrosphere as documented by NOAA GlobalView-CO₂ and WDCGG.

†Post mortem memorial edition

In 1958 Keeling introduced continuous measurements of atmospheric CO₂ using modern NDIR procedure and defined the modern standards of background levels.

Historical CO₂ measurements prior to this year are usually derived from proxies, with ice cores being the favorite. Those done by chemical methods prior to 1960 are often rejected as being inadequate due to poor siting, timing or method. As outlined in Beck (2007) the vast majority of these data has not been evaluated.

In this paper a new data set of annually averaged CO₂ background levels from 1826 to 1960 is presented based on the comprehensive analysis of direct near ground measurements. This was possible by the development of new methods to estimate the annual CO₂ background levels from near-ground data, as described in Massen et al. (2007).

2. Data and methods

An amount of more than 200,000 single samples is available in about 400 historical papers from 1800 to 1960 (Letts and Blake 1899–1902, Stepanova 1952).

The selection process leading from the raw data to the annual CO₂ background averages was as follows (Beck 2007, 2008 and Messen and Beck 2011):

1. Compiling data from available literature (data, stations, methods and literature in separate files)

About 100 000 single samples (97,404 samples from 901 stations at sampling locations from lat -78.8 to +83.7 and long -156.8 to -163.3 most frequent locations: northern hemisphere at latitudes 40 to 80N (~75 %), Europe, averages of double and quadruple sampling) have been selected to calculate a dataset of monthly averages. There are 1172 months with data from 1800 to 1959 including 1998 with data sampled over the oceans, by a total 77 authors. Data from marine, coastal stations or from higher troposphere in 20th century are about 50 % of all. The longest series have been analysed at Montsouris (Paris) 1877–1910 (33 years).

From 1949 to 1951 there has been measurements in a continuous air stream (URAS) as with the modern NDIR. Typical sampling height was 1–50 m above ground (sea surface), literature research has revealed that Andrée 1893, Wigand 1911, Kauko 1936, Bischof 1960 (Lapape 1928, 1929, 1934 ignored because of inconsistent data) have measured CO₂-levels at different altitudes (balloon, aeroplane) so that vertical profiles can be calculated.

The most accurate analysis in 19th century had been conducted by Spring 1883 and Palmqvist 1889 (± 1 –2 %) using high precision and well calibrated chemical gas analysers. In the 20th century Kauko 1935 analysed vertical CO₂ profiles over Helsinki down to ± 0.33 %, Kreutz analysed during 1939 to 1941 with ± 1.5 % accuracy at 4 altitudes, 8 samples per day. An overall accuracy range of ± 3 % can be recognized since 1870.

The year 1960 marked the transition time when a methodical change occurred by no longer using old wet chemical methods, but new physical infrared spectroscopic NDIR methods by analysing a continuous gas stream. Charles Keeling introduced the new method at the Mauna Loa Observatory (Hawaii) in 1958. It is remarkable that no calibration of the new NDIR method versus the old chemical methods can be found in literature.

The data can be traced in two main libraries. 292 papers with CO₂ data in the 19th century are listed in Letts and Blake (1899). 231 papers with data from the 19th and 20th century have been compiled by Stepanova (1952). Additionally, the author has used 16 further papers showing CO₂ data not listed in the two libraries.

Detailed station, sampling, author, and literature information are documented in the supplemental files to this paper.

2. Testing the reliability of data by checking the used methods, local sources and sinks, meteorological conditions (air mass analysis) and comparisons with other geophysical time series if possible.
3. Calculating monthly and yearly averages and estimating the annual background averages by using methods outlined in this paper. Often several data series per year are available. In total 10 linear interpolations fill the gaps of years with no data available since 1870 (31 since 1826)

The selected dataset of about 90 000 values show very high values from 1800, analysed by de Saussure (1830).

The very detailed information on methods, locations, and air masses at the time of the largest volcanic event in recent history (Tambora 1815–1816) justifies the implementation of his data. During expeditions to the Arctic circle and Antarctic areas, either very low values were sampled (Venus 1882 and Charcot 1908 expeditions, analysed by Müntz; Müller 1928, Buch 1936) or very high levels had been documented by Krogh 1902 and Lockhart 1941. The evaluation of the sampling procedures reveals accurate methods using calibrated gas analyzers by skilled persons. Therefore we have to accept these data as real such as high levels of CO₂ near the ice-covered waters. This was documented by different persons using different analysing methods. The very high levels seem to reflect known upwelling of CO₂-enriched waters.

Some corrections have been applied to the dataset because of methodical errors existing in some French data series showing the sulphuric acid absorption problem, (Beck 2007). The Reiset, Müntz and Montsouris data (prior to 1890) have been corrected by an addition of about 20 ppm (20–30 ppm losses was demonstrated by Spring in 1883 using this procedure). Reiset passed his air samples through sulphuric acid, Müntz used a volumetric method and sulphuric acid to free the CO₂ from the alkaline carbonate. Data analysed at Montsouris can be confirmed because parallel analyses were done by other investigators, when the method was changed in 1890. Also the Brown and Escombe and Petermann (1892–93) data produced by a variant of the Reiset method (1898–1901) are influenced by using sulphuric acid absorption. Therefore a correction was necessary. The Feldt, Heimann and Frey data had to be corrected because of too short absorption time in alkaline solution. (For detailed informations please see in the station and author supplemental file)

Figure 1 shows a 3D presentation of the monthly averages according to latitudes. Figure 2a shows their sampling locations.

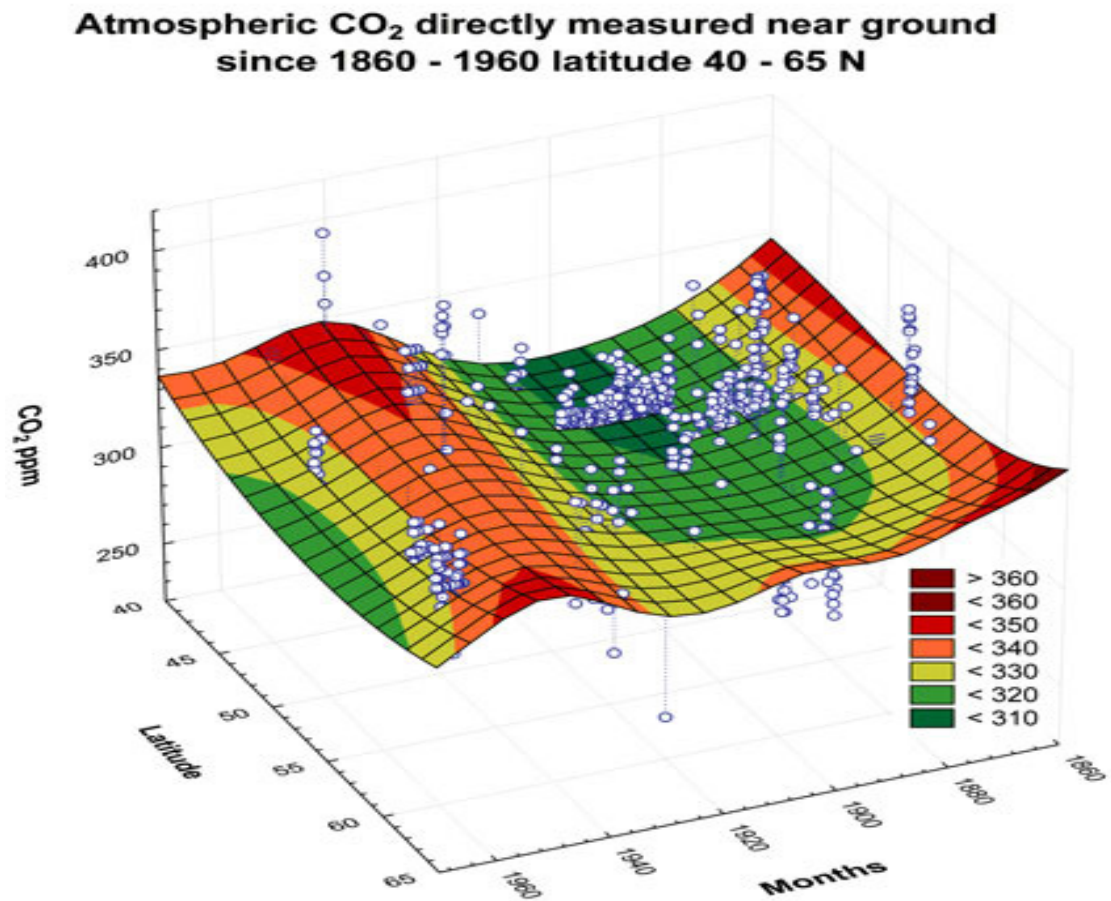


Figure 1. Monthly averages of about 72 % of raw CO₂ samples (latitude 40–65 N) collected 1860–1960 near ground and selected from >200 000 available in literature. Coloured plane = distance weighted least squares fit Statistica (2009); blue circles: monthly averages.

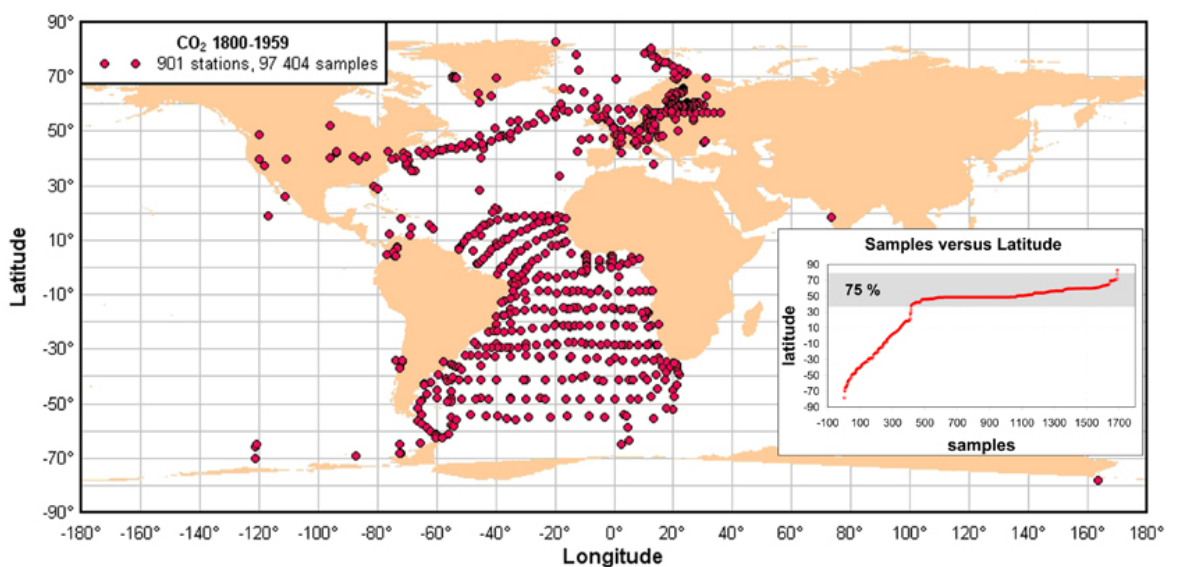
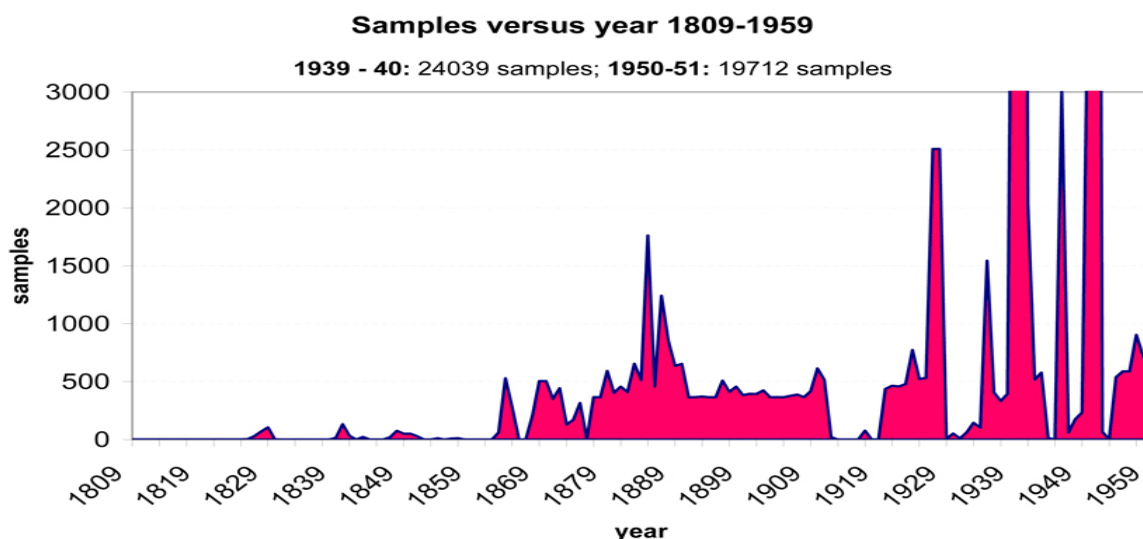


Figure 2a. 901 sampling stations of direct measured CO₂ near ground since 1800–1960 (dPlot2009). To the right: Samples versus latitude; 1172 months with data +Wattenberg/Buch single samples over sea. (e.g. modern WDCGG stations with monthly CO₂ data: 55, Globalview-CO₂ (2008):110)



Figur 2b. Samples per year (see supplemental file *samplesused.pdf*)

About 75 % of the samples were collected between latitudes of 40 and 80 N, about 50 % over sea surface or from the sea at coasts. Samples collected near the sea ice at the Arctic and Antarctic circle usually show very low values because of absorption in ice/water. Samples collected over sea surface near warm ocean currents or in upwelling areas show high values.

2.1 Summary of historical methods of gas analysis prior to *ndir* 1958

Since its early arising in the 18th century, chemical methods as described in Beck (2007, 2008) have been used to analyse fluid and gas mixtures. The typical procedure was to pass a defined volume of air through an alkaline solution of known concentration ($\text{Ba}(\text{OH})_2$, NaOH , KOH) and calculate quantitatively absorbed CO_2 from the induced changes of the system. Up to about 1845 the gravimetric method was in favour by drying and weighting the produced carbonate. The French chemist Regnault introduced the volumetric method by measuring the changed volume of the system. No inter-calibration of the methods can be found in literature.

A landmark in gas analysis was established by the German physician Max v. Pettenkofer in 1857 when he developed a titrimetric method named in honour of him the “Pettenkofer Process”. It was based on the absorption of the CO_2 from air in baryta water and titration of the produced barium carbonate with acid. Since about 1855 inter-calibration of the several methodical variants are available. A typical analysis of an air sample lasted from several hours up to one day.

A theoretical accuracy of $\pm 0.0006\%$ in volume was provided by the Pettenkofer process but in practice the accuracy was about $\pm 2\%$, (Kauko et al. 1935). Special modifications of H. Lundegårdh (1922) resulted in $\pm 1\%$ accuracy. Since about 1883 Otto Pettersson had refined the volumetric method by introducing means of eliminating volume errors caused by heat of absorption. Therefore the former volumetric analyses show erratic values due to temperature dependence. The French school of analysing air had used sulphuric acid to dry the air. This had introduced another error of about 20–30 ppm too low, because of absorption of a fraction of the sampled CO_2 in the acid. The Belgian chemist W. Spring investigated this problem in detail in 1883. In the 20th century August Krogh, D. van Slyke, Y. Kauko and P. Schuftan introduced high precision volumetric, manometric, pH-metric and conductometric methods down to an error range of $\pm 0.33\%$ in 1935 with an analysing time of some minutes. In 1938 the URAS (Ultrared Absorption Writer) gas analyser was invented by Friedrich Luft at BASF, the first continuous monitoring physical device later called NDIR, which is in use today, showing an error range of about $\pm 0.1\%$. (Beck 2007, 2008). Modern physical NDIR devices are calibrated against a manometric CO_2 determination.

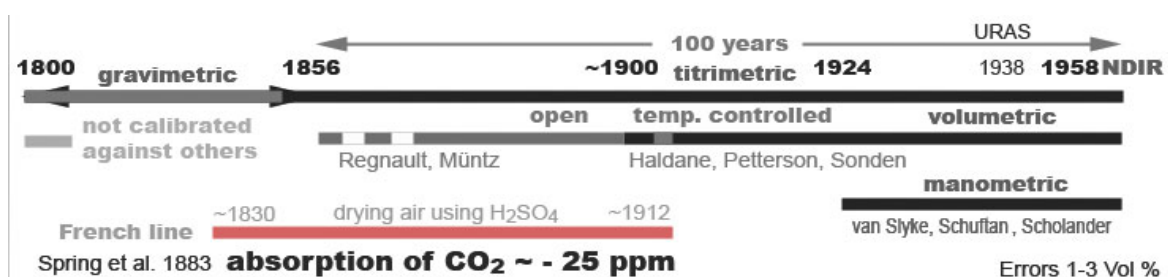


Figure 3. Evolution of analytical methods for chemical CO₂ gas analysis since 1800–1960.

The timeline of the methods in CO₂ gas analysis is summarized in Figure 3.

Kauko in 1934–37 did comparative analysis of well known analytical methods at that time (gravimetric, titrimetric, Pettenkofer, potentiometric, pH-metric, condensation) and Kauko et al. (1935) developed the most accurate CO₂ condensation method (± 0.33 % valid down to CO₂-levels of 0.02 %) in 1935. According to Kauko all methods give comparable results within about ± 3 %, the CO₂-levels concluded from the Pettenkofer method are somewhat lower than the exact levels

Table 1. Comparative chemical methods to quantify atmospheric CO₂-levels (Kauko 1934–1937).

pH method ¹	potentiometric method ²	condensation method ²	Pettenkofer titrimetric ³	gravimetric method ⁴
		0.017	0.0175	
0.036	0.031			
	0.065	0.065	0.069	
0.072	0.0721	0.0723		
0.087	0.088			
	0.122		0.1225	
0.144	1.42	0.143	1.43	1.422
0.18	0.18	0.189	0.172	
0.210			0.209	
0.239		0.236	0.241	
0.261		0.255	0.261	
	0.99	1.0	0.98	0.985
1.28		1.21	1.23	

Values in vol %; (1= Kauko 1934, 2= Kauko et al. 1935, 3= Hempel 1913, 4= Kauko et al. 1935).

Beside the methodical errors of the early gravimetric methods in weighting and drying the precipitate, which are difficult to reconstruct (de Saussure 1830), most of French measurement series, and those who use methods according to the Regnault-Reiset analysers show large errors because of CO₂ loss in drying ore setting free air by sulphuric acid (Reiset, Petermann, partly Montsouris) or a missing means of elimination heat of absorption in volumetric devices (Müntz plus other losses by using sulphuric acid). Other methodical errors derive from using too small volumes of air to analyse (early Pettenkofer methods, Frey, Heimann, Feldt).

All these errors have been quantified and corrected: Reiset: +20 ppm; Müntz: +20 ppm, Montsouris: +18.5 ppm 1877–june 1890, Feldt, Heimann, Frey: +40 ppm, Petermann: +20 ppm.

2.2 Analysis of vertical CO₂ profiles

The vertical CO₂-profiles are the key to estimate background levels from near-ground measurements. They are characterized by large seasonal fluctuation (SEAS) near ground on continents in non well-mixed environments and small variations in the higher troposphere or over sea surface (MBL) in well-mixed environments. Because all CO₂-sources are assumed to come from the lithosphere there is a physical connection from the ground to the higher layers. Figure 4 shows the most important globally CO₂-sources and sinks in the lithosphere-atmosphere boundary layer. Anthropogenic sources and others below 1 % of total emissions according to IPCC (Solomon et al. 2009) have been omitted. Within the atmosphere there exists a CO₂-gradient with a somewhat lower concentration and better mixing in the higher troposphere.

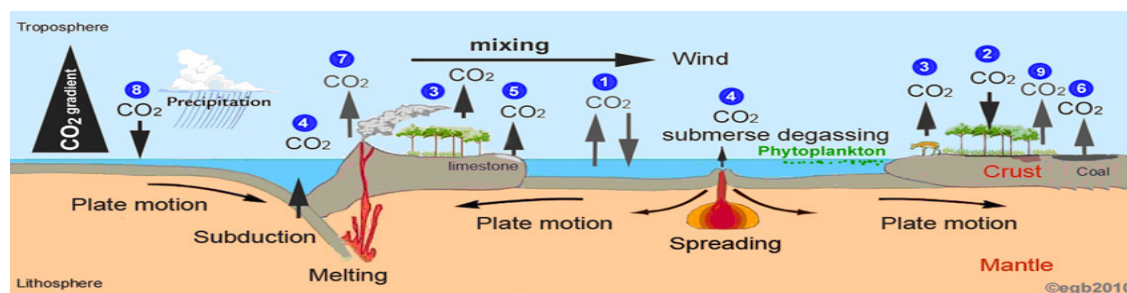


Figure 4. CO₂ sources and sinks in the boundary layer of the lithosphere-troposphere. 1: ocean degassing/absorption, 2: photosynthesis, 3: respiration, 4: submerse geological degassing; 5: limestone weathering, 6: surface coal oxidation, 7: volcanic degassing and subduction degassing, 8: precipitation absorption, 9: soil respiration. CO₂ flux < 1 % of total emissions (IPCC) omitted.

The main globally effective controllers for CO₂-flux in the lithosphere/atmosphere system are the oceans (1) and the biomass (2, 3, 9). The phytoplankton in the surface layer of the oceans act as controlling agent for ocean bound CO₂.

The amount of geological surface flux of CO₂ from continents is greatly underestimated according to Mörner and Etiope (2002). Limestone weathering, surface coal oxidation and non-volcanic degassing are not quantified in detail in the IPCCs carbon cycle. Also the submerse fluxes in the oceans have not been quantified. (IPCC 2007). Local sources and sinks control local mixing ratios.

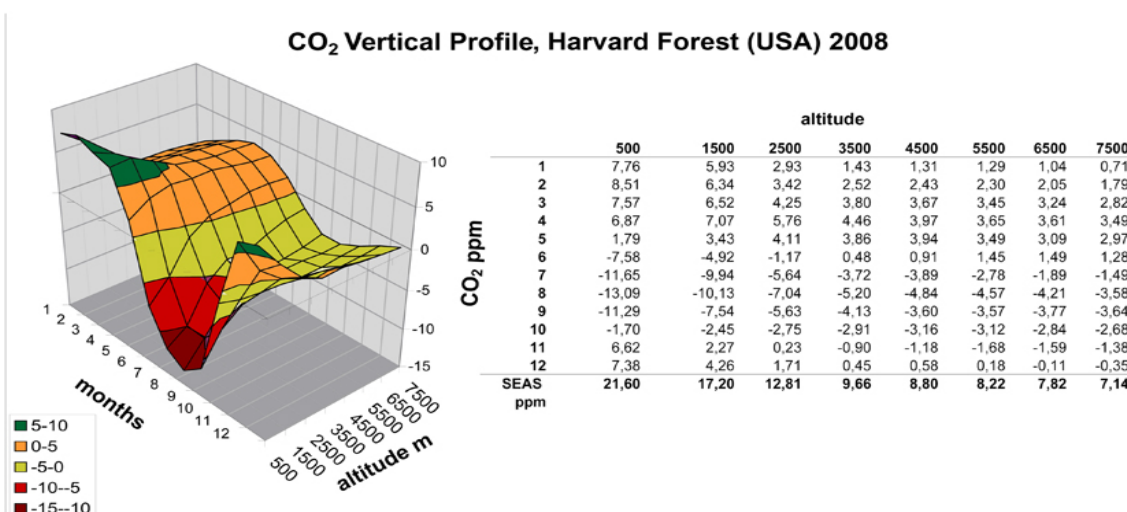


Figure 5. Vertical profile of CO₂ (deviations from 0) at Harvard Forest (USA), lat 42.54N, long -72.17E, measured by aeroplane at different altitudes of 500, 1500, 2500, 3500, 4500, 5500, 6500 and 7500 m. (data from NOAA Globalview-CO₂ 2009)

From the NOAA Globalview-CO₂-sampling locations (NOAA 2009) I have chosen the vertical CO₂-gradient from the Harvard Forest site as an example for a typical continental location with vegetation at a typical latitude (lat 42.547N, long -72.17E).

Figure 5 shows the larger SEAS fluctuation near ground (500 m, 21.60 ppm) and the smaller variation of the background levels at higher altitudes (7500 m: 7.14 ppm). The SEAS average is nearly identical for 500 m: 0, 0.099 and 7500 m: -0.0055 (0.1 ppm difference).

CGER Monitoring of GHGs over Siberia supplies typical continental vertical data profiles (CGER 1996) and the work of Gurk et al. (2008) analysed vertical CO₂-profiles over Europe (land and

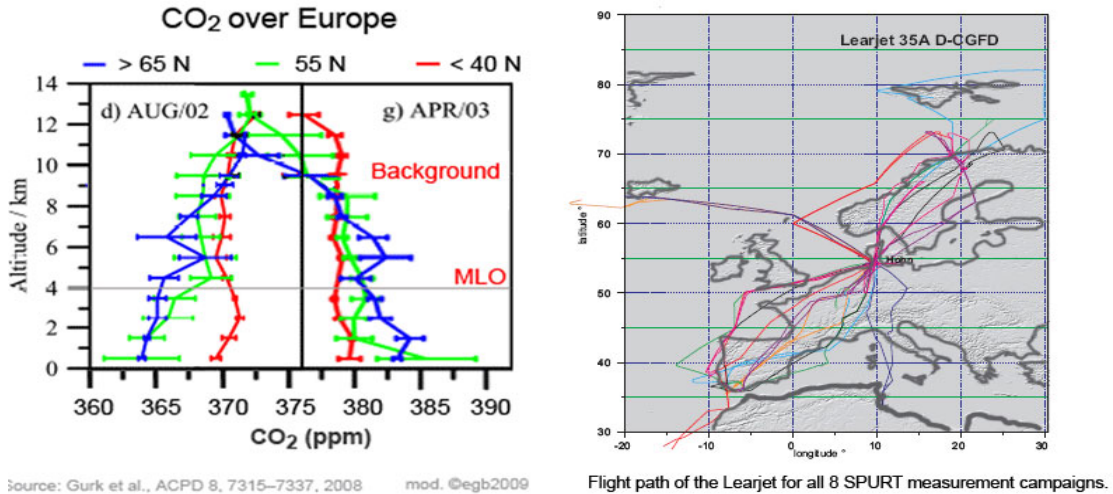


Figure 6. Vertical CO₂-profiles over Europe covering latitudes from 33 N to 79 N sampled by aeroplane during 2002–2003. (Gurk et al. 2008) showing the selected month with largest deviation. Horizontal bars are standard deviations for each km altitude. (flight path from Engel et al. 2006).

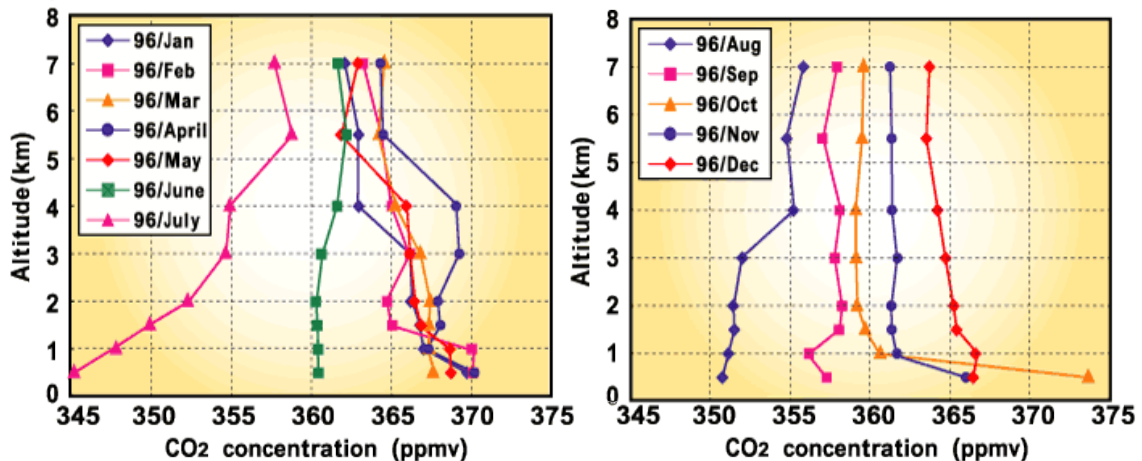


Figure 7. Vertical CO₂-profile sampled over Surgut, Siberia in 1996.

The seasonal variation in the boundary layer was max. 28 ppm. The variation at 4,000 m was 15 ppm. 14 ppm was the difference at the marine boundary layer calculated from Globalview-CO₂ (2008).

The annual average for CO₂ at 55 N at an altitude of 4 km was 373.5 ppm, the annual average at 500 m was 375 ppm, that means a difference of 1.5 ppm (-0.5 % deviation).

Over Surgut we found a seasonal range of 28.4 ppm at 500 m and 42.6 ppm extrapolated near ground. The Surgut data from 1996 show a summer deviation of –17 ppm for July compared to the global MBL background of 361.6 ppm.

Stephens et al. (2007) used average vertical profiles derived from aircraft during midday at 12 global stations at latitudes 40N to 40S with records extending over periods from 4–27 years averaged over different seasonal intervals. (See Figure 1.) The following locations have been chosen according to the NOAA Globalview-CO₂ Sampling locations

<https://gml.noaa.gov/ccgg/globalview/>

Table 2. Locations analysed by Stephens et al. (2007)

	Location	Geographic position: Latitude, longitude
1	Briggsdale, Colorado, United States (CAR)	lat. 40.37 N long. –104.30 E
2	Estevan Point, British Columbia, Canada (ESP)	lat. 49.58 N long. 126.37 E
3	Molokai Island Hawaii (USA) (HAA)	lat. 21.23 N long. 158.95 E
4	Harvard Forest, Massachusetts, United States (HFM)	lat. 42.54 N long. –72.17 E
5	Park Falls, Wisconsin, United States (LEF)	lat. 45.93 N long. –90.27 E
6	Poker Flat, Alaska, United States (PFA)	lat. 65.07 N long. –147.29 E
7	Orleans, France (ORL)	lat. 47.80 N long 2.50 E
8	Sendai/Fukuoka Japan (SEN)	lat. 33.39 N long. 130.21E
9	Surgut, Russia (SUR)	lat. 61N long 73 E
10	Zotina, Russia, Siberia (ZOT)	lat. 60.75 N long. 89.38 E
11	Rarotonga, Cook Islands (RTA)	lat. 21.25 S long. –159.83 E
12	Bass Strait/Cape Grimm Australia (AIA)	lat. 40.53 S long. 144.30 E

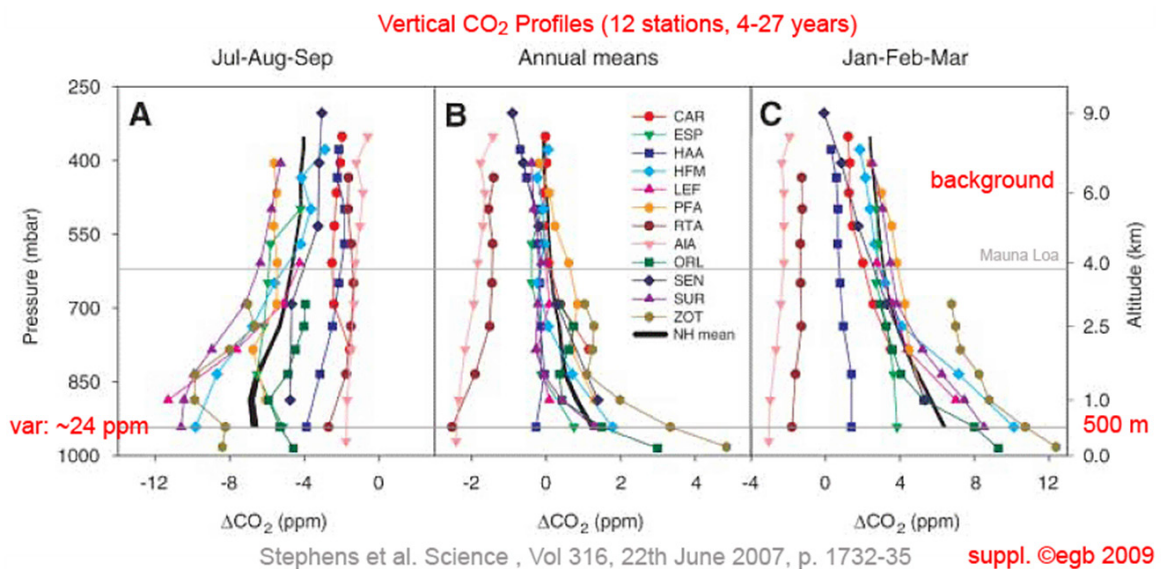


Figure 8. Vertical CO₂-profiles from 12 global stations derived from flask samples collected from aircraft during midday with records extending over periods from 4 to 27 years. (Stephens et al. 2007). Figure 1 of the paper was supplemented by the author. MLO = the Mauna Loa sampling station used as a reference. B has been calculated by subtracting the MLO data.

Figures 8 A and C show the seasonal variation (SEAS) at different altitudes and locations for July to September and January to March. Figure 8 B shows the annual averages of the deviation from the reference data sampled at Mauna Loa. The annual averaged difference of the seasonal variation to the Mauna Loa data in about 4 km altitude is about 2.3 ppm, near ground 8.6 ppm by graphical extrapolation. The average of the Northern Hemisphere data near ground shows a 2.56 ppm difference compared to the Mauna Loa reference at an altitude of about 4000 m. At 500 m we can observe a maximum seasonal variability of 27 ppm (from Globalview-CO₂) of all stations. Near ground by extrapolation this value extends to 30 ppm.

Table 3. Seasonal cycles near ground and background in modern data.

Location	Max.Seasonal variation	ΔCO_2 background -500 m	ΔCO_2 -background -near ground; extrapolated
Europe 33N- 78 N, sea/land average	28 ppm		-
12 global stations 65N – 40S sea/land average	30 ppm	1.13 ppm	2.56 ppm
Surgut 60 N wetland	42.6 ppm	0.2 ppm	3.9 ppm

Analysis of vertical CO₂-profiles revealed that the yearly average of near ground values resembles the yearly average of the background level at altitudes higher than about 4 km at the same location within about 1 %.

2.3 Methods to estimate CO₂-background levels from continental near ground data: CWBA, CPBA, CSMBA, CDMBA

Local anthropogenic emissions, vegetation, soil respiration, geological soil degassing, wind and precipitations are the main influences on the CO₂-mixing ratios on continents near ground.

As the analysis of the vertical gradients at 500 m shows that annual averages are close to the mean, we can correct for the seasonal variations in the higher troposphere.

But near the surface (e.g. 1–50 m) mixing ratios can be much unsteady and CO₂-levels may vary in a wide range, dependent on local sources and sinks. Figures 9–12 show a range of up to 200 ppm at different locations inclusive some anthropogenic influence.

The Ameriflux network supplies a vast amount of high precision CO₂ and meteorological data from more than 130 sampling locations in continental environments with vegetation since 1996 at near ground levels (2–500m). About 30 data sources have been selected to work out methods for estimating annual background levels (Ameriflux 2009). Additionally the long time data series (1972–2008) from Schauinsland and data from some other stations have been used to test the CO₂-wind speed-background approximation (CWBA) developed by Massen et al. (2007), the CO₂-precipitation method (CPBA) (this paper), the summer minimum-background-approximation (CSMBA) (this paper) and the CDMBA, the daily minimum background approximation as proposed by C. Keeling (1958).

Background levels are characterized by well mixed conditions. Massen had shown that inland stations have a typical boomerang or sometimes a bi-lobe pattern investigating the CO₂-levels at rising wind speeds. At higher wind speeds (5–10 m/s) a quasi well mixed situation is achieved and the CO₂-levels represent the yearly average of the background level within a small error range (CWBA). By non-linear regression methods these CO₂-levels can be calculated. Equations from Massen (2004–2007 private communications) were applied to the data series in this paper:

$$\text{CO}_2 = A + B/X \quad (1)$$

X = wind speed or precipitation

Also other models are successful to fit the background levels:

$$Y = A * X^B \quad (2)$$

$$Y = A * e^{(B*X)} \quad (3)$$

$$Y = A + B*\ln(X) \quad (4)$$

$$Y = X / (A + B*X) \quad (5)$$

Since de Saussure 1810 (de Saussure 1830), it is known that precipitation lowers atmospheric CO₂-levels. This can be used to establish another tool to estimate CO₂ background levels per year within a small error range. Here we compare the CO₂-levels to the amount of precipitation. This emulates a quasi well mixed situation at high precipitation rates, because of washing out CO₂ from air to an equilibrium. The CPBA uses the physical effect of dissolution of CO₂ in water during times of precipitation. The remaining lower atmospheric CO₂ level is achieved faster than the CWBA during 2–3 mm precipitation. Again, non-linear regression models allow to estimate these lower CO₂-levels which are very close to the annual averaged MBLs.

Table 4. Data and error ranges for the CWBA and CPBA in Figure 9.

Stations	MBL (NOAA) ppm	wind speed – MBL approx, ppm; w	precipitation – MBL approx, ppm; p	Error %
Harvard Forest	MBL 2004= 376.76	377.67	378.78	w: -0.24, p: 0.53
Park Falls	MBL 2004= 376.76	382.57	383.66	w: -1.51, p: -1.79
Vaira Ranch	MBL 2004= 376.76	379.71	381.5	w: -0.77, p: -1.24
Hartheim	MBL 2003= 374.94	380.91		w: -1.57
Linden ¹	MBL 2008= 384.89	397.64		w: -3.2

Figure 9 shows typical examples for the validity of the CWBA and CPBA at continental locations with forest (Harvard Forest and Park Falls, USA), grassland (Vaira Ranch, USA), and rural area with agricultural use (Linden, Germany) and forest with anthropogenic influence (Hartheim, Germany).

¹ Linden, HLUG, Hessisches Landesamt für Naturschutz, Umwelt und Geologie.
<https://www.hlnug.de/messwerte/datenportal>

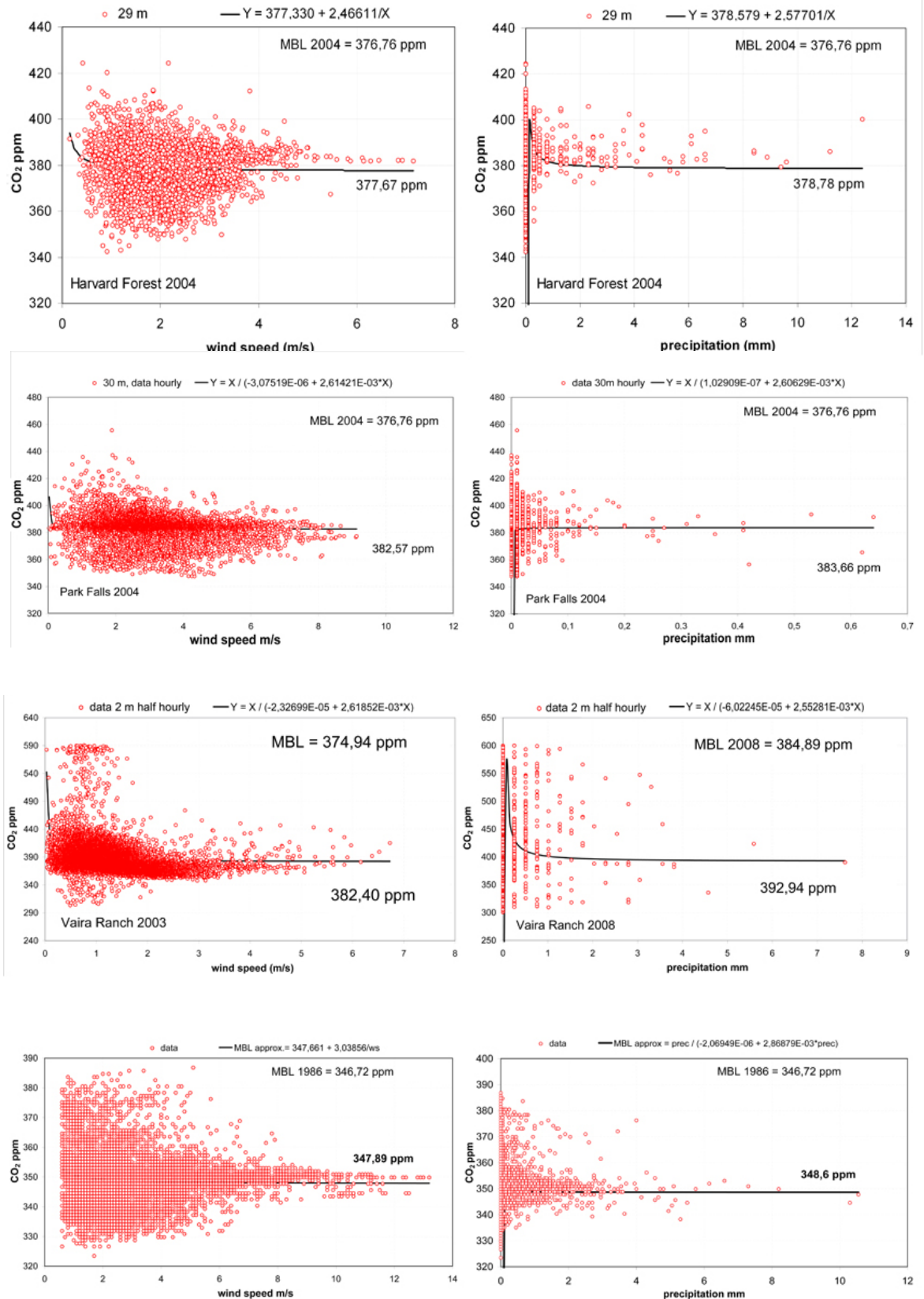


Figure 9. CO₂, wind speed (CWBA) and precipitation (CPBA) at Ameriflux station Harvard forest (lat 42.53N, long 72.17E, 360 masl), Park Falls (lat 45.94N, long -90.27E, 480 masl), Vaira Ranch (USA, lat 38.4N, long -102.95E, 129 masl), Linden (Hessia, Germany: lat 50.32N, long 8.41E, 173 masl); Hartheim, (Rhine valley, lat 47.93N, long 7.62E, 206 masl), Black: linear regression and asymptotic fit from Massen models (1) and (5).

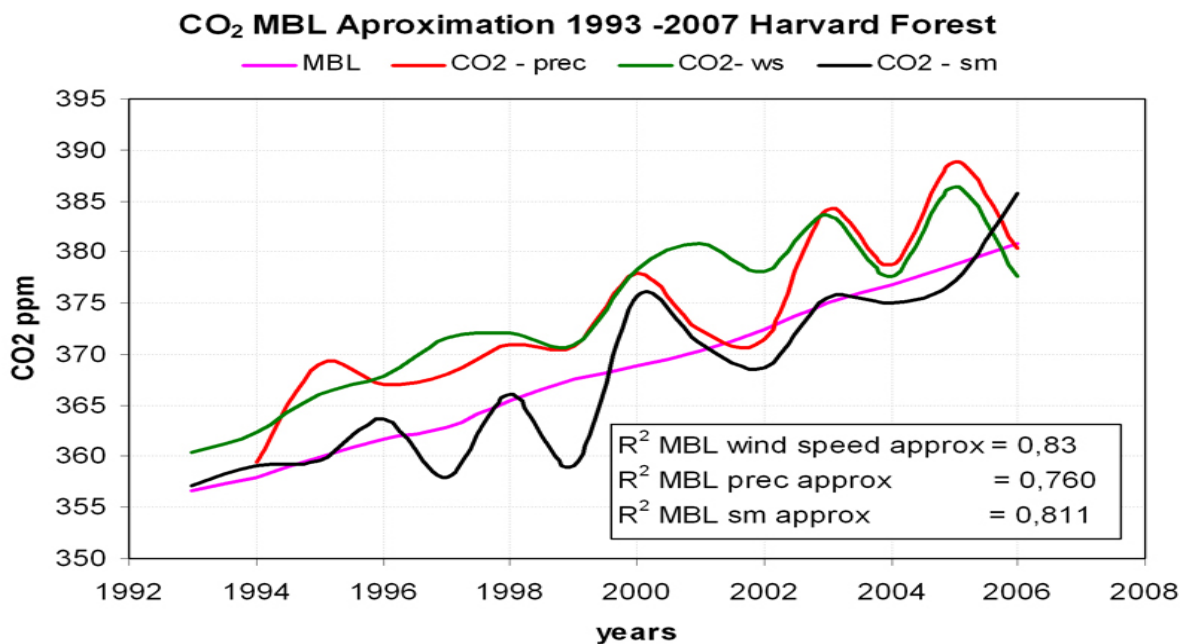


Figure 10. CWBA, CPBA and CSMBA at the Ameriflux station Harvard forest from 1993 to 2006 using hourly samples and their coefficients of determination. (ws = wind speed, sm= summer minimum, prec=precipitation).

Typical forest locations as Harvard Forest and Park Falls show a very good approximation to the MBL annual averages. In contrast to CWBA and CPBA, the CSMBA does not reflect the result of a physical process to establish a quasi well mixed situation. It's based on the simple calculation of the seasonal average from the summer minimum average in June, July, August compared to the total average of the seasonal cycle which appears 2 times a year in April and October/November. Therefore the method is limited by the amount of anthropogenic bias of natural sources and sink mechanisms.

Figure 10 shows the application of CWBA, CPBA and CSMBA to the available data from the Ameriflux station Harvard forest from 1993 to 2006 using hourly samples. 2007 data have been omitted because of too few CO₂ data are available.

The coefficients of determination show the very good correlation of the methods. At Harvard Forest the CWBA fits in average 1.25 % and the CPBA 1.51 % to the MBL (1993–2006).

At grassland environments like Ameriflux Vaira Ranch (lat 38.4 long -120.9, masl 129 m) the CWBA and CPBA resulted in the same approximation limits as can be seen in forested stations. In 2004 the MBL of 376.76 can be approximated to +0.77 % by the CWBA and to +1.24 % by the CPBA. Please note the tri-lobe pattern as outlined by Massen and Beck (2011 in CWBA in their Figure 5 to the right).

The Hartheim and Linden station has been included because of strong local influences. The Hartheim data were collected in the very hot summer 2003/2004 at a Scots pine forest growing in the warm and dry southern upper Rhine plain. The location has mixed vegetation and anthropogenic influence. Schindler et al. (2006) indicated a netto CO₂ emission at that period. Nevertheless the CWBA results in an error of -1.57 % compared to the NOAA MBL.

The Linden station has strong agricultural and forestry influence. Using wind speeds from 1.5 m/s, regression results in 397.64 ppm, the asymptotic value is 396.45 ppm, which is an error of +3 %.

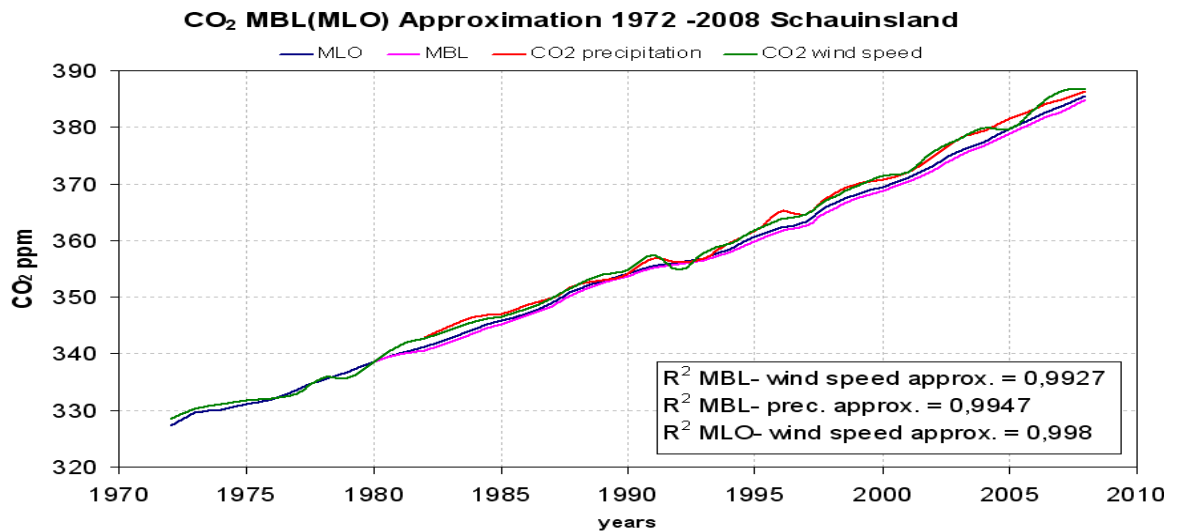


Figure 11. CWBA and CPBA applied to the CO₂ data series from Schauinsland, Germany, 1972–2008 lat (47.92°N, long 7.92°E, 1205 m masl), UBA (2009).

In Figure 11 the CWBA and the CPBA have been applied to estimate the global background levels from the 36 year long data series from Schauinsland (Germany) UBA (2009)². The Schauinsland station (47.55N, 7.55E, 1205 masl) is surrounded by forests and meadows situated about 15 km South-Southwest of Freiburg and west to the Upper Rhine rift and the French boarder. Annual mean precipitation is about 1,780 mm. Annual mean temperature is about 5.6 °C. Prevailing wind is south westerly with anthropogenic influence mainly during nights. R² are the coefficients of determination which show strong positive correlation and a very small error range within about 1 % despite of its vicinity to biogenic and anthropogenic sources and sinks. (Schmidt et al. 2003).

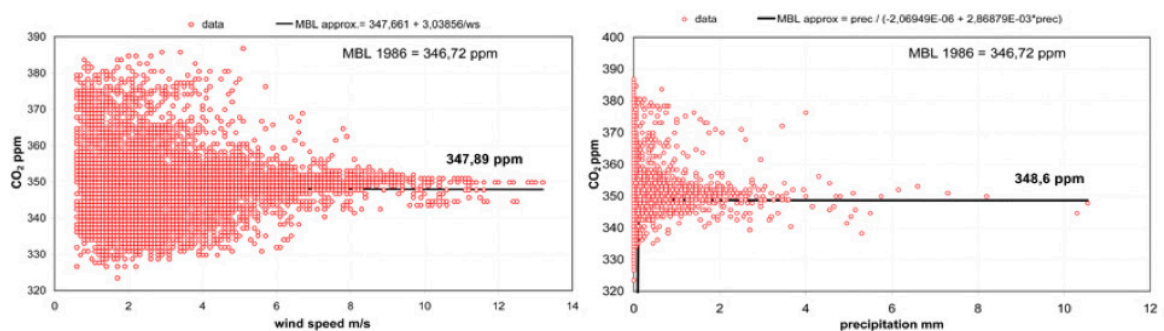


Figure 12. CO₂ wind speed (CWBA) and precipitation (CPBA) at the Schauinsland station during 1986 using 1/2 hourly samples. Black: asymptotic fit

Figure 12 shows a typical example of the CWBA and CPBA applied to the Schauinsland data 1986. Using one of the nonlinear regression models the CWBA results in 347.89 ppm, the CPBA in 348.6 ppm which is an error of +0.33 % and +0.54 % to the 1986 MBL of 346.72 ppm. The CPBA patterns for the period of 36 years at Schauinsland are nearly identical to the CWBA pattern and show that the MBL can be approximated within very small error range from about 4 mm precipitation.

C. Keeling (1958) had found in 1955 minimum daily CO₂ concentrations in the afternoon and observed the same at other locations. He suggested that this is a meteorological phenomenon. This can be used to check if this minimum value represents the MBL or background level in the higher troposphere.

2 Schauinsland data set supplied by Kerin Uhse UBA (Umwelt Bundesamt) 2009, outliers corrected.

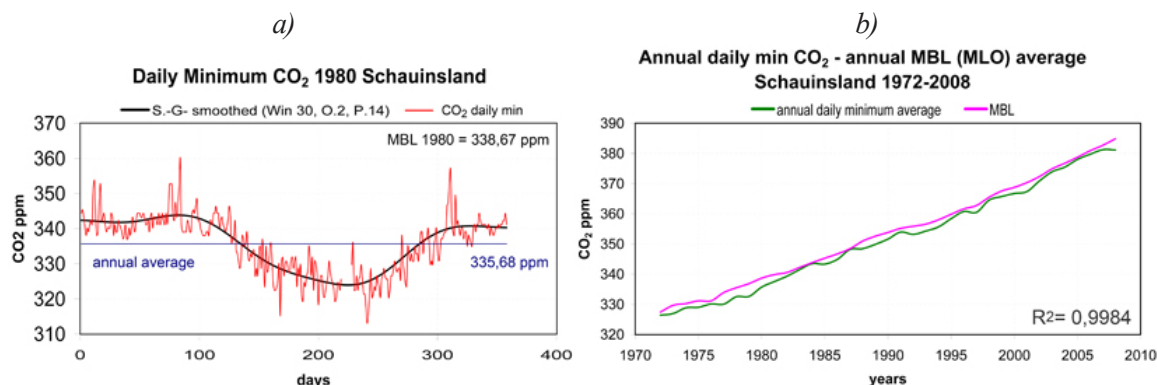


Figure 13a). Daily minimum CO₂-levels 1980 at Schauinsland (Germany) and b) annual average for daily minimum 1972–2008 compared to MBL/MLO annual average

Figure 13b shows the calculation of the daily minimum values for 36 years of annual data at Schauinsland (Germany). As an example the 1980 SEAS is presented as daily minimum smoothed by a Savitzky-Golay Filter (Win 30, order: 2, passes 14). This is shown in Figure 13a.

The daily minimum average (CDMBA = CO₂- daily minimum- background- approximation) at the Schauinsland station 1980 was 335.68 ppm which is only -0.88 % different from the MBL average of 338.67 ppm. The calculation of the CDMBA for the whole 36 years at Schauinsland reveals a very good correlation. Total average for the 36 years is 351.95 ppm and the MBL average 353.85, a -0.54 % difference. The smoothed seasonal amplitude is 17 ppm compared to the averaged 13.8 ppm deduced by Schmidt et al. (2003).

Additionally, the CWBA, CPBA and CSMBA were tested at dozens of other stations for example Mead Rainfall, Duke Forest, Howland Forest, UMBS, Niwot, AMT-Maine, ARM, WLEF, WKT, UCI, UMBS (USA, Canada), Wasserkuppe (Hessia), Hartheim (Germany) and more.

The MBL over typical forest and grassland environments can be modelled by CWBA and CPBA from near ground sampled data within 1 %. The CSMBA method approximates the MBL from near ground data within about ± 1.5 %. At continental environments outside cities even with stronger anthropogenic influence the CWBA, CPBA and CSMBA are valid within about ± 2.5 %. The CDMBA is also valid at mixed continental and marine environments showing errors around 1 %.

2.4 Estimation of atmospheric CO₂ background levels since 1800

We have applied vertical profile analysis, CWBA, CPBA, CSMBA and CDMBA to the historical CO₂ data series. The methods outlined in 2.3 has been applied to the historical data set compiled in the supplemental data files: CO₂MBL_1800–1960.xls and CO₂raw.zip. Daily data in CO₂raw.zip are the basis to calculate monthly averages in CO₂MBL_1800–1960.xls.

CO₂MBL_1800–1960.xls also contains the procedure to estimate the annual CO₂ background levels from these data for each selected station.

In contrast to the continuous sampling since 1958 the historical data have been collected at hundreds of different locations. Sampling periods differ in decades, years, months or days.

A lot of the historic measurement series have been collected only during seasons of the year mostly at summer time on continental stations. Therefore the presented 4 tools CWBA, CPBA, CSMBA and CDMBA have been applied when sampling period had fitted.

Using available meteorological and oceanographic data from each sampling location given in the historical literature to analyse air masses it is possible to estimate annual CO₂ background level within an error range of about ± 3 % (chemical methods). A SEAS range is used between 12.5 and 18.5 ppm for years with MBL average around 315 and 380 ppm. At coastal stations winds from the sea are preferred for calculations, also CWBA, CPBA and CSMBA at continental stations or data sampled on rainy and stormy days.

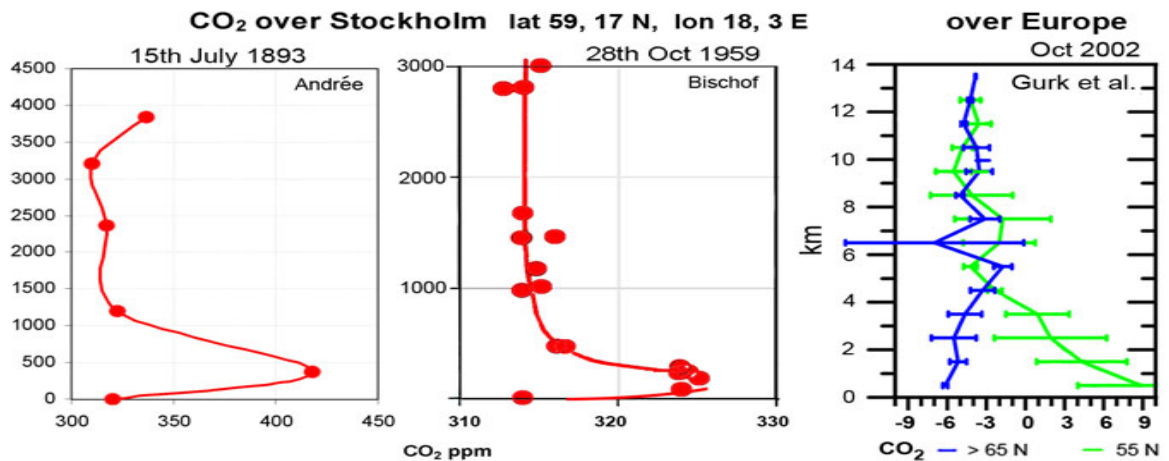


Figure 14. Vertical profiles of atmospheric CO₂ in the air over Stockholm 1893 (Andrée cited in Letts and Blake, Stockholm 1959 (Bischof 1960) and over Europe 2002/2003 (Gurk et al. 2008). On the right: green lines= lat 55°N, blue= >65°N, modified from Gurk et al.

The following examples are typical for the estimation process:

2.4.1 Background estimation for 1890, 1893, 1935 and 1959

Available historical literature supplies 4 vertical profiles measured in 1893 by Andrée (Balloon near Stockholm, up to 3837 m; Petterson gas analyzer; error $\sim \pm 1-2\%$), 1911 by Wigand (Balloon Bitterfeld (Germany) to 9040 m; fractionated condensation method, according to Erdmann, error $< \pm 1\%$), Kauko 1935 over Helsinki up to 1600 m (condensation method $\pm 0.33\%$) and Bischof 1959, near Stockholm as high as 3 km (NDIR $< \pm 1$ ppm) (Letts and Blake 1899–1902, Stepanova 1952, Bischof 1960).

Figure 14 reveals the same CO₂-levels near ground as in the upper troposphere. The latitude of Stockholm is about 60°N so the assumed vertical profile is between the blue and green line which is near the yearly average. The amplitude of 16.5 ppm in Figure 12 used for the reconstruction of the 1893 CO₂ background level has to be reduced by about 10–15 ppm for the data at latitudes around 60°N.

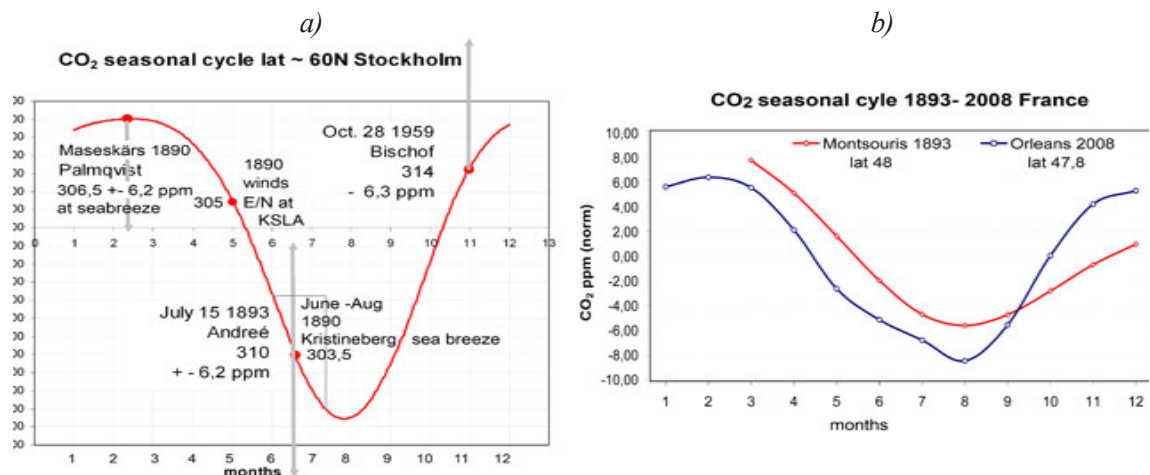


Figure 15a). Calculated atmospheric background CO₂ in the air over Stockholm: 1893 Andrée cited in Letts and Blake (1899), 1959, Bischof (1960), and as a mix of MBL at Pallas and Baltic Sea. The contour (red line) is generated by mixing Pallas and Baltic Sea Globalview-CO₂ SEAS data and fitted according to the Loess Algorithm Cleveland (1993). b) Comparison of smoothed (Savitzky-Golay (Autosignal 2009)) measured SEAS at Montsouris 1893 and Orleans 2008 (Globalview-CO₂) (Montsouris data are without erratic January and February values).

According to the analysis in Figures 14 and 15, I estimate the CO₂ background level in 1893 measured over Stockholm to be 315 ± 6.3 ppm. The MBL in 1959 must be 316.98 ppm (MLO+1). Bischof had measured 314 ppm in Oct. 28th, 1959. The October value must be 3.33 ppm above MBL. If we accept the MLO data, the Bischof value of 314 has an error of +6.3 ppm or +2 %.

A comparison of the SEAS measured at Montsouris in 1893 and the MBL SEAS from Globalview-CO₂ for Orleans in 2008, both at a latitude of around 48°N shows the good fit August as the summer minimum (Montsouris 307.3 ppm). The SEAS shows a good fit in 1893 and 2008 for despite of the difference in amplitude (about 13 ppm Montsouris) and levels (2008 about 380 ppm, 1893 about 310 ppm). The Montsouris data reveal a summer minimum of 307.5 ppm and a MBL level of 313 ppm assuming a 14 ppm amplitude.

Therefore, I conclude with a background summer minimum of 306.5 ppm in 1893 with a MBL average of 315 ± 6.2 ppm for Stockholm 1893 measured by Andrée at latitude of about 60°N. The difference of about 2 ppm accounts for the latitude difference.

For the years 1889/90 we can use the marine and coastal data sampled at Kristineberg (Sweden), the island of Maseskärs (Sweden) and the continental data from Stockholm done by Augusta Palmqvist, Montsouris (Paris), Gembloux (Belgium) and Odessa (Ukraine). The most accurate temperature constant volumetric Pettersson gas analyser was used by Palmqvist (error 1–2 %). The Montsouris and Gembloux-data (Pettenkofer variant) have to be corrected by +18.5 and +20 ppm because of CO₂ absorption losses due to the management of water content and procedural similarities to the lossy Reiset gas analyser in drying acid before absorption in alkaline solution (Stanhill 1983; Beck 2007). Both data series show erratic SEAS all over the years with much too low values during winter time and lacking the typical continental amplitude of about 25–40 ppm. The Montsouris data show an about 20 ppm rise since July 1890 due to changing the procedure (Stanhill 1982).

CO₂ SEAS Montsouris 1877-1910, Petermann 1890

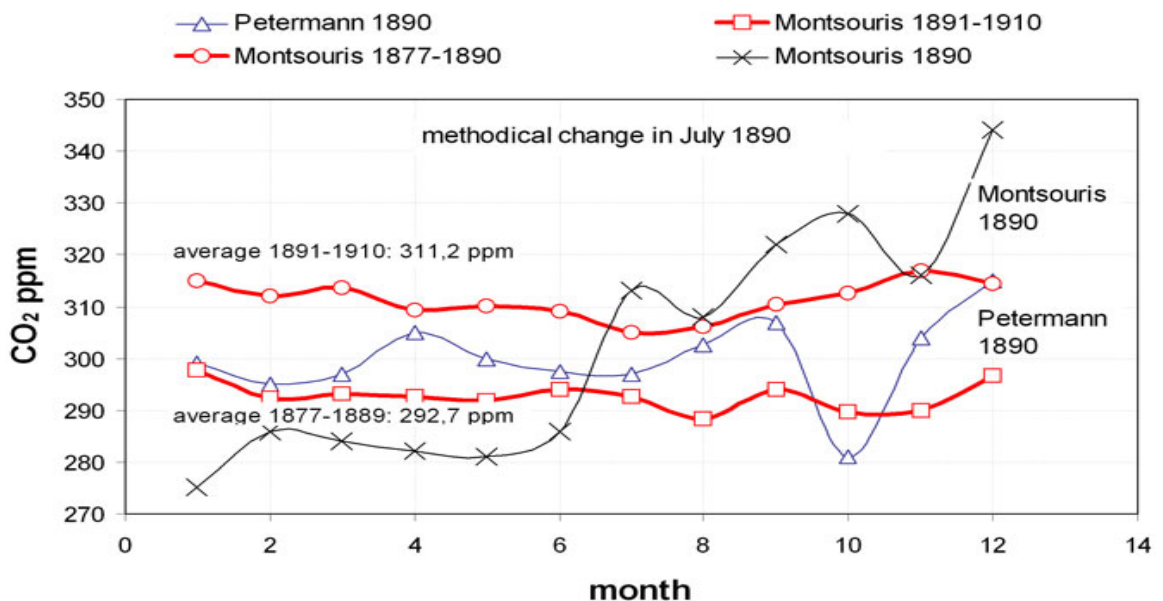


Figure 16. CO₂ SEAS analysed in Montsouris 1877–1910 and Gembloux (Belgium). Letts and Blake (1899). Methodical change in July 1890 leads to a shift up of 18.5 ppm in average SEAS (red). Erratic SEAS measured at Montsouris (black) and Gembloux (blue) 1890.

In 1890 Palmquist (1892) conducted 484 detailed air analyses at Stockholm (lat 59.2 N), Tromsø (Norway, lat 69 N), Maseskär (Sweden, Island, 7 km from the coast in Skagerrak, lat 58.5 N), Kristineberg (Skagerrak) and at the agricultural research station 1.5 km north of Stockholm KSLA) from 281 samples. CWBA and CPBA were not applicable to the Stockholm data (January to May average 323 ppm) because of the lack of precipitation observations in 1890 and only wind speeds of max. 2 m/s. Analysis of wind direction at the Stockholm station reveals lowest CO₂ in winds from eastern and northern direction with an average of 305.2 ppm from 21 samples in May. Winds from the sea at Maseskär island (Sweden) showed a CO₂ level of 306.5 in February which is taken as the reference for 1890 because of a marine location far from sources (stony island without vegetation), samples of air from the sea analysed with the most accurate volumetric temperature compensated equipment at that times (Petterson, 1–2 % accuracy), done by an experienced person.

Table 4 lists the data from 1890 at 7 different locations including 1125 samples. The Tromsø data show a weak influence of the mixed coastal/continental location as can be seen in the Odessa and Stockholm samples. The complete seasonal cycles measured at the continental stations at Paris and Gembloux had to be corrected because of the sulphuric acid loss error and other methodical errors. At Montsouris the method was changed in July 1890 resulting in a large shift upwards in the CO₂ level of in average 18.5 ppm which was added to the whole series after that date.

Callendar (1940, 1958) had listed the Montsouris and Gembloux data, also From and Keeling (1986) and Wigley (1983) had listed the Petermann data series, rejecting it because of the poor quality without discussing methodical aspects.

The amplitude of 16.5 ppm in Figure 15 used for the reconstruction of the 1890 CO₂ background level has to be reduced to about 10–15 ppm for the data at latitudes around 60 N.

Table 5. CO₂ in the atmosphere 1890 over Europe (1125 samples, 484 analyses in Scandinavia)

	CO ₂ ppm	samples	Station/ Author	lat	remarks
1	306.5	38	Maseskär, Palmqvist	58.5	Sea breeze SW, W, NW; February
2	303.5	64	Kristineberg, Palmqvist	59.17	Sea breeze from June, July, August
3	314.4	23	Tromsø, Palmqvist	69	At stormy winds NW/SW
4	305.2	197	Stockholm KSLA, Palmqvist	59.2	Winds from E/N in May
5	304	-	Odessa (Ukraine), Lebedinzeff	46	Average March/April at rural area
6	302.1	365	Montsouris, Levy	46	SEAS average, corrected +18.5 ppm
7	300	365	Gembloux, Petermann	50.5	SEAS average, corrected +20 ppm

Estimation for the background level 1890: 302.5 ± 6.2 ppm (Maseskär: 306.5 - 6 ppm).

Figure 17 b) reveals that the average in about 1.5 km altitude over Europe in January 2002 for similar latitudes is close to 375 ppm. The annual average of CO₂ background at 4 km altitude from Figure 6 is 373.5 ppm which corresponds very well to the global MBL average of the years 2002/2003 of 373.7 ppm Globalview-CO₂ (2009). Figure 7 shows the same deviation of about 2 ppm from the average at similar latitude and altitude (e.g. Surgut). This indicates that in 1935 Kauko had measured the real background CO₂ in the air over Helsinki (lat 60.1 long 25E) of 361 ppm ± 0.33 % in Dec. 7th and 375 ppm ± 0.33 % at 1000 m in Feb. 20th over the clouds. For an estimation of the CO₂ background average for 1935 the modern seasonal averages listed in Globalview CO₂ at similar latitudes of Pallas Finland, lat 68N, Baltic Sea lat 55N, Zotino lat 60N and Shetland lat 60.1N from Globalview-CO₂ are helpful. Globalview MBL CO₂ data since 1980 are comparable to historic times because they exhibit about the same high atmospheric CO₂ range of about 360–380 ppm as the historic data to be evaluated.

The typical seasonal amplitude at the stations varies from 20.4 ppm at Zotino to 14.8 ppm at the Shetland station and 16.8 ppm at Pallas (lat 67.97 N, long 24.12 E).

The larger seasonal amplitude at Zotino (lat 60 N) is due to a typical continental location, the smaller Shetland cycle (60.1 N) corresponds to a typical marine station. The difference between the Baltic Sea seasonal cycle (lat 55 N) and Pallas cycle (lat 68 N) is <1 ppm in amplitude and summer minimum. Therefore, we conclude a seasonal cycle for the air over Helsinki as a coastal station of about 16.8 ppm.

For estimating the 1935 CO₂ background we need to check the available data:

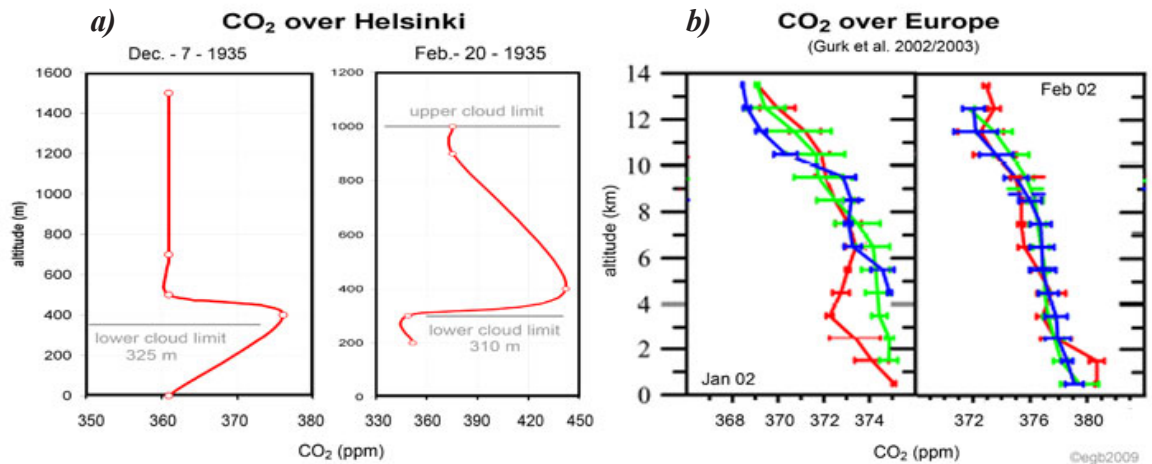


Figure 17a). Vertical profiles of atmospheric CO₂ in the air over Helsinki 1935 by Kauko and b) over Europe 2002/2003 (Gurk et al. 2008). On the right: green lines= lat 55N, blue= >65N, red<40N.

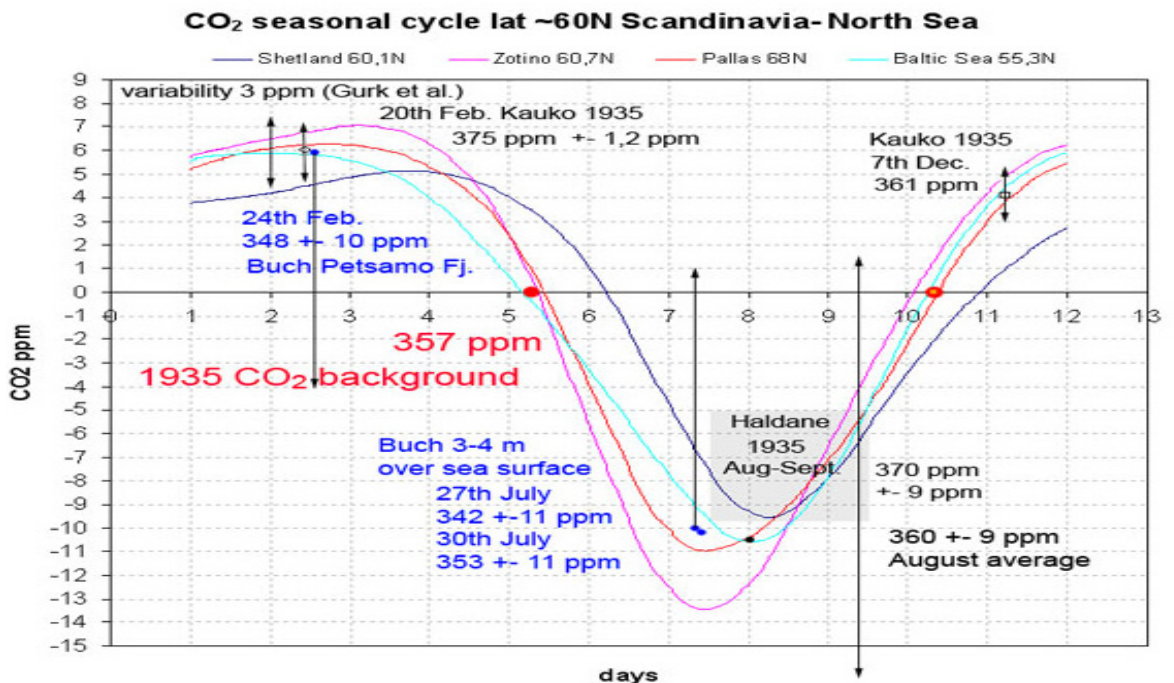


Figure 18. CO₂ seasonal cycles around lat 60N Scandinavia, North Sea (Globalview-CO₂ 2008) and measured CO₂ around 1935 at various stations (troposphere, coast to Barent Sea, Scotland, Northern Atlantic Ocean). Arrows= error bars of sampling method. CO₂ data correct in time scale. Contours of graph fitted with the Loess algorithm.

Table 6. CO₂ in the atmosphere 1935/1936

1	361 ppm \pm 1.2 ppm	1600m altitude, Dec.1935, 1 km above cloud coverage, (Kauko); 3 x 361 ppm from 500 to 1600 m.
2	375 ppm \pm 1.2 ppm	1 km altitude February, directly at the upper cloud limit (Kauko).
3	370 ppm \pm 9.2 ppm	near ground, winds from the sea Aug./Sept. average (Haldane).
4	360 ppm	average in August 1935 at Cloan (Scotland), rural station (Haldane).
5	348 ppm \pm 3 %	1935 at the Petsamo Fjord (Barents Sea) 24th February (Buch).
6	342 ppm \pm 3 %	1935 at Woods Hole USA coast and sea. (Buch).
7	353 ppm \pm 3 %	1935 Crossing the Atlantic Ocean (Buch)
8	>360 ppm	several CO ₂ data 1934 (Buch over the Atlantic Ocean) and 1936 (Buch over the Atlantic Ocean Norway-Spitsbergen)
9	358 ppm	spring 1936 average, Duerst, Switzerland, rural location, only influence of vegetation)
10		Seasonal Cycles GlobalviewCO ₂ lat N 55–68, modelled by the Loess algorithm.

During 1935/1936 another systematic analysis of air in Scotland is available by Haldane (1936). His volumetric gas analyzer was a standard in science for the first 50 years in the 20th century showing an accuracy of about 2.5 % (Beck 2007). The results of 1500 analyses, part of them using country air done at 1.2 m to 21 m above ground in Scotland (Cloan area, lat 56N and Ayrshire coast, lat 55N) since July 1935 are:

1. 153 daily analyses made at Cloan (Perthshire) during August 1935 were 320–400 ppm (average 360 ppm), 15 made at night showed 380–600 ppm. The whole range over ground was 210–440 ppm.
2. Samples of air blowing inland off the sea on to the coast of Ayrshire in August and September averaged 370 ppm of carbon dioxide and reflects the CO₂ rich air over the Firth of Clyde, North Channel and the islands there.

Buch did systematic analysis of air over sea in the northern and Arctic Atlantic Ocean from 1932 to 1936 Buch (1939a,b, 1948) during several travels by ship to Island, Spitsbergen, Woods Hole USA and New York. Furthermore, a data series sampled at Petsamo (Barents Sea) within 1.5 years is available. He used the gas analyser of Krogh and Rehberg (\pm 3 % accuracy).

Duerst at mountains and shores of the Sea of Geneva (Switzerland) collected about 1,500 samples from 1936 to 1938. He used an optimized Pettenkofer method with \pm 3 % accuracy.

361 ppm reflects the December background, measured several times 1 km above clouds by Kauko. The February value of 375 ppm is the result of the influence of clouds. The 370 ppm measured by Haldane at the Scottish coast in August/September 1935 reflects the CO₂ enriched air of the coastal islands. Considering the error range and the fact that the difference continental/marine air at coasts are in the range of 10 ppm, the value has to be corrected by about 8 ppm. The average of 360 ppm at the rural Scottish environment reflects the continental summer minimum there. The value is near the correct CO₂ background within its \pm 2.5 error range of method and CSMBA(see below).

The Buch data supports the CO₂-levels around 360 ppm in 1935. His samples 3–4 m over sea show absorption by the ocean especially near the Arctic circle with lowest values. Samples at 30 m above sea surface had about 10 ppm higher values.

Inspection of adjacent years in 1934 and 1936 show similar data with higher values in 1936. Buch had measured >368 ppm over the North Atlantic Ocean from Norway to Spitsbergen in 1936.

From the above analysis I conclude the average annual CO₂ background for 1935 is equal to 361 -4 ppm = 357 ±1.2 ppm and could have been measured according to the above evaluation of data at the end of May and October 1935 in the air over Helsinki.

2.4.2 Background estimation for 1920–1926

During 1920 to 1926 H. Lundegårdh analysed about 3000 air samples from June to September at Hallands Väderö, an island in Kattegat, southern Sweden using a gas analyser with optimized

Pettenkofer method to ±1 %. (Lundegårdh 1922).

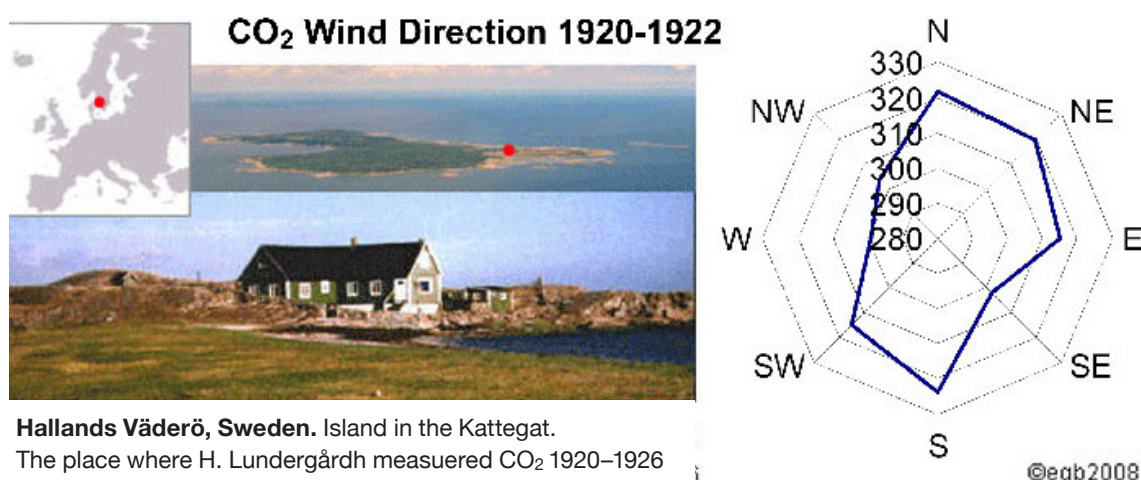


Figure 19. The ecological station of H. Lundegårdh 1920–1926 analysing air samples in the summer at Hallands Väderö (southern Sweden). The CO₂ wind direction 1920–1922 is presented at the right. S = south direction (photo ©<http://www.shvn.se/>); 8 masl; lat: 56° 25.8'N long 12° 34.3'E. (Lundegårdh 1924, 1949).

Wind analysis in Figure 19 shows that winds from the open sea (W, NW) have the lowest CO₂ concentration in summer (about 305 ppm). Air masses from the Northern and North-Eastern forests on the island provide higher CO₂ mixing ratios (about 320 ppm). Data in 1923 show mainly winds from the western direction. The station can be categorized as marine and coastal.

Table 7. CO₂ data (Hallands Väderö summers 1920–26).

	1920	1921	1922	1923	1924	1925	1926
Temperature °C	19.1	17.3	16.5	15.4	16.4		
averaged CO ₂ ppm, measured	329.5	303.1	284.3	300.0	331	312.5	320.0
reconstructed annual CO ₂ background	316	306.8	290.1	301.8	319.9	318.3	321.9

From Lundegårdh (1924, 1949); recalculated data. Data June–August 1920–1926

*data recalculated by using : $ppmv = (mg/m^3)(273.15 + C^\circ) / 12.187(44.01)$

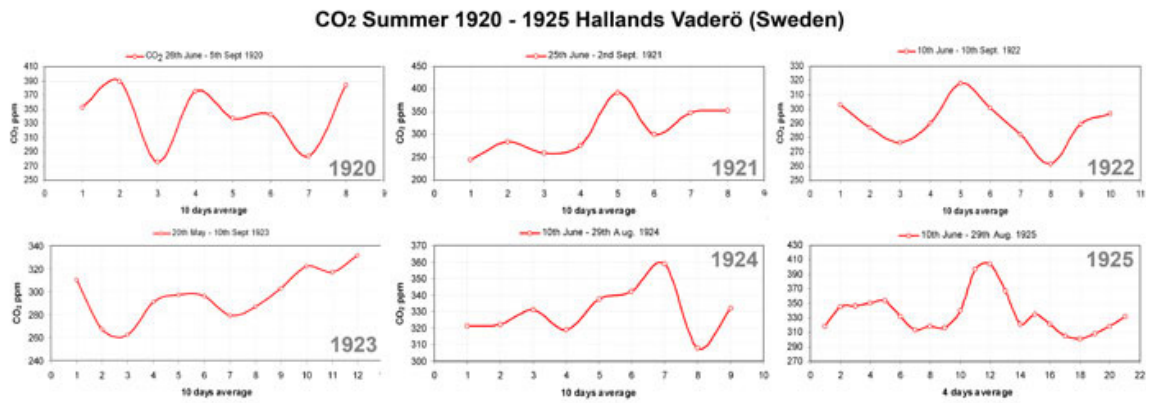


Figure 20. CO₂ in air at the shore of Hallands Väderö during 1920 to 1925 (10 days average June 29–Sept 2).

The June/July data usually show lower CO₂ than the second half of the summer. CPBA for summer 1921 estimates 306.76 ppm as the MBL for 1921 at Hallands Väderö.

The CO₂-levels through these years are characterized by a drop of > 20 ppm in the summer 1923 and reconstituting the former levels within 3 years. At the same time SST and temperature also drop down in the North Atlantic Ocean at lat 45–80N and long 0–15E at about 1.5 °C in average (see Figure 21 left). Figure 21 shows the evolution of three parameters in time as summer averages (June–July–August). SST is taken from COADS (KNMI), air temperature from Copenhagen (NCDC 2009) and CO₂ at Hallands Väderö according to Lundegårdh (1924, 1949).

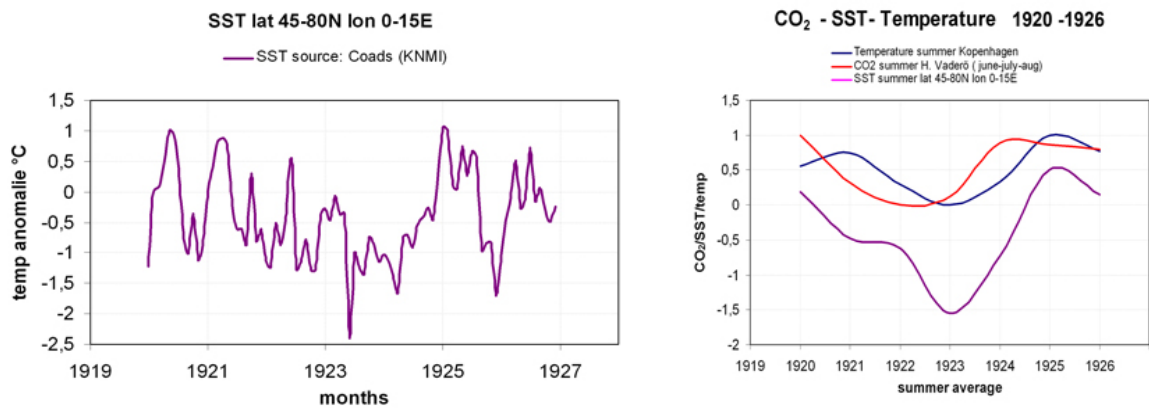


Figure 21. Monthly SST (left violet; COADS, KNMI), right: Copenhagen; summer temperature (blue: NCDC 2009), CO₂ (red): at Hallands Väderö, Kattegat (Lundegårdh (1924, 1949), SST summer (violet). All curves are anomalies.

Cross correlation calculation reveals a lag of 1 month of CO₂ behind SST. In Figure 22 one can see that the CO₂-levels mimic the SST contour with a time lag of about 1 month.

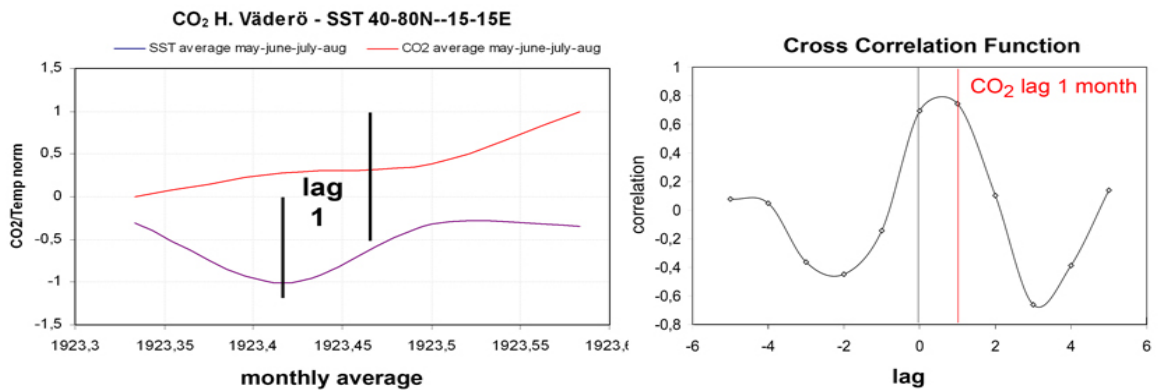


Figure 22. Time lag of CO₂ with respect to SST in 1923 at Hallands Väderö as monthly averages (left); cross correlation calculation (right).

In order to reconstruct the annual CO₂ background mixing ratios from 1920 to 1926 it is necessary to use the seasonal cycle data analysed at a nearby modern station, Baltic Sea (55.35°N, 17.22°E, 28 m; Globalview-CO₂, 2008).

In the summer of 1921, B. Schulz collected sea- and 25 atmospheric CO₂-samples during a cruise by the exploring ships Poseidon in the North Sea, and Skagerak (16th–31th July), and (24th August–17th September) in the Baltic Sea (Schulz 1922). He reported that the surface layers of the sea were always super saturated by CO₂ especially in the Baltic Sea. The Poseidon cruised in the Kattegat along the coast of southern Sweden (Hallands Väderö) and the Baltic Sea. The samples were analysed in the laboratory of the Deutsche Seewarte using the Krogh gas analyser (accuracy $\sim \pm 2$ %).

Table 8. CO₂ level in samples during the cruise of the Skagerak, Kattegat, and Baltic Sea July–Sept 1922.

Samples	1	2	3	4	5	6	7	8	9
CO ₂ ppm	305	290	320	300	275	290	310	290	290

Average: 297 ppm; average sea surface CO₂ 343 ppm (Schulz 1922).

From these data and the average in 1921 at Hallands Väderö we calculate a summer minimum of 301 ppm using the average of 5.1 (+1.7 % ppm from Table 3 and 6.5 ppm as the summer minimum from the seasonal cycle (Baltic Sea) as an addition, resulting in 306.8 ± 4.6 ppm (error level from method 1.5 % method) as the background level in 1921 over Hallands Väderö. The low CO₂-levels in 1922 are estimated as follows:

CWBA summer 1922: 283.9 ppm; CPBA summer 1922: 282 ppm. Lundegård average 284.3 ± 5.8 ppm = 290.1 ± 2.9 ppm.

The levels in 1920 show very high outliers around the 10th, 26th July and 3rd August. Eliminating these values and considering the very different SST values during this year the estimation for 1920 at Hallands Väderö = 318.3 ppm summer minimum $+5.1 = 323.4$ ppm ± 3.2 ppm (error level from method 1 %).

In 1923 the winds came mostly from W/NW at Hallands Väderö with CO₂-levels just below 300 ppm. The summer minimum from data is 296 ppm, CPBA for the summer results in 298.9 ppm, CWBA is 283.85 ppm, so we estimate the CO₂ background level to $296 + 5.8$ ppm = 301.8 ± 3 ppm.

The air in 1924 at Hallands Väderö show higher CO₂-levels again accompanied by a rise of the SST by about +2 °C in average in the Baltic Sea and Kattegat. Correcting outliers around the 22th, 48th, 61th and 66th day leads to $324.9 + 5.8$ ppm = 330.7 ± 3.3 ppm. Summer CPBA is 337.5 ppm. The June average by Lundegårdh was 319.7 ppm, Meinecke at Eberswalde had measured 320 ppm after rain. So we had to correct the CO₂ background for 1924 to 319.9 ppm.

In 1925 E. Rheinau analysed air near ground and around Davos, Switzerland (1600–2500 m elevation) using the Petterson/Sonden gas analyser at the meteorological station Davos in August 1925, Rheinau (1926). 154 samples have an average of 293 ppm. A lot of days show fog and rain, at clear days levels are well beyond 310 ppm. The data are ignored because of too large uncertainties.

Lundegårdh (1949) lists 312.5 ppm in his table 45 p. 32. Digitalization from his graph p. 33 results in an average of 335.5 ppm, outlier and temperature corrected to 329.5 ppm. Because the SSTs are still down in 1925 we use $312.5 + 5.8 = 318.3$ ppm.

Table 9. 1926 summer observations.

Station, author	CO ₂ ppm
Lundegårdh, Hallands Väderö	320
Krogh et al. (1929), Copenhagen, Greenland	318.5, 312, 310, 328
Wattenberg (1933) over sea surface in Atlantic Ocean	313.4
Average	316.9

CO₂ background estimation for 1926: $316.9 + 5 \text{ ppm summer minimum} = 321.9 \text{ ppm}$ as 1926 CO₂ background level.

2.4.3 Background estimation for 1939–40

Figure 23 presents a re-read of the data of W. Kreutz compared to the data presented in Massen and Beck (2011). The CWBA difference is $(392.6 - 390) = 2.6 \text{ ppm} = 0.7 \%$.

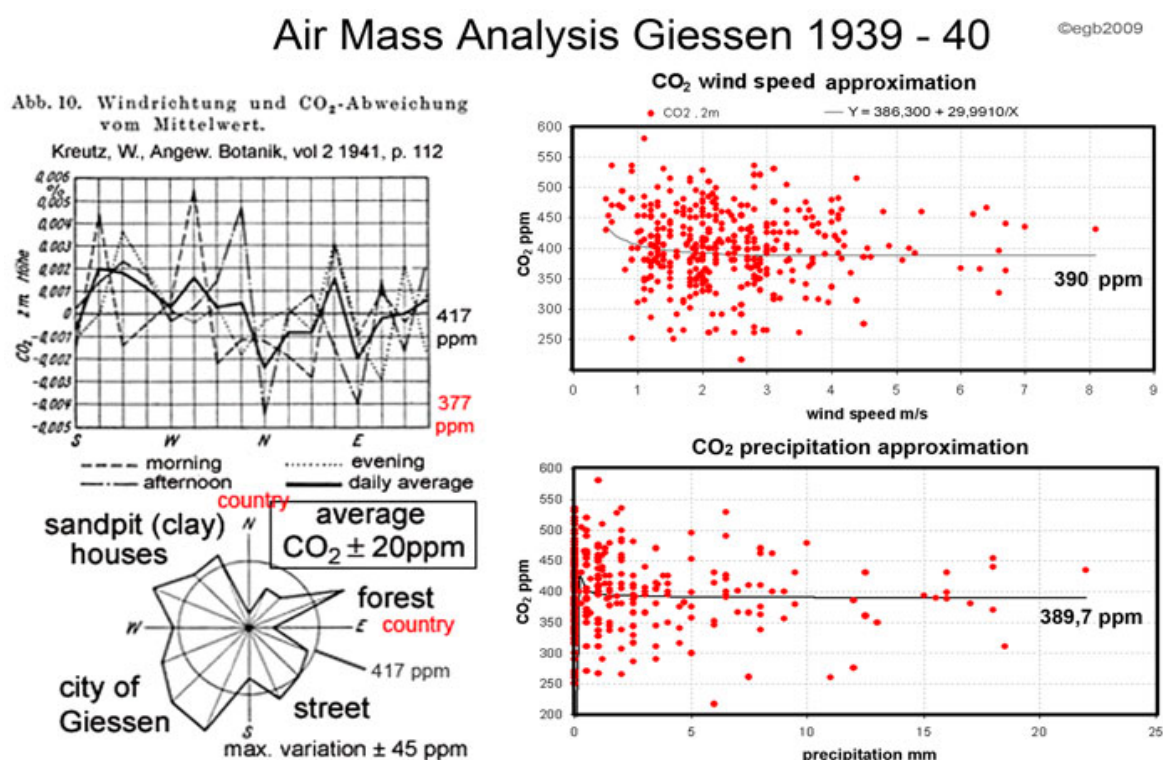


Figure 23. Air mass analysis using Giessen data from 1939–40. CO₂ variation sampled every 90 minutes 2 m above ground. On the left the air mass analysis done by W. Kreutz 1940, on the right the CWBA and CPBA at Giessen sampling station. The Massen model and asymptotic fit shown as grey line. Data from Massen and Beck (2011).

The approximated background level at Giessen 1939/40 by CWBA was 390 ppm and by CPBA it was 389.7 ppm, which is in good agreement to the air masses with the lowest CO₂-levels blowing from the north and east (rural area) at that times as deduced by W. Kreutz in 1942 of about 377 ppm. (Beck 2007). The standard deviation is 6.47. The CSMBA (June-July-August) cannot be calculated because the data series starts in August 1939. The August average is 338.5 ppm and the average for August/September is 347.8 ppm. The October average was 386 ppm.

The accuracy of the volumetric gas analyzer used (RICO C) was $\pm 1.5\%$ (Schuftan 1933, cited in Beck 2007). So we can calculate $\pm 1.7\%$ (CPBA) from the average $(389.7+390)/8 + 386/4 + 377/2 = 382.4 \pm 2.5\%$. This CO₂ level must be therefore considered as CO₂ background level at Giessen in 1939/40.

In a recent paper by Massen and Beck (2011) we presented a CWBA for additional historical data series e.g. at Vienna 1957/58 by F. Steinhauser at the meteorological station Hohe Warte estimating a MBL of 324 ppm.

3. Results and Discussion

The analysis presented above results in the estimation of eleven MBL approximations as examples for the whole data set of historical near ground sampled CO₂ values.

Table 10. Some MBL examples.

Year	Location	MBL estimate	Year	Location	MBL estimate
1890	Scandinavia ~60 N	302.5 \pm 6.2 ppm	1924	Hallands V. 55 N	319.9 \pm 3.3 ppm
1893	Stockholm 60 N	315 \pm 6.2 ppm	1925	Hallands V. 55 N	318.3 \pm 3.2 ppm
1920	Hallands V. 55 N	316 \pm 3.2 ppm	1926	Hallands V. 55 N	321.9 \pm 3.2 ppm
1921	Hallands V. 55 N	306.8 \pm 3 ppm	1935	Helsinki 60N	357 \pm 1.2 ppm
1922	Hallands V. 55 N	290.1 \pm 2.9 ppm	1939	Giessen 48N	382.4 \pm 9.5 ppm.
1923	Hallands V. 55 N	301.8 \pm 3 ppm			

Applying the methods outlined above to all available historical data listed from chemical CO₂-analysis listed in table 1, 134 yearly averages have been calculated representing the estimated CO₂ background levels. Since 1870 to 1960 errors had been estimated to $\pm 0.33 - 3\%$ or max. ± 9 ppm referred to a CO₂ level of 300 ppm accepted as average through the two centuries.

Table 11 lists the annual CO₂ MBL estimations since 1826 to 1960 from data compiled in the files *CO2_MBL_1800-1960.xls* and *CO2_raw_1800-1960.pdf*.

Table 11. Annual CO₂ MBL estimations from 1826 to 1960 from direct measurements

1	2	3	1	2	3	1	2	3	1	2	3	1	2	3
1826	364.50	72.90	1856	335.20	33.52	1886	299.00	8.97	1916	323.40	9.33	1946	336.00	47.04
1827	359.00	71.80	1857	337.00	33.70	1887	302.80	9.08	1917	321.60	10.20	1947	338.00	47.32
1828	358.00	70.80	1858	335.20	33.35	1888	300.00	9.00	1918	317.00	10.46	1948	328.40	45.98
1829	339.00	67.80	1859	333.50	33.50	1889	300.80	6.02	1919	320.20	10.44	1949	316.00	9.48
1830	339.90	67.98	1860	331.80	33.30	1890	302.40	6.05	1920	323.40	10.43	1950	308.85	9.27
1831	340.80	102.24	1861	330.10	33.10	1891	308.10	9.24	1921	305.80	3.07	1951	314.50	9.44
1832	341.70	102.51	1862	328.40	32.90	1892	311.30	9.34	1922	289.40	2.90	1952	314.50	6.29
1833	342.60	102.78	1863	326.70	32.70	1893	310.00	6.30	1923	305.10	3.02	1953	318.90	6.36
1834	343.50	103.05	1864	325.00	32.50	1894	317.00	9.51	1924	330.00	3.20	1954	321.90	6.44
1835	344.40	103.32	1865	310.00	31.00	1895	305.00	9.15	1925	321.30	3.18	1955	318.80	6.38
1836	345.30	103.59	1866	301.20	9.04	1896	313.80	9.41	1926	321.90	3.22	1956	320.50	6.41
1837	346.20	103.86	1867	300.00	9.00	1897	312.00	9.36	1927	327.00	5.89	1957	320.20	6.43
1838	347.10	104.13	1868	298.00	8.94	1898	317.30	9.52	1928	327.00	6.54	1958	318.40	6.37
1839	348.00	174.00	1869	290.00	8.70	1899	313.60	9.41	1929	328.00	6.56	1959	317.80	6.36
1840	347.00	173.50	1870	291.00	8.73	1900	307.50	9.23	1930	328.00	6.56			
1841	341.50	170.75	1871	300.00	9.00	1901	311.50	9.35	1931	329.25	6.58			
1842	336.00	168.00	1872	313.90	9.42	1902	305.90	9.18	1932	326.40	4.90			
1843	325.00	162.50	1873	311.00	9.33	1903	306.50	9.19	1933	328.00	4.89			
1844	328.50	164.25	1874	317.50	9.52	1904	305.50	9.17	1934	331.00	4.96			
1845	332.10	166.05	1875	324.00	9.72	1905	307.00	9.21	1935	357.00	5.36			
1846	335.60	167.80	1876	311.00	9.33	1906	306.00	9.18	1936	349.50	6.99			
1847	339.30	169.65	1877	298.00	8.94	1907	307.10	9.23	1937	354.00	7.08			
1848	319.90	63.98	1878	303.50	9.11	1908	306.50	9.26	1938	354.00	7.08			
1849	330.00	66.00	1879	309.90	9.30	1909	303.30	7.75	1939	382.40	5.74			
1850	330.00	66.00	1880	300.00	9.00	1910	307.80	7.72	1940	376.50	5.65			
1851	323.60	64.72	1881	309.00	9.27	1911	308.20	7.69	1941	376.00	5.64			
1852	325.30	65.06	1882	312.00	9.36	1912	318.50	15.21	1942	379.50	15.18			
1853	328.30	65.66	1883	312.00	9.32	1913	329.00	9.24	1943	383.00	15.32			
1854	331.60	66.32	1884	312.00	9.36	1914	327.15	9.35	1944	367.30	14.69			
1855	333.50	66.70	1885	303.50	9.11	1915	325.30	9.46	1945	352.00	14.08			

1: year; 2: CO₂ MBL estimation; 3: \pm error (ppm) of method

Figure 1 shows about 75 % of the data as monthly averages within a latitude range of 40–80N modelled by a distance weighted least squares fit algorithm. A clearly enhanced CO₂ concentration around 1940 over the whole latitude range can be seen with CO₂ maximum in 1942.

A continuous time series using estimations from Table 11 from 1826 to 1960 is presented in Figure 24.

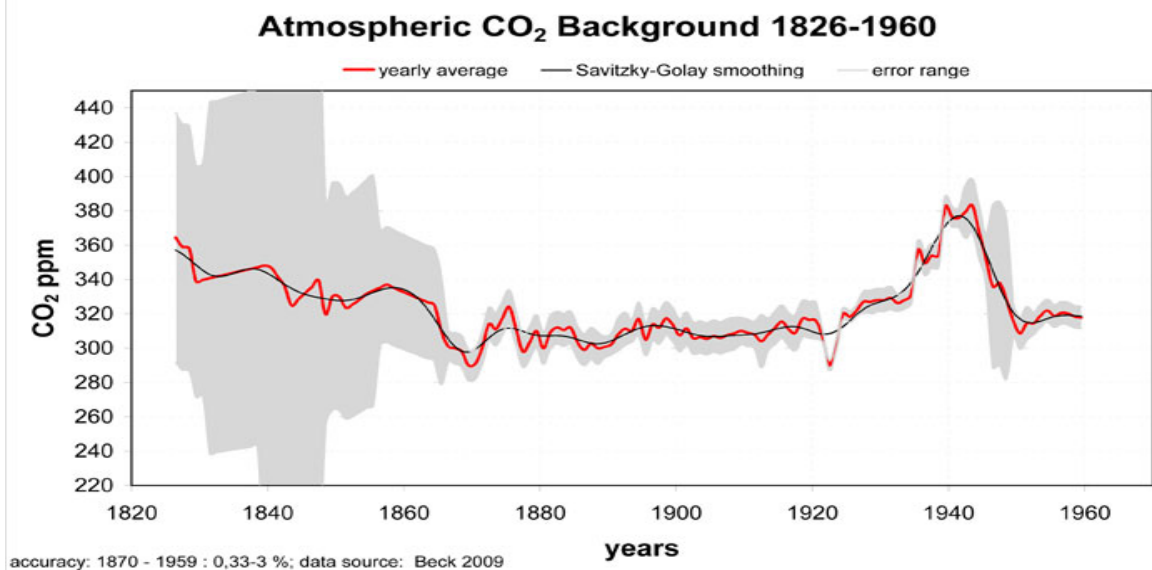


Figure 24. Atmospheric CO₂ background level 1826–1960. CO₂ estimates from directly measured data (red); black line smoothed by a Savitzky-Golay filter, grey area = estimated error range. Savitzky-Golay smoothing parameters (Autosignal): width of the moving window: 5, order: 2; passes: 3. Data from table 11.

Because of some gaps in the annual time series and uncertain data, 40 interpolations are necessary since 1826 (14 since 1870). 44 % coastal data or data from the sea or the higher troposphere since 1870 have been used. The CO₂ maximum in 1942 is based on the work of >25 authors and locations and >60 000 samples within about 20 years from 1930 to 1950. Additionally, the direct measurement of the background level of 357 ppm in 1935 over Helsinki by aeroplane, Kauko (1935) using the most accurate gas analyser in history of chemical methods (0.33 %), supports the existence of 1942 CO₂ maximum. It is most remarkable that literature reveals CO₂ enriched air coming from the sea at several stations when sampling at the coast (Haldane North Sea, Buch 1932–1936 Barents Sea, Northern Atlantic) or over warmer ocean currents in the Northern Atlantic (Buch 1932–1936). This suggests the Northern Atlantic Ocean as the source of the enhanced CO₂-levels.

Using the Savitzky-Golay smoothed data (see Figure 24), the contour of the reconstructed MBL of CO₂ from directly measured data show maxima around 1858 (335.2 ppm) and 1941 (377.1 ppm) in contrast to the monotone rising CO₂-levels reconstructed from ice cores (IPCC). Several small oscillations of the curve prior to the continuously sampled CO₂ since 1958 are within error range of ± 3 % since 1870:

Using a Savitzky-Golay smoothed curve with a wider moving window width of 7 to correct problems around 1880 and 1930 we can observe a periodic cycling with maxima at 1836: 343.9 ppm; 1857: 334.2 ppm; 1878: 309.7 ppm; 1896: 312 ppm; 1915: 320.7 ppm; and 1941: 371.4 ppm.

The average period is 21 years (21, 21, 18, 19, 26 years). The sharp drop in 1922 and the changing period length at those times points to phase change in the time series which supports the findings of Yndestad in the NAW (Northern Atlantic water temperature) (Yndestad et al. 2004). He found strong evidence for the lunar nodal cycle and its harmonics as the controlling forces behind the northern and Arctic climate. At around 1920 there is a phase-reversal of the 18-year temperature cycle in the NAW. Yndestad also identified 55 years as a dominant wavelet cycle and third harmonic of the 18.6 yr lunar nodal cycle. By calculating the best low-frequency harmonic fit using Lyubushin (2009) software of the data since 1870 we get a period of 55.17 years (see Figure 25).

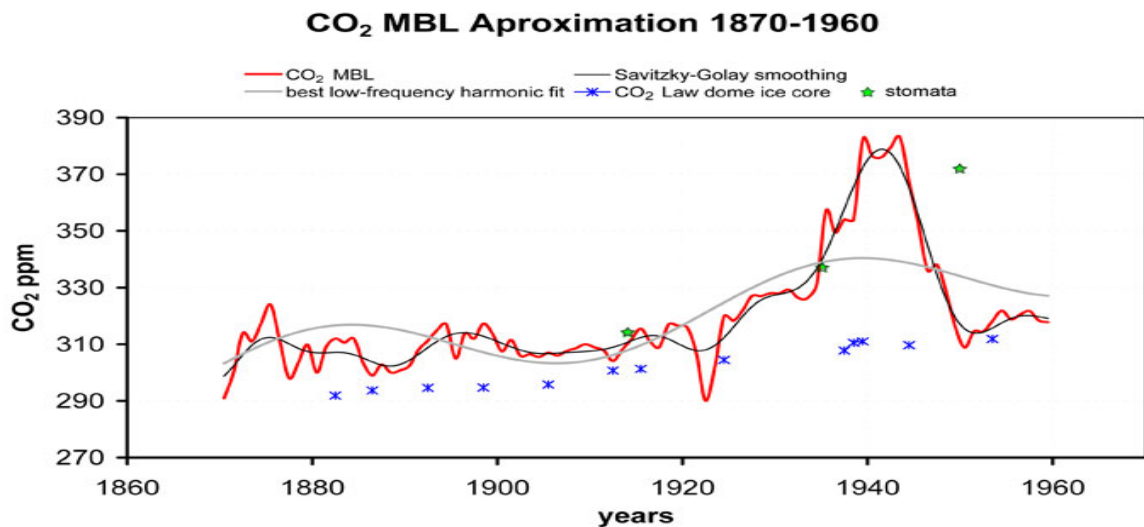


Figure 25. Atmospheric CO₂ background level 1870–1960; black line smoothed by a Savitzky-Golay filter, parameters (Autosignal): width of the moving window: 7, order: 2; passes: 3; grey line= estimated best low-frequency harmonic fit (55.17 years = 18.39 years \times 3); blue stars= CO₂ law dome ice core (Etheridge et al. 1998); green stars= stomata *Tsuga spec.*, Jay Bath, Mount Rainier Washington, USA; (Kouwenberg 2005). 1922: phase reversal.

Figure 25 confirms the early analysis of Callendar (1940) that CO₂-levels in the atmosphere have grown since the late 19th century.

The minimum is 289.4 ppm in 1922, the maximum is 383 ppm in 1943, mean = 324.63 and the standard deviation = 19.63 for the period 1870–1960

The average in the 19th century using the reconstructed MBL (1826–1900) is 322.67 ppm. The average in 20th century using a combination of historical and modern data (NOAA) is 331.38 ppm. This suggests a rise of 8.71 ppm or 2.6 % which is well within observed variability and error range of the methods. Data prior to 1826 are not included because of the great uncertainty. If the estimated higher CO₂-levels had been real at the beginning of the 19th century, there would be no difference in the average CO₂-levels between the last two centuries.

Since 1870 two periods of about 60–70 years (1870–1940) and 1949–2009 can be observed with such a slow rise of the CO₂-levels to a maximum level of about +70 ppm in about 1943 and today. The overall rising CO₂-levels since 1870 to today has also been supported by the reconstructed ice core data despite of its much worse resolution compared to the presented data (see Figure 25). The maxima around 1860 and 1940 are in contrast to the published literature. They can be described by an about 70–80 year cycle.

Stomata are tiny openings in the epidermis of leaves to allow gas exchange of the plants. At high atmospheric CO₂-levels leaves adapt by decreasing their density. At low levels they increase their density to absorb more CO₂. The inverse relation is confirmed over different time scales (Royer 2003; van Hoof 2006, 2008). Several reconstructions of atmospheric CO₂-levels exist in modern times. Wagner (2005) reported of low density of stomata found in several species from the swamps of Florida around 1940–50 and since around 1980–2000. The same low stomata density today as in the first half of the 20th century can be seen in *Quercus spec.* leaves from the Netherlands (van Hoof et al. 2006). CO₂ reconstruction from stomata at Jay Bath, Mount Rainier, Washington, USA (Kouwenberg 2005) in 20th century, show 332 ppm in 1914, 337 ppm in 1935 and 372 ppm in 1950 which fit very well to the CO₂ MBL from direct measurements (Figure 25).

These stomata data confirm the CO₂ MBL reconstruction as well as the raw data showing high CO₂-levels in the 1930s and 40s at higher temperatures. This is the pre-condition for the inverse stomata/CO₂ relation.

If we assume the actual CO₂-levels are near a peak, the levels are expected to drop within the next years. The application of spectrum analysis on the historical data set would give more answers.

4. Conclusion

In this paper a new dataset of directly measured CO₂ samples from 1826 is introduced. They have been sampled and analysed mostly near ground by well known chemical methods (Pettenkofer process and related volumetric methods) by experienced scientists since the early 19th century (see station and author list in the supplemental data) which contributed to the evolution of gas analytical methods. From an estimated total sum of more than 200 000 single samples collected since 1800 in the northern and southern hemispheres, the author has selected 97 404 samples from 901 stations compiled in 87 data files (supplemental data). A thorough literature review revealed that these data are only partly known to climate science and had been rejected and ignored without a thorough validation of the quality, sampling and analysing methods behind. This new dataset contains high quality data including vertical profiles which can be easily compared to today's standards. The selection process was characterized by using only data sampled by known methods and from locations which allow a validation of local influences and air masses.

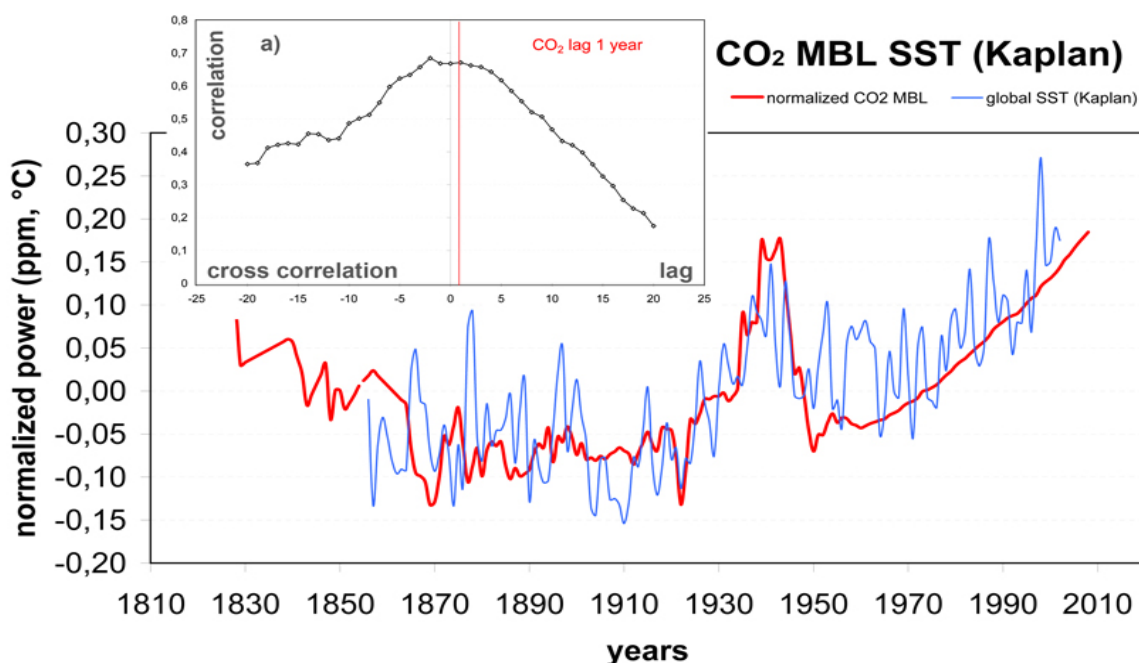


Figure 26. Annual atmospheric CO₂ background level 1856–2008 compared to SST (Kaplan, KNMI); red line: CO₂ MBL reconstruction 1826–1959 (Beck), 1960–2008 (MLO); blue line: Annual SST (Kaplan) 1856–2003; a) cross correlation of SST and CO₂ MBL showing correlation of $r=0.668$ and a lag of 1 year for CO₂ after global SST.

To make these near ground data comparable to modern CO₂ background data compiled under international standards, new methods had to be developed to estimate the marine boundary level (MBL) or background levels in the higher troposphere from near ground data. Using modern vertical profiles available from the WMO and NOAA sampling networks, the author was able to establish 4 estimation methods which allow calculation of the MBL from near ground air mass characteristics. By simple nonlinear regression methods it was possible to estimate the MBL within 1–3 % error range from a comparison of CO₂-levels at higher wind speeds and precipitation levels. The new MBL estimation methods from near ground data are named CWBA, CPBA, CSMBA, CDMBA. They also include a calculation from the daily minimum CO₂-levels initially speculated by C. Keeling (1958)(CDMBA) and an estimate based on the summer minimum levels (CSMBA). These methods have been applied to the 87 historical data series to calculate the historical MBL since 1826 as annual averages within an overall error range of about ± 3 % since 1870 (table 11). Missing years are filled by interpolated values. The resolution of these annual new data series is much better compared to reconstructions from ice core and stomata data. Showing 317.8 ppm in 1959, it fits perfect to the modern values of Mauna Loa based CO₂-levels analysed by NDIR sensors despite a calibration against the old methods is not reported by C. Keeling.

The most remarkable conclusion from the contour of the new CO₂ MBL data is that CO₂-levels between 1930 and 1950 have been as high as today. Furthermore, a distinct dip can be observed around 1922.

The data also suggest higher levels in the first half of the 19th century than reconstructed from commonly used ice cores. Using modern MLO CO₂ data, we can calculate a centennial average for the 20th century 1901–2000 of 331.38 ppm and of a MBL in the 19th century (1826–1900) of 322.67. This is a growth rate of +2.6 % in contrast to about 30 % as derived from ice cores and therefore within measurement variability. Analysing the new series of directly measured CO₂ MBL levels from 1926 to 2010 suggests a possible cyclic behaviour.

The CO₂ MBL levels since 1826 to 2008 show a good correlation to the global SST (Kaplan, KNMI; see Figure 26) with a CO₂ lag of 1 year after SST from cross correlation (Figure 26a). Kuo et al. (1990) had derived 5 months lag from MLO data alone.

Table 12. Summary of acronyms and abbreviations

Ameriflux	The AmeriFlux network was established in 1996. The network provides continuous observations of ecosystem level exchanges of CO ₂ , water, energy and momentum spanning diurnal, synoptic, seasonal, and interannual time scales and is currently composed of sites from North America, Central America, and South America
BASF	Badische Anilin und Soda Fabrik
C	Celsius
CDMBA	CO ₂ daily minimum background approximation
CGER	Center for Global Environmental Research
COADS	Comprehensive Ocean-Atmosphere Data Set
CPBA	CO ₂ precipitation background approximation
CSMBA	CO ₂ summer minimum background approximation,
CWBA	CO ₂ wind speed background approximation
E	east
GlobalView-CO2	is a product of the Cooperative Atmospheric Data Integration Project. The project is coordinated and maintained by the Carbon Cycle Greenhouse Gases Group of the National Oceanic and Atmospheric Administration, Earth System Research Laboratory (NOAA ESRL),
IPCC	Intergovernmental Panel on Climate Change
KNMI	Koninklijk Nederlands Meteorologisch Instituut
KSLA	Kungl. Skogs- och Lantbruksakademien, (Royal Swedish Academy of Agriculture and Forestry)
m	meter
MBL	marine boundary layer
mg	milli gram
MLO	Mauna Loa Observatory, Hawaii
N	north
NCDC	National Climatic Data Center
NDIR	nondispersive infrared sensor
NOAA	National Oceanic and Atmospheric Administration
ppm	parts per million (volume)
ppmv	parts per million per volume
prec	precipitation
RICO C	Riedel gas analyser type C
S	south
SEAS	seasonal cycle
Sm	summer minimum
SST	sea surface temperature
URAS	Ultrarot-Absorptionsschreiber (infrared absorption writer),
W	west
WDCGG	World Data Centre for Greenhouse Gases
WMO	World Meteorological Organisation
ws	wind speed

Acknowledgments

The author thanks Prof. Dr. Harald Yndestad for the very helpful discussions and help in organizing the paper, Prof. Dr. Ole Humlum and Prof. Jan-Erik Solheim for their valuable comments.

The guest editor thanks Harald Yndestad for making the manuscript available. Francis Massen, Stein Storlie Bergsmark and Arild Eugen Johansen have assisted with proofreading and layout.

References

- Ameriflux 2009. <https://ameriflux.lbl.gov/>
- Autosignal 1.7 2009. <https://sigmaplot.com/resources>
- Beck E-G 2007, **180 Years of Atmospheric CO₂ Gas Analysis by Chemical Methods**, *Energy & Environment* **18**, 259–282. <https://doi.org/10.1177/0958305X0701800206>
- Beck E-G 2008, **50 years of continuous measurement of CO₂ on Mauna Loa**, *Energy & Environment* **19**, 1017–1028. <https://doi.org/10.1260/095830508786238288>
- Bischof W 1960, **Periodical Variations of the Atmospheric CO₂-content in Scandinavia**, *Tellus* **12**, 2, 216–226. <https://doi.org/10.3402/tellusa.v12i2.9360>
- Buch K 1939a, **Beobachtungen über das Kohlensäuregleichgewicht und über den Kohlensäureaustausch zwischen Atmosphäre und Meer im Nord-Atlantischen Ozean**, *Acta Academiae Aboensis, Mathematica et Physica* **11**, 9, 28–31.
- Buch K 1939b, **Kohlensäure in der Atmosphäre und Meer an der Grenze zum Artikum**, *Acta Academiae Aboensis, Mathematica et Physica* **11**, 9, 1–40.
- Buch K 1948, **Der Kohlendioxydgehalt der Luft als Indikator der Meteorologischen Luftqualität**, *Geophysica* **3**, 63–79.
- Cleveland WS, *Visualizing Data*, 1993, Hobart Press, Summit, NJ. ISBN 0-9634884-0-6.
- de Saussure T 1830, **Sur les variation de l'acide de carbonique atmosphérique**, *Annales de Chimie et Physique*, 44, 5–28.
- de Saussure T 1830, **Sur les variation de l'acide de carbonique atmosphérique**, *Annales de Chimie et Physique*, 44, 5–28.
- dPlot 2009, *Graph Software for Scientists & Engineers*, <http://www.dplot.com/index.htm>
- Etheridge DM., Steele LP, Langenfelds RL, Francey RJ, Barnola J-M, and Morgan VI 1998, **Historical CO₂ records from the Law Dome DE08, DE08-2, and DSS ice cores**. In *Trends: A Compendium of Data on Global Change*, Carbon Dioxide Information Analysis Center, Oak Ridge National Laboratory, U.S. Department of Energy, Oak Ridge, Tenn., U.S.A. <https://cdiac.ess-dive.lbl.gov/trends/CO2/lawdome.html>
- From E and Keeling CD 1986, **Reassessment of late 19th century atmospheric carbon dioxide variations in the air of western Europe and the British Isles based on an unpublished analysis of contemporary air masses by G. S. Callendar**, *Tellus* **38B**, 87–105. <https://doi.org/10.1111/j.1600-0889.1986.tb00092.x>
- Globalview-CO₂ 2008, *Cooperative Atmospheric Data Integration Project - Carbon Dioxide*, CD-ROM, NOAA ESRL, Boulder, Colorado. Also: https://daac.ornl.gov/ISLSCP_II/guides/globalview_CO2_point.html, later <https://gml.noaa.gov>

- Gurk C, Fischer H, Hoor P, Lawrence MG, Lelleveld J, and Wernli H 2008, **Airborne in-situ measurements of vertical, seasonal and latitudinal distributions of carbon dioxide over Europe**, *Atmos. Chem. Phys.* **8**, 6395–6403. <https://doi.org/10.5194/acp-8-6395-2008>
- Haldane JBS 1936, **Carbon Dioxide Content of Atmospheric Air**, *Nature* **137**, 575. <https://doi.org/10.1038/137575a0>
- Hempel W 1913, *Gasanalytische Methoden*, 4. Auflage 1913, Vieweg Braunschweig. http://www.archive.org/stream/gasanalytische00hempuoft/gasanalytische00hempuoft_djvu.txt
- van Hoof TB, Kürschner WM, Wagner F and Visscher H 2006, **Stomatal index response of Quercus robur and Quercus petraea to the anthropogenic atmospheric CO₂ increase**, *Plant Ecology* **183**, 237–243. <https://doi.org/10.1007/s11258-005-9021-3>
- van Hoof T, Wagner-Cremer F, Kürschner WM, and Visscher H 2008, **A role for atmospheric CO₂ in preindustrial climate forcing**, *PNAS* **105** (41), 15815–15818. <https://doi.org/10.1073/pnas.0807624105>
- Solomon SD, Qin D, Manning M, Chen Z, Marquis M, Averyt KB, Tignor M and Miller HL (eds.) 2009, *Contribution of Working Group I to the Fourth Assessment Report of the Intergovernmental Panel on Climate Change*, Cambridge University Press, Cambridge, United Kingdom and New York, NY, USA. https://archive.ipcc.ch/publications_and_data/ar4/wg1/en/ch7s7-3.html
- Kauko Y 1934, **Zur Bestimmung der Kohlensäure in der Luft mit Hilfe von pH Messungen**, *Angewandte Chemie* **47**, 164–167. <https://doi.org/10.1002/ange.19340471104>
- Kauko Y 1935, **Ein Apparat zur potentiometrischen Bestimmung der Luftkohlensäure**, *Angewandte Chemie* **48**, 539–540. <https://doi.org/10.1002/ange.19350483204>
- Kauko Y et al. 1935, **Eine genaue Methode zur Bestimmung des CO₂-gehaltzes der Luft**, *Z. anorg. allg. Chem.* **223**, 33–44. <https://doi.org/10.1002/zaac.19352230105>
- Keeling C 1958, **The concentration and isotopic abundances of atmospheric carbon dioxide in rural areas**, *Geochimica et Cosmochimica Acta* **13**, 322–333. [https://doi.org/10.1016/0016-7037\(58\)90033-4](https://doi.org/10.1016/0016-7037(58)90033-4)
- Kouwenberg L, Kürschner WM and Visscher H 2005, **Atmospheric CO₂ fluctuations during the last millennium reconstructed by stomatal frequency analysis of Tsuga heterophylla needles**, *Geology* **33**, 33–36. <https://doi.org/10.1130/G20941.1>
- Krogh A and Brandt-Rehberg P 1929, **CO₂-Bestimmungen in der atmosphärischen Luft durch Mikrotitration**, *Biochemische Zeitschrift* **205**, 265–272.
- Kuo C, Lindberg C and Thomson DJ 1990, **Coherence established between atmospheric carbon dioxide and global temperature**, *Nature* **343**, 709–714. <https://doi.org/10.1038/343709a0>
- Letts E and Blake R 1899–1902, **The carbonic anhydride of the atmosphere**, *Royal Dublin Society Scientific Proceedings* **9**.
- Lundegårdh H 1922, **Neue Apparate zur Analyse des Kohlensäuregehalts der Luft**, *Biochem. Zeitschr* **131**, 109
- Lundegårdh H 1949, *Klima und Boden und ihre Wirkung auf das Pflanzenleben*, Gustav Fischer, Jena.
- Lyubushin AA 2009, *Software for Point Processes Periodicity Detecting and Scalar Time Series Data Mining*. http://alexeylyubushin.narod.ru/Software_for_Point_Processes_Periodicity_and_Scalar_Time_Series_Data_Mining.pdf

- Massen F, Kies, A, Harpes N et al. 2007, **Seasonal and Diurnal CO₂ Patterns at Diekirch, LU 2003—2005**. [https://meteo lcd.lu/papers/CO₂_patterns/CO₂_patterns.html](https://meteo lcd.lu/papers/CO2_patterns/CO2_patterns.html)
- Massen F and Beck E-G 2011, **Accurate Estimation of CO₂ Background Level from Near Ground Measurements at Non-Mixed Environments**. In: *Leal Filho, W. (eds) The Economic, Social and Political Elements of Climate Change, Climate Change Management*. Springer: Berlin, Heidelberg. https://doi.org/10.1007/978-3-642-14776-0_31
- Mörner NA and Etiope G 2002, **Carbon degassing from the lithosphere**, *Global and Planetary Change* **33**, 185–203. [https://doi.org/10.1016/S0921-8181\(02\)00070-X](https://doi.org/10.1016/S0921-8181(02)00070-X)
- NCDC 2009, <http://www.ncdc.noaa.gov/oa/ncdc.html>
- Palmqvist A 1892, **Undersökningar öfver Atmosferens Kolsyrehalt**, *Bihang till Kungliga Svenska Vetenskapsakademiens handlingar* **18** Afd.2:no 2.
- Petermann A 1892–93, **Acide carbonique contenu dans l'air atmospherique**, Brux. *Mémoires couronnés et autres mémoires publiés par l'Académie Royale des Sciences, des Lettres et des Beaux-Arts de Belgique* coll.in-8 **47**, 2. Abt. S. 5
- Rheinau E 1926, *Praktische Kohlensäuredüngung in Gärtnerei und Landwirtschaft*, Springer Verlag, Berlin.
- Rorsch A 2007, **Climate Science and the Phlogiston Theory: Weighing the Evidence**, *Energy & Environment* **18**, 441–448. <https://doi.org/10.1260/095830507781076158>
- Royer DL 2003, **Estimating Latest Cretaceous and Tertiary atmospheric CO₂ from stomatal indices**. In: *GSA Special Papers*, vol. 369, *SL Wing, PD Gingerich, B Schmitz and E Thomas, Causes and consequences of globally warm climates in the early Paleogene*, p. 79-93. <https://doi.org/10.1130/0-8137-2369-8.79>
- Schindler D, Türk M, Mayer H 2006, **CO₂ fluxes of a Scots pine forest growing in the warm and dry southern upper Rhine plain, SW Germany**, *European Journal of Forest Research*, **125**, 201–212. <https://doi.org/10.1007/s10342-005-0107-1>
- Schmidt M, Graul R, Sartorius H and Levin I 2003, **The Schauinsland CO₂ record: 30 years of continental observations and their implications for the variability of the European CO₂ budget**, *Journal of Geophysical Research* **108 D19**, 4619–4626. <https://doi.org/10.1029/2002JD003085>
- Schulz B 1922, **Hydrographische Beobachtungen insbesondere über die Kohlensäure in der Nord- und Ostsee im Sommer 1921**: (Forschungsschiffe ‚Poseidon‘ und ‚Skagerak‘), *Archiv der Deutschen Seewarte*, Hamburg: Hammerich & Lesser **40**, 2.
- Stanhill G 1982, **The Montsouris series of carbon dioxide concentration measurements 1877–1910**, *Climatic Change* **4**, 221–237. <https://doi.org/10.1007/BF02423398>
- Statistica 8 2009. <http://www.statsoft.de/>
- Stepanova NA 1952, **A Selective Annotated Bibliography of Carbon Dioxide in the Atmosphere**, *Meteorological Abstracts* **3** 137–170.
- Stephens, B. et al. 2007, **Weak Northern and Strong Tropical Land Carbon Uptake from Vertical Profiles of Atmospheric CO₂**, *Science* **316**. no. 5832, 1732 – 1735. <https://www.science.org/doi/10.1126/science.1137004>

Wattenberg H 1933, **Die Deutsche Atlantische Expedition auf dem Forschungs- und Vermessungsschiff „Meteor“... 1925–1927**. In: *Wissenschaftliche Ergebnisse Band VIII; Das chemische Beobachtungsmaterial und seine Gewinnung, I. Teil des chemischen Materials*, Verlag von Walter de Gruyter&CO, Berlin

Wagner F, Dilcher DL, and Visscher 2005, **Stomatal frequency responses in hardwood-swamp vegetation from Florida during a 60-year continuous CO₂ increase**, *American Journal of Botany* **92**(4), 690–695. <https://doi.org/10.3732/ajb.92.4.690>

Wigley TML 1983, **The pre-industrial carbon dioxide level**, *Climate Change* **5**, 315–320. <https://doi.org/10.1007/BF02423528>

Yndestad H, Turrell W and Ozhigin V. 2004, **Temporal linkages between Faroe-Shetland time series and Kola section time series**, *ICES CM/M:01, Regime Shifts in the North Atlantic Ocean: Coherent or Chaotic?*

Supplemental data:

- 1) CO2_raw_1800-1960.pdf
- 2) Calculated monthly averages and reconstruction of annual CO₂ MBL (1826–1960): CO2_MBL_1826–1960.xls
- 3) CO2_Literature_1800-1960.pdf
- 4) CO2_stations_1800-1960.pdf
- 5) Samplesused-jan2010.xls

Ernst-Georg Beck Dipl. Biol.

19 February 2010.

Guest editor: Jan-Erik Solheim, June 2022

CO₂ 1800-1960 Historical References, Chemical Methods

Links to digitized sources

©Ernst-Georg Beck 2006-2009

Note: Montsouris 1877-1910

1800	Théodore. de Saussure; Sur les variation de l'acide de carbonique atmosphérique Annales de Chimie et Physique, 44[1830], p. 5 http://www.archive.org/stream/annalesdechimie51unkngoog#page/n10/mode/1up
1801	
1802	E. Letts and R. Blake , (1899) The carbonic anhydride of the atmosphere; Roy. Dublin Soc. Sc.Proc., N. S., Vol.9, 1899-1902; Scientific Proceedings of the Royal Dublin Society, p. 167 http://www.biokurs.de/treibhaus/literatur/letts-blake/letts_blake_biblio.doc http://www.biokurs.de/treibhaus/literatur/letts-blake/letts_blake.doc
1803	
1804	
1805	
1806	
1807	
1808	
1809	Theodore de Saussure, Notes sur les variations du gaz acide carbonique dans l'atmosphere , en hiver et en ete. ; Annales de Chimie et Physique 1816, p 199 http://books.google.de/books?id=6sUNBwXDbAkC&pg=PA5&lpg=PA5&dq=Annales+de+Chimie+et+Physique+1816&source=bl&ots=cpEMtYnXP-&sig=9PumQQ1w0XwKTLuMN83DvbRpsOI&hl=de&ei=XePJSvirCNmM4gaWrbXHAQ&sa=X&oi=book_result&ct=result&resnum=1#v=onepage&q=Annales%20de%20Chimie%20et%20Physique%201816&f=false
1810	Theodore de Saussure, Notes sur les variations du gaz acide carbonique dans l'atmosphere , en hiver et en ete. ; Annales de Chimie et Physique 1816, p 199 E. Letts and R. Blake, (1899) The carbonic anhydride of the atmosphere; Roy. Dublin Soc. Sc.Proc., N. S., Vol.9, 1899-1902; Scientific Proceedings of the Royal Dublin Society, p 167
1811	Theodore de Saussure, Notes sur les variations du gaz acide carbonique dans l'atmosphere , en hiver et en ete. ; Annales de Chimie et Physique 1816, p 199 E. Letts and R. Blake, (1899) The carbonic anhydride of the atmosphere; Roy. Dublin Soc. Sc.Proc., N. S., Vol.9, 1899-1902; Scientific Proceedings of the Royal Dublin Society, p 167
1812	Theodore de Saussure, Notes sur les variations du gaz acide carbonique dans l'atmosphere , en hiver et en ete. ; Annales de Chimie et Physique 1816, p 199 E. Letts and R. Blake, (1899) The carbonic anhydride of the atmosphere; Roy. Dublin Soc. Sc.Proc., N. S., Vol.9, 1899-1902; Scientific Proceedings of the Royal Dublin Society, p 167/
1813	Theodore de Saussure, Notes sur les variations du gaz acide carbonique dans l'atmosphere , en hiver et en ete. ; Annales de Chimie et Physique 1816, p 199 E. Letts and R. Blake, (1899) The carbonic anhydride of the atmosphere; Roy. Dublin Soc. Sc.Proc., N. S., Vol.9, 1899-1902; Scientific Proceedings of the Royal Dublin Society, p 167
1814	Theodore de Saussure, Notes sur les variations du gaz acide carbonique dans l'atmosphere , en hiver et en ete. ; Annales de Chimie et Physique 1816, p 199 E. Letts and R. Blake, (1899) The carbonic anhydride of the atmosphere; Roy. Dublin Soc. Sc.Proc., N. S., Vol.9, 1899-1902; Scientific Proceedings of the Royal Dublin Society, p 167
1815	Theodore de Saussure, Notes sur les variations du gaz acide carbonique dans l'atmosphere , en hiver et en ete. ; Annales de Chimie et Physique 1816, p 199 E. Letts and R. Blake, (1899) The carbonic anhydride of the atmosphere; Roy. Dublin Soc. Sc.Proc., N. S., Vol.9, 1899-1902; Scientific Proceedings of the Royal Dublin Society, p 167
1816	Theodore de Saussure, Notes sur les variations du gaz acide carbonique dans l'atmosphere , en hiver et en ete. ; Annales de Chimie et Physique 1816, p 199
1817	
1818	
1819	
1820	
1821	
1822	
1823	
1824	
1825	
1826	Théodore. de Saussure; Sur les variation de l'acide de carbonique atmosphérique

	Annales de Chimie et Physique, 44[1830], p. 5 http://www.archive.org/stream/Annalesdechimie51unkngoog#page/n10/mode/1up
1827	Théodore. de Saussure; Sur les variation de l'acide de carbonique atmosphérique Annales de Chimie et Physique, 44[1830], p. 5
1828	Théodore. de Saussure; Sur les variation de l'acide de carbonique atmosphérique Annales de Chimie et Physique, 44[1830], p. 5
1829	Théodore. de Saussure; Sur les variation de l'acide de carbonique atmosphérique Annales de Chimie et Physique, 44[1830], p. 5
1830	Théodore. de Saussure; Sur les variation de l'acide de carbonique atmosphérique Annales de Chimie et Physique, 44[1830], p. 5
1831	
1832	
1833	
1834	
1835	
1836	
1837	
1838	
1839	J. B. Boussingault, « Recherche sur la quantité d'acide carbonique <i>contenue dans l'air de la ville de Paris</i> », 1844, p. 456 , http://gallica.bnf.fr/ark:/12148/bpt6k34751c.image.r=boussingault.f455.tableDesMatières.langFR
1840	J. B. Boussingault, « Recherche sur la quantité d'acide carbonique <i>contenue dans l'air de la ville de Paris</i> », 1844, p. 456
1841	J. B. Boussingault, « Recherche sur la quantité d'acide carbonique <i>contenue dans l'air de la ville de Paris</i> », 1844, p. 456
1842	
1843	J. B. Boussingault, OBSERVATIONS SIMULTANÉES FAITES A PARIS ET A ANDILLY, PRÈS MONTMORENCY, POUR RECHERCHER LA PROPORTION D'ACIDE CARBONIQUE CONTENUE DANS L'AIR ATMOSPHERIQUE ->, p. 470 http://gallica.bnf.fr/ark:/12148/bpt6k34751c.image.r=boussingault.f469.tableDesMatières.langFR
1844	
1845	
1846	
1847	A. Lewy Sur la constitution de l'atmosphère, Annales de chimie et de physique, 34, 1852 p. 5 http://gallica.bnf.fr/ark:/12148/bpt6k34775c.image.f4.langFR
1848	A. Lewy Sur la constitution de l'atmosphère, Annales de chimie et de physique, 34, 1852 p. 5
1849	E. Letts and R. Blake, (1899) The carbonic anhydride of the atmosphere; Roy. Dublin Soc. Sc.Proc., N. S., Vol.9, 1899-1902; Scientific Proceedings of the Royal Dublin Society, p. 167 http://www.biokurs.de/treibhaus/180CO2_supp.htm
1850	E. Letts and R. Blake, (1899) The carbonic anhydride of the atmosphere; Roy. Dublin Soc. Sc.Proc., N. S., Vol.9, 1899-1902; Scientific Proceedings of the Royal Dublin Society, p. 167
1851	M. Mène, Dosage I, acide carbonique de l'air; Comptes Rendus 57, 1863, p. 155 http://gallica.bnf.fr/ark:/12148/bpt6k30143.image.r=acide+carbonique.f155.langEN
1852	
1853	
1854	A. Vogel, Untersuchung der atmosphärischen Luft während der Choleraepidemie zu München 1854, Chemisch-Pharmaceutisches Centralblatt, Nr. 1, 4. Januar 1854, 25. Jahrgang, p. 875 http://books.google.de/books?id=UZw4AAAAIAAJ&dq=chemisches+Centralblatt+1854&printsec=frontcover&source=bl&ots=A-eCSNlpPF&sig=Is2pU9tsiU2aehFvs4N0fh9gP4A&hl=de&ei=WxjKSrPyAcP94Ab97qXHAQ&sa=X&oi=book_result&ct=result&resnum=1#v=onepage&q=&f=false
1855	
1856	H. v.Gilm, Über die Kohlensäurebestimmung der Luft Sitzungsberichte d. kaiserl. Akademie d. Wissenschaften Volume 24, 1857, p. 279 http://www.biodiversitylibrary.org/item/31064
1857	H. v.Gilm, Über die Kohlensäurebestimmung der Luft Sitzungsberichte d. kaiserl. Akademie d. Wissenschaften Volume 24, 1857, p. 279
1858	
1859	
1860	
1861	

1862	
1863	F. Schulze, Landwirtschaft. Versuchsstationen, Bd. 9, 1867, S.217, Bd. 10, 1868, S.515, Bd. 12, 1870, S.1; Bd. 14 1871, S. 366; http://www.biokurs.de/treibhaus/180CO2_supp.htm A.Smith, On the composition of the atmosphere, Memoirs and Proceedings of the Manchester Literary & Philosophical Society (1868), p. 1-56+181+ http://www.archive.org/stream/memoirsandproce40socigoog#page/n13/mode/1up
1864	F. Schulze, Landwirtschaft. Versuchsstationen, Bd. 9, 1867, S.217, Bd. 10, 1868, S.515, Bd. 12, 1870, S.1; Bd. 14 1871, S. 366;
1865	T. E. Thorpe, On the <i>amount of Carbonic Acid contained in the Air above the Irish Sea</i> ; Memoirs and Proceedings of the Manchester Literary & Philosophical Society (1868), p. 152 http://www.archive.org/stream/memoirsandproce40socigoog#page/n161/mode/1up
1866	T. E. Thorpe, cited in John S. Billings, Ventilation and Heating, 1893, Engineering Record (New York), p. 62 http://www.archive.org/stream/ventilationheati00billuoft#page/62/mode/2up
1867	
1868	F. Schultze; Landwirtschaft. Versuchsstationen, Vol. 10, 1868, p.515, vol. 12, 1870, p.1; vol. 14 1871, p. 366 F. Schultze Jahresbericht über die Fortschritte auf dem Gesamtgebiete der Agrikultur-Chemie, vol 13-15, 1874, Die Chemie der Luft: p. 113 http://www.archive.org/stream/jahresberichtbe303unkngoog#page/n128/mode/1up
1869	F. Schultze; Landwirtschaft. Versuchsstationen, Vol. 10, 1868, p.515, vol. 12, 1870, p.1; vol. 14 1871, p. 366 F. Schultze Jahresbericht über die Fortschritte auf dem Gesamtgebiete der Agrikultur-Chemie, vol 13-15, 1874, Die Chemie der Luft: p. 113
1870	F. Schultze; Landwirtschaft. Versuchsstationen, Vol. 10, 1868, p.515, vol. 12, 1870, p.1; vol. 14 1871, p. 366 F. Schultze Jahresbericht über die Fortschritte auf dem Gesamtgebiete der Agrikultur-Chemie, vol 13-15, 1874, Die Chemie der Luft: p. 113
1871	F. Schultze; Landwirtschaft. Versuchsstationen, Vol. 10, 1868, p.515, vol. 12, 1870, p.1; vol. 14 1871, p. 366 F. Schultze Jahresbericht über die Fortschritte auf dem Gesamtgebiete der Agrikultur-Chemie, vol 13-15, 1874, Die Chemie der Luft: p. 113
1872	J.A. Reiset, Compt. Rend., T. 88, 1879, p.1007, T. 90, p.1144,1457 (1879-1880) http://gallica.bnf.fr/ark:/12148/bpt6k30457.image.r=acide+carbonique.f1001.langEN E. Risler, Quantité d'acide carbonique contenue dans l'air a Caleve pres Nyon (Suisse) Comptes Rendus T94, 1882, p.1390 http://gallica.bnf.fr/ark:/12148/bpt6k3050z.image.langFR.f1392.tableDesMatières E. Risler, Gazette hebdomadaire de médecine et de chirurgie; série 2, tome 19. - Paris : G. Masson, 1882. W. Henneberg, Der Kohlensäuregehalt der atmosphärischen Luft; Jahresbericht über die Fortschritte auf dem Gesamtgebiete der Agrikultur-Chemie, vol 13-15, 1874, Die Chemie der Luft: p. 117 http://www.archive.org/stream/jahresberichtbe303unkngoog#page/n133/mode/1up
1873	P. Truchot, Sur la proportion d'acide carbonique existent dans l'air atmospherique,. Compt. Rend., 77, 1873, S. 675 http://gallica.bnf.fr/ark:/12148/bpt6k3034n.image.r=carbonique.f675.langEN.tableDesMatières
1874	F. Farsky, Bestimmungen der atmosphärischen Kohlensäure in den Jahren 1874-1875 zu Tabor in Böhmen, Wien, Akadem. Sitzungsberichte, 74, 1877, Abt. 2, S. 67 http://www.archive.org/stream/sitzungsbericht138klasgoog#page/n80/mode/1up P. Hässelbarth et al, Lokale Schwankungen im Kohlensäuregehalt der Luft, Chem. Centralblatt, 1879, p.750 http://www.archive.org/stream/chemischeszentr32chemgoog#page/n805/mode/1up
1875	F. Farsky, Bestimmungen der atmosphärischen Kohlensäure in den Jahren 1874-1875 zu Tabor in Böhmen, Wien, Akadem. Sitzungsberichte, 74, 1877, Abt. 2, S. 67 G. Tissandier, l'acide carbonique de l'air, La Nature, Paris, 1875 : Troisième année, premier semestre : n° 79 à 104, p 331 http://cnum.cnam.fr/CGI/fpage.cgi?4KY28.4/335/100/433/0/0
1876	P. Hässelbarth und J. Fittbogen, Beobachtungen über lokale Schwankungen im Kohlensäuregehalt der atmosphärischen Luft, Landw. Jahrbücher, 8, 1879, S. 669 Jahresbericht über die Fortschritte auf dem Gesamtgebiete der Agrikultur-Chemie, v. 22 1879, p. 66 http://www.archive.org/stream/jahresberichtb22berl#page/66/mode/2up E. Moss, Notes on arctic air, Österreichische Zeitschrift f. Meteorogie, 15, 1880, p. 492 http://www.archive.org/stream/zeitschriftders11metegoog#page/n527/mode/1up J.P. Claesson, Chemisches Centralblatt, 7, 1876, p. 296 http://www.archive.org/stream/chemischeszentr37chemgoog#page/n333/mode/1up
1877	G. Stanhill, The Montsouris series of Carbon dioxide Concentration Measurements 1877 –1910, Climatic Change 4 (1982) 221-237)

	http://www.biokurs.de/treibhaus/literatur/montsouris/stanhill1-23.pdf
1878	
1879	<p>J.A. Reiset, Recherches sur la proportion de l'acide carbonique dans l'air, Comptes Rendus, T90, 1880, p. 1144 http://gallica.bnf.fr/ark:/12148/bpt6k3047v.image.r=reiset.f1139.langEN</p> <p>George Frederick Armstrong; On the Diurnal Variation in the Amount of Carbon Dioxide in the Air, <i>Proc. R. Soc. Lond. January 1, 1879</i> 30:343-355 http://www.biokurs.de/treibhaus/literatur/sonstige/armstrong1880.pdf</p> <p>H. Macagno; A series of analyses of air, chem.. Centralblatt 11, 1880, p.225 http://www.archive.org/stream/chemischeszentr04chemgoog#page/n268/mode/1up</p>
1880	<p>G. Stanhill, The Montsouris series of Carbon dioxide Concentration Measurements 1877 –1910, Climatic Change 4 (1982) 221-237)</p> <p>J.A. Reiset, Recherches sur la proportion de l'acide carbonique dans l'air, Comptes Rendus, T90, 1880, p. 1144</p> <p>F. Nansen, tidsskrift.dk; Geografisk Tidsskrift, Bind 12 (1893 - 1894) http://www.tidsskrift.dk/print.jsp?id=66857 http://www.archive.org/stream/firstcrossingofg00nansuoft#page/44/mode/2up</p>
1881	<p>G. Stanhill, The Montsouris series of Carbon dioxide Concentration Measurements 1877 –1910, Climatic Change 4 (1982) 221-237)</p> <p>A. Müntz, E. Aubin, Determination de l'acide carbonique de l'air, Comptes rendus, 1881/1, T92, p. 247, 1229 http://gallica.bnf.fr/ark:/12148/bpt6k7351t.image.f246.langFR</p>
1882	<p>A. Müntz, E. Aubin, Determination de l'acide carbonique de l'air dans les stations d'observation du passage de Venus, Comptes rendus, 1883, T96, p. 1793 http://gallica.bnf.fr/ark:/12148/bpt6k3052k.image.r=acide+carbonique.langEN.f1792.tableDesMatières</p> <p>A. Müntz, Sur le dosage de l'acide carbonique de l'air a effectuer Cape Horn; Comptes Rendus T94 1882 p. 1651 http://gallica.bnf.fr/ark:/12148/bpt6k3050z.image.r=m%C3%BCntz.langEN.f1653.tableDesMatières</p>
1883	<p>G. Stanhill, The Montsouris series of Carbon dioxide Concentration Measurements 1877 –1910, Climatic Change 4 (1982) 221-237)</p> <p>W. Spring Spring, W., Roland, L. Untersuchungen über den Kohelnsäuregehalt der Luft; Chemisches Centralblatt Nr. 6, 10.2.1886, 3. Folge 17. Jahrgang and Mémoires couronnés par l' Academie royal de Belgique, 37, 1885, p. 3 http://www.biokurs.de/treibhaus/literatur/spring/spring.doc http://www.biokurs.de/treibhaus/literatur/spring/spring_data.rar</p> <p>S.A. Andree cited in A. Arrhenius, Lehrbuch der kosmischen Physik 2. part, Leipzig 1903, p. 481 http://www.archive.org/stream/lehrbuchderkosmi02arrhuoft#page/480/mode/2up</p>
1884	<p>G. Stanhill, The Montsouris series of Carbon dioxide Concentration Measurements 1877 –1910, Climatic Change 4 (1982) 221-237)</p> <p>E. Ebermayer, Die Beschaffenheit der Waldluft und die Bedeutung der atmosphärischen <i>Kohlensäure</i> für die Waldvegetation«[341] Stuttg. 1885</p> <p>W. Hempel, Die Sauerstoffbestimmung in der atmosphärischen Luft, Beichte der deutsch. Chem. Gesellschaft , 1885, 18, p. 267 http://gallica.bnf.fr/ark:/12148/bpt6k90702f.image.f269.langFR</p>
1885	<p>G. Stanhill, The Montsouris series of Carbon dioxide Concentration Measurements 1877 –1910, Climatic Change 4 (1982) 221-237)</p> <p>Every year up to 1910</p> <p>W. Marcet at al. An Instrument for the Speedy Volumetric Determination of Carbonic Acid <i>Proceedings of the Royal Society of London</i>, Vol. 41, (1886), pp. 181-195 http://www.jstor.org/pss/114483</p>
1886	<p>THOMAS C. VAN NUYS and BENJAMIN F. ADAMS, JR; Carbonic Acid In The Air; Amer. Chem. Journal, 9 1887, p. 191. http://chestofbooks.com/crafts/scientific-american/sup5/Carbonic-Acid-In-The-Air.html Roster, Giorgio</p> <p>L'acido carbonico dell'aria e del suolo di Firenze : Indagini sistematiche eseguite nel 1886 Firenze : Tip. Dei Succ. Le Monnier, 1889. 8 fig. p. 98, cited in J.S.Billings, Ventillation and Heating, The Engineering Record, New York 1893, p. 76 http://www.archive.org/stream/ventilationheati00billuoft#page/78/mode/2up</p> <p>W. Marcet at al. An Instrument for the Speedy Volumetric Determination of Carbonic Acid <i>Proceedings of the Royal Society of London</i>, Vol. 41, (1886), pp. 181-195</p>

	http://www.jstor.org/pss/114483 V. Feldt, „Der Kohlensäuregehalt der Luft in Dorpat bestimmt in den Monaten Februar bis Mai 1887“, Inaug. Dissert. Dorpat 1887; see Letts&Blake http://dspace.utlib.ee/dspace/bitstream/10062/5708/1/kohlen.pdf J. Uffelmann, Luftuntersuchungen ausgeführt im hygienischen Institute der Universität Rostock, Archiv für Hygiene 8, 1888. p262 http://www.biokurs.de/treibhaus/literatur/uffelmann/uffelmann1.doc Selander, N.E., Luftundersökningar vid Vaxhims fästning, Bih. Kgl. Svenska Vet. Handlingar, Bd. 13, 1888, Afd. II, No. 9 cited in H. Lundegardh, Der Kreislauf der Kohlensäure in der Natur. Fischer, Jena (680) (1924), Fig. 10 http://www.biokurs.de/treibhaus/literatur/Lundegardh/lundegardh3.doc cited in L. G. Rommell, Meddelanden från Statens Skogsförsöksanstalt, 1922, p. 255 http://www.archive.org/stream/meddelandenfrn1920stat#page/n265/mode/2up Montsouris see above
1887	J. Heimann, „Der Kohlensäuregehalt der Luft in Dorpat bestimmt in den Monaten Juni bis September 1888“, Inaug. Dissert. Dorpat 1888; see Letts&Blake http://dspace.utlib.ee/dspace/bitstream/10062/5805/4/heimann_derkohlenocr.pdf E. v. Frey, „Der Kohlensäuregehalt der Luft in Dorpat bestimmt in den Monaten September 1888 bis Januar 1889“, Inaug. Dissert. Dorpat 1889; see Letts&Blake http://dspace.utlib.ee/dspace/bitstream/10062/9139/2/frey_kohlensauregehaltocr.pdf Montsouris see above
1888	A. Petermann et al., Untersuchungen über die Zusammensetzung der Atmosphäre, Teil I cited in Jahresbericht über die Fortschritte auf dem Gesamtgebiete der Agrikultur-Chemie, vol 35, 1892, p. 7 http://www.archive.org/stream/jahresberichtb35berl#page/6/mode/2up http://www.biokurs.de/treibhaus/literatur/petermann/pertmann.doc Recherches sur la composition de l'atmosphere premier partie, Bruxelles Mem. Couronn. (8 vo.)47, 1892-1893 A. Palmqvist, cited in O. Petterson, Forhandlingar ved de Skandinaviske Naturforskere vol 14 1892, p. 397 http://www.archive.org/stream/forhandlingerved141892skan#page/398/mode/2up Montsouris see above
1889	Recherches sur la composition de l'atmosphere premier partie, Bruxelles Mem. Couronn. (8 vo.) 47, 1892-1893 A. Palmqvist, Undersökningar öfver Atmospherens Kolsyrehalt, Bihang till K.Sv.Vet.akad.handl. ; Bd 18:Afd.2:no 2, 1892 http://www.biokurs.de/treibhaus/literatur/palmqvist/palmqvist1888-90-2.pdf Montsouris see above
1890	Recherches sur la composition de l'atmosphere premier partie, Bruxelles Mem. Couronn. (8 vo.) 47, 1892-1893 A. Palmqvist, Undersökningar öfver Atmospherens Kolsyrehalt, Bihang till K.Sv.Vet.akad.handl. ; Bd 18:Afd.2:no 2, 1892 http://www.biokurs.de/treibhaus/literatur/palmqvist/palmqvist1888-90-2.pdf A. Lebedinzeff, Neue Modifikation der Dalton-Pettenkofer'schen Methode zur Bestimmung der Kohlensäure in der Luft, Berichte der deutschen chemischen Gesellschaft, A24, 1991, p. 839 http://gallica.bnf.fr/ark:/12148/bpt6k90724r.image.f840.langFR Chemisches Centralblatt vol 62, pt. 1, 1891, p. 221 http://www.archive.org/stream/chemischeszentr08gesegoog#page/n250/mode/1up Zeitschrift für Analytische Chemie (1891) 30:267-279, December 01, 1891 Montsouris see above
1891	Recherches sur la composition de l'atmosphere premier partie, Bruxelles Mem. Couronn. (8 vo.) 47, 1892-1893 Montsouris see above
1892	S.A. Andree, Über die Kohlensäure der Atmosphäre, Chemisches Centralblatt, 1897, Vol. 1, p. 790 http://www.archive.org/stream/chemischeszentr30chemgoog#page/n833/mode/1up Montsouris see above
1893	Montsouris see above
1894	Montsouris see above
1895	Montsouris see above
1896	Carleton Williams, Die Menge der in der Atmosphäre vorhandenen Kohlensäure; Berichte der chemischen Gesellschaft, 20, 1897, Bd.2 p. 1450 http://gallica.bnf.fr/ark:/12148/bpt6k90747d.image.f378.langFR

	Chemisches Centralblatt, 1887, Bd. 1, p. 1095 http://www.archive.org/stream/chemischeszentr27chemgoog#page/n1117/mode/1up Montsouris see above
1897	A. Letts and R.F. Blake, The carbonic anhydride of the atmosphere, http://www.biokurs.de/treibhaus/literatur/letts-blake/letts_blake_biblio.doc http://www.biokurs.de/treibhaus/literatur/letts-blake/letts-blake.rar http://www.biokurs.de/treibhaus/literatur/letts-blake/letts-datap225.jpg Montsouris see above
1898	H.Brown, F. Escombe. On the Variations in the Amount of Carbon Dioxide in the Air of Kew during the Years 1898-1901; Proc. R. Soc. Lond. B April 22, 1905 76:118-121; http://www.biokurs.de/treibhaus/literatur/brown_Escombe/b_e1.doc Montsouris see above
1899	H.Brown, F. Escombe. On the Variations in the Amount of Carbon Dioxide in the Air of Kew during the Years 1898-1901; Proc. R. Soc. Lond. B April 22, 1905 76:118-121; Montsouris see above
1900	H.Brown, F. Escombe. On the Variations in the Amount of Carbon Dioxide in the Air of Kew during the Years 1898-1901; Proc. R. Soc. Lond. B April 22, 1905 76:118-121; Montsouris see above
1901	H.Brown, F. Escombe. On the Variations in the Amount of Carbon Dioxide in the Air of Kew during the Years 1898-1901; Proc. R. Soc. Lond. B April 22, 1905 76:118-121; Montsouris see above
1902	A. Krogh, The abnormal CO ₂ -Percentage in the Air in Greenland and the General Between Atmospheric and Oceanic Carbonic Acid. Meddelelser om Grønland Vol 26 No 8. p.408 http://www.archive.org/stream/meddelelseromgr2526denm#page/406/mode/2up F. Benedict, The composition of the atmosphere, Carbegie Institution 1912 p. 62 http://www.archive.org/stream/carnegieinstitut166carn#page/n5/mode/2up Montsouris see above
1903	Montsouris see above
1904	Montsouris see above
1905	R. Legendre, sur la teneur en acide carbonique de l'air marine; Comptes Rendus T143 1906, p. 526 http://gallica.bnf.fr/ark:/12148/bpt6k30977.image.r=acide+carbonique.f526.langEN Montsouris see above
1906	Montsouris see above
1907	Montsouris see above
1908	J. Charcot, Deuxième expédition antarctique française (1908-1910); Masson Paris 1913, p. 20 http://www.archive.org/stream/deuximeexpdi1913hchar#page/20/mode/2up Montsouris see above
1909	J. Charcot, Deuxième expédition antarctique française (1908-1910); Masson Paris 1913, p. 20 http://www.archive.org/stream/deuximeexpdi1913hchar#page/20/mode/2up F. Benedict, The composition of the atmosphere, Carbegie Institution 1912, p. 69 http://www.archive.org/stream/carnegieinstitut166carn#page/n5/mode/2up Montsouris see above
1910	J. Charcot, Deuxième expédition antarctique française (1908-1910); Masson Paris 1913, p. 20 http://www.archive.org/stream/deuximeexpdi1913hchar#page/20/mode/2up F. Benedict, The composition of the atmosphere, Carbegie Institution 1912, p. 69 http://www.archive.org/stream/carnegieinstitut166carn#page/n5/mode/2up Montsouris see above
1911	A. Wigand. Die Änderung der Zusammensetzung der Luft mit der Höhe Meteorologische Zeitschrift Band 33, 1916 Heft 10 http://www.biokurs.de/treibhaus/literatur/wigand/wigand1911.pdf F. Benedict, The composition of the atmosphere, Carbegie Institution 1912, p. 69 http://www.archive.org/stream/carnegieinstitut166carn#page/n5/mode/2up
1912	
1913	J. Kendall, THE SPECIFIC CONDUCTIVITY OF PURE WATER IN EQUILIBRIUM WITH ATMOSPHERIC CARBON DIOXIDE, Jour. Amer. Chem. Soc. 38: 1480-1497. 1916 pp 1480 – 1497 http://www.biokurs.de/treibhaus/literatur/kendall/kendall1913.pdf
1914	
1915	
1916	
1917	A. Krogh, The composition of the atmosphere, København : A.F. Høst, 1919. Serien: Mathematisk-fysiske meddelelser , bd. 1, nr. 12. http://www.biokurs.de/treibhaus/literatur/krogh/krogh1919.doc
1918	A. Krogh, The composition of the atmosphere, København : A.F. Høst, 1919. Serien: Mathematisk-fysiske

	meddelelser , bd. 1, nr. 12.
1919	
1920	H. Lundegardh, Der Kreislauf der Kohlensäure in der Natur. Fischer, Jena (680) (1924) http://www.biokurs.de/treibhaus/literatur/Lundegardh/lundegardh2.doc http://www.biokurs.de/treibhaus/literatur/Lundegardh/lundegardh3.doc http://www.archive.org/stream/zeitschriftfrb16jena#page/n271/mode/2up H. Lundegardh, Klima und Boden und ihre Wirkung auf das Pflanzenleben, Jena 1949
1921	H. Lundegardh, Der Kreislauf der Kohlensäure in der Natur. Fischer, Jena (680) (1924) H. Lundegardh, Klima und Boden und ihre Wirkung auf das Pflanzenleben, Jena 1949 B. Schulz, Hydrographische Beobachtungen insbesondere <i>über die</i> Kohlensäure in der Nord- und Ostsee im Sommer 1921. (Archiv d. Deutschen Seewarte, XL. Jahrgang, No. 2 1922), data p. 16; sampling on the ship Poseidon: 16.-31.August 1921; on Skagerak: 24.-17.September 1921 http://www.biokurs.de/treibhaus/literatur/schulz1921/schulz1.jpg
1922	H. Lundegardh, Der Kreislauf der Kohlensäure in der Natur. Fischer, Jena (680) (1924) H. Lundegardh, Klima und Boden und ihre Wirkung auf das Pflanzenleben, Jena 1949
1923	H. Lundegardh, Der Kreislauf der Kohlensäure in der Natur. Fischer, Jena (680) (1924) H. Lundegardh, Klima und Boden und ihre Wirkung auf das Pflanzenleben, Jena 1949 E. Rheinau, Rheinau, E. Praktische Kohlensäuredüngung in Gärtnerei und Landwirtschaft, Springer Verlag Berlin, 1927 http://www3.interscience.wiley.com/journal/112256490/abstract?CRETRY=1&SRETRY=0
1924	H. Lundegardh, Der Kreislauf der Kohlensäure in der Natur. Fischer, Jena (680) (1924) H. Lundegardh, Klima und Boden und ihre Wirkung auf das Pflanzenleben, Jena 1949 Th. Meinecke, Die Kohlenstoffernährung des Waldes, Berlin. Verlag Jul. Springer. 1927. http://www3.interscience.wiley.com/journal/114096877/abstract
1925	H. Lundegardh, Der Kreislauf der Kohlensäure in der Natur. Fischer, Jena (680) (1924) H. Lundegardh, Klima und Boden und ihre Wirkung auf das Pflanzenleben, Jena 1949 Wattenberg, H., Die Deutsche Atlantische Expedition auf dem Forschungs- und Vermessungsschiff "Meteor"... 1925-1927. Wissenschaftliche Ergebnisse Band VIII; Das chemische Beobachtungsmaterial und seine Gewinnung, 1.Teil des chemischen Materials, Verlag von Walter de Gruyter&CO, Berlin 1933 p.240 – 307 http://www.biokurs.de/treibhaus/literatur/wattenberg/meteor-reise.jpg http://www.biokurs.de/treibhaus/literatur/wattenberg/watt1.pdf http://www.biokurs.de/treibhaus/literatur/wattenberg/watt2.pdf http://www.biokurs.de/treibhaus/literatur/wattenberg/watt3.pdf
1926	H. Lundegardh, Der Kreislauf der Kohlensäure in der Natur. Fischer, Jena (680) (1924) H. Lundegardh, Klima und Boden und ihre Wirkung auf das Pflanzenleben, Jena 1949 Wattenberg, H., Die Deutsche Atlantische Expedition auf dem Forschungs- und Vermessungsschiff "Meteor"... 1925-1927 A. Krogh u. P.B.Rehberg, CO ₂ -Bestimmung in der atmosphärischen Luft durch Mikrotitration, Biochemische Zeitschrift, 205 (1929) 265 http://www.biokurs.de/treibhaus/literatur/krogh/krogh1929.doc D. Florentin, Sur la composition de l'air des rues de Paris, Comptes Rendus, vol T185, 1927, p. 1538 http://gallica.bnf.fr/ark:/12148/bpt6k31384.image.r=Florentin.f1538.langFR
1927	Wattenberg, H., Die Deutsche Atlantische Expedition auf dem Forschungs- und Vermessungsschiff "Meteor"... 1925-1927 R. Gut, le Gaz carbonique de l'atmosphère forestière, Ders. Journ. Forest. Suisse 9/10,11,12,1929 http://e-collection.ethbib.ethz.ch/eserv/eth:21435/eth-21435-02.pdf D.D. van Slyke, Carbon dioxide factors for the manometric blood gas analysis, http://www.jbc.org/cgi/reprint/73/1/127.pdf#search=%22A%20Gas%20Analysis%20Apparatus%20Accurate%20to%200%E2%80%A2001%25%20%22
1928	R. Gut, le Gaz carbonique de l'atmosphère forestière, Ders. Journ. Forest. Suisse 9/10,11,12,1929 D. Müller, Die Kohlensäureassimilation bei arktischen Pflanzen und die Abhängigkeit der Assimilation von der Temperatur, Planta, 1928, vol. 6, Nr. 1 Juli 1928, p. 22-39 http://www.springerlink.com/content/j27457141865x213/
1929	
1930	P. Lehmann, Messungen der freien Kohlensäure in und über dem Boden einiger der bioklimatischer Stationen im Lunzer Gebiet, Plant systematics and Evolution, Volume 80, Number 2 / Juni 1931 http://www.springerlink.com/content/k65354w513111v5k/
1931	D.D. van Slyke, MANOMETRIC ANALYSIS OF GAS MIXTURES: I. THE DETERMINATION, BY SIMPLE ABSORPTION, OF CARBON DIOXIDE, OXYGEN, AND NITROGEN IN MIXTURES OF THESE GASES <i>J. Biol. Chem.</i> 1932 95: 509-529. http://www.jbc.org/content/95/2/509.full.pdf+html?sid=1f2f8d69-1f4f-4b65-852e-538de1540cba

	<p>MANOMETRIC ANALYSIS OF GAS MIXTURES: II. CARBON DIOXIDE BY THE ISOLATION METHOD <i>J. Biol. Chem.</i> 1932 95: 531-546. http://www.jbc.org/content/95/2/531.full.pdf+html?sid=1f2f8d69-1f4f-4b65-852e-538de1540cba</p> <p>MANOMETRIC ANALYSIS OF GAS MIXTURES: Part III March 1, 1932 <i>The Journal of Biological Chemistry</i>, 95, 547-568. http://www.jbc.org/content/95/2/547.full.pdf+html?sid=1f2f8d69-1f4f-4b65-852e-538de1540cba</p>
1932	<p>K. Buch, Der Kohlendioxydgehalt der Luft als Indikator der Meteorologischen Luftqualität," <i>Geophysica</i>, vol. 3, 1948, pp. 63-79. http://www.biokurs.de/treibhaus/literatur/buch/buch1948.doc</p>
1933	<p>Buch K, Kohlensäure in der Atmosphäre und Meer an der Grenze zum Artikum, ABO Akademi, 1939 http://www.biokurs.de/treibhaus/literatur/buch/buch1939.pdf</p> <p>k. Buch, Beobachtungen über das Kohlensäuregleichgewicht und über den Kohlensäureaustausch zwischen Atmosphäre und Meer im Nord-Atlantischen Ozean" . <i>Acta Acad. Aboensis, Math. et Physica</i>, v. 11, no. 9, 32 pp., 1939. Abo, Finland.</p> <p>T. Moyer, Precise Automatic Apparatus for Continuous Determination of Carbon Dioxide in Air <i>Ind. Eng. Chem. Anal. Ed.</i>, 1933, 5 (3), pp 193–198 http://pubs.acs.org/doi/abs/10.1021/ac50083a021</p>
1934	<p>K. Buch, Der Kohlendioxydgehalt der Luft als Indikator der Meteorologischen Luftqualität," <i>Geophysica</i>, vol. 3, 1948, pp. 63-79.</p> <p>Buch K, Kohlensäure in der Atmosphäre und Meer an der Grenze zum Artikum, ABO Akademi, 1939</p> <p>Waugh <i>Precise Determination of Carbon Dioxide in Air. Hand-Operated Apparatus</i> <i>Ind. Eng. Chem. Anal. Ed.</i>, 1937, 9 (2), pp 96–100 http://pubs.acs.org/doi/abs/10.1021/ac50106a018 http://www.biokurs.de/treibhaus/literatur/waugh/waugh1934.pdf</p>
1935	<p>K. Buch, Der Kohlendioxydgehalt der Luft als Indikator der Meteorologischen Luftqualität," <i>Geophysica</i>, vol. 3, 1948, pp. 63-79.</p> <p>Buch K, Kohlensäure in der Atmosphäre und Meer an der Grenze zum Artikum, ABO Akademi, 1939</p> <p>Kauko, Y., Yli-Uotila, T., Zur Kenntnis der absoluten Kohlensäure der Luft, <i>Meteorologische Zeitschrift</i>, Band 54, 1937, S. 30-33</p> <p>Y. Kauko, V. Mantere ; Eine genaue Methode zur Bestimmung des CO₂-Gehaltes der Luft <i>Zeitschrift für anorganische und allgemeine Chemie</i>, Volume 223, Issue 1, 1935. Pages 33-44</p> <p>Y. Kauko, einige orientierende Versuche über den Kohlensäuregehalt der Luft über der Stadt Helsinki, <i>Suomen, Kemistilehti</i>, , Vol. 7-8, 1936, p. 65 http://www.biokurs.de/treibhaus/literatur/kauko/helsinki1936.jpg</p> <p>J.B.S Haldane. Carbon dioxide content in atmospheric air; <i>Nature</i>, 4,4, p. 575, 1936 http://www.biokurs.de/treibhaus/literatur/Haldane/haldane1.doc</p>
1936	<p>K. Buch, Der Kohlendioxydgehalt der Luft als Indikator der Meteorologischen Luftqualität," <i>Geophysica</i>, vol. 3, 1948, pp. 63-79.</p> <p>Buch K, Kohlensäure in der Atmosphäre und Meer an der Grenze zum Artikum, ABO Akademi, 1939</p> <p>U. Duerst, "Neue Forschungen über Verteilung und Analytische Bestimmung der wichtigsten Luftgase als Grundlage für deren hygienische und tierzüchterische Wertung," <i>Schweizer Archiv für Tierheilkunde</i>, vol. 81, No. 7/8, August 1939, pp.305-3 17. http://www.biokurs.de/treibhaus/literatur/duerst/duerst1939.doc</p>
1937	<p>U. Duerst, "Neue Forschungen über Verteilung und Analytische Bestimmung der wichtigsten Luftgase als Grundlage für deren hygienische und tierzüchterische Wertung," <i>Schweizer Archiv für Tierheilkunde</i>, vol. 81, No. 7/8, August 1939, pp.305-3 17.</p>
1938	<p>U. Duerst, "Neue Forschungen über Verteilung und Analytische Bestimmung der wichtigsten Luftgase als Grundlage für deren hygienische und tierzüchterische Wertung," <i>Schweizer Archiv für Tierheilkunde</i>, vol. 81, No. 7/8, August 1939, pp.305-3 17.</p>
1939	<p>W. Kreutz, "Kohlensäure Gehalt der unteren Luftschichten in Abhängigkeit von Witterungsfaktoren," <i>Angewandte Botanik</i>, vol. 2, 1941, pp. 89-117, http://www.biokurs.de/treibhaus/literatur/kreutz/kreutz.zip</p>
1940	<p>W. Kreutz, "Kohlensäure Gehalt der unteren Luftschichten in Abhängigkeit von Witterungsfaktoren," <i>Angewandte Botanik</i>, vol. 2, 1941, pp. 89-117</p> <p>LOCKHART, ARNOLD COURT; OXYGEN DEFICIENCY IN ANTARCTIC AIR ; Monthly weather report, Vol 70, No. 5, 1942 http://docs.lib.noaa.gov/rescue/mwr/070/mwr-070-05-0093.pdf</p> <p>H.C. Bazett, A MODIFIED HALDANE GAS ANALYZER FOR ANALYSIS OF MIXTURES WITH ONE HUNDRED PER CENT ABSORBABLE GAS <i>J. Biol. Chem.</i> 1941 139: http://www.jbc.org/content/139/1/81.full.pdf</p>
1941	<p>LOCKHART, ARNOLD COURT; OXYGEN DEFICIENCY IN ANTARCTIC AIR ;</p>

	<p>Monthly weather report, Vol 70, No. 5, 1942</p> <p>Fuller, H. J. 1948. Carbon dioxide concentrations of the atmosphere above Illinois forest and grassland. <i>Amer. Mid. Nat.</i>, 39: 247-249. Gut, R. C. 1929 http://www.biokurs.de/treibhaus/literatur/fuller/fuller1941.pdf</p>
1942	<p>R.K., Misra, Studies on the Carbon Dioxide factor in the air and soil layers near ground, <i>Indian Journal of Meteorology and Geophysics</i>, 1 (4): 275-286, 1950 http://www.biokurs.de/treibhaus/literatur/misra/misra1941.doc</p>
1943	<p>R.K., Misra, Studies on the Carbon Dioxide factor in the air and soil layers near ground, <i>Indian Journal of Meteorology and Geophysics</i>, 1 (4): 275-286, 1950</p>
1944	<p>E. Glückauf, <i>Nature</i>, may 20 1944, vol. 153, p. 620 http://www.biokurs.de/treibhaus/literatur/glueckauf/glueckauf1944.pdf</p>
1945	
1946	<p>P. F. Scholander ; ANALYZER FOR ACCURATE ESTIMATION OF RESPIRATORY GASES IN ONE-HALF CUBIC CENTIMETER SAMPLES ; <i>J. Biol. Chem.</i> 1947 167: 235-250 http://www.jbc.org/cgi/reprint/167/1/235</p>
1947	<p>R. Hock, P. Scholander, COMPOSITION OF THE GROUND-LEVEL ATMOSPHERE AT POINT BARROW, ALASKA, <i>Journal of Atmospheric Sciences</i>, vol. 9, Issue 6, pp.441-441 http://ams.allenpress.com/archive/1520-0469/9/6/pdf/i1520-0469-9-6-441.pdf</p>
1948	<p>R. Hock, P. Scholander, COMPOSITION OF THE GROUND-LEVEL ATMOSPHERE AT POINT BARROW, ALASKA, <i>Journal of Atmospheric Sciences</i>, vol. 9, Issue 6, pp.441-441</p>
1949	<p>H.W. Chapman , W.E. Loomis, <i>Plant Physiol.</i> 1953 October; 28(4): 703–716. http://www.pubmedcentral.nih.gov/picrender.fcgi?artid=540433&blobtype=pdf</p>
1950	<p>H.W. Chapman , W.E. Loomis, <i>Plant Physiol.</i> 1953 October; 28(4): 703–716. https://kb.osu.edu/dspace/bitstream/1811/3939/1/V52N04_187.pdf K. Egle, W. Schenk, Die Anwendung des Ultrarotabsorptionsschreibers in der Photosyntheseforschung <i>Ber. d. dtsh. bot. Ges.</i>, 64, 180 1951.</p>
1951	<p>H.W. Chapman , W.E. Loomis, <i>Plant Physiol.</i> 1953 October; 28(4): 703–716. de Selm, H.R., Carbon Dioxide Gradients in Beech Forest in Central Ohio, <i>Ohio Journal of Science</i> 52 (4) 187, July 1952 https://kb.osu.edu/dspace/bitstream/1811/3939/1/V52N04_187.pdf B. Huber, Der Einfluß der Vegetation auf die Schwankungen des CO₂-Gehaltes der Atmosphäre Theoretical and Applied Climatology, Volume 4, Number 2 / Oktober 1952 http://www.springerlink.com/content/p321g0540656599k/</p>
1952	<p>H. W. Chapman, L. S. Gleason, and W. E. Loomis The Carbon Dioxide Content of Field Air <i>Plant Physiol.</i> 29: 500-503 http://www.plantphysiol.org/cgi/reprint/29/6/500?maxtoshow=&HITS=10&hits=10&RESULTFORMAT=&author1=Chapman+&searchid=1&FIRSTINDEX=0&sortspec=relevance&resourcetype=HWCIT de Selm, H.R., Carbon Dioxide Gradients in Beech Forest in Central Ohio, <i>Ohio Journal of Science</i> 52 (4) 187, July 1952</p>
1953	
1954	<p>S. Fonselius, Microdetermination of CO₂ in the <i>air</i>, with current Data for Scandinavia., <i>Tellus</i> 7, 1955, pp. 259–265. 66 http://www.biokurs.de/treibhaus/literatur/Fonselius/Fonselius1_2.doc</p>
1955	<p>S. Fonselius, Microdetermination of CO₂ in the <i>air</i>, with current Data for Scandinavia., <i>Tellus</i> 7, 1955, pp. 259–265. 66 C. Keeling, The concentration and isotopic abundances of atmospheric carbon dioxide in rural areas, <i>Geochim. et Cosmochim. Acta</i> 13, pp. 322—33 http://www.biokurs.de/treibhaus/literatur/keeling/Keeling_1955.doc</p>
1956	<p>S. Fonselius, Microdetermination of CO₂ in the <i>air</i>, with current Data for Scandinavia., <i>Tellus</i> 7, 1955, pp. 259–265. 66</p>
1957	<p>S. Fonselius, Microdetermination of CO₂ in the <i>air</i>, with current Data for Scandinavia., <i>Tellus</i> 7, 1955, pp. 259–265. 66 Steinhauser, F. Der Kohlendioxidgehalt der Luft in Wien und seine Abhängigkeit von verschiedenen Faktoren, <i>Berichte des deutschen Wetterdienstes</i>, Nr. 51, S 54, 1958 http://www.biokurs.de/treibhaus/literatur/steinhauser/steinhauser.doc</p>
1958	<p>S. Fonselius, Microdetermination of CO₂ in the <i>air</i>, with current Data for Scandinavia., <i>Tellus</i> 7, 1955, pp. 259–265. 66</p>
1959	<p>S. Fonselius, Microdetermination of CO₂ in the <i>air</i>, with current Data for Scandinavia., <i>Tellus</i> 7, 1955, pp. 259–265. 66 Bischof, W. (1960) Periodical variations of the atmospheric CO₂ content in Scandinavia. <i>Tellus</i> 12, 216-226. http://www.biokurs.de/treibhaus/literatur/bischof/Bischof.pdf</p>

CO₂ Sampling Stations - Chemical Methods 1800-1960

©Ernst-Georg Beck 2006-2010

Note: Montsouris 1877-1910; all stations listed with their first year

year	Station	Method
97 409 samples used at 901 stations		
1809	<p>•Investigator: Theodore de Saussure, Prof. mineralogy, geology University Geneva (Switzerland)</p> <p>•Location: Meadow near the village of Chambesy near Geneva (Switzerland), slightly inclined, 250 m from the Lake of Geneva, well ventilated, soil: clay, , rural area;</p> <p>•Lat 46,15N. Lon: 6,8 E.</p> <p>•Elevation: 1,3 m above ground, 16 m above sea level of Lake Geneva, 388m masl</p> <p>•Mountains around Chambesy 900 – 1300m height</p> <p>Sampling time: 1809-1816, at noon 1826-1830</p> <p>Samples: 225 since 1809, since 1826 205; 8 samples at mountains</p> <p>Meteorolog. Parameters: daytime, precipitation, weather</p> <p>Station 1, 2</p>	<p>•Gravimetric determination of Barium carbonate (sulphate)</p> <p>•Sampling: Simultaneous measurements day/night -city/rural area-water/land, vegetation, mountains, rain, winter, summer; 6 times sampling in one location, 225 single samples since 1826</p> <p>•Duration of analysis: 24 hours.</p> <p>•Methodical details: 35-45 Litre round flask with fixed lock, stop cocks and seals, air pumping by air pump; measurement of temperature, air pressure and humidity; 100 g baryta water, absorption time 1 h. (60-80 x shaking/minute); Barium carbonate in baryta water was separated after absorption to wash flask; Elution with HCl several times rest of baryta in flask (1mass unit HCl on 15 mass units water = about. 0,8M), joining precipitations and precipitation with Na₂SO₄.;Sufficient absorption time of solutions (-24 hours). Resulting dry barium carbonate was weighed (mg scales) and mass of bound CO₂ was calculated.</p> <p>Remarks and Errors:</p> <p>•Results relatively stable on a high level compared to later series 1830-1850; minimum 0,2 mg weighing error because of variable mass of absorption equipment [Warburg 1905; Hlasiwetz 1856 p.9]; 3rd procedure according to Thenard: weight of Ba(CO₃): 0,966g ; 391 ppm CO₂; min. ~21% error, seals in leather is a cause of erroneous high values after Müntz (1880); max. 2,5% error by hygroscopic glass walls; resulted weights of CO₂ by using around 30 l is in the order of about 30 mg using 330 ppm. Weight errors of glass apparatuses are in then same error range up to 32 mg [Hlasiwetz 1856]</p> <p>Estimated error: 20%</p>
1839	<p>Investigator: Jean-Baptiste Boussingault, Prof. chemistry Lyon, Paris</p> <p>Location: Paris (48N 2E), periphery, Alsace Pechelbronn (Alsace, France) lat 48,93N, 7,83E Liebfrauenberg (Alsace) lat 48,23N 7,38E Andilly lat 49N 2,3E, rural area</p> <p>Elevation: 1-2 m Paris: 129 masl Pechelbronn: masl 153-199 m Liebfrauenberg: masl 222m Andilly: masl 278</p> <p>Sampling time: 1839-1843; at Paris 1839-1841 during 142 days In Alsace Nov.- 1839-March 1840 during 49 days; at Andilly and Paris, College de France 1843 Sept—</p>	<p>• Gravimetric determination of Sodium sulfate Citation from Hlasiwetz 1856: Method after Carl Emmanuel Brunner, Professor of chemistry in Bern (Switzerland)</p> <p>•About 25 Litre air flows through tubes with H₂SO₄ on pumice, then through tubes with KOH, then again through tubes with H₂SO₄. Amount of CO₂ was calculated by rise of mass in the tubes with KOH and H₂SO₄.</p> <p>Citation from Brunner, M. 'Détermination de l'acide carbonique'; Annales de Chimie, 3, 1841, p. 312</p> <p>Remarks and errors:</p> <p>•U-tubes containing H₂SO₄ absorb CO₂, therefore resulting in too low values (~20 ppm according to Spring 1885, 7-10% according to Hlasiwetz</p>

	<p>Nov. Samples: Alsace 19, Paris 190, Paris/Montmorency 1843: 22; total: 231 Meteorolog. Parameters: daytime, precipitation, weather</p>	<p>1856); Amount of CO₂ too small for accurate weighing; min. 0,2mg error [Warburg 1902]; max. 2,5% error by hygroscopic glass walls; resulted weights of CO₂ by using around 30 l is in the order of about 30 mg using 330 ppm. Weight errors of glass apparatuses are in then same error range up to 32 mg [Hlasiwetz 1856]; large fluctuation of values (-100%) shown by most series done by several authors</p> <p>Estimated error: 50%</p>
1847	<p>Investigator: Bernhard Carl Lewy, (Danmark), Prof. chemistry, Bogota Location: France, Atlant. Ocean, Caribbean, Colombia, rural area Sept. 1847 at Paris (48N 2E), Nov./Dec. 1847 Le Havre (49N, 0,1E) Atlantic Ocean Dec. 1847: 47,3N, -8,5E, 47N, -11E, 33,4N, -18,35E, 21,45N, -39,3E, 21,9N, -40,25E, 20,35N, -41,35E, 15,49N, -62,48E, 14,6N, -68,4E, 12,5N, -76E Colombia: Rio Magdalena San Bernardo 4,4N, -74,2, Ambalema 4,78N, -76,7E, Esperanza 7,39N, -73,37E, Santa Ana 7,14N, -73,29E, Honda 7,28N, -73,25E, Guaduas, 5,7N, -74,5E, Bogota 4N, Elevation: Paris, 30 masl, Le Havre 8 masl, Rio Magdalena 38 masl, Ambalema 282 masl, Esperanza 396 masl, Honda 242 masl, Guaduas 996 masl, Santa Ana 998 masl, Bogota 2645 masl Sampling time: Sept 1847-Aug 1848, High amount of volcanoes in the Rio Magdalena area, high CO₂ low O₂ Samples: Paris 5, Le Havre: 4, Atlantic Ocean: 11, Colombia: 11; Bogota 14: total: 45 Meteorolog. Parameters: daytime, temperature, pressure, precipitation, weather</p>	<p>Volumetric determination according to Regnault/Reiset Part of samples in flasks are analysed 18-20 months after sampling at Paris •Hydrogen Eudiometer; air flow trough tubes with pumice and KOH, then baryta water. Adding H₂SO₄ the potassium carbonate is transformed to potassium sulphate liberating CO₂, after that measuring change of volume. • Remarks and errors: Open system using long connections between CO₂ absorption and Eudiometer, partly consisting of caoutchouc; no control of heat of absorption temperature (approx. 20,000 cal/g Mol; Schuftan 1933): Temperature change gas of 1° = change of vol/pressure by 0.34 %; [Schuftan 1933]. Further methodical errors by absorption of CO₂ in H₂SO₄ resulting in too low values (about -20 ppm). (Using H₂SO₄ for drying air see Regnault/Reiset, Annales de chimie, 24, 1871 p.258 [Regnault 1871]) Standard dev. of samples from Columbia= 641,3</p>
1848	<p>Investigator: Richard F. Marchand, Prof. chemistry at Halle (Germany) Conditions not researchable Sampling time 1848-1850 Samples: 150 No further details researchable</p>	<p>Gravimetric method similar Brunner Several samples showing very high and low levels Estimated error: >20-50%</p>
1851	<p>Investigator: Ch. Mène Location: Paris (48N 2E), Sampling time: Aug 1851 Samples: 12 Meteorolog. Parameters: daytime, temperature, No further details researchable</p> <p>Investigator: Adolf Schlagintweit, Prof. geography Munich (Germany) Location: Swiss/Italian Alps (45N, 7,51E), rural area Elevation: 1370-1862 masl Sampling time: Sept 1851 Samples: 16 (Alps+ Berlin) Meteorolog. Parameters: daytime, temperature, pressure, weather</p>	<p>Mène: Method according to Boussingault and titrimetric Remarks and errors: Drying air by sulphuric acid, -20 ppm error according to Spring and Hlasiwetz Estimated error: selected data >20 % No further details researchable</p> <p>Schlagintweit: gravimetric; passing air through tubes of sulphuric acid or CaCl₂ solution for drying; absorption in 3 tubes with KOH;. Weighing the absorbed solution; Remarks and errors: Drying air by sulphuric acid, -20 ppm error according to Spring and Hlasiwetz; weighing errors, gravimetric see Brunner (Boussingault. Estimated error: selected data >20 %</p>

1854	<p>Investigator: August Vogel jun., Prof. organic chemistry Munich (Germany) Location: Munich (48N, 11,35E), city free place Elevation: 519 masl Sampling time: Aug. 1854 Samples: 11 Meteorolog. Parameters: -</p>	<p>Gravimetric after Brunner see above Remarks and errors: Drying air by sulphuric acid, -20 ppm error according to Spring and Hlasiwetz; weighing errors, gravimetric see Brunner (Boussingault. Estimated error: selected data about 20 % using selected data</p>
1856	<p>Investigator: Hugo v. Gilm., Prof. chemistry Innsbruck (Austria) Location: Innsbruck (Austria) (47N, 11,39E) garden of the university Elevation: 573 masl Sampling time: Nov. 1856- March 1857 Samples: 19 Meteorolog. Parameters: temp. pressure, state of the atmosphere</p> <p>Station 16</p>	<p>Gravimetric/volumetric, Aspiration of approx. 60 L air and absorption in baryta water; dilution of filtrated Barium carbonate in HCl, drying of produced Barium chloride. Subsequent determination of Chlorine by titration after Mohr; amount Chlorine = CO₂. Calibration: Determination of a weighed amount of BaCO₃ in a CO₂ free flask. Decomposition of BaCO₃ by H₂SO₄, measurement of deliberated amount of CO₂, result: Remarks and errors: weighing errors, gravimetric see Brunner/ Boussingault. Estimated error: 10%; about 2,8 % using selected data</p>
1863	<p>Investigator: Franz Schulze., Prof. chemistry Rostock (Germany) Location: western balcony of university of Rostock (54N, 12,06E) , free ventilation Elevation: about 19 masl Sampling time: Oct. 1863- Dec 1864 Samples: 431 Meteorolog. Parameters: daytime, temp. pressure, Wind direction, precipitation, state of the atmosphere</p> <p>Station 18</p>	<p>Pettenkofer titrimetric •Flask method/tube method; approx. 25 Litre air per analysis by using 2 l flasks/tubes; baryta water for absorption of CO₂ and oxalic acid for titration of CaCO₃; indicator for showing endpoint of titration; about 30 minutes per analysis. Remarks and errors: Independent on temperature, easy design, fast speed, (30 min) high accuracy possible (1-3% Kauko 1935), errors possible by sampling air, contamination of baryta water during titration and too small air volume for testing. Schulze had used max. 25 l air for one analysis . Estimated error: +--10%</p>
1864	<p>Investigator: Agnus Smith., Dr. chemistry Manchester (UK) Location: various places Scotland, (56,1-3N, - 3,23E) rural areas, hills 1 Elevation: 250-1400 masl Sampling time: 1864-1865 Samples: 200 London/Manchester, 158 Scotland total: 358 Meteorolog. Parameters: daytime, temp. pressure, wind, state of the atmosphere Station-57</p>	<p>Pettenkofer flask method as Schulze Baryta water, Oxalic acid, titration Estimated error: +--10%</p>
1865	<p>Investigator: T.E Thorpe, Prof. chemistry Leeds (UK) Location: along the coasts, (54,21N, -2,11E) Irish sea Elevation: 2 masl Sampling time: summer 1865-summer 1866 Samples: 77 Irish channel; 31 in tropical Brasil (Letts&Blake) Meteorolog. Parameters: daytime, temp. pressure, wind direction, speed, state of the atmosphere</p>	<p>Pettenkofer flask method as Schulze 5l flasks,modified Baryta water, Oxalic acid, titration Estimated error: +--3%</p>

	Station 157	
1868	<p>Investigator: Franz Schulze., Prof. chemistry Rostock (Germany) Location: university of Rostock (54N, 12,06E), direction Blücherplatz, periphery of the city, free ventilation Elevation: about 19 masl Sampling time: Oct. 1868- July 1871, 2 samples daily Samples: 1600 Meteorolog. Parameters: daytime, temp. pressure, wind direction, precipitation, state of the atmosphere station 158</p>	<p>Pettenkofer flask method , titrimetric, modified 25 l flasks, 66 l Aspirator Baryta water, Oxalic acid, titration</p> <p>Estimated error: +--3%</p>
1872	<p>Investigator: J.A Reiset., Prof. chemistry Paris Location: 8m from Dieppe (France) (49N, 1,07E), agricultural station, rural area, free ventilation Elevation: about 96 masl Sampling time: Sept. 1872 – Oct. 1873, Samples: 92 field, 27 young forest, 14 clover/alfalfa Meteorolog. Parameters: daytime, temp. pressure, wind direction, precipitation, state of the atmosphere station 161</p> <hr/> <p>Investigator: Eugène Risler., Prof. agronomie, Paris Location: Calèves (Nyon, Switzerland) (46N, 6,63E), rural area, free ventilation Elevation: 420 masl Sampling time: Aug. 1872 – July 1873 Samples: 365 Meteorolog. Parameters: not known Station 162</p> <hr/> <p>Investigator: Wilhelm Henneberg., Prof. chemistry Göttingen (Germany) Location: Weende (Germany) (51,5N, 9,95E), agricultural station, rural area Elevation: about 237 masl Sampling time: May - July 1872, Samples: >17 Meteorolog. Parameters: temperature Station 163</p>	<p>Reiset: Pettenkofer variant mobile analyser, 600 l aspirator (Reiset's tower); drying by sulphuric acid, absorption in barium hydroxide; titration by resulting carbonate by sulphuric acid. Remarks and errors: Sulphuric acid error of about 20-30 ppm according to Hlasiwetz [1848] and Spring (1883); Bunsen absorption coefficient H₂SO₄ at 25°C = 0,96; H₂O at 25°C=0,759 [IUPAC NIST Solubility database]</p> <p>Estimated error: correction by +20 ppm; error+--3%</p> <hr/> <p>Risler: Pettenkofer variant no more details researchable</p> <hr/> <p>Henneberg, Weende: Pettenkofer flask method as Schulze 5l flasks,modified Baryta water, Oxalic acid, titration</p> <p>Estimated error: +--3%</p>
1873	<p>Investigator: Pierre Truchot., Prof. chemistry, Clermont-Ferrand Location: some kms from Clermont-Ferrand, (45N, 1,05E), rural area, free ventilation Elevation: near Clermont Ferrand 395 masl; Sampling time: July-Aug. 1873, day/night Samples: 49 Meteorolog. Parameters: temp., pressure Station 164</p>	<p>Pettenkofer method 10-20l air absorbed in baryta water, titration the carbonate with sulphuric acid</p> <p>Estimated error: +--3-10%</p>

Supplemental file to: Reconstruction of atmospheric CO₂ Background levels since 1826

1874	<p>Investigator: Franz Farsky., Dr. chemistry, director of the agricultural station at Tabor, Czech Republic Location: agricultural station outside Tabor, (49,25N, 14,6E), rural area, free ventilation, 4,48m above ground NNW Elevation: 423 masl; Sampling time: Oct. 1874 -Aug. 1875 Spring /summer afternoon, autumn/winter at noon Station 165 Samples: 295 Meteorolog. Parameters: temp., pressure, wind direction, precipitation, weather</p> <p>Investigator: P. Hässelbarth, Dr. chemistry, J. Fittbogen Prof. chemistry, director agricultural station Dahme Location: Dahme (Prussia) lat 51N, 11,04 lon; agricultural station, rural area Elevation: 87 masl, sampling height: 2,85m Sampling time: Sept. 1874-Aug 1875 Samples: 347 Meteorolog. Parameters: temp., pressure, wind direction, precipitation, weather Station 166</p>	<p>Pettenkofer variant of Fittbogen Air passing from outside (4,48m elevation) NNW in CaCl₂ tubes (drying) and then in a absorption tube with baryta water then in a Brunner 30 l aspirator. Absorbing time 4 h. Titration was done with hydrochloric acid or oxalic acid.</p> <p>Estimated error: +--3%</p> <p>Pettenkofer variant of Fittbogen Air passing from eastern, outside of laboratory (2,85m elevation) in CaCl₂ tubes (drying) and then in a absorption tube with baryta water then in a 32 l aspirator. Absorbing time 5 h. Titration was done with oxalic acid.</p> <p>Estimated error: +--3%</p>
1875	<p>Investigator: Gaston Tissandier, Location: Paris : 890 masl 1000 masl during balloon flight (Zenith) Elevation: 87 masl, sampling height: 2,85m Sampling time: March. 1874 Samples: 2 Meteorolog. Parameters: temp., pressure, wind direction, weather Station 167</p> <p>Investigator: Peter Claesson, Dr. chemist Location: Lund (Sweden) lat 55, 13,12E lon Elevation: 47 masl Sampling time: Nov/Dec. 1875 Samples: 31 Meteorolog. Parameters: - Station 168</p>	<p>Volumetric determination according to Regnault/Reiset •air flow trough tubes with pumice and KOH, then baryta water. 22 l Aspirator. Adding H₂SO₄ the potassium carbonate is transformed to potassium sulphate liberating CO₂, after that measuring change of volume. Using 66 l air</p> <p>Remarks and errors: Open system using long connections between CO₂ absorption and Eudiometer, partly consisting of caoutchouc; no control of heat of absorption temperature (approx. 20,000 cal/g Mol; Schuftan 1933): Temperature change gas of 1° = change of vol/pressure by 0.34 %; [Schuftan 1933]. Further methodical errors by absorption of CO₂ in H₂SO₄ resulting in too low values (about -20 ppm).</p> <p>Estimated error: +--8%</p> <p>Claesson Pettenkofer method 50 air passed through CaCl₂, absorbed in baryta water, titration the carbonate</p> <p>Estimated error: +--3-10%</p>
1876	<p>Investigator: E.L. Moss, Dr. physician Location: Arctic, Greenland lat 82,7, -20E lon Elevation: - Sampling time: Dec 1875, Jan/Feb. 1876 Samples: 3 Meteorolog. Parameters: temp., pressure, weather Station 169</p>	<p>Pettenkofer method 47, 95, 19 l samples of air absorbed in baryta water, titration the carbonate</p> <p>Estimated error: +--3-10%</p>

1877	<p>Investigator: Hippolyte Marié-Davy, Prof. physicist, Montpellier; Albert Lévy, Dr. physicien</p> <p>Location: Paris 48,58N, 2,27E Montsouris observatory</p> <p>Elevation: 75 masl</p> <p>Sampling time: daily 1877-1912, noon</p> <p>Samples: 12 000</p> <p>Meteorolog. Parameters: temp., pressure, wind, precipitation, weather</p> <p>Station 170</p>	<p>Pettenkofer method Absorption of dry air in baryta water /sodium hydroxide, titration with HCl (since 1892 H₂SO₄) Changing method in July 1890 leads to a shift of + 18,5 ppm in SEAS</p> <p>Remarks and errors: First years 1877-July 1890 values too low, corrected by +18,5 Estimated error: +--3%</p>
1879	<p>Investigator: J.A Reiset., Prof. chemistry Paris</p> <p>Location: 8km from Dieppe (France) (49N, 1,07E), agricultural station, rural area, free ventilation, the North Sea in NE direction</p> <p>Elevation: about 96 masl +4m sampling height</p> <p>Sampling time: June – Nov. 1879, day/night, June-Aug. 1880</p> <p>Samples: 91 (1879), 37 (1880),</p> <p>Meteorolog. Parameters: daytime, temp. pressure, wind direction, precipitation, state of the atmosphere</p> <p>station 171</p>	<p>Reiset: Pettenkofer and volumetric variant according to Regnault mobile analyser, 600 l aspirator (Reiset's tower); , drying by sulphuric acid, absorption in barium hydroxide (12 hours); titration the resulting carbonate by sulphuric acid. Furthermore volumetric determination.</p> <p>Remarks and errors: Sulphuric acid error of about 20-30 ppm according to Hlasiwetz [1848] and Spring (1883); Bunsen absorption coefficient H₂SO₄ at 25°C = 0,96; H₂O at 25°C=0,759 [IUPAC NIST Solubility database]</p> <p>Estimated error: correction by +20 ppm; error+--3%</p>
	<p>Investigator: George F. Armstrong, Prof. engineering, Leeds (UK)</p> <p>Location: village of Grasmere 54,45N, -3,0E , rural area at Lake Grasmere surrounded by hills, meadow</p> <p>Elevation: 61 masl +1,50 sampling height</p> <p>Sampling time: July - Oct. 1879, day/night</p> <p>Samples: 115 (53 day, 62 night)</p> <p>Meteorolog. Parameters: temp., pressure, wind, precipitation, weather</p> <p>Station 172</p>	<p>Armstrong: Pettenkofer variant 4 x 10l jars; air passed through Baryta water titrated with sulphuric acid, quadruple sampling</p>
	<p>Investigator: Ippolito Macagno, Prof., chemistry, director of the royal agricultural station of Palermo (Sicilia))</p> <p>Location: Palermo, astronomical observatory 38,6N, 13,21E ,</p> <p>Elevation: 72 masl</p> <p>Sampling time: Feb - Aug. 1879</p> <p>Samples: 21 (3 per month)</p> <p>Meteorolog. Parameters: temp., pressure, O₂, precipitation</p> <p>Station 173</p>	<p>Macagno: Assumption: Pettenkofer variant data measured in 100 l air</p> <p>Estimated error: -3-10%</p>
1881	<p>Investigator: Achille Müntz, Prof., chemistry, National Institute of Agronomy Paris</p> <p>Location: Paris, 48N, 2,14E, Plaines de Vincennes (rural area) 48,84N, 2,44E; Pic Midi 38,6N, 13,21E ,</p> <p>Elevation: Paris:129 masl , Pleines des Vincennes 52 masl, Pic Midi: 2877 masl</p> <p>Sampling time: Dec. 1880. - Dec. 1881</p> <p>Samples: Paris: 42, Plaine d. V.: 35, Pic Midi: 14</p> <p>Meteorolog. Parameters: temp., pressure, weather, precipitation</p>	<p>Volumetric after Regnault 300l air dried by sulphuric acid was absorbed in KOH; addition of sulphuric acid set free CO₂, volume measured by manometer.</p> <p>Remarks and errors: Open system, no means of controlling heat of absorption; sulphuric acid absorbed parts of CO₂, error of about 20-30 ppm according to Hlasiwetz [1848] and Spring (1883); Bunsen absorption coefficient H₂SO₄ at 25°C = 0,96; H₂O at</p>

Supplemental file to: Reconstruction of atmospheric CO₂ Background levels since 1826

	Station 174-176	25°C=0,759 [IUPAC NIST Solubility database] Estimated error: correction : + 20 ppm , after correction: +--3%
1882	<p>Investigator: Achille Müntz, Prof., chemistry, National Institute of Agronomy Paris</p> <p>Location: Venus expedition: Haiti 18N, -72E, Florida 29,9N, -81E, Martinique 14N, -61E, Mexico 26N, -111E, Santa Cruz 34,35S, -71,74E, Chubut 43,18S, -65E, Cerro Negro 36,9S, -72,5 E</p> <p>Elevation: Haiti 355 masl , Florida 4 masl, Martinique 1masl , Mexico, Santa Cruz 520 masl, Chubut 50 masl, Cerro-Negro 153 masl</p> <p>Sampling time: Haiti Nov. 1882. - Jan. 1883; Florida Nov-Dec. 1882, Martinique Oct. -Dec. 1882, Mexico Nov.-Dec. 1882, Santa Cruz Patagonia Oct-Dec. 1882, Chubut Nov.-Dec 1882,, Cerro-Negro Dec 1882</p> <p>Samples: Haiti: 8, Florida: 7, Martinique: 5, Mexico 3, Santa Cruz 10, Chubut 2, Cerro Negro (Chile) 5; total 38 (1882); 2 at Haiti 1883</p> <p>Meteorolog. Parameters: temp., pressure, wind, weather, precipitation</p> <p>Station 177-183</p> <p>The French expedition to Cap Horn Sept 1882-1883</p> <p>Investigator: Sampling by Dr. Paul Hyades, physician of the expedition; A. Müntz, Prof. chemistry, Paris</p> <p>Location: Orange Bay Hoste Island, 55,3N, - 68,05E</p> <p>Elevation: 6 masl</p> <p>Sampling time: Sept. 1882-Sept. 1883</p> <p>Samples: 6 (1882), 39 , + 6 (=44 in 1883) on the ship in south Atlantic, 1 islands of Cape Verde</p> <p>Meteorolog. Parameters: temp., pressure, wind direction, precipitation, weather</p> <p>Station 184, 185</p>	<p>Volumetric after Regnault</p> <p>Trained persons on the ships of the expedition sampled air by passing it through prepared flasks filled with KOH. They had been analysed back in Paris by a modified apparatus since 1881 with a 160 l aspirator,</p> <p>Remarks and errors:</p> <p>Sulphuric acid error, values too low; correction + 20 pp (according to Spring 1883). Blocked upwelling, by ice, therefore too low values, not used (Poisson et al. 1987, Deep Sea Research, Vol 34, no. 7, p. 1255); possible absorption or decomposing error in glass vessels stored for max. 1 year by reaction to potassium silicate, changing solution equilibrium and freeing CO₂.</p> <p>Estimated error: correction : + 20 ppm , after correction: +--3%</p> <p>French expedition to Cap Horn</p> <p>Air was sampled in glass flasks filled with KOH, locked and stored in a metal closing. Analysis was done later in 1883 in Paris using the Müntz volumetric gasometer (see above).</p> <p>Remarks and errors:</p> <p>See above</p>
1883	<p>Investigator: Walthère Spring et al., Prof., mine engineering, chemistry, university of Liege (Belgium)</p> <p>Location: Chemical institute at Liege, 50,3N, 5,5E , direction the river of Meuse</p> <p>Elevation: 63 masl + 5 m sampling height</p> <p>Sampling time: Feb. 1883 –Feb. 1884</p> <p>Samples: 266</p> <p>Meteorolog. Parameters: temp., pressure, wind speed/direction, weather</p> <p>Station 186</p> <p>E. Ebermayer see 1884</p> <p>Location: Tölz, Forsthaus 47,8N, 12,5E,</p> <p>Samples: june 1883 - December: 29</p>	<p>Pettenkofer variant</p> <p>Passing air through baryta water and an aspirator of 114,6 l, titration by hydrochloric acid without drying. Checking for optimal passage, absorption speed of air stream, absorption of CO₂ by caustic, and absorption if using sulphuric acid for drying.</p> <p>Remarks and Errors:</p> <p>Calibrated apparatus and carefully controlled conditions, enhanced CO₂ level in the city by winds from the industrial centres, enhanced levels by carbon oxidation from coal in the soil</p> <p>Estimated error: +--2-3%</p>
1884	<p>Investigator: Ernst Ebermayer, Prof. agricultural chemistry, university of Munich</p> <p>Location: Bavarian forests, 47,6N, 12,5E ,</p> <p>Elevation: 813 masl + 1,5 m sampling height</p> <p>Sampling time: Oct. 1883 –Nov. 1884</p> <p>Samples: 68 (40 in 1884)</p> <p>Meteorolog. Parameters: temp., pressure, wind speed/direction, weather</p>	<p>Pettenkofer method</p> <p>Estimated error: +- 3%</p>

Supplemental file to: Reconstruction of atmospheric CO₂ Background levels since 1826

	<p>Station 187 Investigator: Walther Hempel, Prof. chemistry, university of Dresden Location: Dresden, 51,3N, 13,7E , Elevation: 111 masl + 15 m sampling height Sampling time: Oct. 1884 –Dec. 1884 daily Samples: 63 Meteorolog. Parameters: temp., pressure, wind speed/direction, weather Station 188</p>	<p>Hempel Volumetric Constant volume, constant temperature 15°C, variable pressure, Air from the roof of the laboratory or 100ccm glass flasks; Measurement of gases in H2O saturated state In parallel check of 1 l air with Pettenkofer-Hesse method Estimated error: +--3%</p>
1885	<p>Investigator: William Marcet, Dr. pysician, Edinburgh/London Location: Geneve, 46,3N, 1E , Elevation: 388 masl + mountains Sampling time: Aug. 1885 –Sept. 1885 Samples: 51 Meteorolog. Parameters: temp., pressure, wind speed/direction, weather Station 189 Investigator: Reinhart Blochmann Prof. chemistry, University of Koenigsberg Location: Koenigsberg /East Prussia, 53,7N, 20,5E Elevation: 15 masl Sampling time: 1885 Samples: 1345 (1200 on land, 44 over sea) Station 703</p>	<p>Volumetric Absorption in KOH and volumetric determination of change of air volume after absorption, Heat control by placing the absorbing vessel in temperature controlled bath Estimated error: +--2-3%</p> <p>Blochmann Pettenkofer variant Air is absorbed in baryta water and titrated Estimated error: +- 3%</p>
1886	<p>Investigator: Thomas van Nuys Prof. chemistry, University of Indiana Location: University park near Bloomington /Indiana, 39,10N, -86,5E Elevation: 228 masl + 50 cm Sampling time: April 1886 10:00 am Samples: 18 Meteorolog. Parameters: temp., pressure, wind speed/direction, weather Station 190 Investigator: Giorgio Roster Prof. chemistry, University of Florence Location: Florence, 43N, 11,15E Elevation: 38 masl + 18 m Sampling time: Jan-Dec 1886 Samples: 9 Station 191</p>	<p>Pettenkofer variant Absorption of air in baryta water</p> <p>Roster Pettenkofer variant Remarks and Errors: Inverted SEAS (summer high, winter low) Estimated error: +--3% in summer</p>
	<p>Investigator: Julius Uffelman Prof. physician, University of Rostock, director of the institute of hygiene Location: Rostock, 54N, 12E court of the university 20 cm above pavement, outside the city, shore of Baltic Sea Elevation: 19 masl + 6 m Sampling time: Oct 1886 – Sept 1887 daily 11:00 am Samples: 92 in 1886; total 420 (26 in rural area) Meteorolog. Parameters: temp., pressure, wind speed/direction, weather Station 193 Investigator: Nils Edvard Selander Dr. physician, Karolinska University Solna (Sweden) Location: Stockholm, 59N, 18,3E , fortress vaxholm directly at the sea side</p>	<p>Uffelman Pettenkofer method Air passed through 4l glass flasks, shaking for 1minute and leaving flasks for 24 hours before titration with oxalic acid. Checking time before titrating: ½ hour 330 ppm, 8 hours 342 ppm (+3.6 %)</p> <p>Selander Not researched, Pettenkofer or volumetric Petteson Estimated error: +- 2-3%</p>

	<p>Elevation: 10 masl Sampling time: Oct 1887 – June 1888 Samples: total 263; 92 in 1886 Meteorolog. Parameters: temp., pressure, wind speed/direction, weather Station 194</p>	
1887	<p>Investigator: Victor Feldt Dr. physician, University of Tartu Location: Tartu, 55N, 26,7E Elevation: 38 masl + 36 m place of the church “Domplatz” Sampling time: Feb – May 1887 several times a day Samples: 377 Meteorolog. Parameters: temp., pressure, wind speed/direction, weather Station 195 Montsouris see above</p>	<p>Pettenkofer method Air stream passed baryta water, , three 6l flasks were filled, shaken for ½ hour, titration by oxalic acid without waiting for a precipitate 20 l aspirator, titration directly in unclear baryta water Remarks and Errors: Too low values (- 187 ppm) 16th April 1887) because of small air volume, titration directly in the unclear baryta water without waiting; methodical problems see the same values day and night. Correction +40 ppm Estimated error: +--3 after correction</p>
1888	<p>Investigator: Jacob Heimann Dr. physician, University of Tartu Location: Tartu, 55N, 26,7E Elevation: 38 masl + 36 m place of the church “Domplatz” Sampling time: June – Sept 1888 several times a day Samples: 350 Meteorolog. Parameters: temp., pressure, wind speed/direction, weather</p> <p>Investigator: Eugen v. Frey Dr. physician, University of Tartu Location: Tartu, 55N, 26,7E Elevation: 38 masl + 36 m place of the church “Domplatz” Sampling time: Oct – Jan 1889 several times a day Samples: 556 (104 outside the city at Ratshof rural area) Meteorolog. Parameters: temp., pressure, wind speed/direction, weather Station 196</p> <p>Investigator: Dr. F. Nansen /Augusta Palmqvist/. assistant of O. Pettersson teacher in natural science Location: travel over the Atlantic to Greenland, 59,48,5N, -3 – 66,8N, -25,2E Elevation: 6 masl + 5 m over sea Sampling time: May 1888 – June 1888 sea, Sept 1888 Greenland (2300 masl) Samples: 35 over sea, 3 over Greenland in 1888, 395 1888 -1890 Meteorolog. Parameters: temp., pressure, wind speed/direction, weather Station 229</p>	<p>Pettenkofer method Air stream passed baryta water, , three 8-10l flasks were filled, shaken for ½ hour, filtration of the precipitation, titration by oxalic acid 20 l aspirator, titration directly in unclear baryta water Remarks and Errors: Too low values (- 187 ppm) 16th April 1887) because of small air volume titration directly in the unclear baryta water without waiting; methodical problems see the same values day and night. Correction +40 ppm Estimated error: +--3 after correction</p> <p>Pettenkofer as Feldt and Heimann</p> <p>Remarks and Errors: Too low values (- 187 ppm) 16th April 1887) because of small air volume titration directly in the unclear baryta water without waiting; methodical problems see the same values day and night. Correction +40 ppm Estimated error: +--3 after correction</p> <p>Pettersson volumetric Flask samples done by F. Nansen on his expedition 1888, analysed by A. Palmqvist in laboratory of O. Pettersson Absorption of CO₂ in KOH, subsequently measurement of volume change of CO₂-free gas by mercury. Absorbing vessels in tempered water bath ; Temperature control of heat of absorption (H₂CO₃ approx. 20 000 cal/gMol; [Schuftan 1933]) much better than older systems (open e.g. Müntz, Regnault); Remarks and Errors: result dependent on temperature and pressure after v. Slyke [van Slyke 1932]. Estimated error: +- 1-2%</p>

1889	<p>Investigator: Arthur Petermann Prof. acricultural chemistry, director of the agricultural station at Gembloux (Belgium) Location: near Gembloux, 50,5N, 4,41E agricultural station Elevation: 150 masl + 5 m over a meadow Sampling time: May 1889 – April 1891 daily from 9 am Samples: 525 Meteorolog. Parameters: temp., pressure, wind speed/direction, weather Station 230</p> <p>Investigator: Augusta Palmqvist/. assistant of O. Pettersson, teacher in natural science Location: Stockholm, 59,17,5N, 18,3E Elevation: 20 masl + 2 m Sampling time: July 1889 – May 1890, Sept 1888 Greenland Samples: 77 in 1889 experimental station Meteorolog. Parameters: temp., pressure, wind speed/direction, weather Station 231</p>	<p>Pettenkofer variant (Schlössing-Reiset) Air was passed trough washing flasks (sulphuric acid) and then absorbed by baryta water in a Pettenkofer tube and titrated by oxalic acid.</p> <p>Remarks and Errors: Sulphuric acid error of about 20-30 ppm according to Hlasiwetz [1848] and Spring (1883); Bunsen absorption coefficient H₂SO₄ at 25°C = 0,96; H₂O at 25°C=0,759 [IUPAC NIST Solubility database]</p> <p>Estimated error: correction by +20 ppm; error+--3%</p> <p>Pettersson volumetric See above Remarks and Errors: result dependent on temperature and pressure after v. Slyke [van Slyke 1932]. Very accurate Estimated error: +- 1- 2% [Johansson 1898, Skand. Arch. Phys. Bd. 8, p. 93]</p>
1890	<p>Investigator: Augusta Palmqvist/. assistant of O. Pettersson, teacher in natural science Location: Stockholm, 59,17N, 18,3E Tromsö: Husa: 63,48N, 13,11E Skagerak: 57,8N, 13,58E Maseskär: 58,5N, 11,05E Kristineberg: 59,17N, 18E Elevation: 20 masl + 2 m Sampling time: Jan 1890 – May 1890, Tromsö: Feb- March 1890 Husa: Feb- March 1890 Maseskär: Feb- March 1890 Skagerak: Feb 1890 Kristineberg: June –Aug 1890 Samples: 120 in 1890 experimental station Tromsö: 23, Husa: 29, Maseskär: 38, Skagerak: 7, Kristineberg: 64; 1888 -1890: 395 samples Meteorolog. Parameters: temp., pressure, wind speed/direction, weather Station 236</p> <p>Investigator: Arsenius Lebedinzeff, Dr. chemist, University of Odessa Location: Odessa, 46,48N, 30,7E Elevation: 50 masl Sampling time: April-May 1890</p> <p>Samples: 7 Meteorolog. Parameters: temp., pressure, weather Station 704</p>	<p>Pettersson volumetric See above Remarks and Errors: result dependent on temperature and pressure after v. Slyke [van Slyke 1932]. Very accurate Estimated error: +- 1-2%</p> <p>Pettenkofer variant Air was passed trough baryta water and titrated by oxalic acid.</p> <p>Estimated error: error+--3%</p>
1893	<p>Investigator: Salomon August Andrée, engineer Location: over Stockholm, 59,17N, 18,3E , Elevation: 0-3830 masl (0, 380, 1200, 2370, 3200, 3830) Sampling time: 15th July 1893 Samples: 6 Meteorolog. Parameters: temp., pressure, wind,</p>	<p>Volumetric determination , Pettersson gas analyzer Remarks and Errors: see above; first vertical profile by balloon flight Estimated error: +- 1-2%</p>

Supplemental file to: Reconstruction of atmospheric CO₂ Background levels since 1826

	weather Station 237	
1896	Investigator: Carleton Williams, Prof. chemistry, university of Sheffield Location: garden 2,4 km west of Sheffield (UK), 53,4N, 1,5E , Elevation: 110 masl Sampling time: Dec 1896-April 1897 Samples: 142, + 21 in the city of Sheffield Meteorolog. Parameters: temp., pressure, wind, weather Station 238	Pettenkofer variant according to Smith Air passed in 10l flask and the for absorption in baryta water, filtration of unclear baryta water, titration with oxalic acid Estimated error: +--3%
1897	Investigator: E.A. Letts, Prof. chemistry, Queens university of Belfast Location: 53,55N, -2.4333E, garden of university Elevation: 0 masl +2m Sampling time: March July 1887 Samples: 46 Meteorolog. Parameters: : temp., pressure, wind, weather Station 239	Pettenkofer variant 20 l air were absorbed in baryta water and titrated with HCl Estimated error: +--3%
1898	Investigator: Horace Brown, Dr. chemistry, Jodrell Lab. Kew Gardens London Location: Kew Gardens lat 51,5N; 029W Elevation: 15 masl + 1, 5 m Sampling time: July 1898 July 1901 Samples: 91 (16 in 1898, 18 in 1899, 29 in 1900, 28 in 1901) Meteorolog. Parameters: : weather Station 240	Pettenkofer variant according to Reiset 100- 200 l air was passed trough washing flasks (sulphuric acid) and then absorbed by NaOH and double titrated by sulphuric acid. Remarks and Errors: Sulphuric acid error of about 20-30 ppm according to Hlasiwetz [1848] and Spring (1883); Bunsen absorption coefficient H ₂ SO ₄ at 25°C = 0,96; H ₂ O at 25°C=0,759 [IUPAC NIST Solubility database] Estimated error: correction by +20 ppm; error+--3%
1902	Investigator: August Krogh, Prof., zoology university of Copenhagen, Nobel awardist 1920 Location: Disko Island and coast of Greenland 69,75N, -53,5E, Kuganguak 70,28N, -53,9E, Ingnagnak, Napasiligsuak 70,3N, -54,48E, Igdlorpait 60,45N, -45,33, Avatarpait 70,08N -54,8E, Nordfjord 69,95N -54,5E, Ivisarkut 69,73N, -54,78E, Mellemfjord 69,75N, -54,6E, Dikofjord 69,4N, -53,9E, Sioranguak 69,4N, -53,9E, Uvivak 63,0N, -41,4E Elevation: 0 -670 masl + 1, 5 m Sampling time: July – August 1902 Samples: 59 Meteorolog. Parameters: : pressure, wind direction/speed, weather Station 251	Volumetric using a modified Haldane apparatus air in flasks was connected to an absorption vessel with KOH , the volume change of the system was determined by a capillary manometer, heat control is maintained by placing vessels for analysis in water bath. Double determinations Remarks and Errors: Original Haldane analyser was modified to get better accuracy as normal of about +- 8-16,6 % Upwelling of warmer water with high phyto/zooplankton bloom in June/July/August at Disko island explains high CO ₂ values. Moss 1875 using the Pettenkofer method received the same high values in Greenland 1875/76 (642, 483, 536 ppm) Winds with highest CO ₂ from N,W,S Oxygen values about constant, conclusion: CO ₂ from water Estimated error: modified +--3,3 % or +- 10 ppm (300 ppm; +- 1,6% 600 ppm)
1906	Investigator: René Legendre, Prof. biology, director biological station at Concarneau Location: Concarneau (Normandie) 47,5N, -3,85E Elevation: 15 masl Sampling time: Aug/Sept, 1906, July/Aug. 1907 Samples: 12 in 1906, 12 in 1907, (total 24)	Pettenkofer variant used at Montsouris Observatory Paris see above Remarks: Data sampled in July /Aug.1907 directly from the roof of the laboratory at the front of the Atlantic sea

	Meteorolog. Parameters: : temperature, pressure, wind direction, weather Station 252	Estimated error: +--3 %
1907	Investigator: Jens P. Lindhard, Dr. physiology, Danish North East Greenland expedition Location: Greenland Denmarkshavn 76°46'N, 18°46'W Elevation: 11 masl Sampling time: 1907-1908 Samples: 23 Meteorolog. Parameters: : temperature, pressure, wind direction, weather Station 253	Haldane volumetric variant , same as Krogh 1902 Remarks: Same upwelling on some days found as Krogh Normal average 350 ppm, 2 days <300 ppm, 5 days >400 ppm, max 620 ppm (cited in Benedict 1912) Estimated error: modified +--3,3 % or +- 10 ppm (300 ppm; +- 1,6% 600 ppm)
1908	Investigator: Jean Charcot, Dr. physician, 2 nd French Antarctic Expedition 1908-1910 CO ₂ Analysis: A. Müntz, Paris Location: Cape Horn-Antarctic coast 58S -70S, -65- -121E Elevation: 3-10 masl Sampling time: 1908-1910 Samples: 10 (1 in 1908) Meteorolog. Parameters: : temperature, pressure, wind direction, weather Station 263	Volumetric after Müntz Trained persons on the ships of the expedition sampled air by filling it in prepared flasks (5 l). They had been analysed back in Paris by a modified apparatus. The flask air was passed through KOH and the connected to a volumeter which measures the volume of freed CO ₂ by adding sulphuric acid. Remarks and errors: Sulphuric acid error, values too low ; correction + 20 pp (according to Spring 1883). Blocked upwelling, by ice, therefore too low values, not used (Poisson et al. 1987, Deep Sea Research, Vol 34, no. 7, p. 1255); Not used because of strong ocean absorption near ice shields (see Buch) Estimated error: correction : + 20 ppm , after correction: +--3%
1909	Investigator: Francis G. Benedict, Prof. physiology, Director Boston Nutrition Laboratory Location: Boston, west side of nutrition laboratory 42,3N, -71E, ocean, Pikes Peak Elevation: Boston 13 masl +10 m; Pikes Pike 4312 masl Sampling time: 1909-1912 Samples: Boston :212, ocean air 43, Pikes Peak 9 (1909: 42 samples, 1910: 248, 1911, 297, 1912: 17) total 604 Meteorolog. Parameters: : temperature, pressure, wind direction, weather Station 265	Pettersson – Sonden volumetric See above Remarks and Errors: result dependent on temperature and pressure after v. Slyke [van Slyke 1932]. Very accurate Estimated error: +- 1-2%
1911	Investigator: James Kendall, Prof. chemistry, Columbia University New York Location: Edinburg 55,5N, -10E, Petrograd 54,38N, 62,42E, Stockholm 59,2N, 18E, Columbia University 42,8N, -74,5E Elevation: Petrograd 180, Edinburgh 32, Stockholm 20, New York 9 masl Sampling time: Edinburg Mar 1911 Petrograd Jan 1913, Nobel institute Stockholm June 1913, Columbia University July 1915 Samples: 18 Edinburg, 10 Petrograd, 8 Stockholm, 24 New York, total: 60 Meteorolog. Parameters: : not available Columbia Institut fresh breeze from the Hudson river Station 269	Pettenkofer method, Walker modification (Walker, J., Estimation of atmospheric carbon dioxide; Chem. Soc, Trans. 77, 1110 (1900)) see Letts and Blake p 219-229 double determinations Remarks: No meteorological and station conditions available Lowest value March 1911:356 ppm, near the city Lowest value Jan 1913: 356 ppm, near the city Lowest value June 1913: 321ppm rural area Lowest value July 1915 :326 ppm Winds from Hudson River Estimated error: at least +- 3%

	Investigator: August Krogh, Prof., zoology university of Copenhagen, Nobel awardist 1920 Location: Copenhagen Elevation: 6 masl Sampling time: April 1911- Jan 1912, Samples: 200 Meteorolog. Parameters: : pressure, wind direction/ speed, weather	Volumetric using a modified Haldane apparatus See 1902
1912	Investigator: Albert Wigand, Prof. meteorology, Hamburg Location: Bitterfeld (Germany) 51,6N, 12,3E Elevation: 3260, 4990, 6350, 9100 masl Sampling time: . Aug. 1911-Sept 1912 Samples: 4 (CO ₂) Meteorolog. Parameters: : temperature, pressure, wind, weather Station 270	Fractionated Condensation (Erdmann 1910) (Erdmann et al. Berichte der deutschen chemischen Gesellschaft, 43, (1910), p. 1702/1708 Air was sampled during ballon flights in 2 l flasks and analysed in the chemical laboratory of Halle (Germany) Remarks: CO ₂ in upper troposphere much lower than expected, possible problem of the condensation method by Erdmann correction by +15 ppm Estimated error: at least +- 5%
1917	Investigator: August Krogh, Prof., zoology university of Copenhagen, Nobel awardist 1920 Location: Copenhagen lat 55,7 N, 12,5E Elevation: 6 masl Sampling time: . May. 1917 - June 1918, Samples: 76 Meteorolog. Parameters: : - Station 271	Volumetric similar Haldane /Pettersson 3 gas burettes each for O ₂ /N ₂ /CO ₂ , one measuring burette for saturing with H ₂ O, reading of volume change before and after absorption of moist air in KOH Remarks: Air in Copenhagen is between 310 -370 ppm 2 very accurate values after calibration: 305, 300 ppm (average: 302,5 ppm) Temperature constancy in laboratory Error: O ₂ /N ₂ /CO ₂ = <= 0,001% Standard deviation in double determinations for CO ₂ is 0,00025 %; +-2,5 %.
1920	Investigator: Henrik Lundegardh, Prof., botany Central institute for agricultural research Stockholm Location: Hallands Väderö, lat 55,5N, 12,55E Elevation: 8 masl Sampling time: . 1920 - 1926, May - Sept Samples: > 3000 Meteorolog. Parameters: : - temperature, pressure, wind , weather Station 272	Pettenkofer variant Automatic absorption of moist air in baryta water, titration by HCl controlled by phenolphthalein. Temperature control; result CO ₂ concentration in mg/l Remarks: Half -automatic apparatus Additional volumetric analysis of soil air and air over crop fields Error: +-1% or +-0,0003 Vol %
1921	Investigator: Bruno Schulz, Prof., hydrography University Hamburg, institute of oceanography Location: North Sea, Baltic sea, 55N, 12,4E Elevation: 8 masl Sampling time: . 1921, July- August 1921 Samples: 25 Meteorolog. Parameters: : - temperature, most important oceanographic parameters Station 297	Volumetric apparatus by Krogh see 1917 Remarks: Surface water of Baltic Sea supersaturated with CO ₂ more than North Sea Error: +-2,5%
1924	Investigator: Theodor Meinecke Jr., Dr.phil., Dr., forestry science, University Hannover,	Pettersson – Sonden volumetric See above

	Location: Eberswalde, 52,8N, 13,7E Elevation 5 masl Sampling time: 1924, June- October Samples: >334 Meteorolog. Parameters: temperature, wind, weather Station 298	Remarks and Errors: result dependent on temperature and pressure after v. Slyke [van Slyke 1932]. Very accurate selected data 5-32 m over ground after rain Estimated error: +- 1-2%
1925	Investigator: Erich Reinau, Prof., ecologic agriculture Location: Davos, 46,8N, 9,7E Elevation: 2 masl Sampling time: August 1925 Samples: 53 Meteorolog. Parameters: : - temperature, weather Station 299 Investigator: Hermann Wattenberg, Prof. Dr., chemist, Hydrography Location: southern Atlantic ocean 0S-72S, Elevation: 0 masl Sampling time: June 1925 – May 1927 Samples: >10 000, 312 calculated CO ₂ values over sea surface Meteorolog. Parameters: : - temperature, weather oceanographic parameters Station 611	Pettersson – Sonden volumetric See above Remarks and Errors: result dependent on temperature and pressure after v. Slyke [van Slyke 1932]. Very accurate selected data after rain Estimated error: +- 1-2% Volumetric apparatus by Krogh modified by Buch see 1917 Buch, K. Über die Alkalinität, Wasserstoffionenkonzentration, Kohlensäure und Kohlensäureretension im Wasser der Finland umgebenden Meere, Helsingfors : Societas scientiarum fennica, 1917. Remarks: Measured values higher according to Buch Error: +-1-2 %
1926	Investigator: D. Florentin, Dr., chemist, Laboratoire municipale de Paris Location: Paris, Laboratoire de Villejuif, 48N, 2,19E Elevation: 120 masl Sampling time: Jan 1926 – Nov 1927 Samples: 27 (one selected: 4 th Dec 1926, strong wind) Meteorolog. Parameters: : - temperature, wind, weather Station 612 Investigator: August Krogh, Prof., zoology university of Copenhagen, Nobel awardist 1920; Dr. Odum Location: Greenland /Danmark Elevation: - Sampling time: summer 1926 Samples: - Meteorolog. Parameters: : - Station 613	Pettenkofer variant after Vandenberghe Passing air through baryta water and titration Remarks: Only one value selected : altitude 120 m, strong winds Error: +-1-2 % Pettenkofer variant Passing air through baryta water and titration by HCl Remarks: Error: +-3 %
1927	Investigator: Robert Gut, Dr., forest engineer Zurich Location: Zuerichberg, forests near Zurich, 4 stations, Elevation: 622, 619, 642, 646 masl, 34, 28, 23, 18, 13, 10, 5, 1 m altitude+ more altitudes Sampling time: July 1927 – July 1928 Samples: 5000 Meteorolog. Parameters: : - temperature, wind, weather Station 617	Volumetric apparatus by Gut similar to Haldane apparatus absorption of air in KOH, manometric reading of changed air volume over solution temperature and pressure controlled as Krogh apparatus Remarks: Temperature sensible, too low levels at higher temperature errors in CO ₂ absorption heat, large diurnal variation the same as measured in modern with somewhat higher CO ₂ levels; no calibration against Pettenkofer Error: +-2-3%

	<p>Investigator: Donald D. van Slyke, Prof. Dr., biochemist Location: Rockefeller Institute laboratory , New York Elevation: Sampling time:. 1927 Samples: >2 Meteorolog. Parameters: : - temperature Station 618</p>	<p>Volumetric apparatus by Van Slyke (manometric) Absorption of air in NaOH Manometric reading of pressure change</p> <p>Remarks: Comparison with the Haldane apparatus Error: +-1 %</p>
1930	<p>Investigator: Paul Lehmann, Dr., Klimatologie der Hochschule für Bodenkultur Location: Lunz, biological station Seehof lat 47,8N, 15E Elevation: 1280 masl + 2m Sampling time:. 1927 Samples: >44 soil and air (29) Meteorolog. Parameters: : - temperature , pressure, wind, weather Station 619</p>	<p>Pettenkofer variant Krogh/ Rehberg 1928 Passing air through baryta water and titration by HCl</p> <p>Remarks: Measurements over crops, 2, over Topinambur; photosynthesis absorption reduction: Error: +-3 %</p>
1931	<p>Investigator: Donald D. van Slyke, Prof. Dr., biochemist Location: Rockefeller Institute laboratory , New York lat 40,30N, -45,10E Elevation: 8 masl Sampling time:. 1931 Samples: >2 Meteorolog. Parameters: : - temperature Station 620</p>	<p>Volumetric apparatus by Van Slyke (manometric) Absorption of air in NaOH Manometric reading of pressure change</p> <p>Remarks: Comparison with the Haldane apparatus Error: +-1 %</p>
1932	<p>Investigator: Kurt Buch, Prof. Dr., chemistry Institute of ocean research, Helsingfors</p> <p>Location: northern Atlantic ocean lat 56,41N 5,5E, 55,56N, -6,21E, 59,07N, -6,14E, 62,01N, -5,3E, 64,5N, -10,4E, + locations at the northern icelandic coast</p> <p>Elevation: 8 masl Sampling time:. summer 1932 (7th July – 9th Sept) Samples: 28 (double determinations) Meteorolog. Parameters: : - temperature, weather Station 632</p>	<p>Pettenkofer variant Krogh/ Rehberg 1928 Variant by Buch</p> <p>Passing air through baryta water and titration by HCl</p> <p>Remarks: Sampling over sea surface:</p> <p>Error: +-2 %</p>
1933	<p>Investigator: Kurt Buch, Prof. Dr., chemistry Institute of ocean research, Helsingfors</p> <p>Location: Liinahamari, Petsamofjord (now Russian) lat 69° 38' 29 N, Longitude: 31° 20' 36 E Elevation: 8 masl Sampling time:. 31 October 1933 – 4 May 1935 Samples: weekly, 52 (double determinations) Meteorolog. Parameters: : - temperature, wind, weather Station 633</p> <p>Investigator: Thomas Moyer, Dr., chemistry AMERICAN SMELTING AND REFINING COMPA.NY, Utah , USA Location: 5 km out of Salt Lake City, Utah, lat 69°</p>	<p>Pettenkofer variant Krogh/ Rehberg 1928 Variant by Buch</p> <p>Passing air through baryta water and titration by HCl</p> <p>Remarks: Sampling over sea surface:</p> <p>Error: +-2 %</p> <p>Thomas Moyer Autometer Absorption of CO₂ from air stream with 300 ccm/min in 0,005N NaOH; measuring the electrical conductance of the solution at constant temperature</p>

	<p>40 N, Longitude: -111 E Elevation: ~1900 masl Sampling time: 19 Jan 1933 – 13 Feb 1933 Samples: >135 (continuous air stream) Meteorolog. Parameters: -</p> <p>Station 634</p>	<p>with a recording Wheatstone bridge, making use of the fact that sodium hydroxide solution has about twice the conductance of the equivalent sodium carbonate solution. Temperature thermostat controlled Source: Air pollution and plant life J. N. B. Bell, Michael Treshow, p.7; Wiley 2002 Remarks: One of the first automatic systems, calibration against Pettenkofer titrimetric method: difference max+0,3-0,6% Error: +-1 %</p>
1934	<p>Investigator: John.G. Waugh, Dr., physicist Cornell university Ithaca, USA Location: Ithaca, Plant science building, roof, rural area Elevation: 135 masl Sampling time: 11 April 1934 – 11 Oct 1934 Samples: >37 Meteorolog. Parameters:</p> <p>Station 635</p>	<p>Thomas Moyer Autometer variant Absorption of CO₂ from air stream with 350 ccm/min in 0,00488N NaOH; measuring the electrical resistance of the solution at constant temperature with a recording Wheatstone bridge. 2,5 l air samples in flasks, 2-3 determinations/hour Remarks: Double determination in outside air Error: average +-1 %</p>
1935	<p>Investigator: Yrjö Kauko, Prof. Dr., chemist University of Helsinki Location: over Helsinki, by aeroplane, vertical profile Elevation: 0-1500 masl Sampling time: 20 Feb 1935, 7 Dec 1935, 13 Dec 1935 Samples: 15 Meteorolog. Parameters: Temperature, wind, weather</p> <p>Station 636</p> <p>Investigator: J.B.S. Haldane, Prof. Dr., chemist University of Helsinki Location: Scotland rural and coast, Elevation: 1,2-21 masl Sampling time: July - December 1935 August: Cloan (Perthshire) day/night Samples: 1500 153 samples at Cloan (Perthshire)= 324 ppm day/386ppm night; samples coast of Ayreshire (Aug/Sept)= 370 ppm wind from the sea; night air at Oxford in October to Nov= 330 ppm av and 380 av; Meteorolog. Parameters: wind, weather Station 639</p>	<p>Kryogenic Condensation Method 30 l air was passed through conc. H₂SO₄, stream of 10l/std measured by difference manometer, passed through cooling coils, and sampled in flasks filled with CaCl₂ and determined by weighting the volume of the displaced solution. Remarks: Most accurate method Calibration against potentiometric method (+-1%) and Pettenkofer Error: average +-0,33 %</p> <p>Haldane volumetric, improved See above Remarks: All pipettes in the same water bath Also measurements of CO₂ from soils and combustion (London) Estimated error: modified +--2,5 %</p>
1936	<p>Investigator: Kurt Buch, Prof. Dr., chemistry Institute of ocean research, Helsingfors</p> <p>Location: travel to Spitsbergen lat 69° N - 80N, lon 0°E- 20 E Elevation: 8 masl Sampling time: 14 Aug – 24 Aug 1936 Samples: 13 in flasks Meteorolog. Parameters: - temperature, wind, weather Station 652</p>	<p>Pettenkofer variant Krogh/ Rehberg 1928 Variant by Buch</p> <p>Passing air through baryta water and titration by HCl</p> <p>Remarks: Sampling over sea surface: Error: +-2 %</p>

Supplemental file to: Reconstruction of atmospheric CO₂ Background levels since 1826

	<p>Investigator: Johann Ulrich Duerst, Prof. Dr., veterinary science Institute veterinary hygiene University of Bern (Switzerland)</p> <p>Location: Ins (near Bern Switzerland) lat 47° N, lon 7,1 E , rural area Elevation: 499 masl Sampling time:. 1936-1938, max. 6 samples/day Samples:, 1000 Meteorolog. Parameters: : temperature, wind, weather Station 653</p>	<p>Pettenkofer variant Hesse Calibration with Pettesson Sonden analyser Passing air though baryta water and titration by HCl</p> <p>Remarks: Sampling 1m over meadow surrounded by:shrubs and trees</p> <p>Error: +-3 %</p>
1938	<p>Investigator: Kurt Buch, Prof. Dr., chemistry Institute of ocean research, Helsingfors Location: Baltic sea, lat 65 -50, lon 17-29 ; see separate file Elevation: 0 masl Sampling time:. 1927-1938, day night Samples:, 185 at 185 different stations Meteorolog. Parameters: : temperature, oceanographic parameters Station 838</p>	<p>Pettenkofer variant Krogh/ Rehberg 1928 Variant by Buch</p> <p>Passing air though baryta water and titration by HCl</p> <p>Remarks: Sampling over sea surface:</p> <p>Error: +-2 %</p>
1939	<p>Investigator: Wilhelm Kreutz, Dr., chemistry Director of the weather station at Giessen (Germany), Reichswetterdienst</p> <p>Location: Giessen periphery, near rural area Elevation: 499 masl Sampling time:. August 1939- January 1941, 16 samples per day, otherwise samples at 7:00, 14:00, 21:00 at 4 altitudes; (total 550 days) Samples:, >30 000; > 25 000 used soil samples: 1647, special CO2/temperature analyses: 1098 + analysis in higher air layers + 2176 diurnal sampling every 1,5 hours+ preexaminations at Heidelberg; 7054 in 1939, 16773 in 1940, 1429 in 1941 Meteorolog. Parameters: : temperature, wind, precipitation, radiation, pressure, humidity, cloud coverage, weather Station 839</p> <p>Investigator: J. Verduin, Dr., botany; IOWA state university Location: IOWA Agricultural experimental station; cornfield, lat 42,024N, -93,6E Elevation: 299 masl, 1 m Sampling time:. July/Aug 1939/40 Samples:1939: 53; 1940: 203 Meteorolog. Parameters: - Station 840</p>	<p>Manometric Riedel C gas analyser designed by Schuftan 0,5 l flask sampling , Pressing air sample through KOH by turning vessel by 90 degree, reading volume change by capillary manometer</p> <p>Remarks: Sampling in 4 altitudes: 0, 0,5, 2, 14 m; monitoring radiation, precipitation, cloud cover, wind speed, pressure, humidity. Temperature, CO2 Analysis in temperature controlled room</p> <p>Error CO2: +-1,5 %</p> <p>Pettenkofer according to Heinicke and Hoffmann, modified Absorption of CO2 in NaOH, precipitation in BaCl2, titration with HCl, phenolphthalein</p> <p>Remarks: 25% absorption at 1 m over cornfield from normal level Error: 3%</p>
1940	<p>Investigator: Wilhelm Bazett, Prof. Dr., physiology; University of Pennsylvania, Philadelphia Location: Philadelphia Elevation: 105 masl Sampling time:. 1940 Samples: 9 Meteorolog. Parameters: - Station 841</p>	<p>Haldane volumetric gas analyser variant See above Remarks: No date and other parameters available Estimated error: modified +-13 %</p>
1941	<p>Investigator: Ernest Earl Lockhart, Dr.,</p>	<p>Haldane volumetric portable gas analyser</p>

	<p>physiologist, Harvard university, Boston USA, Arnold Court, meteorologist, US weather Bureau Location: Antarctica, West Base 78,29S, -163,5 E Elevation: 244 masl Sampling time: July 1940 –Jan 1941 Samples: 26 Meteorolog. Parameters: wind, temperature, pressure, weather, O2 Station 842 Investigator: Harry J. Fuller, Prof., botanist, University of Illinois Location: Campaign county forest and grassland, Illinois, Urbana 40,1N, -88,1 E Elevation: about 214 masl Sampling time: 22 June 1941 –9 July 1941, 1pm Samples: 144 (4 locations) Meteorolog. Parameters: - Station 846</p>	<p>See above Remarks: Calibrated according to van Slyke Estimated error: +-5% Haldane volumetric gas analyser 100ml glass tubes, analysed in laboratory Remarks: Quadruple determinations Estimated error: +-2,5%</p>
1943	<p>Investigator: R.K. Misra, Dr., chemist, Central Agricultural Meteorological Observatory Poona , India Location: experimental fields near Poona, rural area; lat 18,5N, 73,8 E Elevation: about 555 masl Sampling time: Dec 1941 –Nov 1943, Samples: atmosphere >1532; soil > 1500 Meteorolog. Parameters: temperature, wind, precipitation Station 847</p>	<p>Pettenkofer Passing air through baryta water and titration by oxalic acid, Phenolphthalein as indicator Remarks: Flask samples analysed in laboratory Double determinations, difference in the 3rd decimal Error: +-4 %</p>
1944	<p>Investigator: Eugen Glückauf, Dr., chemist, University Science Laboratories Durham (UK) Location: 4-10km over England; Kew garden; lat 51,5N; 0,29W Elevation: about 4000-1000 masl; Kew Garden 15 masl Sampling time: winter/spring 1944, Samples: 12 in troposphere, several near ground London Meteorolog. Parameters: - Station 849</p>	<p>Condensation method Freezing out CO2 and H2O by liquid air, measuring the pressure of CO2 Remarks: Author states CO2 in water was negligible, no check Error: 10% (see reference p. 621; 0,001% CO2)</p>
1946	<p>Investigator: Per F. Scholander, Prof. Dr., botanist, 1946 at Edward Martin Biological Laboratory, Swarthmore College Swarthmore Location: Swarthmore lat 39.90N, -75.35E , rural area Elevation: Edward Martin laboratory 77 masl Sampling time: 1946 Samples: >3000 Meteorolog. Parameters: - Station 850</p>	<p>Manometric Scholander Analyser Absorption of air in KOH, automatically measuring pressure change Remarks: checked against Haldane analyser: same accuracy Error: paper 1946 +- vol 0,015% stddev of tests 58 (mean 349)=16,5% improved analyser=</p>
1947	<p>Investigator: Per F. Scholander, Prof. Dr., botanist, 1947 at Location: Point Barrow Arctic Laboratory lat 71,3N, -156,64W, Elevation: 2 masl Sampling time: Oct 1947 – March 1949 Samples: : ~350 Meteorolog. Parameters: O2 Station 851</p>	<p>Manometric Scholander Analyser Absorption of air in KOH, automatically measuring pressure change Remarks: checked against Haldane analyser: same accuracy Error: paper 1946 +- vol 0,015% stddev of tests 58 (mean 349)=16,5% improved analyser=</p>

1949	<p>Investigator: H. W. Chapman, Dr., botanist, University of Nebraska, Lincoln</p> <p>Location: near Alliance Nebraska, rural area lat 42,4N, -103E</p> <p>Elevation: 1220 masl</p> <p>Sampling time: June-Aug 1949 -1951</p> <p>Samples: :. 1949: 220 ; 1950: 148, 1951: 177</p> <p>Meteorolog. Parameters: temperature Station 852</p>	<p>Pettenkofer according to Heinicke and Hoffmann, modified; Absorption of CO₂ in KOH, precipitation in BaCl₂, titration with HCl, phenolphthalein</p> <p>Remarks: Control tower 10-30 cm over potato plants; 28% variability in CO₂ absorption by potato leaves Absorption by potato plants: average 14%,</p> <p>Error: 3%</p>
1950	<p>Investigator: Hal R. de Selm, Prof., botanist, Ohio state university; later University of Tennessee, Knoxville</p> <p>Location: near Blacklick Creek Ohio, rural area lat 40,1N, -82,4E</p> <p>Elevation: 327 masl, 0,9m, 9,m, 12m above ground</p> <p>Sampling time: April - July 1950 , 4 hourly at day</p> <p>Samples: :.>127</p> <p>Meteorolog. Parameters: temperature, pressure, humidity, wind Station 853</p> <p>Investigator: Karl Egle, Prof., botanist, Director of the institute of applied botany Hamburg, later on president of the botanical society of Germany</p> <p>Location: Frankfurt botanical institute lat 50,1N, 8,6E</p> <p>Elevation: 348 masl, + 6-10 m</p> <p>Sampling time: 19 may 1950, 5:00AM-1:30PM</p> <p>Samples: :.>1620,</p> <p>Meteorolog. Parameters: temperature, pressure, humidity, wind; rainy day Station 853</p> <p>Investigator: Siegfried Strugger, Prof., botanist, University Muenster (Germany)</p> <p>Location: botanical garden university Muenster, rural area, grassland lat 51,9N, 7,61E</p> <p>Elevation: 65 masl; 3-4m above ground</p> <p>Sampling time: 18/29 July-1950, 8:00am-6am</p> <p>Samples: :. > 2640</p> <p>Meteorolog. Parameters: weather Station 854</p>	<p>Pettenkofer according to Heinicke and Hoffmann, modified by Böhning 1948; http://www.plantphysiol.org/cgi/reprint/24/2/222</p> <p>Absorption of CO₂ in KOH, precipitation in BaCl₂, titration with HCl, phenolphthalein</p> <p>Remarks: Measurements in forest</p> <p>Error: 3%</p> <p>URAS continous sampling and plotting (NDIR), drying air by streaming through silica gel ; infrared absorption by CO₂</p> <p>Remarks: Continuous gas stream; sample analysis within every 30 sec</p> <p>Error: < +- 1% (0,0001 Vol%)</p> <p>URAS continous sampling and plotting (NDIR), drying air by streaming through silica gel ; infrared absorption by CO₂</p> <p>Remarks: Continuous gas stream; sample analysis within every 30 sec</p> <p>Error: < +- 1% (0,0001 Vol%)</p>
1951	<p>Investigator: Bruno Huber, Prof., botanist, forest and botanical institute, University Munic (Germany)</p> <p>Location: over wheat field in Duernast (48,4N, 11,691E) Freising agricultural faculty Weihenstephan TU Munic</p> <p>Elevation: 476 masl; 50cm-1,2m, 4,5m, 22,5 m beside the field, 50-100m balloon</p> <p>Sampling time: 15 May- 14 Aug 1951</p> <p>Samples: :. > 15 000</p> <p>Meteorolog. Parameters: weather, temperature, rain Station 855</p>	<p>URAS continous sampling and plotting (NDIR), drying air by streaming through silica gel ; infrared absorption by CO₂</p> <p>Remarks: Continuous gas stream; sample analysis within every 30 sec</p> <p>Error: < +- 1% (0,0001 Vol%)</p>
1952	<p>Investigator: H. W. Chapman, Dr., botanist,</p>	<p>Pettenkofer according to Heinicke and Hoffmann,</p>

Supplemental file to: Reconstruction of atmospheric CO₂ Background levels since 1826

	Iowa state College, Ames, Iowa Location: cornfield, Iowa state college television tower, rural area lat 42,4N, -103E Elevation: 1220 masl; 1m, 20m above corn field ; TV tower 10m, 30m, 152m Sampling time: July-Oct1952, 3AM-midnight Samples: :. > 66 Meteorolog. Parameters: temperature, pressure wind Station 856	modified; Absorption of CO ₂ in KOH, precipitation in BaCl ₂ , titration with HCl, phenolphthalein Remarks: Error: 3%
1954	Investigator: Stig Fonselius, Dr., meteorologist, Institute of marine research Helsingfors Finland Location: 15 stations throughout Scandinavia; data from Plönninge Sweden lat 56,8N, 12,9E and Tvärminne Finland 59,8N, 22,9E selected Elevation: Plönninge 59; Tvärminne 14,9 masl Sampling time: Nov 1954-Dec 1959, 1 st , 10 th , 20 th of each month , 1PM Samples: > 2700 Meteorolog. Parameters: temperature, wind, pressure, weather Station 851	Pettenkofer variant by Krogh/ Rehberg 1929 Passing a small amount of air through Ba(OH) ₂ ; titration by HCl see above Remarks: air samples collected in flasks analysed in laboratories at Stockholm and Sweden 6 sampling location ² in Sweden, 4 in Finland, 3 in denmark, 2 in Norway; only data from Plönninge Sweden and Tvärminne (Finland seashore) used Error: +-3 %
1955	Investigator: Charles Keeling, Dr., chemist, California institute of Technology , Pasadena USA Location: see below Elevation: 1. 10 masl +1 m; 2. 1950 masl 1m 3. 2500 masl; 4. 3000 masl; 5. 3800 masl; 6. 4000 masl 7. 4300 masl; 8. 1900 masl 9. 0 masl; 10. 170 masl Sampling time: 1. Big Sur State Park: 18-19 May 55 2. Yosemite National Park, Tamarack: 2-3 June 1955 3. Yosemite National Park, Lake Tenaya: 3 June 1955 4. Yosemite National ParkTioga Pass: 3 June 1955 5. Inyo Mountains,: Mt. Barcroft 8 July 1955 6. Inyo Mountains, Mountain divide: 8-9 July 1955 7. Inyo Mountains, white Mountain summit: 9 July 1955 8. Hart's Pass 1 Sept 1955 9. Olympic National Parc Beach trail: 6-7 Sept 1955 10. Olympic National Hoh River Ranger st.: 6-7 Sept 1955 11. Rock Lake 10-11 Sept 1955 + further locations see reference in 1956 Samples: 50 Meteorolog. Parameters: temperature, wind,	Cryogenic condensation method Condensation of sample by liquid nitrogen, freeing the condensate from water by fractionated distillation and identifying gas by mass spectroscopy and determination quantity by a manometer. Remarks: air samples collected in 5 ltr. flasks analysed in laboratory, additionally determination of C13 isotope Error: +-1 %

	pressure, humidity, weather Station 862	
1956	<p>Investigator: Charles Keeling, Dr., chemist, Scripps Institute of Oceanography, USA</p> <p>Location: see below</p> <ol style="list-style-type: none"> 1. Coastal Redwood Canyon, 6-7 June; 150 masl 2. Coastal Redwood Valley 5-6 June; 70 masl 3. Sierra Nevada Pine and Fir Forest California 10-11 June 1956; 1950 masl 4. Mogollan Rim Pine Forest Arizona; 16-17 May 1956; 2100 masl 5. Borrego desert; 02. Feb 56, 340masl 6. Inyo Mountains; 9-14 March 1956; 3800 masl 7. Sonora desert; 21-22 April 1956, 550 masl <p>Elevation: 1-7: 70 -3800 masl see above</p> <p>Sampling time: See above</p> <p>Samples: 51</p> <p>Meteorolog. Parameters: - Station 869</p>	<p>Cryogenic condensation method Condensation of sample by liquid nitrogen, freeing the condensate from water by fractionated distillation and identifying gas by mass spectroscopy and determination quantity by a manometer.</p> <p>Remarks: air samples collected in 5 ltr. flasks analysed in laboratory, additionally determination of C13 isotope</p> <p>Error: +-1 %</p>
1957	<p>Investigator: Ferdinand Steinhauser, Prof., meteorologist, Zentralanstalt für Meteorologie und Geodynamik, Vienna, Austria</p> <p>Location: weather station Hohe Warte Vienna, Austria, lat 48,25N, 6.35E</p> <p>Elevation: 205 masl +25 m tower</p> <p>Sampling time: Jan 1957- June 1958, daily 1PM</p> <p>Samples: 546</p> <p>Meteorolog. Parameters: wind, (temperature, pressure, weather: other data set) Station 870</p>	<p>Pettenkofer variant by Krogh/ Rehberg 1929 Passing a small amount of air through Ba(OH)₂; titration by HCl see above</p> <p>Remarks: Air collected from the tower of the institute and analysed in laboratory</p> <p>Error: +-2 %</p>
1959	<p>Investigator: Walter Bischof, Dr., engineer University of Stockholm,</p> <p>Location: near/ over Stockholm, Sweden lat 48,25N, 6.35E; Dalarö: lat 59.13N, 18.4E (island) Bryggan:, lat 59.78N, 14.13E, Golf course 1 km away, Djursholm</p> <p>Elevation: 100 m -3 km masl over Stockholm; Dalarö: 0 masl; Djursholm: 16 masl, Bryggan: 154 masl</p> <p>Sampling time: 28 October 1959 over Stockholm, 11-13 Aug and 15-17 Sept 1959 at Golfbanan, 15/16 Aug Dalarö , 28 July at Bryggan and a golf course 1km away (1 Sept, 8 Dec.)</p> <p>Samples: 92</p> <p>Meteorolog. Parameters: eastern winds Station 875</p>	<p>NDIR gas analyser</p> <p>Remarks: used since May 1959</p> <p>Error: +-1-4 %</p>

Note: Montsouris 1877-1910

© Ernst-Georg Beck, Dipl. Biol. Institute for Biology III, University Freiburg, Schaenzlestr. 1, D-79104 Freiburg
December 2009